19th Australian Organic Geochemistry Conference

December 4 - 7, 2016

Esplanade Hotel, Fremantle

Conference Handbook and Abstracts

HOSTED BY

SPONSORS

Organising Committee

Sonya McCarthy

Nicole Sing

Annie Burgos

Gemma Spaak

Matthew Campbell

Calum Fox

Bettina Schaefer

Callum Bonnar

Dr Alan Scarlett

Dr Svenja Tulipani

Scientific Committee

Prof Kliti Grice

A/ Prof Marco Coolen

Dr Paul Greenwood

Dr Alison Blyth

Dr Linda Stalker

Venue

Conference and Icebreaker

Esplanade Hotel Fremantle

46 – 54 Marine Terrace, Fremantle, WA 6160

+61 8 9432 4000

Free Wi-Fi will be available for all conference participants.

Conference Dinner

Bathers Beach House

47 Mews Road, Fremantle, WA 6160

+ 61 8 9335 2911

Wireless Internet:

The following Conference Internet Access Code has been generated:
AOGC

Once connected to **Rydges-EVENT**, please open a new browser and you will be directed to enter an Access Code, select *Visitor* and enter your *Code* (**AOGC**). Each user is required to enter the Access Code.

Contents

Welcome to the 2016 AOGC Conference

“Palaeoclimates, Environments, Ecosystems & Our Resources”

The Organising Committee of the 16th Australian Organic Geochemistry Conference welcomes you to Fremantle for ‘So much serenity’.
All of the members of the local Organising and Scientific Committee wish you a superb conference experience.
Finally we’d like to thank our dedicated volunteers, corporate sponsors and exhibitors. And thank you all for making this a truly great AOGC.

Kliti Grice and team

Conference themes:
Modern and ancient environments
Palaeoclimate
Petroleum geochemistry
Geomicrobiology
Organic-inorganic interfaces
New tools and technologies
Other (e.g. minerals)

The Australian Organic Geochemistry Medal:

1991-2014

Since 1991 the AOGC has awarded a medal to distinguished members of our community for lifetime achievement in the field of Organic Geochemistry.

The previous winners of the AOGC medal are:

1991 John Smith (CSIRO, North Ryde, NSW)

1993 Basil Johns (University of Melbourne, VIC)

1995 Trevor Powell (AGSO, Canberra, NSW)

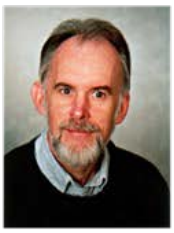

1996 David McKirdy (University of, Adelaide, SA)

1998 Robert Alexander (Curtin University, WA)

2000 Barry Batts (Macquarie University, NSW)

2002 Roger Summioms (MIT, USA)

2004 John Volkman (CSIRO Marine Research, TAS)

2006 Michael Wilson (University of Western Sydney, NSW)

2008 Robert Kagi (Curtin University, WA)

2010 Christopher Boreham (Geoscience Asutralia, ACT)

2012 Simon George (Macquarie University, NSW)

2014 Kliti Grice (Curtin University, WA)

2016 Australian Organic Geochemistry Medal Recipient: Andrew P. Murray

The AOGC Conference first awarded a medal for lifetime achievement in the field of organic geochemistry in 1991. At each conference we recognize a distinguished member of our Australian community for their scientific leadership, commitment to teaching and education, and for their contributions to knowledge in the subject areas of organic geochemistry, biogeochemistry and petroleum geochemistry.

Andrew Murray received B.App.Sc. degree from the Royal Melbourne Institute of Technology followed by B.Sc. (Hons Class 1) in 1981 and an M.Sc in 1987 from Deakin University, Geelong, Australia. He was awarded a Ph.D from the Curtin University of Technology in 1998 based on the dissertation entitled: Factors controlling the abundance and carbon isotopic composition of land plant derived compounds in crude oils.

Andrew began his career as an analytical chemist at the Department of Minerals and Energy, Victoria followed by a period, 1980-1987, as a marine chemist at the Victorian Marine Science Laboratories. From 1988-91 he was a Lecturer in analytical and environmental chemistry at the University of Brunei Darussalam. Andrew then joined the Australian Geological Survey Organisation as a research scientist where he instigated a new research program focused on innovative approaches to evaluate the contributions of land plants to crude oils. He conducted ground-breaking research into the biomarker and C-isotopic characteristics of Cenozoic oils from different paleoenvironmental settings. This led him to study and document how fundamental differences in the physiologies and chemistries of conifers and flowering plants could explain the distinctive chemical compositions of oils from the Gippsland and Taranaki basins, Papua New Guinea and the land plant-sourced oils from S.E Asia. Following his interests in environmental chemistry he studied the chemistry and ocean transport of fossil dammar resin and bitumens that can be found stranded along the coastlines of northern, western and southern Australia after storms. He established the National Oils of the Sea Database and methodologies that could be used to quickly and robustly identify the origins of spills were an accident to occur with the petroleums that are routinely transported around the Australian coastline.

In 1998, Andrew decided to apply his knowledge and skills to petroleum exploration and joined Woodside Energy Ltd. as a Senior Geochemist. He was seconded as a Senior Staff Geochemist to the Shell Research and Technology Centre in Rijswijk, The Netherlands from 2002-2005, before returning to the Woodside Perth office as Principal Petroleum Systems Analyst. In these roles, and subsequently as a Petroleum Systems Advisor, Andrew exercised his critical skills in basin modelling, exploration geochemistry, reservoir geochemistry, and in fact, all aspects of the full life-cycle of exploration and production activities. In early 2014 he started Murray Partners PPSA to offer training and support to exploration geoscientists who are not specialists in geochemistry or basin modelling.

Throughout his distinguished career, Andrew has demonstrated the importance of critical thinking, sound scientific knowledge and judgment and professional integrity. His work has bridged the often significant gulf between bench science and its application to practical problems in industry and environmental custodianship. Andrew has always been, and continues to be the exemplar of the collaborative and collegial scientist, teacher and leader. Young people starting out on their STEM careers today have an outstanding role model in Andrew Murray.

Roger Summons
Schlumberger Professor of Geobiology
EAPS Department
Massachusetts Institute of Technology
Cambridge MA 02139
http://summons.mit.edu
rsummons@mit.edu

PUBLICATIONS:

1. Murray, A.P., Dawson D., Carruthers, D. and Larter S. (2013)
Reservoir Fluid Property Variation at the Metre-scale: Origin, impact and mapping in the Vincent Oil Field, Exmouth Sub-Basin. Proceedings of the West Australian Basins Symposium, Petroleum Exploration Society of Australia, Perth.

2. Larter S.R., Head, I.M., Huang, H. Bennet B., Jones, M., Aplin A.C., Murray A., Erdmann M., Wilhelms A. and Di Primio R. (2005) Biodegradation, gas destruction and methane generation in deep subsurface petroleum reservoirs: an overview. In Dore A.G. and Vining B. (eds) Petroleum Geology: North West Europe and Global Perspectives - Proceedings of the 6th Petroleum Geology Conference, Geological Society of London.

3. Summons R.E, Metzger P., Largeau C., Murray A.P. and Hope J.M.
Polymethylsqualanes from *Botryococcus braunii* in lacustrine sediments and crude oils. (2002). Org. Geochem. 33, 99-109

4. Longley, I.M., Buessenschuett, C., Clydsdale, L., Cubitt1, C.J., Davis, R.C., Johnson, M.K., Marshall, N, M., Murray, A.P., Somerville, R., Spry, T.B & Thompson, N.B. (2002) The North West Shelf of Australia – A Woodside perspective. Proceedings of the Western Australian Basins Symposium, Petroleum Exploration Society of Australia, Perth.

5. Jiang, C.-Q; Alexander, R., Kagi, R.I. and Murray, A.P. (2000) Origin of perylene in ancient sediments and its geological significance. Org. Geochem., 31 1545-1559.

6. Jiang C.-Q., Alexander R., Kagi R.I., and Murray A.P (1998). Polycyclic aromatic hydrocarbons in ancient sediments and their relationships to palaeoclimate, Org. Geochem. 29, 1721-1735

7. Murray A.P., Edwards D.E., Hope J.M, Boreham C.J., Alexander R. and Summons R.E. (1998). Carbon isotope biogeochemistry of plant resins and derived hydrocarbons. Org. Geochem. 29, 1199-1214

8. Murray A.P., Sosrowidjojo I.B., Alexander R. and Summons R.E. (1997). Locating effective source rocks in deltaic petroleum systems: Making better use of land-plant biomarkers. Proceedings of the IPA/AAPG/APEA symposium of petroleum systems of Southeast Asia and Australasia., Jakarta, May, 1997

9. Murray A.P., Sosrowidjojo, I.B., Alexander R., Kagi R.I., Norgate C.M. and Summons, R.E. (1997). Oleananes in oils and sediments: Evidence of marine influence during early diagenesis ? Geochim. Cosmochim. Acta, 61, 1261-1276

10. Volkman J.K., Revill A.T. and Murray A.P. (1997). Applications of biomarkers for identifying sources of natural and pollutant hydrocarbons in aquatic environments. Ch.8. In: Molecular Markers in Environmental Chemistry. (Ed. R. Eganhouse). American Chemical Society Special Publication.

11. Francis D. and Murray A.P. (1996) Source rock study relates to exploration potential outside Taranaki. Pet. Explor. Assoc. NZ Newsletter, 1-3.

12. Summons R.E., Boreham. C.J., Foster C.B., Murray A.P. and Gorter J. D. (1995) Chemostratigraphy and the composition of oils in the Perth Basin, Western Australia. APEA Journal. 35. 613-632

13. Dowling L.M., Boreham C.J., Hope J.M., Murray A.P. and Summons R.E. (1995). Carbon isotopic composition of hydrocarbons in ocean-transported bitumens from the coastline of Australia. Org.Geochem. 23, 729-737.

14. Murray A.P., Summons, R.E., Boreham, C.J. and Dowling L.M. (1994). Biomarker and n-alkane isotope profiles for Tertiary oils: relationship to source rock depositional setting. Org. Geochem. 22, 521-542.

15. Murray A.P., Summons, R.E. Boreham, C.J., Reed, J.D. and Francis, D.A. (1994). Geochemistry of oils and source rocks of the East Coast Basin and implications for the Taranaki Basin, New Zealand. In: Proc. 1994 NZ Petroleum Conference, Ministry of Commerce, New Zealand, 338-351.

16. Murray A.P., Padley, D., McKirdy, D.M., Booth, W.E. and Summons, R.E. (1994). Oceanic transport of fossil dammar resin - The chemistry of coastal resinites from South Australia. Geochim. Cosmochim. Acta. 58, 3049-3059.

17. Bradshaw M.T., Bradshaw J., Murray A.P., Needham D.J., Spencer L., Summons R.E., Wilmot J. and Winn S. (1994). Petroleum systems in West Australian Basins. In: Purcell, P.G. and R.R. (Eds), The sedimentary Basins of Western Australia: Proceedings of Petroleum Exploration Society of Australia Symposium, Perth, 1994.

18. Lee C.S., Galloway M.C. Willcox J.B. Moore A.M.G., Fraser A.R., Heggie D.T, Murray A.P., Apostol J.R.L., Trinidad N.D., Abando R.P., Panganiban D.V., Guazon E.B., Cortez E.E. and Reyes E.N. (1994). Petroleum potential of Ragay Gulf, southeast Luzon, Philippines. APEA Journal, 34, 707-727

19. Summons R.E., Bradshaw J., Brooks D.M., Goody A.K., Murray A.P, and Foster C.B. (1993). Hydrocarbon composition and origins of coastal bitumens from the Northern Territory, Australia. PESA Journal, 21, 31-42.

20. Murray A.P., Summons R.E., Bradshaw J. and Pawih B. (1993). Cainozoic oil in Papua New Guinea - Evidence from geochemical analysis of two newly discovered seeps. In: Petroleum Exploration and Development in New Guinea: Proceedings of the 2nd PNG petroleum convention (eds. G and Z. Carman), Port Moresby, 1993. pp. 489-498.

21. Bradshaw M., Bradshaw J., Loutit T. Murray A.P. and Summons R. (1993). Petroleum systems and geologic processes. Australian Geological Survey Organisation Record., p17.

22. Padley D., McKirdy D.M., Murray A.P. and Summons R.E. (1993). Oil strandings on the beaches of Southern Australia: Origins from natural seepage and shipping. In: Organic Geochemistry: Poster sessions from the 16th international meeting on organic geochemistry, Stavanger, 1993. (ed. K. Oygard), Falch Hutigtrykk (Publ.), Norway.

23. Gibbs C.F., Fabris J.G. and Murray A.P. (1999). Chemical Analysis of Water. In: Expert Evidence (eds. I. Freckleton and H. Selby), the Law Book Company, Sydney.

24. Gibbs C.F., Fabris J.G. and Murray A.P. (1999). Forensic Identification of Spilled Oil. In: Expert Evidence (eds. I. Freckleton and H. Selby), the Law Book Company, Sydney

25. Richardson B.J., Ashton P.H. and Murray A.P. (1993). Bioaccumulator monitoring in Victoria: Past, present and future perspectives. In: Proceedings of a bioaccumulation workshop: Assessment of the distribution, impacts and bioaccumulation of contaminants in aquatic environments. (ed. A.G. Miskiewicz), Water Board and Australian Marine Sciences Association Inc., Sydney

26. Phillips D.J.H., Richardson B.J., Murray A.P. and Fabris J.G. (1992). Trace metals, organochlorines and hydrocarbons in Port Phillip Bay (Victoria): A historical review. Mar. Pollut. Bull. 25, 200-217.

27. Murray A.P., Richardson B.J. and Gibbs C.F. (1991). Bioconcentration factors for petroleum hydrocarbons, PAHs, LABs and biogenic hydrocarbons in the Blue Mussel. Mar. Pollut. Bull. 22, 595 - 603.

28. Murray A.P. and Richardson B.J. (1988). Bioaccumulation factors for hydrocarbons in mussels from Port Phillip Bay (Australia). In: Pollution in the Urban Environment, Vol. 2, Hills, Keen, Lam, Leung, Oswell, Stokes and Turner (Eds.), 556-564, Vincent Blue Copy Co. Hong Kong, 1988.

29. Murray A.P., Gibbs C.F. and Kavanagh P.E. (1987). Linear alkyl benzenes in the sediments of Port Phillip Bay (Australia). Mar. Environ. Res. 23, 65-76.

30. Murray A.P., Gibbs C.F, Longmore A.R. and Flett D.J. (1986). Determination of chlorophyll in marine waters: Intercomparison of a rapid HPLC method with full HPLC, spectrophotometric and fluorometric methods. Mar. Chem. 19, 211-227.

31. Murray A.P., Gibbs C.F. and Kavanagh P.E. (1983). Estimation of total aromatic hydrocarbons in environmental samples by high pressure liquid chromatography. Intern. J. Environ. Anal. Chem. 16, 167-195.

MAP

ESPLANADE HOTEL TO CONFERENCE DINNER

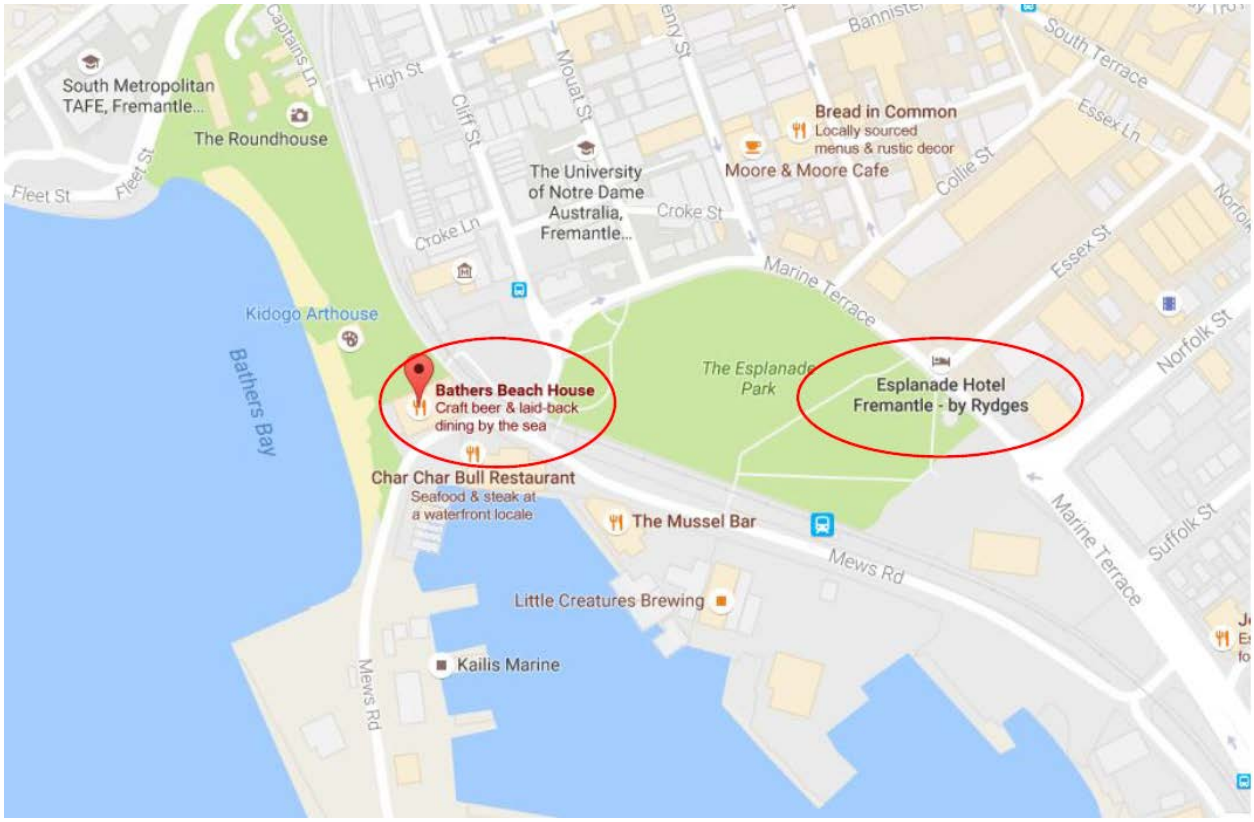

CONFERENCE PROGRAMME

Sunday 4th December

5.30 – 8.30pm Icebreaker and Registration at the **Esplanade Hotel**, Fremantle

Monday 5th December

8.00 – 8.30 Registration and poster set up
Tea and coffee

8.20 – 8.30 **Welcome and Opening**

Session 1 **Paleoclimate and Ancient Environment I**
Chair Eelco Rohling

Keynote

8.30 – 9.00 Exploiting imperfect records of the carbon isotope excursion at the Palaeocene-Eocene Thermal Maximum to infer changes in soil carbon cycling
Francesca A. McInerney, A. Baczynski, S. Wing, M. Kraus, J. Bloch, K. Freeman

9.00 – 9.20 The Neogene expansion of C_4 dominated ecosystems: an Australian perspective
Jake W. Andrae, F. A. McInerney, J. J. Tyler, P. A. Hall

9:20 – 9.40 Cryostane, a new C_{28} sterane from 820 to 740 Ma old pre-Snowball sediments: a biomarker for early sponges and toxic protists?
Jochen J. Brocks, A. Jarrett, E. Sirantoine, F. Kenig, P. Adam, P. Schaeffer, M. Moczydlowska, S. Porter

9.40 – 10.00 Investigation of palaeoenvironmental conditions through the middle Cambrian in the Georgina Basin, central Australia
Anais Pagès, S. Schmid, D. S. Edwards, S. Barnes, N. He, K. Grice

10.00 – 10.30 Morning tea

Session 2 **Petroleum I**
Chair Jamie Burgess

Keynote

10.30 – 11.00 Decision making in petroleum exploration and production: How does organic geochemistry make a difference?
Andrew P. Murray

11.00 – 11.20 Geochemical characteristics of some biodegraded crude oils from the Liaodong Bay, Bohai Bay Basin: Insights into the source and the history of accumulation
Xiong Cheng, D. Hou, C. Xu, F. Wang

11.20 – 11.40 A revised oil family classification scheme and geochemical weathering proxies for South Australian coastal bitumen strandings
Alexander J. Corrick, P. A. Hall, D. M. McKirdy, S. Gong, C. Trefry, C. Dyt, Z. Angelini, A. S. Ross, R. Kempton, S. Armand, C. White

11. 40 – 12.00 The North West Shelf of Australia: Molecular and isotopic approach to discriminate organic facies; and their potential applications for– source rock characterisation
Jaime Cesar, K. Grice

12.00 - 1.30 Lunch

Session 3 Geomicrobiology and Paleoclimates

Chair Lorenz Schwark

1.30 – 1.50 Investigations into the cause of the initial organic carbon isotope excursion at St. Audrie's Bay during the end-Triassic mass extinction using sterane and hopanes biomarkers
Calum P. Fox, K. Grice, J. H. Whiteside, P. Olsen, J. Sepúlveda, R.E. Summons

1.50 – 2.10 The end-Cretaceous mass extinction event – Recovery and evolution of life
Bettina Schaefer, M. J. L. Coolen, K. Grice

2.10 – 2.30 Climate oscillations reflected in the Arabian Sea subseafloor microbiome
Marco J. L. Coolen, W. D. Orsi, L.-H. He, C. Wuchter, K. D. More, X. Irigoien, G. Chust, C. Johnson, J. D. Hemingway, M. Lee, V. Galy, L. Giosan

2.30 – 2.50 Planktonic and benthic eukaryote community responses to glacial-interglacial climate variability in the Arabian Sea
Kuldeep More, K. Grice, M. J. L. Coolen

2.50 – 3.10 Multi-proxy geochemical analyses of Indus submarine fan sediments sampled by IODP Expedition 355: implications for sediment provenance and palaeoclimate reconstructions
Sophia Aharonovich, S. C. George, J. Bendle, H. Liddy, P.D. Clift, D. K. Kulhanek, S. Ando, M. Tiwari, B.-K Khim, E. Griffith, S. Steinke, K. Suzuki, J. Lee, K. Newton, S. Tripathi, Expedition 355 Scientific Party

3.10 – 3.50 Poster Summary/Speed Talks

3.50 – 5:30 Poster Session
Snacks and beverages

Tuesday 6th December

8.00 – 8.30 Registration

Tea and coffee

Session 4 Modern Environments

Chair Francesca A. McInerney

Keynote

8.30 – 9.00 Beached up!: The fascinating story of ambergris
Steve J. Rowland, P. A. Sutton

9.00 – 9.20 How can we use the stable carbon isotope composition of Holocene organic sediments for paleoclimate reconstruction?
Grzegorz Skrzpek, Z. Engel

9:20 – 9.40 Reduced early Holocene moisture availability in central Tibetan Plateau: Evidence from δD values of sedimentary *n*-alkanes
Chuanfang Jin, F. Guenther, S. Li, C. Cao, G. Gleixner

9.40 – 10.00 Effect of hydrocarbon contamination on the soil microbiome in Western Australia's pristine Kimberley region
Deirdre B. Gleeson, T. Lardner, A. S. Ball, K. Grice, A. Trolove, M. Nicholas, G. Bending, S. Hilton, M. Ryan

10.00 – 10.30 Morning tea

Session 5 Paleoclimate and Ancient Environment II

Chair Zeev Aizenstat

Keynote

10.30 – 11.00 Sea level and climate sensitivity
Eelco J. Rohling

11.00 – 11.20 The first occurrence of ergostane and aromatic ergosteroid in the rock record
Tharika M. Liyanage, E. Sirantoine, J. M. Hope, I. Bobrovskiy, J. J. Brocks

11.20 – 11.40 Geochemical and palynological evidence of the earliest land plants in Middle Ordovician shallow marine environments: Implications for paleoclimate and early plant evolution
Gemma Spaak, K. Grice, C. Foster, D. Edwards

11.40 – 12.00 Interpreting shifts in *n*-alkane average chain length in sedimentary records: what are the key drivers?
Sian. Howard, F. A. McInerney, E. Reed, M. Farrell

12.00 – 12.20 Biomarkers from the Ediacaran macrofossil Beltanelliformis
Ilya *Bobrovskiy, J. M. Hope, T. M. Liyanage, J. J. Brocks*

12.30 - 1.30 **Lunch**

Session 6 Geomicrobiology and Paleoclimates

Chair Alison J. Blyth

Keynote

1.30 – 2.00 The Great Oxidation Event and its biological impacts: Insights from geochemistry and molecular clocks
D. A. Gold, A. Caron, G. P. Fournier, Roger E. Summons

2.00 – 2.20 Combined organic and inorganic geochemical characterisation approach of Toarcian carbonate concretions
Chloe Plet, K. Grice, M. J. L. Coolen, A. Pages, W. Ruebsam, L. Schwark

2.20 – 2.40 Occurrence of microbially mediated black sludge and cobble formations after a cyclonic event in Shark Bay, Western Australia
Matthew Campell, K. Grice, M. J. L. Coolen, C. Wuchter, W. Di Fulvio, T. Morris, P. Visccher, R. Bush, G. Choppala

2.40 – 3.00 Molecular, Isotopic and Genetic composition of human gallstones: a Geomedical study.
Sureyya Kose, M. J. L. Coolen, K. Grice, M. Ballal

3.00 – 3.30 Afternoon Tea

Session 7 Petroleum II

Chair Andrew P. Murray

3.30 – 3.50 A case study of oil-oil correlation in the Tarim Basin, China
Shaojie Li, X.-X. Wang, K. Liu, K. Grice, A. I. Holman, P. Hopper

3.50 – 4.10 Helium isotopic distribution of Australian natural gases
Chris J. Boreham, D. S. Edwards, R. J. Poreda

4.10 – 4.30 The stable carbon isotopic compositions of individual *n*- alkanes and isoprenoids provide evidence of source contributions for petroleum generated from the Xihu Depression, East China Sea
Huiyuan Xu, S.C. George, D. Hou

6:00 **Conference Dinner at Bathers Beach House**

AOGC Medal Presentation

Wednesday 7th December

8.00 – 8.30 Registration

Tea and coffee

Session 8 **Petroleum III**
Chair Emmanuelle Grosjean

8.40 – 9.00 Organic geochemical characterisation of aliphatic fractions of Pliocene sapropels from ODP Sites 964 and 967, Eastern Mediterranean Basin
Simon C. George, H. Xu, S. C. Löhr, M. J. Kennedy

9.00 – 9.20 Thoughts on the carbon isotopic composition of fluid inclusion gases from Scott Reef area in Browse Basin
Se Gong, S. Sestak, S. Armand, J. van Holst, J. Bourdet, R. Kemton, E. Grosjean

9:20 – 9.40 Shale petroleum resources of Western Australia:an overview
Ameed R. Ghori

9.40 – 10.00 Geochemistry of dew point petroleum systems, Browse Basin, Australia
Dianne S. Edwards, E. Grosjean, T. Palu, N. Rollet, L. Hall, C. J. Boreham, A. Zumberge, J. Zumberge, A. P. Murray, P. Palatty, N. Jinadasa, K. Khider, T. Buckler

10.00 – 10.30 Morning tea

Session 9 **Organic-Inorganic and New Tools**
Chair Roger E. Summons

Keynote

10.30 – 11.00 Multiproxy reconstruction of redox conditions during Permian Kupferschiefer deposition in the Thuringian Basin based on trace elements, molybdenum isotopes and biomarkers
Lorenz Schwark, W. Ruebsam, K. Grice, S. Tulipani, A. Dickson

11.00 – 11.20 Carbon isotope records of thermochemical sulfate reduction corrosion effects on carbonate minerals, Upper Permian and Lower Triassic carbonates, NE Sichuan Basin, China
Kaikai Li, S. C. George, C. Cai

11.20 – 11.40 Wettability alteration measurements of Indiana lime stone due to effect of crude oil composition during immiscible CO_2 flooding
Muhammad Ali, S. Iglauer, N. U. H. Dahraj, A. Arif

11.40 – 12.00 Uranium radiolytic impacts on aromatic hydrocarbon composition of Mulga rock sediments
Chao Shan, Paul F. Greenwood, A. I. Holman, K. Grice

12.00 – 12.20 Unusual association of organic matter and metals in the Cambrian black shales of South China
A. Pagès, Steve Barnes, S. Schmid, M. Le Vaillant, C. Ryan, D. Paterson, H. Fan, H. Wen

Session 10 New Tools I

Chair Alan Scarlett

Keynote

1.30 – 2.00 Sulfur isotope variability of DMS(P) in specific environments and phytoplankton species
Alon Amrani

2.00 – 2.20 $\delta^{34}S$ of Organic Sulfur Compounds and the Sulfur Cycle of Petroleum Systems
Nannan He, K. Grice, P.F, Greenwood

2.20 – 2.40 Developments in new conversion processes of biomass to liquid fuels versus the formation of high-end energy saving chemicals
E. Meller, Y. Sasson, Zeev Aizenstat

2.40 – 3.00 Challenges in Rhenium-Osmium (Re-Os) Isotope Dating of Hydrocarbons in Petroleum Systems
Zhen Li, X.-C. Wang, K. Liu, X.-M. Yang

3.00 – 3.30 Afternoon Tea

Session 11 New Tools II

Chair Steve J. Rowland

3.30 – 3.50 NanoMin; a quantum step in understanding the diagenetic and depositional history of organic carbon rich shale
Martin Kennedy, S. Löhr, H. Rahman, S. Abassi

3.50 – 4.10 Constraining the impact of benthic meiofaunal activity on organic carbon burial in ancient oxygen-depleted sedimentary environments
Stefan C. Löhr, M. J. Kennedy, S. C. George

4.10 – 4.30 Iron cemented sandstone in coastal regions of Western Australia: Mechanisms of Formation and Impacts on Groundwater
Mewish Ali, A. Heitz

4.40 – 5.00 **Closing Remarks and Awards**
Best overall student talks sponsored by Woodside
Best overall student posters sponsored by Woodside

Posters

Sub-marine mass slide as a potential biomarker reservoir: preliminary results from IODP Expedition 355, Arabian Sea
Sophia Aharonovic, Denise K. Kulhanek, Peter D. Clift, and Simon C. George

Using GC x GC-TOF-MS to identify individual naphthenic acids within a degraded crude oil sample
Callum Bonnar, Alan Scarlett, Kliti Grice

Geochemical and sedimentological characterisation of the shallow marine-fluvial Permian succession, Cadda Terrace, northern Perth Basin.
Caroline Butland and Annette D. George

Diamond Like Carbon (DLC) coating in combat for flow assurance
Jamie M. Burgess, Amy E. Kelly, Nancy Utech

Biodegradation of tricyclic terpanes in crude oils from the Bohai Bay Basin
Xiong Cheng, Dujie Hou, Changgui Xu, Feilong Wang

Using neo-pentane to probe the source of gases in accumulations of the Browse and northern Perth basins
Emmanuelle Grosjean, Dianne Edwards, Chris Boreham, Ziqing Hong, Junhong Chen, Jacob Sohn

Sulfur isotopic composition of individual organic sulfur compounds and pyrite during the Permian/Triassic extinction
Hendrik Grotheer, Paul F. Greenwood, Michael Böttcher, Roger E. Summons, Kliti Grice

Microbial diversity and palaeoenvironmental reconstruction of the 4 Ga Roper Seaway, McArthur Basin, northern Australia
Amber J. M. Jarett, G. M. Cox, J. J. Brocks, C. J. Boreham, D. S. Edwards

Petroleum Analysis and Fingerprinting Using Comprehensive Two-dimensional Gas Chromatography (GC×GC)
Robert K. Nelson and Christopher M. Reddy

Understanding natural analogues of mineral carbonation to inform the development of industrial CO_2 storage
Hans C. Oskierski and Bogdan Z. Dlugogorski

Investigations of metal-rich black shales of South China and the Nick prospect
Anais Pagès, Steve Barnes, Ray Coveney, Susanne Schmid, Margaux Le Vaillant, Chris Ryan, David Paterson, Haifeng Fan, Hanjie Wen

Vibrational Spectroscopy Characterisation of Shales from the Canning and Perth Basins *Bobby Pejcic, Claudio Delle Piane, Charles Heath*

Combining GCxGC and CSIA of diamondoids to unravel the sources of (biodegraded) hydrocarbons in the Browse Basin
Gemma Spaak, Kliti Grice, Dianne S. Edwards, Alan G. Scarlett, Emmanuelle Grosjean

An organic geochemical investigation of the late Holocene vegetation and hydrological dynamics of the TROPICAL arid Pilbara (NW Australia)
Alexandra Rouillard, Paul F. Greenwood, Kliti Grice, Grzegorz Skrzypek, Shawan Dogramaci, Chris Turney, Pauline F. Grierson

Unravelling the food-web structure of the subterranean invertebrate communities of arid zone Western Australia.
Mattia Saccò, Alison Blyth, Bill Humphrey, Bill Bateman, Kliti Grice

Analyses of biomarkers using reverse-phase comprehensive two-dimensional gas chromatography time-of-flight mass spectrometry (GC×GC-TOFMS) employing an extremely polar ionic liquid capillary GC columns
Alan G Scarlett, Peter Hopper, Kliti Grice

Hydrocarbon-source correlation of the post-mature Neoproterozoic Dengying giant gas system from the Sichuan Basin, southwestern China: insights from carbon isotopes of individual *n*-alkanes
Chunhua Shi, Jian Cao, Kliti Grice, Alex I. Holman, Xiucheng Tan, Bing Luo, Wei Zeng, Wenxuan Hu

Classification of Australian crude oils by artificial neural network and geochemical hydrocarbon characteristics
Jacob Sohn, Dianne S. Edwards, J. Chev, Chris J. Boreham

Coagulation optimisation using aluminium sulfate for the removal of natural organic matter from a surface water in the South West of Western Australia
Madina N. Tsuntsaeva, Anna Heitz

Oral Presentation Abstracts

SESSION 1 PALEOCLIMATE AND ANCIENT ENVIRONMENT I

Exploiting imperfect records of the carbon isotope excursion at the Palaeocene-Eocene Thermal Maximum to infer changes in soil carbon cycling

Francesca McInerney[1,*], Allison Baczynski[2], Scott Wing[3], Mary Kraus[4], Jonathan Bloch[5], Katherine Freeman[2]

[1] Sprigg Geobiology Centre and Earth Sciences, University of Adelaide University, Adelaide SA 5005 AU
[2] Geosciences, Pennsylvania State University, State College PA 16801 USA
[3] Paleobiology, Smithsonian Institution, Washington DC 20013 USA
[4] Geological Sciences, University of Colorado Boulder, Boulder CO 80309 USA
[5] Natural History, Florida Museum of Natural History and University of Florida, Gainesville FL 32611 USA
(corresponding author: cesca.mcinerney@adelaide.edu.au)*

The Palaeocene-Eocene Thermal Maximum (PETM, 56 Ma) was a period of abrupt and extreme global warming driven by a massive release of organic carbon. This event represents an opportunity to examine carbon cycle feedbacks that can be difficult to quantify in the modern day, but are critical to anticipating future carbon cycle changes. Soil respiration is the largest carbon flux from land to the atmosphere and acts as an important carbon cycle feedback: CO_2-induced warming drives increased soil respiration, releasing more CO_2, driving more warming. However, quantifying the sensitivity of soil respiration to changes in temperature and precipitation in the modern has proven challenging. Here we examine carbon isotope ratios of bulk soil organic matter and leaf wax *n*-alkanes from the Bighorn Basin, Wyoming, USA to examine changes in rates of soil organic matter degradation in relationship to climate change.

During the PETM, the addition of ^{13}C-depleted organic carbon to the ocean, atmosphere and biosphere caused a wholesale shift in carbon isotope ratios. This negative carbon isotope excursion (CIE) is the hallmark of the PETM, but details of the CIE vary between different archives and across the paleolandscape. In the southeastern Bighorn Basin, we are able to locate the PETM with biostratigraphy and chemostratigraphy and trace marker beds across the ~16 km field area to develop a stratigraphic context for multiple sections. Within this framework, we compare the CIE preserved in local sections across the paleolandscape. We find that the shape and magnitude of the CIE varies widely, suggesting that soil organic matter does not record a global excursion. Instead, the soil organic matter signal must be influenced by degradation of organic matter in soils and/or addition of allochthonous organic carbon (Baczynski et al., 2013).

In contrast, leaf wax *n*-alkanes record a larger and more sustained CIE than soil organic matter, suggesting that the original CIE experienced by plants is recorded unaltered (Baczynski et al., 2016). Therefore, the carbon isotope ratios of leaf wax *n*-alkanes provide estimates for the carbon isotope ratios of plant matter in the Bighorn Basin across the PETM interval. We can exploit the discrepancy between the high molecular weight *n*-alkane and soil organic carbon CIEs, to model the effects of soil organic matter degradation and inputs of allochthonous fossil carbon. We model the soil organic matter degradation as a Rayleigh distillation following Wynn et al. (2005). Having estimated the effect of soil organic matter degradation, we determine the proportion of allochthonous carbon required to reconcile the bulk organic matter records with the leaf wax *n*-alkane record. The allochthonous carbon was likely derived from Mesozoic marine rocks from the nearby Bighorn Mountains, as supported by the presence of reworked Mesozoic palynoflora, zircons and shark teeth. We calculate that the PETM warming of ~5˚C was associated with a doubling of microbial degradation rates, and that the proportion of reworked fossil carbon rose to ~28–63% of the total organic carbon preserved during the PETM.

The doubling of soil respiration during the PETM represents an important positive feedback on warming, and the increase in reworked organic matter suggests increased erosion and redeposition that is consistent with the reconstructed increased seasonality of precipitation. These results highlight the importance of periods of past climate change in charcterising carbon-cycle feedbacks that are relevant to anticipating future climate change scenarios.

References

Baczynski, A.A., McInerney, F.A., Wing, S.L., Kraus, M.J.,Bloch, J.I., Boyer, D.M., Secord, R., Morse, P.E., and Fricke, H.C., 2013, Chemostratigraphic implicationsof spatial variation in the Paleocene-Eocene thermal maximum carbon isotope excursion, SE Bighorn Basin, Wyoming: Geochemistry Geophysics Geosystems 14: 4133–4152.

Baczynski, A. A., McInerney, F. A., Wing, S. L., Kraus, M. J., Morse, P. E., Bloch, J. I., Chung, A. H., and K. H. Freeman. 2016. Distortion of carbon isotope excursion in bulk soil organic matter during the Paleocene-Eocene Thermal Maximum. Geological Society of America Bulletin.

Wynn, J.G., Bird, M.I., and Wong, V.N.L., 2005, Rayleigh distillation and the depth profile of C-13/C-12 ratios of soil organic carbon from soils of disparate texture in Iron Range National Park, Far North Queensland, Australia: Geochimica et Cosmochimica Acta 69: 1961–1973.

The Neogene expansion of C_4 dominated ecosystems: an Australian perspective.

Jake W. Andrae[1,*], Francesca A. McInerney[1], Jonathan J. Tyler[1], Tony Hall[1]

[1]Sprigg Geobiology Centre, The University of Adelaide, Adelaide, 5005, Australia
(corresponding author: jake.andrae@adelaide.edu.au)*

The C_4 photosynthetic pathway is proposed to have evolved a number of times in different plant lineages during the Oligocene and early Miocene (~30-20 Ma), but existed only as a minor component of Earth's floral ecosystems until at least the late Miocene (Fox and Koch, 2004; Gowik and Westhoff, 2011). A number of studies have reported that a widespread expansion of C_4 dominated ecosystems initiated at that time. Variations in CO_2 fixation mechanisms in the C_4 pathway as an adaptation to more extreme conditions mean that the carbon isotope signature ($^{13}C/^{12}C$ ratio; designated as $\delta^{13}C$) of modern and ancient plants using the C_4 pathway is offset to that of plants using the C_3 pathway (O'Leary, 1981). Variation in the carbon isotope signature of geological substrates containing plant carbon can thus be recognised as a regional shift in dominant photosynthetic pathway. Though the expansion of C_4 dominated ecosystems has been identified during the late Neogene across much of the Earth, Australia remains thoroughly understudied. At present, the timing of initiation of C_4 expansion and possible drivers remains unconstrained for the Australian continent.

What drove the expansion of C_4 ecosystems is debated. The C_4 pathway incorporates biophysical and biochemical processes that result in it being favoured over the C_3 pathway across an array of extreme environments (conditions of low atmospheric carbon dioxide (CO_2) and high light intensity) and climatic conditions (arid desert and tropical to sub-tropical savanna) (Long, 1999). Large scale changes in regional hydrology may have resulted in shifts towards more seasonally arid environments during the late Miocene (Huang et al., 2007; Passey et al., 2009). This would have led to more favourable conditions for C_4 dominated ecosystems to proliferate at the expense of C_3 dominated ecosystems. Thus, hydrological changes and associated feedbacks are considered theoretically as a major driver of the expansion of C_4 dominated ecosystems (Tipple and Pagani, 2007). Plant derived geological substrates containing hydrogen are useful in trying to understand regional hydrology in a temporal context. The primary control on the hydrogen isotope signature of a plant is the hydrogen isotope signature of the source water that it utilises. This is known to be influenced by climate. Hydrogen isotope signatures are also influenced by changes in the isotopic composition of leaf water, primarily brought about by variation in relative humidity (Sachse et al., 2012).

Leaf wax lipid compounds in ancient sediments have been shown to be an excellent terrestrial plant derived geological substrate for analysis of carbon and hydrogen isotopes (Freeman and Colarusso, 2001; Uno et al., 2016). Compounds are transported from continental landmasses into fluvial, lacustrine and marine geological settings through aeolian distribution of terrestrial particulate matter. This particulate matter includes dust, wind ablated leaf wax particles and decaying plant organic matter (Schefuss et al., 2003). The indicative nature of long chain (*n*-C25-*n*-C35) normal (*n*)-alkane homologs as terrestrial plant biomarkers as well as their robustness and aversion to degradation makes them particularly useful for these types of studies (Eglinton and Hamilton, 1967; Jetter et al., 2006).

An isotope geochemical study is currently underway to address the lack of information around proliferation of C_4 dominated ecosystems on the Australian continent, and to evaluate whether regional hydrological changes drove such an event. The study is composed of compound specific isotope analysis (CSIA) of carbon and hydrogen in long chain *n*-alkane homologs extracted from deep marine (pelagic) sediments. Carbon isotope signatures are used to quantify shifts in regional photosynthetic pathway dominance on either side of the Australian continent in a temporal context. Hydrogen isotope signatures are utilised as a signal primarily for variations in source water isotopic composition, and therefore as a temporal proxy of the hydrological environment and climate (Sachse et al., 2012).

A pilot study of 23 deep ocean drilling pelagic sediment samples evaluated the chain length distribution of the *n*-alkanes extracted. The carbon preference index (CPI) exceeds one in all 23 pilot samples, in most cases by a significant amount. This indicates a terrestrial plant origin for the *n*-alkanes present. The pilot study also determined that sufficient quantities of the *n*-alkane homologs required for carbon and hydrogen CSIA (*n*-C29 and *n*-C31) are present in the deep sea drilling sediments (see Figure 1).

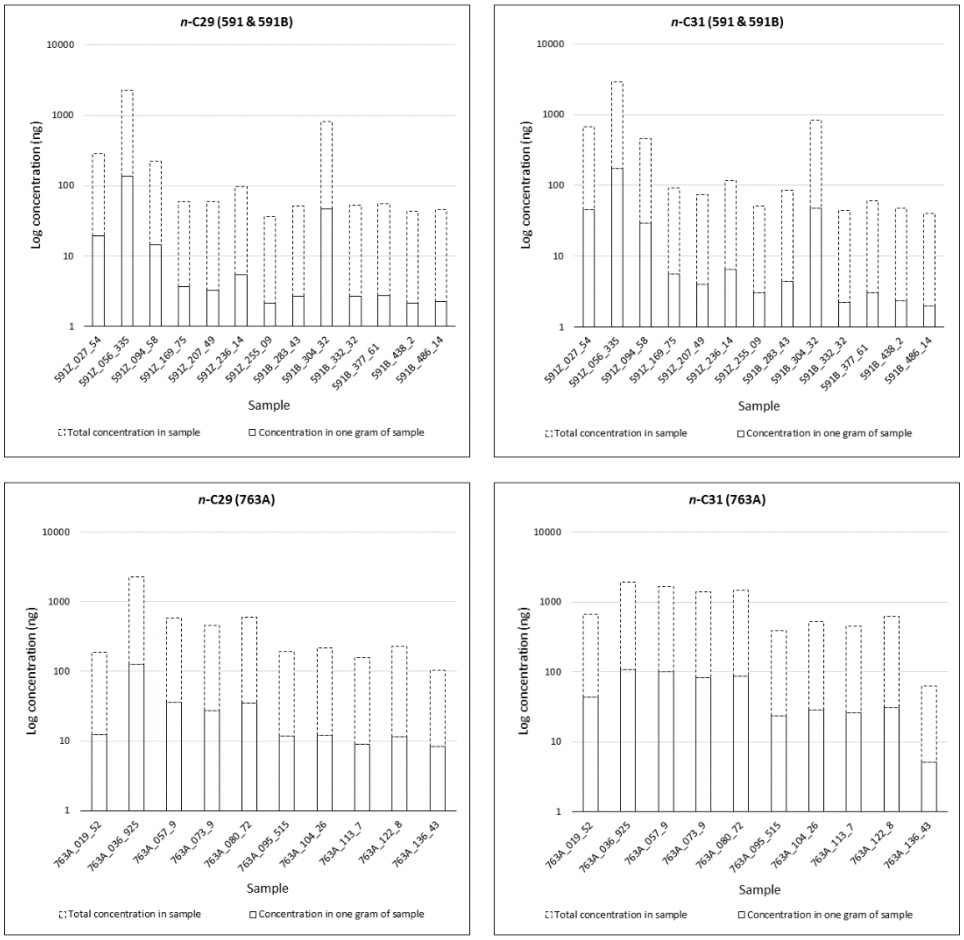

Fig. 1. Concentration of *n*-alkane homologs (*n*-C29; *n*-C31) in pelagic sediment samples from pilot study. Concentration plotted on log scale for clarity.

References

Eglinton, G., Hamilton, R.J., 1967. Leaf epicuticular waxes. Science 156, 1322-1335.

Fox, D.L., Koch, P.L., 2004. Carbon and oxygen isotopic variability in Neogene paleosol carbonates: constraints on the evolution of the C4-grasslands of the Great Plains, USA. Palaeogeography, Palaeoclimatology, Palaeoecology 207, 305-329.

Freeman, K.H., Colarusso, L.A., 2001. Molecular and isotopic records of C4 grassland expansion in the late Miocene. Geochimica et Cosmochimica Acta 65, 1439–1454.

Gowik, U., Westhoff, P., 2011. The path from C3 to C4 photosynthesis. Plant Physiology 155, 56-63.

Huang, Y., Clemens, S.C., Liu, W., Wang, Y., Prell, W.L., 2007. Large-scale hydrological change drove the late Miocene C4 plant expansion in the Himalayan foreland and Arabian Peninsula. Geology 35, 531–534.

Jetter, R., Kunst, L., Samuels, A.L., 2006. Composition of plant cuticular waxes, in: Riederer, M., Muller, C. (Eds.), Biology of the plant cuticle. Blackwell Publishing, Oxford, UK, pp. 145-181.

Long, S.P., 1999. Environmental Responses, in: Sage, R.F., Monson, R.K. (Eds.), C4 Plant Biology. Academic Press, London, pp. 215-249.

O'Leary, M.H., 1981. Carbon isotope fractionation in plants. Phytochemistry 20, 553-567.

Passey, B.H., Ayliffe, L.K., Kaakinen, A., Zhang, Z., Eronen, J.T., Zhu, Y., Zhou, L., Cerling, T.E., Fortelius, M., 2009. Strengthened East Asian summer monsoons during a period of high-latitude warmth? Isotopic evidence from Mio-Pliocene fossil mammals and soil carbonates from northern China. Earth and Planetary Science Letters 277, 443-452.

Sachse, D., Billault, I., Bowen, G.J., Chikaraishi, Y., Dawson, T.E., Feakins, S.J., Freeman, K.H., Magill, C.R., McInerney, F.A., van der Meer, M.T.J., Polissar, P., Robins, R.J., Sachs, J.P., Schmidt, H.-L., Sessions, A.L., White, J.W.C., West, J.B., Kahmen, A., 2012. Molecular paleohydrology: interpreting the Hydrogen-isotopic composition of lipid biomarkers from photosynthesizing organisms. Annual Review of Earth and Planetary Sciences 40, 221-249.

Schefuss, E., Ratmeyer, V., Stuut, J.-B.W., Jansen, J.H.F., Damste, J.S.S., 2003. Carbon isotope analyses of n-alkanes in dust from the lower atmosphere over the central eastern Atlantic. Geochimica et Cosmochimica Acta 67, 1757-1767.

Tipple, B.J., Pagani, M., 2007. The early origins of terrestrial C4 photosynthesis. Annual Review of Earth and Planetary Sciences 35, 435–461.

Uno, K.T., Polissar, P.J., Jackson, K.E., deMenocal, P.B., 2016. Neogene biomarker record of vegetation change in eastern Africa. PNAS 113, 6355-6363.

Cryostane, a new C_{28} sterane from 820 to 740 Ma old pre-Snowball sediments: a biomarker for early sponges and toxic protists?

Jochen J. Brocks[1*], Amber Jarrett[1], Eva Sirantoine[1], Fabien Kenig[2], Pierre Adam[3], Philippe Schaeffer[3], M. Moczydłowska[4], Susannah Porter[5]

[1] The Australian National University, Canberra, ACT 2601, Australia
[2] University of Illinois at Chicago, USA
[3] ECPM, Université de Strasbourg, 67200 Strasbourg, France
[4] Uppsala University, 75236 Uppsala, Sweden
[5] University of California at Santa Barbara, CA 93106, USA
(corresponding author: Jochen.Brocks@anu.edu.au)*

The mid-Neoproterozoic, the period between 800 and 717 million years (Ma) ago in the lead-up to the Sturtian Snowball glaciation, saw an increase in the diversity of eukaryotic microfossils as well as the appearance of several modern eukaryotic groups. To afford an independent and complementary view of this evolutionary event, we studied the distribution of eukaryotic biomarkers from three pre-Sturtian basins across the supercontinent Rodinia, the ~780 Ma Kanpa Formation of Western Australian, the ~800 – 740 Ma Visingsö Group in Sweden, and the 740 Ma Chuar Group, Arizona. The distribution of eukaryotic steranes was remarkably similar in the three pre-Sturtian basins but distinct from all other known younger and older sterane assemblages. Cholestane (C_{27}) was the only conventional structure, while indigenous steranes alkylated in position C-24, such as ergostane (C_{28}), stigmastane (C_{29}) and the C_{30} steranes 24-isopropylcholestane and 24-*n*-propylcholestane were below detection limits. This unique sterane distribution appears to be age-diagnostic for the mid-Neoproterozoic and attests to the distinct evolutionary state of pre-Snowball eukaryotes with a taxonomic disparity still much lower than in the Ediacaran (635 – 541 Ma).

Intriguingly, hydrocarbons from all three basins revealed a new sterane that elutes in MRM m/z 386 → 217 mass chromatograms significantly after ergostane and lacks the isomer duplets characteristic for ergostane (Figure 1). Theoretical considerations of elution and isomer behaviour predicted that the unknown structure is 26-methylcholestane (Brocks et al. 2015), an assignment now confirmed by chemical synthesis of a co-injection standard by the Strasbourg group.

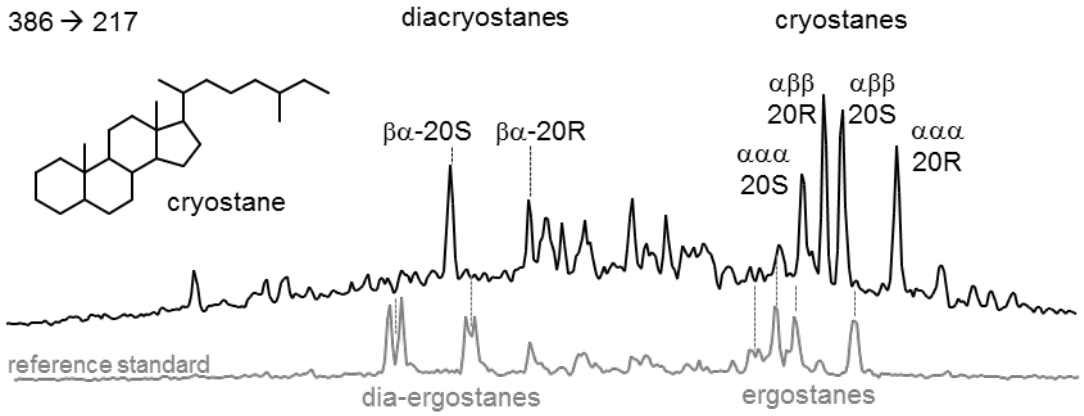

Fig. 1. Confirmed structure of the diagnostic mid-Neoproterozoic sterane biomarker 'cryostane' and MRM chromatograms contrasting the C_{28} sterane distributions of the interior extract of 740 Ma Chuar Group sample 10J093 (black traces, top) with the AGSO-II industrial standard, a mixture of representative Phanerozoic oils (grey traces, bottom).

This new sterane, named cryostane, possesses an alkylation in C-26 position, an unusual modification that, among extant organisms, is solely produced by sponges. Sponges are indeed a plausible source because molecular clocks place the appearance of this earliest animal branch into the mid-Neoproterozoic. However, little is known about the sterol biosynthetic capacity of most heterotrophic protists that may be alternative sources of the unknown compound. Thus, rather than assigning cryostane to sponges or any other clade, it is more instructive to elucidate the function of unusual side-chain alkylated sterols in general. An intriguing hypothesis posits that such sterols may protect organisms against their own membranolytic toxins. Protists release lytic toxins to deter predators and kill eukaryotic prey. This interpretation of cryostane supports fossil evidence of predation in the Visingsö and Chuar groups (Figure 2) and promotes hypotheses about the proliferation of eukaryophagy (eukaryotes that devour eukaryotes) in the lead-up to the Cryogenian Snowball Earth Glaciations (Brocks et al., 2015).

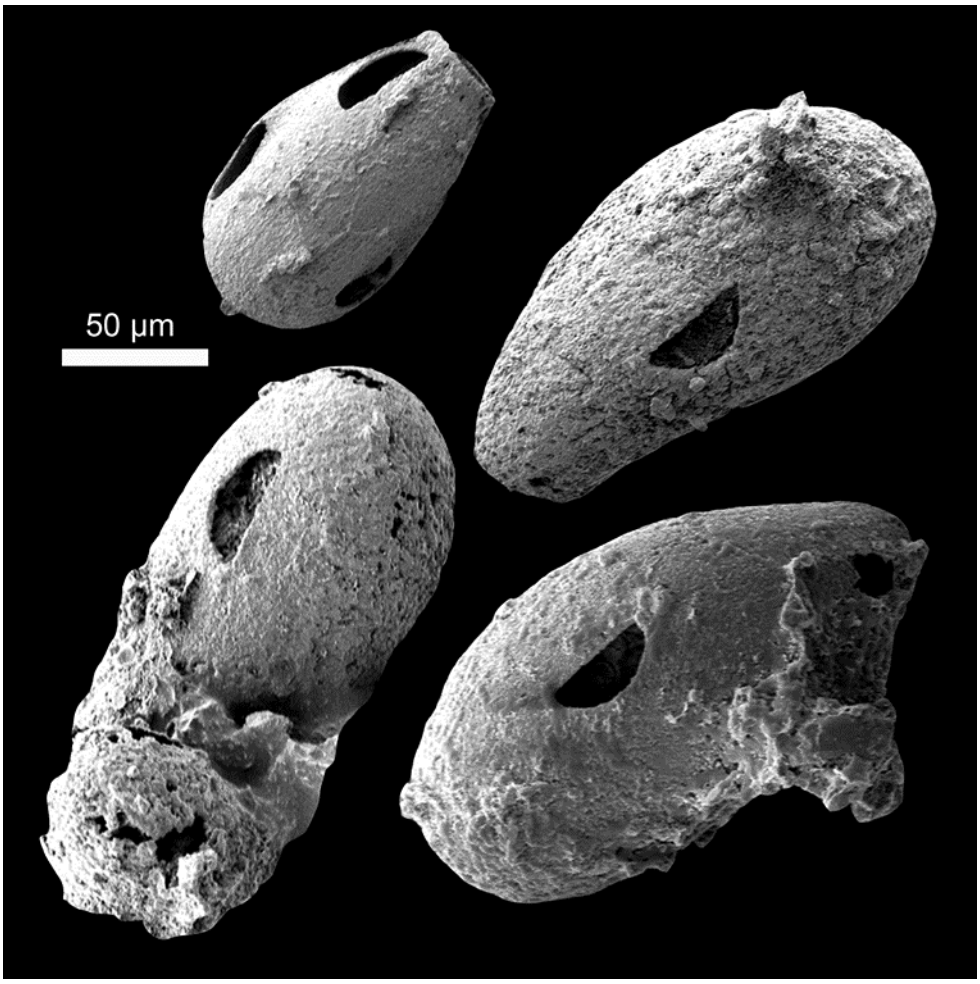

Fig. 2. Vase-shaped microfossils from the Chuar Group showing semi-circular holes in the sides of their tests. The origin of these holes is not known, but they have been hypothesized to be predatory borings (modified from Porter et al., 2003).

References

Brocks, J. J., Jarrett A., Sirantoine E., Kenig F., Moczydłowska M., Porter S., Hope J. (2015) Early sponges and toxic protists: possible sources of cryostane, an age diagnostic biomarker antedating Sturtian Snowball Earth. Geobiology, 14, 129-149.

Porter SM, Meisterfeld R, Knoll AH (2003) Vase-shaped microfossils from the Neoproterozoic Chuar Group, Grand Canyon: a classification guided by modern testate amoebae. Journal of Paleontology, 77, 409-429.

Investigation of palaeoenvironmental conditions through the middle Cambrian in the Georgina Basin, central Australia

Anais Pagès[1,2*], Susanne Schmid[1], Dianne Edwards[3], Stephen Barnes[1], Nannan He[2], Kliti Grice[2]

[1]CSIRO Mineral Resources, 26 Dick Perry Avenue, Kensington, WA6151, Australia
[2]WA Organic and Isotope Geochemistry Centre, Department of Chemistry, The Institute for Geoscience Research, Curtin University, GPO Box U1987, Perth, WA 6845, Australia
[3]Geoscience Australia (GA), Resource Division, Energy Systems Branch, GPO Box 378, Canberra, ACT 2601, Australia
(corresponding author: **Anais.pages@csiro.au**)*

The Cambrian period marks an important point in Earth's history. The Cambrian explosion is the most significant evolutionary event in the history of life on the planet, with a rapid transition from primitive microbial forms to a predominance of protists and taxonomically diverse multicellular organisms (Gould, 1989). The Cambrian explosion is commonly described as a complex succession of cycles of extinction and radiations (Knoll and Walter, 1992). While the first stages of the Cambrian radiation of metazoan life and spreading of skeletal reef fauna occurred in the early Cambrian (Terreneuvian and Series 2), metazoan reef systems had collapsed worldwide by the middle Cambrian (Boucot, 1990). This period was followed by the longest post-extinction metazoan reef gap of the Phanerozoic, longer even than that the Permian–Triassic extinction (Boucot, 1990). Hence, the early–middle Cambrian represents a key point in the history of life.

This study integrates biomarkers and their compound-specific stable carbon isotopes to investigate the palaeoenvironmental depositional conditions in middle Cambrian (Series 3) sedimentary rocks from the Undilla Sub-basin in the eastern Georgina Basin, central Australia (Pagès et al., 2015). The occurrence of photic zone euxinia (PZE) was revealed by the identification of green sulfur bacteria *Chlorobiaceae*-derived biomarkers, including a series of 2,3,6-aryl isoprenoids and the intact biomarker isorenieratane. Co-variations of Molybdenum and Uranium enrichment factors, successfully used in previous studies to characterise redox conditions (Algeo and Tribovillard, 2009; Tribovillard et al., 2012), also supported the occurrence of euxinic conditions. Pulses of enhanced PZE conditions were followed by possible blooms of phytoplankton, as demonstrated by the increase in algal-derived biomarker concentrations and compound-specific isotopes. These observations confirm that palaeoenvironmental conditions could have been similar to those reported for the Permian/Triassic (Grice et al., 2005) and Triassic/Jurassic (Jaraula et al., 2013) mass extinction events.

A previous study on $\delta^{34}S$ isotopes of the Monastery Creek Phosphorite member, deposited at ca. 510Ma elsewhere in the Georgina Basin (Templetonian, Series 3; Hough et al., 2006), highlighted an abrupt increase in $\delta^{34}S$, as a result of green-house warming associated with the volcanic eruption of the Kalkarindji Province in Northern Australia that could have triggered the collapse of early metazoan reefs. The present findings are consistent with previous studies and suggest that although a rise in atmospheric oxygen during the Cambrian has been previously associated with the rapid evolution of metazoans, the ecological challenges related to widespread anoxia must have had a major influence on the evolution of life in Cambrian oceans.

References

Algeo, T.J., Tribovillard, N., 2009. Environmental analysis of paleoceanographic systems based on molybdenum–uranium covariation. Chem. Geol. 268, 211–225.
Boucot, A., 1990. Phanerozoic extinctions: how similar are they to each other? In: Kauffman, E.G., Walliser, O.H. (Eds.), Extinction Events in Earth History. Springer, pp.5–30.
Gould, S., 1989. Wonderful Life: The Burgess Shale and the Nature of History. Cam-bridge Univ. Press, Cambridge, UK. 347 pp.
Grice, K., Cao, C., Love, G.D., Bottcher, M.E., Twitchett, R., Grosjean, E., Summons, R.E., Turgeon, S.E., Dunning, W., Jin, Y., 2005. Photic zone euxinia during the Permian–Triassic superanoxic event. Science 307, 706–709.
Hough, M.L., Shields, G.A., Evins, L.Z., Strauss, H., Henderson, R.A., Mackenzie, S., 2006. A major sulphur isotope event at c. 510Ma: a possible anoxia-extinction-volcanism connection during the Early–Middle Cambrian transition? Terra Nova 18, 257–263.
Jaraula, C., Grice, K., Twitchett, R., Boettcher, M., Lemetayer, P., Dastidar, A.G., Opazzo, L.P., 2013. Elevated pCO2leading to end Triassic extinction, photic zone euxinia and rising sea levels. Geology 41, 955–958.
Knoll, A., Walter, M., 1992. Latest Proterozoic stratigraphy and Earth history. Na-ture356, 673–678.
Tribovillard, N., Algeo, T.J., Baudin, F., Riboulleau, A., 2012. Analysis of marine environmental conditions based on molybdenum–uranium covariation—applications to Mesozoic paleoceanography. Chem. Geol. 324-325, 46–58.

Decision making in Petroleum Exploration and Production: How does organic geochemistry make a difference?

Andrew Murray[1]

[1]Director, Murray Partners PPSA Pty. Ltd.

Organic geochemistry has a well established role in petroleum exploration and applications continue to grow, stimulated and underpinned by new developments such as clumped isotope analysis, GCxGC and and ultra-high resolution mass spectrometric methods. The latter has given rise to the (potentially) new discipline of “petreolomics”.

The value that organic geochemistry studies provide is rarely (nowadays) questioned but it is often unclear how this value is added or which kinds of studies add most. Many reports from service providers and academic partners languish in company files or buried in well completion reports and never produce value equivalent to their cost. Everything a company does or supports should be subject to a “value of information (VOI)” test, especially so in times of low oil price. Information only has value to the extent that it changes decisions, usually in the short or near term. Bayesian reasoning sometimes shows information appearing initially to be of high value to actually be worth little and vice-versa.

Traditionally, the questions that organic geochemistry addresses are: 1. Is there a source rock present in this basin ? 2. Where is it (geographically and stratigraphically) ? 3. Will it result in mainly oil or gas being discovered ? 4. Is it thermally mature and if so where ? These are the primary questions in the exploration phase. Value can also be added in the appraisal and development stages by addressing questions such as how connected is my reservoir, should I expect bulk properties to differ from one part of my field to another (including whether there is an oil rim present in a gas field) and will any contaminants affect the value or produceability of my products ?

The presence or absence of a source rock is often cited as the critical factor driving exploration in the high-risk “frontier” basins of the world. Exploration success rates are as low as 1: 13 in frontier basins. Much effort is expended in analysing cuttings and outcrop sediments in an attempt to prove or disprove source presence: It can be shown that this is actually a low value activity and often not worthwhile. In contrast, the presence of any migrated hydrocarbon fluid is highly polarising for decision making, especially when sufficient sample exists to allow “reverse engineering” of source rock depositional environment. Even here, though, there are dangers in misinterpreting or over-interpreting the data and hence making incorrect inferences about the petroleum system.

“Maturity” is a term so commonly used in relation to petroleum source rocks that its meaning is rarely considered. In fact, maturity is a nebulous concept that cannot be defined out of a particular context. This has become abundantly clear with the frequent drilling of source rocks consequent to the rise of “unconventional” hydrocarbon production. All reservoired hydrocarbons are mixtures and significant variability in properties can and does occur within single fields. Some fields, considered as single entities from a production or legal point of view, even host hydrocarbons created by completely distinct petroleum systems. This needs to be kept in mind when seeking to define petroleum systems at the basin or regional level based on single samples from discovery wells.

This presentation will briefly review how decisions are made in E &P companies where organic geochemistry is involved. Examples will show the disconnect which can occur between the kinds of information traditionally generated and that which can most affect decisions.

Geochemical characteristics of some biodegraded crude oils from the Liaodong Bay, Bohai Bay Basin: Insights into the source and the history of accumulation

Xiong Cheng[1*] Dujie Hou[1], Changgui Xu[2], Feilong Wang[2]

[1] School of Energy Resources, China University of Geosciences, Beijing 100083, China
[2] Exploration and Development Research Institute, Tianjin Branch of China National Offshore Oil Corporation, Tianjin 300452, China
(corresponding author: xcheng2015@cugb.edu.cn)*

Petroleum formation and accumulation is a dynamic process, particularly in a subsiding basin (e.g. Volkman et al., 1983; Alexander et al., 1983). Three sets of good source rocks, i.e., the Ed3, Es1 and Es3 members deposited in the Liaodong Bay area, Bohai Bay Basin in China. This combines with the heavy to severe biodegradation process occurred in reservoirs make the oil-source correlations and the accumulation history of petroleum ambiguous and controversial.

To identify the sources of the crude oils and their accumulation history, a suite of biodegraded crude oils from the Liaodong Bay area were analyzed by using gas chromatography-mass spectrometry. The result shows that the samples were biodegraded to varying degrees, which is evident by the intact to almost completely removed *n*-alkanes, isoprenoids, hopanes and regular steranes and varying concentrations of 25-norhopanes (Fig. 1). The preferential removal of the 4-methyl steranes and hopanes over regular steranes and gammacerane, respectively, leads to variation of the commonly used oil-source correlation parameters (the ratios of 4-methyl steranes to C_{29} regular steranes decline and gammacerane to C_{30} hopane increase), and therefore exaggerate the contribution of the Es1 source rock interval. The ratio of gammacerane to C_{30} hopane can be calibrated as gammacerane /(C_{30} hopane + C_{29} 25-norhopane) based on the mother-daughter relationship between C_{30} hopane and C_{29} 25-norhopane (e.g., Reed, 1977; Rullkötter and Wendisch, 1982; Volkman et al., 1983; Peters et al., 1996; Bennett et al., 2006; Wang et al., 2013). The decrease of the ratio of 4-methyl steranes to C_{29} regular steranes is minor, and can be negligible when steranes and 4-methyl steranes are slightly biodegraded; whereas the decrease must be taken into account when severely degraded. The sources of the crude oils were identified by the distribution pattern of tricylic terpane and C_{24} tetracyclic terpane and the above mentioned parameters with consideration of the effect of biodegradation. Almost all of the crude oil samples from the JX1-1 and LD6-2 oil fields and half of the samples from the SZ36-1 oil field are sourced by the Es3 source rock and the rest are mixtures with contribution of both the Es1 and Es3 source rocks. However, the contribution of the Es1 may be limited.

The co-occurrence of *n*-alkanes, acyclic isoprenoids and abundant 25-norhopanes in the samples indicating that there have been at least two accumulation episodes occurred in the reservoirs (Fig. 1). The initial accumulations of petroleum were biodegraded to level 5 to 7 on Peters and Moldowan (1993) biodegradation scale (abbreviated as PM level 5–7), as evident by nonbiodegradation to considerable alteration of the hopanes and regular steranes. Subsequently these oils were augmented by a minor input of *n*-alkane-rich petroleum at a stage when conditions in the reservoirs were less conducive to biodegradation. In this stage, biodegradation proceeded to PM level 0–4. Although the accumulation history of the most degraded crude oils (e.g., No. 9 in Fig. 1) is unclear, the latest accumulations of these oils were subjected to severe biodegradation (PM level 7-8).

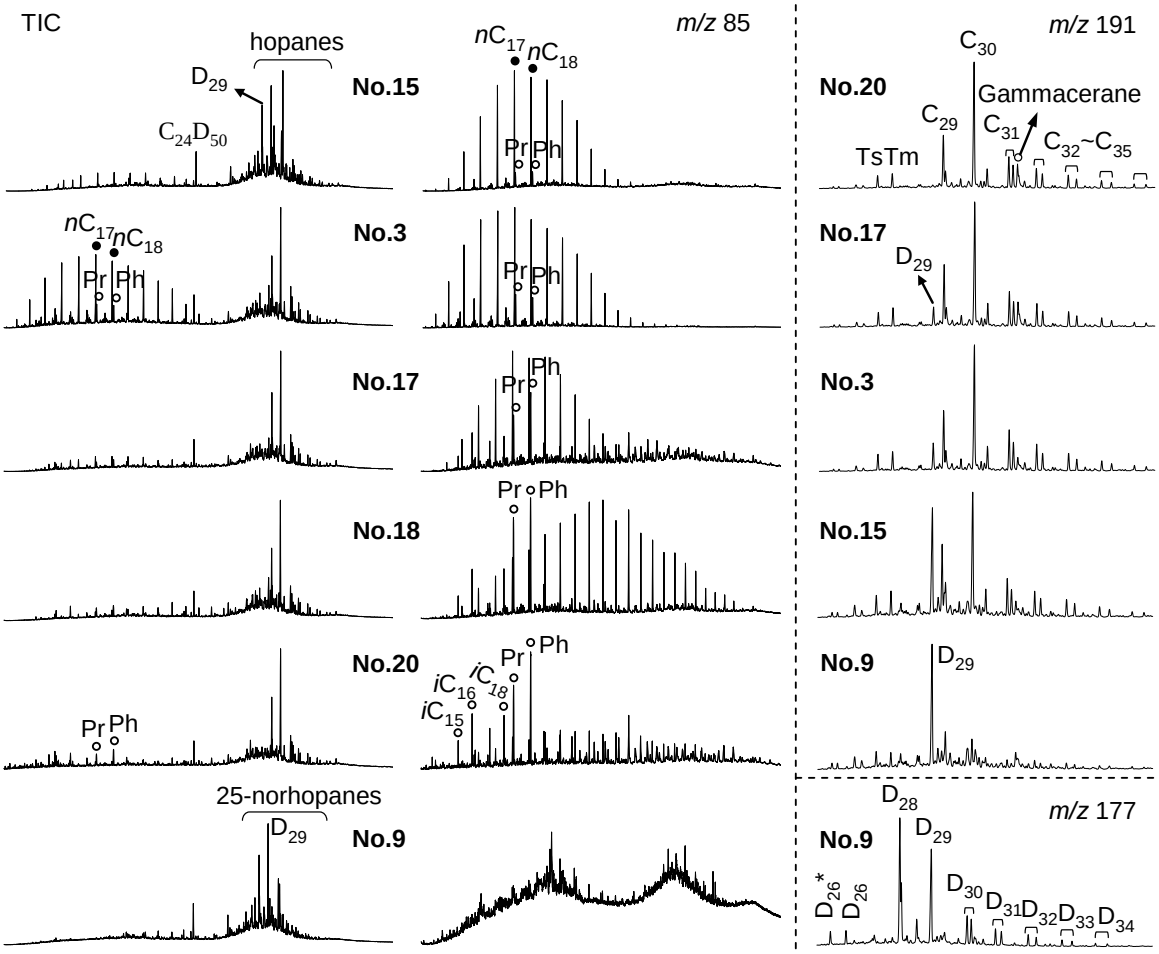

Fig. 1. Total iron chromatograms (TICs, left) and *m/z* 85 (middle), *m/z* 191 and *m/z* 177 (right) mass chromatograms of selected biodegraded crude oil samples from the Liaodong Bay area showing varying biodegradation extents and multiple accumulation. C_{29}–C_{35}: C_{29}–C_{35} hopanes; D_{26}–D_{34}: C_{26}–C_{34} 25-norhopane; D_{26}*: C_{26} 18α-22,25,29,30-tetranorneohopane.

References

Alexander, R., Kagi, I. R., Woodhouse, W., Volkman, J.K., 1983. The geochemistry of some biodegraded Australian oils. APEAJ 23, 53–63.

Bennett, B., Fustic, M., Farrimond, P., Huang, H.P., Larter, S.R., 2006. 25-Norhopanes: formation during biodegradation of petroleum in the subsurface. Organic Geochemistry 37, 787–797.

Peters, K.E., Moldowan, J.M., 1993. The Biomarker Guide. Interpreting Molecular Fossils in Petroleum and Ancient Sediments. Prentice Hall, Englewood Cliffs.

Peters, K.E., Moldowan, J.M., McCaffrey, M.A., Fago, F.J., 1996. Selective biodegradation of extended hopanes to 25-norhopanes in petroleum reservoirs. Insights from molecular mechanics. Organic Geochemistry 24, 765–783.

Reed, W.E., 1977. Molecular compositions of weathered petroleum and comparison with its possible source. Geochimica et Cosmochimica Acta 41, 237–247.

Rullkötter, J., Wendisch, D., 1982. Microbial alteration of 17α(H)-hopane in Madagascar asphalts: removal of C-10 methyl group and ring opening. Geochimica et Cosmochimica Acta 46, 1543–1553.

Volkman, J.K., Alexander, R., Kagi, R.I., Noble, R.A., Woodhouse, G.W., 1983. A geochemical reconstruction of oil generation in the Barrow Sub-basin of Western Australia. Geochimica et Cosmochimica Acta 47, 2091–2105.

Wang, G., Wang, T.-G., Simoneit, B.R.T., Zhang, L., 2013. Investigation of hydrocarbon biodegradation from a downhole profile in Bohai Bay Basin: Implications for the origin of 25-norhopanes. Organic Geochemistry 55, 72–84.

A revised oil family classification scheme and geochemical weathering proxies for South Australian coastal bitumen strandings

A.J. Corrick[1], P.A. Hall[1], D.M. McKirdy[1], S. Gong[3], C. Trefry[2], C. Dyt[2], Z. Angelini[4], A.S. Ross[2], R. Kempton[2], S. Armand[3] and C. White[2]

1) Department of Earth Sciences, School of Physical Sciences, University of Adelaide, SA 5005, Australia (E-mail: alexander.corrick@adelaide.edu.au)
2) Energy, CSIRO, Kensington, WA, 6151 Australia
3) Energy, CSIRO, North Ryde, NSW, 2113 Australia
4) Civil and Environmental Engineering, University of New Hampshire, Durham, NH, United States

Reports of coastal bitumen stranding along the southern coastline of Australia date back to the mid-1800s [1]. These strandings were previously classified into several different oil families on the basis of differences in their geochemistry [1]. The two predominant types are referred to as waxy bitumen and asphaltite. The waxy bitumens may be further classified into sub-families based primarily on their content of botryococcane, a C_{34} acyclic isoprenoid biomarker derived from the freshwater alga *Botryococcus braunii*. These waxy bitumens are attributed to hydrocarbon seeps within the Indonesian Archipelago, and are transported to the southern coast of Australia via the Leeuwin Current [1]. Conversely, the asphaltites are hypothesised to be of a local origin, emanating from seafloor seeps or tar mats exposed by submarine canyons incised into the continental slope of the Bight Basin and/or the offshore Otway Basin [2]. However, recent surveys have yet to identify hydrocarbon seeps in the region [3] and thus their point of origin remains undetermined. Previous geochemical assessment suggests that the asphaltites are derived from a Cretaceous marine shale deposited during an ocean anoxic event [4].

While these bitumens remain in the ocean and/or are stranded on the beach, they progressively degrade due to cumulative weathering processes, with the exterior more prone to alteration. This is a key difficulty when attempting to effectively model the oceanic transportation of these various types of coastal bitumen back to potential seepage sites. Individual specimens may be returned to the ocean during storm activity and undergo secondary migration from beach to beach, obscuring their original stranding location. Additionally, due to seasonal variation in the ocean currents along Australia's southern margin [5-6], the timing of stranding is also key to accurately modelling their migration pathways. In order to reduce these uncertainties, it is necessary to select only the freshest samples for oceanographic modelling, as these are the least likely to have undergone significant secondary migration.

We present the results of interior *versus* exterior analyses of more than 200 coastal bitumen samples collected over two annual surveys of 31 beaches along the South Australian coastline. The data reveal a large range of weathering-related alteration of their saturated hydrocarbons, with little comparable loss of exterior relative to interior alkanes in some specimens to near total loss in others (Fig. 1). Using this information, we provisionally revise the established oil family classifications, propose family-specific geochemical weathering proxies and discuss their ability to constrain the extent of weathering to inform future oceanographic provenance models.

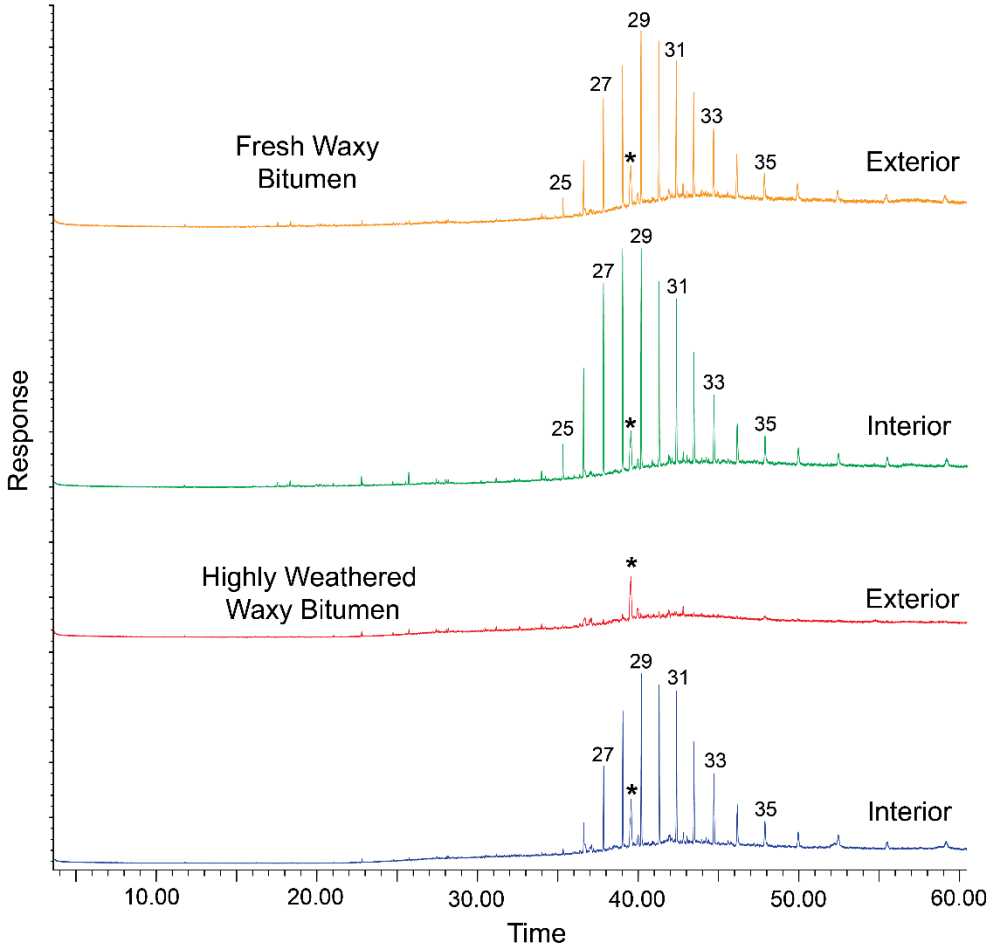

Fig 1: Comparison of whole-oil GC-MS total ion chromatograms from the exterior and interior of a fresh waxy bitumen (sample W13/007552A) and a highly weathered waxy bitumen (sample W13/007559), both collected from the same stranding location in the Canunda National Park. Numbers indicate chain length of n-alkanes. * = botryococcane, a freshwater algal biomarker which is demonstrably recalcitrant to weathering in comparison to the adjacent n-alkanes.

References

[1] Padley, D., 1995 Petroleum geochemistry of the Otway Basin and the significance of coastal bitumen strandings on adjacent southern Australian beaches. PhD thesis, University of Adelaide.

[2] Hall, P. A., McKirdy, D. M., Grice, K. & Edwards, D. S., 2014. Australasian asphaltite strandings: Their origin reviewed in light of the effects of weathering and biodegradation on their biomarker and isotopic profiles. *Mar. Pet. Geol.* **57,** 572–593.

[3] Totterdell, J. M. & Mitchell, C. (editors), 2009. Bight Basin Geological Sampling and Seepage Survey: R/V Southern Surveyor Survey SS01/2007. *Geoscience Australia Record 2009/024.*

[4] Edwards, D., McKirdy, D. M. & Summons, R. E., 1998. Enigmatic asphaltites from the southern Australian margin: molecular and carbon isotopic composition. *PESA J.* **26,** 106–129.

[5] Middleton, J.F. & Platov, G., 2003. The mean summertime circulation along Australia's southern shelves: a numerical study. *J. Phys. Oceanogr.* **33,** 2270–2287.

[6] Cirano, M. & Middleton, J. F., 2004. Aspects of the mean wintertime circulation along Australia's southern shelves: numerical studies. *J. Phys. Oceanogr.* **34,** 668–684.

The North West Shelf of Australia: Molecular and isotopic approach to discriminate organic facies; and their potential applications for source rock charaterisation

Jaime Cesar[1], Kliti Grice[1]

[1]WA Organic and Isotope Geochemistry Centre, The Institute for Geoscience Research, Curtin University, Department of Chemistry, Perth, WA, Australia (E-mail: jaime.cesarcolmenares@curtin.edu.au).

The North West Shelf of Australia is a world class petroleum system and yet uncertainties still exist around fluid provenance. The fluids in the basins are largely fluids (condensates) that derive from mixed marine/terrigenous sources; additionally, low concentration of key organic compounds and alteration processes (*e.g.* biodegradation, evaporative fractionation, and water washing) are challenging and limit the discrimination power of traditional biomarker and isotopic methods [1]. A relevant example occurs in the Northern Carnarvon Basin, specifically in the Dampier sub-Basin, where the source of fluid in the Rankin Platform reservoirs remains uncertain. A fundamental investigation has been undertaken to improve our understanding of different petroleum families, both within the known reserves and those yet to be identified, enabling explorationists to evaluate new plays in this region. To assess this, a novel combination of molecular and isotopic parameters has been used to help de-convolute the overlaps between the organic facies (Triassic *vs* Jurassic). For source rock screening, a new approach has been developed based on the distribution of certain higher plant biomarkers and combustion-derived polycyclic aromatic hydrocarbons (PAHs) as well as their stable carbon isotopic composition which clearly distinguished marginal marine facies from back/mid deltaic facies. Potential applications of benzo[*b*]naphtho[*d*]furan isomers for source rock characterisation have also been reported for the first time. The formation of [1,2]BNF seems to be influenced by clay catalysis and the ratio [2,1]/[1,2]BNF can be used to describe lithofacies.

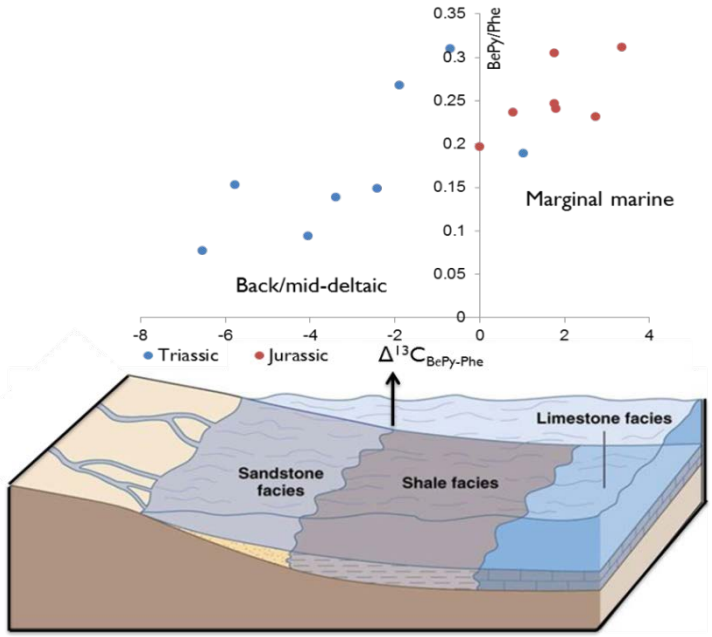

Fig. 1. Facies discrimination by implementing the ratio Benzo[*e*]pyrene/Phenanthrene *vs* the difference in $\delta^{13}C$ values for the same molecules, in Triassic (Mungaroo and Brigadier Fms.) and Jurassic (Legendre Fm.) source rock samples.

References

[1] Longley, I., Buessenschuett, C., Clydsdale, L., Cubitt, C., Davis, R., Johnson, M., Marshall, N., Murray, A., Somerville, R., Spry, T., Thompson, N., 2002. The North West Shelf of Australia – a Woodside Perspective, in: Keep, M., Moss, S. (Eds.), The Sedimentary Basins of Western Australia 3: Proceedings of the Petroleum Exploration Society of Australia Symposium. Petroleum Exploration Society of Australia, Perth, Australia.

Investigations into the cause of the initial organic carbon isotope excursion at St. Audrie's Bay during the end-Triassic mass extinction using sterane and hopanes biomarkers

Calum P. Fox[1*], Kliti Grice[1], Jessica H. Whiteside[2], Paul Olsen[3], Julio Sepúlveda[4], Roger Summons[5]

[1] WA-OIG, Department of Chemistry, The Institute for Geoscience Research, Curtin University, GPO Box U1987, Perth, 6845, Australia
[2]Ocean & Earth Science, National Oceanography Centre, University of Southampton, Southampton, SO17 1BJ, UK
[3]Earth & Environmental Sciences, Lamont-Doherty Earth Observatory of Columbia University, 61 Route 9W, Palisades, NY
[4]Dept. of Geological Sciences, University of Colorado Boulder, 450 UCB, Boulder, CO 80309-0450
[5]Earth, Atmospheric and Planetary Sciences, MIT, Cambridge, MA 02142,
(corresponding author:* calum.fox@postgrad.curtin.edu.au*)*

The end-Triassic mass extinction occurred ~201 million years ago and is one of six recognised mass extinction events in Earth's history. St. Audrie's Bay (SAB) is a heavily studied section during this period where the iconic initial and main negative organic carbon isotope ($\delta^{13}C_{org}$) excursion is identified. Similar isotopic patterns can be observed in widespread geographic locations with differing timings and magnitude. These initial excursions are typically attributed to the dissociation of methane clathrates with very light isotopic signatures. Recent investigations at SAB show a marine to freshwater transition with periodic exposure during the initial excursion as evidenced through biotic and sedimentological evidence. Three other investigated UK sections (Whitehead, Lavernock, and St. Mary's Well Bay) show an initial $\delta^{13}C_{org}$ isotopic pattern comparable with SAB in both timing and magnitude with similar environmental change indicated the SAB $\delta^{13}C_{org}$ and correlated oligohaline record is characteristic of a very large area. Investigated hopane and sterane biomarker data indicative of changing redox and ecological conditions also suggests that the initial excursion was the result of local biotic community changes resulting from a dramatic relative sea level drop and influx of freshwater. At the time of the initial carbon isotope relative abundances of red algae, chrysophytes, and prasinophytes decrease whilst those of green algae increase. During this time C_{28} 28, 30 bis*nor*hopanes decrease and the Homohopane Index increases indicating a change in microbial communities as a result of a drop in water-depth and increases in microbial activity, respectively. Greater abundances of hopanes (largely produced by bacteria) compared to steranes (predominantly attributed to eukaryotes) in what has already been determined a sub-oxic to aerobic environment indicate greater bacterial activity in a lacustrine environment. Simple interpretation of this data set indicates the initial excursion is the result of bacterial community changes with increased bacterial activity, due to the efficiency of bacteria fractionation compared to eukaryotes. These recent results demonstrate the need for further multi-proxy biomarker investigations into other end-Triassic mass extinction, particularly those that demonstrate isotopic patterns very similar to SAB.

The End Cretaceous Mass Extinction Event – Recovery and Evolution of Life

Bettina Schaefer*, Marco J. L. Coolen, Kliti Grice

Western Australian-Organic and Isotope Geochemistry, Department of Chemistry, The Institute for Geoscience Research,
Curtin University, Perth, WA 6000, Australia
(corresponding author: bettina.schaefer@postgrad.curtin.edu.au)*

The End-Cretaceous Mass Extinction Event was one of the five largest mass extinction events in the Phanerozoic (Wiese and Reitner, 2011) and the only one proven to be associated with a meteorite impact (e.g. Hildebrand, 1991; Schulte et al., 2010). The impact crater at Chicxulub in Mexico is the largest terrestrial crater with a peak ring and a global ejecta area. For the first time the peak ring of the crater has been drilled by the Integrated Ocean Drilling Program (IODP) 364 drilling expedition "*Chicxulub: Drilling the K-T Impact Crater*" in April – May 2016 and the newly obtained samples will be used to study the impact crater with a novel approach. While the impact event has been fairly well studied for fossilising taxa, the post impact recovery and evolution of the majority of "soft-bodied" plankton and invertebrates is largely unknown. In this study molecular fossils will be analysed using organic and isotopic geochemistry parallel to a molecular biological approach. It has been shown that ancient DNA can be preserved for hundreds of thousand years and be used for ecosystem reconstruction (Coolen and Overmann, 2007) . For this project, it will be explored to what extent ancient plankton and vegetation DNA can be recovered from Cenozoic marine sediments overlying the Chicxulub impact crater and if this DNA is suitable to study the post-impact recovery and if possibly living bacteria in the Cenozoic record can provide information about post-impact environmental and depositional conditions. Further, the study of microbial metagenomics in the impact breccia and the peak ring below the marine Cenozoic sediments will reveal the diversity and function of microbial communities that at some point in history must have been able to recolonise the fractured impact rocks after the crater had sufficiently cooled down to sustain microbial life. The coupling of the obtained paleogenomic and deep subsurface microbiome datasets with organic, isotopic, and general geochemistry data and in the context of geological data through collaboration with the other IODP 364 science party members will contribute to a deeper understanding of environmental factors that control life in the deep biosphere, its ability to recover and evolve after major extinction events, and the possibility of life to form beyond Earth (Grice et al., 2000; Orsi et al., 2016; Whiteside and Grice, 2016).

References

Coolen, M.J., Overmann, J., 2007. 217 000-year-old DNA sequences of green sulfur bacteria in Mediterranean sapropels and their implications for the reconstruction of the paleoenvironment. Environ Microbiol 9, 238-249.

Grice, K., Alexander, R., Kagi, R.I., 2000. Diamondoid hydrocarbon ratios as indicators of biodegradation in Australian crude oils. Organic Geochemistry 31, 67-73.

Hildebrand, A.R., 1991. Chicxulub crater: a possible Cretaceous/Tertiary boundary impact crater on the Yucatan Peninsula, Mexico. Geology 19, 867-871.

Orsi, W.D., Coolen, L.M.J., He, L., Wuchter, C., More, K.D., Irigoien, X., Chust, G., Johnson, C., Hemingway, J.D., Lee, M., Galy, V., Giosan, L., 2016. Climate oscillations reflected in the microbiome of Arabian Sea sediments. Nat Commun, in review.

Schulte, P., Alegret, L., Arenillas, I., Arz, J., xe, A, Barton, P.J., Bown, P.R., Bralower, T.J., Christeson, G.L., Claeys, P., Cockell, C.S., Collins, G.S., Deutsch, A., Goldin, T.J., Goto, K., Grajales-Nishimura, J., xe, M, Grieve, R., xc, F., Gulick, S.P.S., Johnson, K.R., Kiessling, W., Koeberl, C., Kring, D.A., MacLeod, K.G., Matsui, T., Melosh, J., Montanari, A., Morgan, J.V., Neal, C.R., Nichols, D.J., Norris, R.D., Pierazzo, E., Ravizza, G., Rebolledo-Vieyra, M., Reimold, W.U., Robin, E., Salge, T., Speijer, R.P., Sweet, A.R., Urrutia-Fucugauchi, J., Vajda, V., Whalen, M.T., Willumsen, P.S., 2010. The Chicxulub Asteroid Impact and Mass Extinction at the Cretaceous-Paleogene Boundary. Science 327, 1214-1218.

Whiteside, J.H., Grice, K., 2016. Biomarker Records Associated with Mass Extinction Events. Annual Review of Earth and Planetary Sciences 44, 581-612.

Wiese, F., Reitner, J., 2011. Critical Intervals in Earth History, in: Reitner, J., Thiel, V. (Eds.), Encyclopedia of Geobiology. Springer Netherlands, Dordrecht, pp. 293-306.

Climate oscillations reflected in the Arabian Sea subseafloor microbiome

Marco J. L. Coolen[1*], William D. Orsi[2,3], Lijun He[4], Cornelia Wuchter[3], Kuldeep D. More[1], Xabier Irigoien[5], Guillem Chust[6], Carl Johnson[3], Jordon D. Hemingway[3,7], Mitchell Lee[3], Valier Galy[3] and Liviu Giosan[8]

1. Western Australia Organic and Isotope Geochemistry Centre, Department of Chemistry, Curtin University, Bentley, WA 6102, Australia.
2. Department of Earth and Environmental Sciences, Paleontology & Geobiology, Ludwig-Maximilians-Universität Munich, Germany.
3. Department of Marine Chemistry and Geochemistry, Woods Hole Oceanographic Institution, Woods Hole, MA 02543, USA.
4. State Key Laboratory of Estuarine and Coastal Research, East China Normal University, Shanghai, 200062, China.
5. King Abdullah University of Science and Technology, Red Sea Research Center, Thuwal 23955-6900. Saudi Arabia.
6.AZTI-Tecnalia, Marine Research Division, Txatxarramendi ugartea z/g, 48395 Sukarrieta (Bizkaia), Spain.
7. Massachusetts Institute of Technology-Woods Hole Oceanographic Institution Joint Program in Oceanography/Applied Ocean Science and Engineering.
8. Department of Geology and Geophysics, Woods Hole Oceanographic Institution, Woods Hole, MA 02543, USA.
(corresponding author: marco.coolen@curtin.edu.au)*

Marine sediment contains a vast microbial biosphere that influences global biogeochemical cycles over geological timescales. However, the environmental factors controlling the stratigraphy of subseafloor microbial communities are poorly understood. Using the highest resolved sedimentary metagenomic profile to date together with paleoceanographic proxies, we show that millennial-scale paleoenvironmental conditions correlate with the metabolism and diversity of bacteria and archaea over the last glacial-interglacial cycle in the Arabian Sea[1]. The metabolic potential for denitrification correlates with climate-driven oxygen minimum zone (OMZ) strength and concomitant nitrogen stable isotope fractionation, whereas catabolic potential reflects changing marine organic matter sources across the Last Glacial Maximum. These results indicate that the subsisting microbial communities had been stratified to a large extent by paleoceanographic conditions at the time of deposition. As cells are buried in the subsurface, deeply buried populations surviving with weak selection[2] may provide a genomic record of biogeochemical cycling over long geological timescales, as this phenomenon appears to extend into the deep biosphere[3].

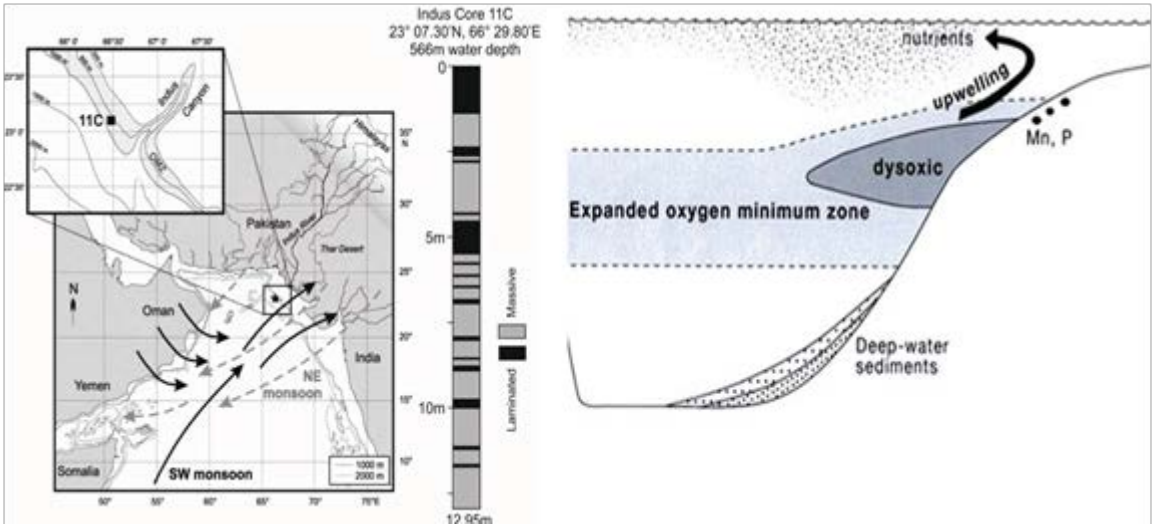

Fig. 1. Map of coring location within the Arabian Sea OMZ. The 13 m-long core covers the last 58 Kyr of deposition. Organic-rich sediments were deposited during warm interstadial climate stages and extensive OMZ formation and are embedded in oxygenated and bioturbated sediments, which were deposited during cold interstadials and reduced OMZ formation.

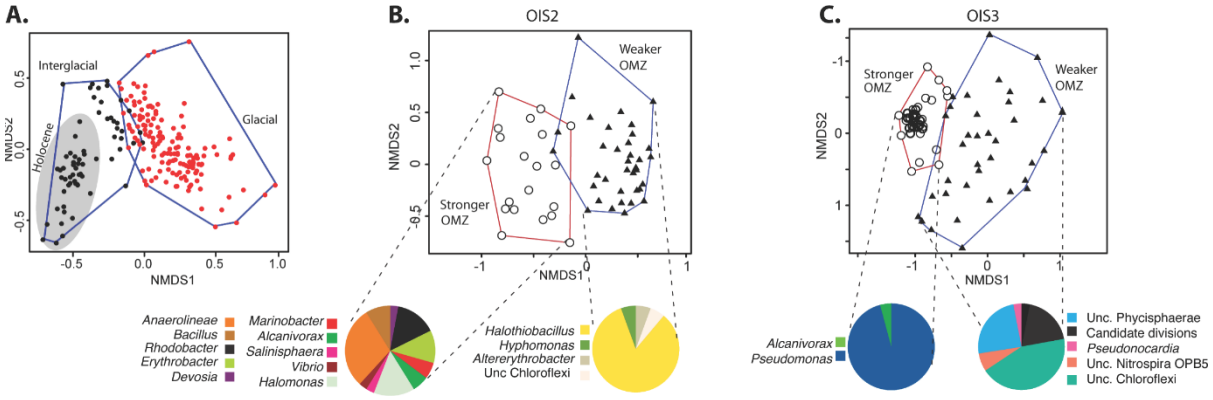

Fig. 2. Stratigraphy of microbial diversity. Non-metric multidimensional scaling (NMDS) of entire microbial populations in 214 analysed sediment intervals spanning the last 58 Kyr of deposition shows that: (A) Holocene (grey area), interglacial (black circles), and glacial (red symbols) periods have significantly (ANOSIM: P = 0.001) different communities of Bacteria. In Oxygen Isotope Stage 2 (OIS 2) (B) and OIS3 (C), bacterial communities in sapropelic interstadials (white circles) are significantly (P = 0.001) different compared to organic poor stadials (black triangles). Pie charts show the distribution of significant indicator taxa for stronger and weaker OMZ periods, pie slices are proportional to the number of OTUs assigned as indicator taxa.

References:

[1]Orsi, W.D., Coolen, M.J.L., He, L., Wuchter, C., More, K.D., Irigoien, X., Chust, G., Johnson, C., Hemingway, J.D., Lee, M., Galy, V., Giosan, L., Climate oscillations reflected in the microbiome of Arabian Sea sediments. Nat Commun, In review.
[2]Hoehler, T.M., Jörgensen, B.B., 2013. Microbial life under extreme energy limitation. Nat Rev Microbiol 11, 83-94.
[3]Inagaki, F., Hinrichs, K.-U., Kubo, Y., Bowles, M.W., Heuer, V.B., et al., 2015. Exploring deep microbial life in coal-bearing sediment down to ~2.5 km below the ocean floor. Science 349, 420-424.

Planktonic and benthic eukaryotic community responses to glacial-interglacial climate variability in the Arabian Sea

Kuldeep More, Kliti Grice, Marco J.L. Coolen

WA Organic and Isotope Geochemistry Centre, Department of Chemistry, Department of Environmental and Agriculture, The Institute for Geoscience Research, Curtin University of Technology, Perth, WA, Australia (E-mail: k.more@postgrad.curtin.edu.au)

Oxygen minimum zones (OMZ) occur when the respiratory oxygen demand during degradation of organic matter exceeds oxygen supply in aquatic systems. Rise in the sea surface temperature results in the OMZ expansion and is predicted to continue due to global warming[1, 2]. The most extensive OMZ is observed in the northern Arabian Sea where intensity of the OMZ is largely triggered by Monsoon-influenced surface-water productivity[3, 4]. In the Monsoon-impacted NE Arabian Sea, organic matter-rich and bioturbated sediments record fluctuations in OMZ intensity that also correlate with North Atlantic climate oscillations over the last glacial-interglacial cycle. Information on how these climatic shifts affect marine planktonic and benthic communities is mainly based on recent observations and modelling experiments[7], but how paleoenvironmental climate variability affected the past planktonic communities is still largely unknown, which is the main focus of this study. As the majority of planktonic taxa lack diagnostic features preserved upon fossilization, we here apply palaeontological-independent method (i.e., ancient DNA stratigraphy[8]) to reconstruct ecosystem-climate interactions. For this analysis a 13 m-long sediment core from the classical OMZ coring location off the Indus Canyon spanning key climate intervals of the last 52,000 years was collected. We performed the highest resolved sedimentary metagenomic profile to date and coupled it with multiple paleoceanographic proxies. Here we present 18S rDNA data showing significant climate-induced changes in eukaryotic planktonic communities. For example, Non Metric Multidimensional Scaling (NMDS) and Analysis of Similarity (ANOSIM) revealed significant differences in the overall community structure during the glacial vs. interglacial and also during shorter-term warm interstadial vs. cold stadial climate stages over the last 52 Ka. Dinoflagellates, uncultured marine avelolata group I, prasinophytes, cercozoans, and jellyfish were among the most significant indicator taxa for the interglacial as well as warm climate intervals (e.g. Dansgaard/Oeschger events), while ascomycete fungi as well as chlorophytes (i.e. *Chlorella*) were significant indicator taxa for the glacial and cold climate stages such as Heinrich events and the Younger Dryas. Our results show that ancient DNA stratigraphy can amend lipid biomarker geochemistry to record plankton community changes in response to climate variability at centennial to millennial scale resolution, covering at least the last glacial interglacial cycle.

References

1. Helm, K.P., Bindoff, N.L., Church, J.A., 2011. Observed decreases in oxygen content of the global ocean. Geophys Res Lett 38.
2. Keeling, R.F., Kortzinger, A., Gruber, N., 2010. Ocean Deoxygenation in a Warming World. Annu Rev Mar Sci 2, 199-229.
3. Altabet, M.A., Francois, R., Murray, D.W., Prell, W.L., 1995. Climate-related variations in denitrification in the Arabian Sea from sediment 15 N/ 14 N ratios. Nature 373, 506-509.
4. Reichart, G.J., Lourens, L.J., Zachariase, W.J., 1998. Temporal variability in the northern Arabian Sea Oxygen Minimum Zone (OMZ) during the last 225,000 years. Palaeoceanography 13, 607-621.
5. Schulte, S., Rostek, F., Bard, E., Rullkotter, J., Marchal, O., 1999. Variations of oxygen-minimum and primary productivity recorded in sediments of the Arabian Sea. Earth and Planetary Science Letters 173, 205-221.
6. Von Rad, U., Lueckge, A., Berger, W.H., Rolinski, H.D., 2006. Annual to millennial monsoonal cyclicity recorded in Holocene varved sediments from the NE Arabian Sea. Journal of the Geological Society of India 68, 353-368.
7. Blackford, J.C., Burkill, P.H., 2002. Planktonic community structure and carbon cycling in the Arabian Sea as a result of monsoonal forcing: the application of a generic model. Journal of Marine Systems 36, 239-267.
8. Coolen, M.J.L., Balkema, C., Quince, C., Harris, K., Orsi, W., Sylva, S., Filipova-Marinova, M., Giosan, L., 2013. Evolution of the plankton paleome in the Black Sea from the Deglacial to Anthropocene. Proceedings of the National Academy of Sciences, USA.

Multi-proxy geochemical analyses of Indus Submarine Fan sediments sampled by IODP Expedition 355: implications for sediment provenance and palaeoclimate reconstructions

Sophia Aharonovich[1*], Simon C. Geroge[1], James Bendle[2], Hannah Liddy[3], Peter D. Clift[4], Dhananjai K. Pandey[5], Denise K. Kulhanek[6], Sergio Andò[7], Manish Tiwari[5], Boo-Keun Khim[8], Elizabeth Griffith[9], Stephan Steinke[10], Kenta Suzuki[11], Jongmin Lee[8], Kate Newton[2], Shubham Tripathi[5], and the Expedition 355 Scientific Party

[1] Macquarie University, North Ryde, Sydney, NSW, Australia
[2] University of Birmingham, Edgbaston, United Kingdom
[3] University of Southern California, Los Angeles, CA, USA
[4] Louisiana State University, Baton Rouge, LA, USA
[5] National Centre for Antarctic and Ocean Research, Vasco da Gama, Goa, India
[6] Texas A&M University, College Station, TX, USA
[7] University of Milano Bicocca, Milan, Italy
[8] Pusan National University, Busan, Republic of Korea
[9] University of Texas at Arlington, Arlington, TX, USA
[10] MARUM, University of Bremen, Bremen, Germany
[11] Hokkaido University, Sapporo, Japan
(corresponding author: sophia.aharonovich@mq.edu.au)*

The correlation between development of the Asian monsoon and continuing tectonic activity in the Himalaya and Tibetian Plateau is crucial to 70% of Earth's population. This correlation is perhaps the most compelling example of the relationship between climate and the solid Earth. To understand it the sediments and sedimentary rocks from the Laxmi Basin were drilled during the International Ocean Discovery Program (IODP) Expedition 355 – Arabian Seam Monsoon in 2015 (Pandey et al., 2015). Drilling operations at Site U1456 (Fig. 1) penetrated through 1109.4 m of sediments and sedimentary rocks, with the oldest sediment dated to 13.5–17.7 Ma.

Here we present the results of a multiproxy palaeoenvironmental study on samples from the IODP Site U1456. We use a wide variety of organic geochemical data coupled with bulk geochemistry, mineralogy, and isotopic analyses. For direct comparison between various data sets, we divided whole round residues from the interstitial water analyses (squeeze cakes) among ten laboratories, with each receiving 50–300 g (dry mass). These preliminary results include initial sediment provenance data based on bulk petrography and heavy mineral analyses, geochemical data, isotope compositions, and biomarker analyses.

The samples show a low extent of diagenesis and intrastratal dissolution of heavy minerals. Based on the amphibole-epidote assemblages and the volume percentage of heavy minerals (2-5%) a provenance from the orogenic Himalaya is suggested (Garzanti and Andò, 2007). The Indus River is interpreted to be the main source of sediment input into Laxmi Basin from ~ 8 Ma.

Preliminary organic geochemistry data suggest low levels of biodegradation and thermal maturity of the organic matter. The results indicate an increase of the terrigenous organic matter input into sediment starting around ~8 Ma, followed by a strong decrease in the last 1 Ma (Fig. 2). Moreover, the detailed compound specific isotope analyses suggest variation in the C3 vs. C4 vegetation cover in the area in the last 10 Ma. The recovered glycerol dialkyl glycerol tetraether (GDGT) and alkenone lipids provide the first sea surface temperature (SST) record for the eastern Arabian Sea (Fig. 2). The SST data based on the GDGT proxy suggest a decreasing temperature trend from the Middle Miocene Climatic Optimum. The alkenone based SST reconstruction shows no noticeable temperature trend. Possible reason for that could be an upper temperature limit of 29-30°C for this proxy (Conte et al., 2006).

This research provides an exceptional opportunity to apply a multiproxy approach for reconstruction of the provenance, the erosional processes, and the palaeoclimatic evolution in the eastern Arabian Sea region.

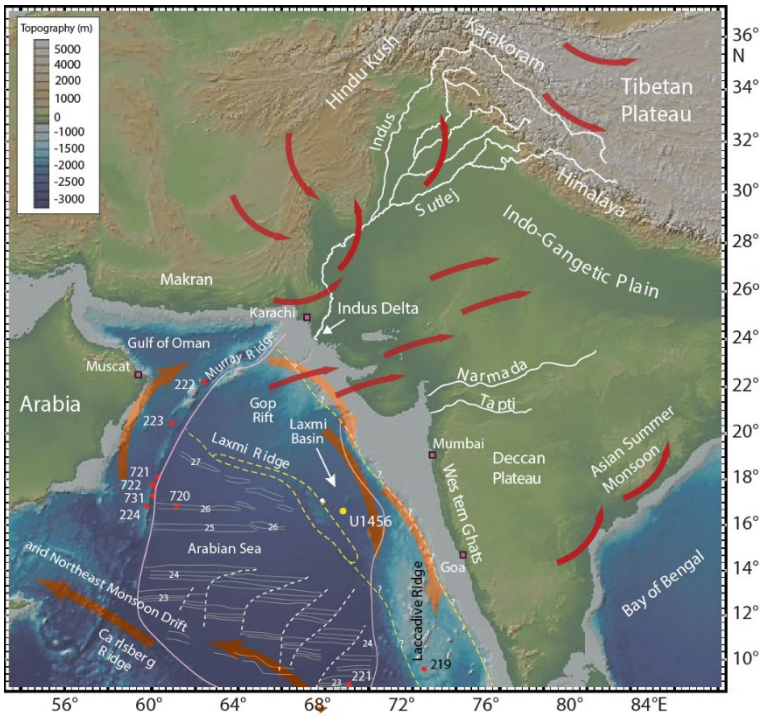

Fig. 2: IODP Expedition 355 drilling location, including modern currents (orange arrows) and summer monsoon (red arrows) directions.

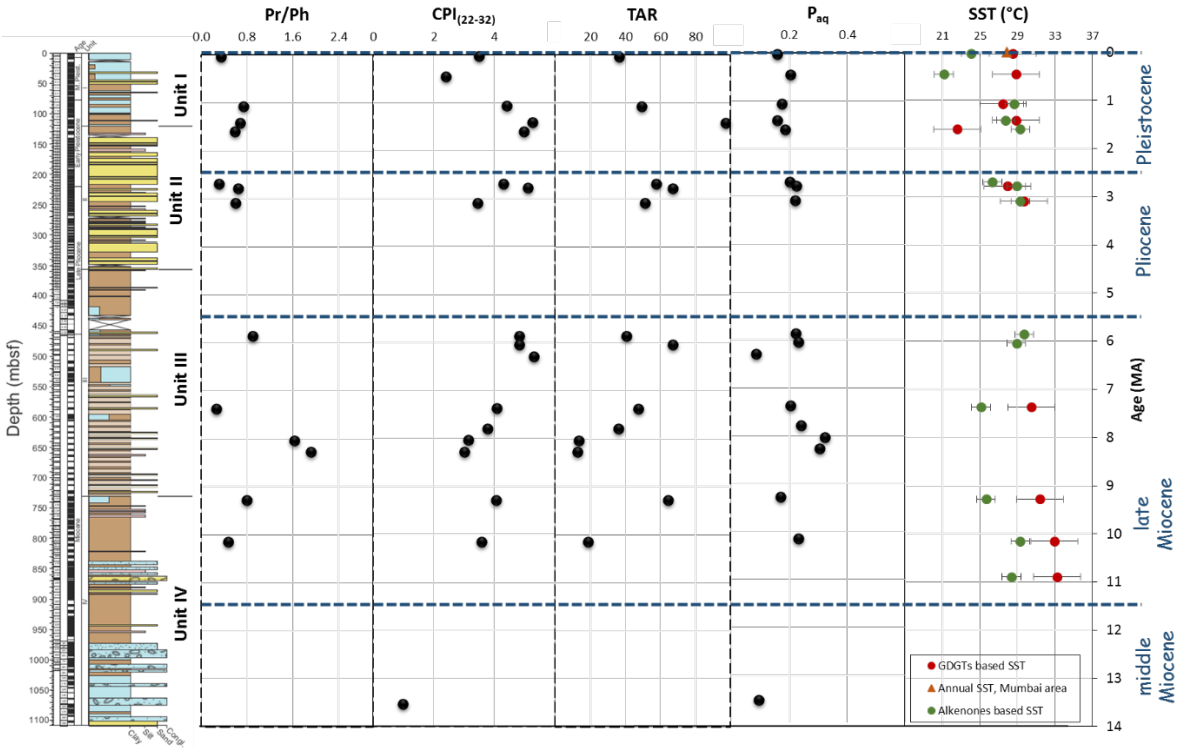

Fig.3: IODP Expedition 355 Site U1456 partial organic composition relative to lithology and geological periods where Pr-pristane, Ph-phytane, CPI – carbon preference index, TAR – terrigenous/aquatic ratio, and P_{aq} – submerged/floating aquatic macrophyte input vs. emergent and terrestrial plant input.

References

Conte, M.H., Sicre, M.A., Rühlemann, C., Weber, J.C., Schulte, S., Schulz-Bull, D., Blanz, T., 2006. Global temperature calibration of the alkenone unsaturation index (UK′ 37) in surface waters and comparison with surface sediments. Geochemistry, Geophysics, Geosystems 7.

Garzanti, E., Andò, S., 2007. Chapter 20 Heavy Mineral Concentration in Modern Sands: Implications for Provenance Interpretation, in: Maria, A.M., David, T.W. (Eds.), Developments in Sedimentology. Elsevier, pp. 517-545.

Pandey, D.K., Clift, P.D., Kulhanek, D.K., et al., 2015. Expedition 355 Preliminary Report: Arabian Sea Monsoon. International Ocean Discovery Program. http://dx.doi.org/10.14379/iodp.pr.355.2015

Beached Up!: The fascinating story of ambergris.

Steve J Rowland and P A Sutton

Jetsam ambergris is a heterogeneous organic deposit or coprolith, found on beaches worldwide. Ambergris originates from Sperm or Pygmy Sperm whales (about 1 to 4 in a hundred); after the death of the whales it is altered by environmental oxidation in the sea, before eventually becoming jetsam. For many centuries, ambergris was highly valued by perfumers as a fixative and odorant and there are still frequent media and press reports of occurrences of jetsam ambergris, but such reports are often based on subjective, or even no, evidence.

Since an objective scientific method of identification is clearly needed for jetsam ambergris, we describe methods for determination of the major components, using authentic samples to confirm or refute the assignments. Ambergris samples were assayed by infrared spectroscopy (FTIR), high temperature gas chromatography (HTGC), HTGC-mass spectrometry (HTGC-MS) and GC-MS, with and without treatment with each of two silylation reagents. Three sub-samples of a museum-archived sample of impeccable provenance, three ancient perfumery samples, and six putative jetsam samples, were also examined. The results suggest that confident assignment of an unknown jetsam sample as ambergris can be made in a tiered analytical approach. Where is the geochemistry? The methods allow us to examine fossil ambergris reported recently from the Pleistocene in central Italy using a classical ‘chemical fossil’ approach.

How can we use the stable carbon isotope composition of Holocene organic sediments for paleoclimate reconstruction?

Grzegorz Skrzypek[1,*], Zbyněk Engel[2]

*[1]West Australian Biogeochemistry Centre, School of Plant Biology, The University of Western Australia, Crawley 6009, Australia [2]Department of Physical Geography and Geoecology, The Charles University in Prague, 128 43 Praha 2, Czech Republic (*corresponding author: Grzegorz.skrzypek@uwa.edu.au)*

The $\delta^{13}C$ value is most commonly studied in bulk organic matter, in extracted cellulose or in other specific compounds. A few studies reported a systematic offset between the $\delta^{13}C$ of cellulose and that of the bulk organic matter in mosses, but this offset seems to be quite constant in well preserved peat. This may suggest that the stable isotope composition of bulk organic matter is a valid reflection of the variation in environmental parameters. Here, we present multiple case studies from Europe [1], USA [2] and South America [3] how $\delta^{13}C$ of bulk organic matter could be interpreted and used for paleoclimate studies and applied for interpretation of paleoclimate records from the Central Andes [4,5]. In this study, we used an alternative proxy for interpretation of palaeoclimate conditions based on a peat core taken from the southern Peruvian Andes (15°30´S, 71°43´W, 4809m a.s.l.), where other proxies are very limited due to high altitudes and relatively low precipitation. The ($\delta^{13}C$) value of Distichia peat reflects mainly the relative variation of the mean air temperature during subsequent growing seasons [3], and allows reconstructions of palaeotemperature changes. In contrast, peat organic carbon concentration (C % wt) records mainly wetness in the valley, directly corresponding to the changes in runoff in the upper part of the catchment.

The most prominent climate changes recorded in the peat over last 4000 years occurred between 3040 and 2750 cal. yrs BP. The initial warming turned to a very rapid cooling to temperatures at least 2°C lower than the mean for the Late Holocene. Initially drier conditions within this event turned to a short wet phase after 2780 cal. yrs BP, when the temperature increased again. This event coincides with significant changes in peat and ice core records in the Central Andes that match the timing of the global climate event around 2.8 cal. ka BP. Climatic conditions in the study area became relatively dry and stable after the event for about 800 years. Highly variable temperatures and humidity prevailed during the last 2000 years, when an extended warm and relatively humid period occurred between 640–155 cal. yrs BP, followed by predominantly colder and drier conditions [4,5].

Our studies demonstrates how the $\delta^{13}C$ value and carbon content variations in Distichia peat can be interpreted and used for verification of other multiproxy records, particularly these which are challenging for accurate dating, even potential limitations of the use for bulk organic matter exist.

References

[1] Skrzypek G., Jezierski P., Szynkiewicz A., 2010, Preservation of primary stable isotope signatures of peat-forming plants during early decomposition – observation along an altitudinal transect. Chemical Geology 273: 238–249.
[2] Skrzypek G., Paul D., Wojtuń B., 2013, The altitudinal climatic effect on the stable isotope compositions of Agave and Opuntia in arid environments - a case study at the Big Bend National Park, Texas, USA. Journal of Arid Environment 92: 102-112.
[3] Skrzypek, G., Engel, Z., Chuman, T., Šefrna, L., 2011. Distichia peat - A new stable isotope paleoclimate proxy for the Andes. Earth Planet. Sci. Lett. 307(3–4), 298–308.
[4] Engel, Z., Skrzypek, G., Chuman, T., Šefrna, L., Mihaljevič, M., 2014. Climate in the Western Cordillera of the Central Andes over the last 4300 years. Quat. Sci. Rev. 99, 60–77.
[5] Engel Z., Skrzypek G., 2014. Reply to the comment by A. Sáez et al. on Climate in the Western Cordillera of the Central Andes over the last 4300 years. Quat. Sci. Rev. 109: 128-130.

Reduced Early Holocene moisture availability in central Tibetan Plateau: Evidences from δD values of sedimentary *n*-alkanes

Chuanfang Jin[1, 2*], Franziska Günther[3], Shijie Li[2, 4], Changqun Cao[1], Gerd Gleixner[3]

[1] State Key Laboratory of Palaeobiology and Stratigraphy, Nanjing Institute of Geology and Palaeontology, Chinese Academy of Sciences, Nanjing 210008, China
[2] State Key Laboratory of Lake Sciences and Environment, Nanjing Institute of Geography and Limnology, Chinese Academy of Sciences, Nanjing 210008, China
[3] Max Planck Institute for Biogeochemistry, Jena 07745, Germany
[4] Institute of Geochemistry, Chinese Academy of Sciences, Guiyang 550002, China
**corresponding author: cfjin@nigpas.ac.cn*

The Tibetan Plateau is the focus of global geo-science research. Uplifting of Tibetan Plateau and its significance to the global material and energy transportation and balance, to the forming and evolution of atmospheric circulation pattern and Asian monsoon, has become the high lights of geo-science. Several projects have revealed that the strongest summer monsoon occurred in combination with warm and humid conditions during the early Holocene on the Tibetan Plateau (e.g. Shen et al., 2005; Zhou et al., 2004). However, the exact timing, duration, and amplitudes of the Holocene monsoon maximum appear to vary in different regions. Pollen records from the Zoige Basin, for example, show that the maximum monsoon occurred in the middle rather than the early Holocene (Zhao et al., 2011). Further analysis based on Chinese cave records indicate the maximum precipitation intensity seems to take place much later after the summer insolation maximum in the region between Dongge and Heshang caves (Hu et al., 2008). Possible reasons for such spatial heterogeneities are not well known, and need to be investigated through additional regional records.

Zigetang Co and Lake Cuona are situated in the central Tibetan Plateau, southern Tanggula Mountains, and belong to Amdo County, Xizang Autonomous Region, China. The water supply in both lake systems mainly depend on precipitation and seasonal inflows due to lacking glacial meltwater inputs in the catchment. This provides excellent sediments for palaeoclimatic and palaeoenvironmental reconstruction. Based on the advancements in the field of gas chromatography (GC)/thermal conversion (TC)/isotope ratio mass spectrometry (IRMS), sedimentary *n*-alkanes and compound-specific hydrogen isotopes in both lake systems were analyzed to explore the process of the source, transport and storage of the biomarkers in the lake system and its climatic and environmental significance.

The short chain *n*-alkanes $C_{15/16/17}$, probably derived from aquatic algae, plankton and photosynthetic bacteria, dominate the *n*-alkane composition in lacustrine sediments in both lake systems. The variation of *n*-alkane indicator ratios (e.g. ACL and CPI values) and δD values reveal that cold-wet conditions in the terminal Pleistocene, warm-dry environment but frequent fluctuation in the early-mid Holocene, cool-wet conditions in the mid-late Holocene and warm-dry settings in the late Holocene, that is, higher effective moisture availability occurred for our study in the middle rather than the early Holocene. This challenged the present interpretation on monsoonal dynamics on the Tibetan Plateau are either strongly influenced by the presence of glaciers in the catchment or that during cold periods the air masses on the Tibetan Plateau mainly derived from the Westerly air masses. Our sediment records provide further evidences for the complex relationship of insolation-induced temperature, evaporation and precipitation affecting the regional climate changes on the Tibetan Plateau

References:

Hu, C. Y., Henderson, G. M., Huang, J. H., Xie, S. C., Sun, Y., Johnson, K. R., 2008. Quantification of Holocene Asian monsoon rainfall from spatially separated cave records. Earth and Planetary Science Letters 266, 221-232.

Shen, J., Liu, X. Q., Wang, S. M., Ryo, M., 2005. Palaeoclimatic changes in the Qinghai Lake area during the last 18,000 years. Quaternary International 139, 131-140.

Zhao, Y., Yu, Z., C., Zhao, W. W., 2011. Holocene vegetation and climate histories in the eastern Tibetan Plateau: controls by insolation-driven temperature or monsoon-drived precipitation changes? Quaternary Science Reviews 30, 1173-1184.

Zhou, W. J., Yu, X. F., Timothy Jull, A. J., Burr, G., Xiao, J. Y., Lu, X. F., Xian, F., 2004. High-resolution evidence from southern China of an early Holocene optimum and a mid-Holocene dry event during the past 18,000 years. Quaternary Research 62, 39-48.

Effect of hydrocarbon contamination on the soil microbiome in Western Australia's pristine Kimberley region

Deirdre B. Gleeson[1*], Tim Lardner[1], Andrew S. Ball[2], Kliti Grice[3], Alastair Trolove[4], Megan Nicholas[4], Gary Bending[5], Sally Hilton[5], Megan Ryan[1]

[1]University of Western Australia, 35 Stirling Highway, Crawley 6009, AUSTRALIA
[2]RMIT University, Bundoora VIC 3083, AUSTRALIA
[3]Curtin University, Kent Street, Bentley 6102, AUSTRALIA
[4]Horizon Power, 18 Brodie Hall Drive, Bentley 6102, AUSTRALIA
[5]University of Warwick, Coventry VC4 7AL, UK
*(*deirdre.gleeson@uwa.edu.au)*

Extensive use of petroleum products represents a constant threat of oil spills to onshore and offshore environments. These spills result in significant environmental problems and cleaning up can be difficult and expensive – this is especially true in pristine and delicate environments such as West Australia's Kimberley region. The risk presented by petroleum contamination can be assessed by measuring total recoverable hydrocarbons (TRH), in addition to using a variety of ecotoxicity assessments that more directly assess risk by measuring the effect of the contaminated soil on the growth and survival of a range of test organisms after exposure. Soil microorganisms can use petroleum hydrocarbons as a source of energy and thus the soil microbial community plays a major role in the removal of contaminant petroleum hydrocarbons from the environment, with biodegradation by indigenous soil microbial communities representing one of the primary mechanisms by which they can be eliminated. The rate of microbially mediated biodegradation depends on factors such as the nature of the contamination and the suitability of the conditions for microbial activity. Harnessing soil microbes to breakdown hydrocarbon contaminants is a low-cost and environmentally friendly way in which to remediate contaminated sites. Here we aimed to assess the impact of long term hydrocarbon contamination from legacy spills at a variety of sites across the Kimberley region of Western Australia. This region is unique with a rich and unusual biodiversity – soils here are nutrient poor and in their natural state harbour a vast microbial diversity which will likely be impacted by the presence of contaminating hydrocarbons.

Samples were collected from three sites (Camballin, Fitzroy Crossing and Kununurra) under the control of the regional power generator, Horizon Power, in the Kimberley region of Western Australia. At all sites there were areas with legacy hydrocarbon contamination due to activities associated with power generation. At each of the three sites, we compared soil properties including measures of TRH, microbial communities and ecotoxicity between areas predicted to be contaminated and areas predicted to be uncontaminated. Our objective was to assess the remaining hydrocarbon contamination and its ecotoxicity and determine whether the soils show potential to further bioremediate naturally through the actions of the soil microbial communities. We further aimed to characterise the effect of hydrocarbon on the soil microbial communities and the networks they form for optimal functioning.

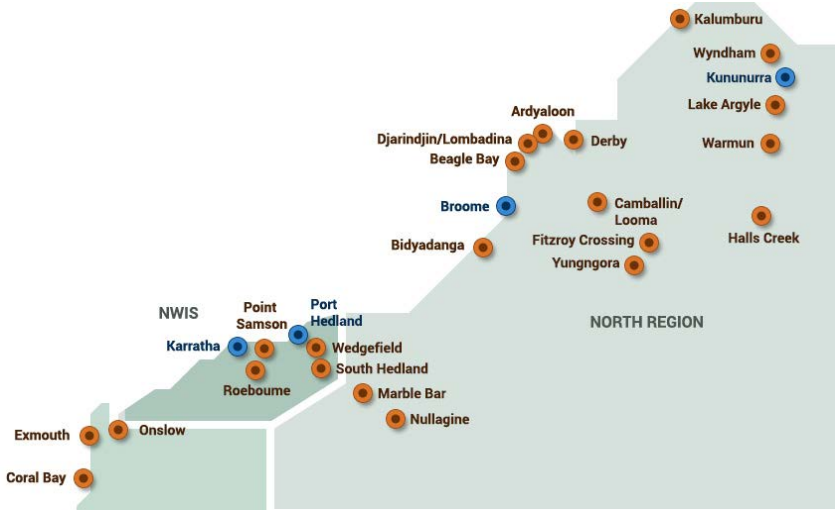

Fig 1: Sites sampled across the Kimberley: Camballin, Kunnunurra and Fitzroy Crossing. Both control and hydrocarbon contaminated soils were collected at each location from the 0-15 and 15-30cm soil layers.

TRHs were present in most contaminated samples, with the concentrations lowest at Camballin and highest at Fitzroy Crossing and Kununurra. All sites had very sandy soils, with low levels of organic matter and very low concentrations of essential nutrients. Soils were mostly very dry at the time of sampling. There was little change in soil characters with depth. Four soil properties were significantly associated with total TRHs: ammonium-N, extractable P and organic C (all positive effects), and pH (negative effect). The largest effects were for pH and organic C. Ecotoxicity was measured in three ways: germination of radish and lucerne, earthworm survival, and Microtox®. All measures indicated that little to no toxicity remained at the sites and that the toxicity that did remain was likely associated with factors other than TRHs.

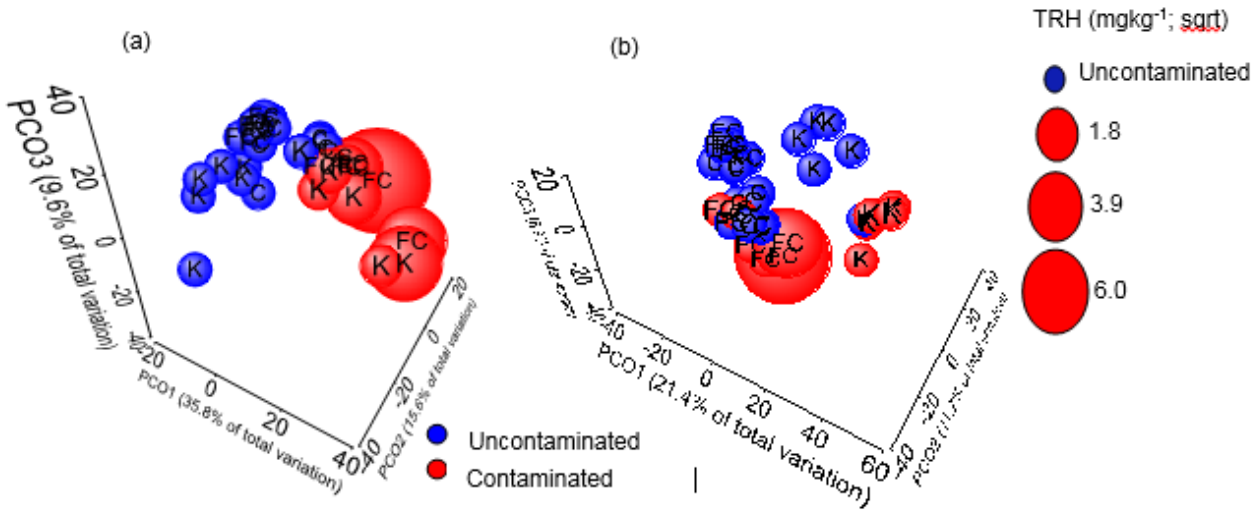

Fig 2: Principal coordinate analysis depicting (a) bacterial and (b) fungal community structure at each of the three sites sampled (C Camballin; FC Fitzroy Crossing; K Kununurra). The size of the bubble represents the level of total hydrocarbon (total recoverable hydrocarbon; TRH) contamination

Contamination affected bacterial community structure; highly contaminated samples were most different from uncontaminated samples (Figure 2a). These trends were less evident for fungal communities (Figure 2b). Bacterial and fungal community diversity and evenness was higher in uncontaminated samples than contaminated samples at each of the sampled sites. The prominent differences between contaminated and uncontaminated samples at Camballin was unexpected as TRHs were low at this site. Possible explanations include presence of low concentrations of highly toxic hydrocarbons, or breakdown products, not present at other sites or other contaminants being present. SIMPER analysis was used to detect which bacterial and fungal taxa were responsible for differences observed between contaminated and uncontaminated samples. The bacterial families Mycobacteriaceae, Rhodospirillaceae and Syntrophobacteraceae were elevated in contaminated samples, whereas Actinobacteria-MB-A2, Gaiellaceae, and Gemmatimonadetes-Gemm-1 and were elevated in uncontaminated samples. The fungal families Pleosporales, Herpotrichiellacaea and Trichocomaceae were elevated in contaminated samples whereas Sordariales and Ascomycota were elevated in the uncontaminated samples. Contaminated soils had a distinctly different microbiome than uncontaminated samples with contamination resulting in lower diversity in contaminated soils. Ecotoxicity data suggest that little toxicity remains at these sites indication natural attenuation has been successful in bioremediating the sites.

Sea level and climate sensitivity

Eelco J. Rohling[1]

[1]*Research School of Earth Sciences, The Australian National University, 2601 Canberra.*

Apart from the obvious need for understanding sea-level variability in response to climate change, there is also a need for detailed records of sea-level variability in studies of climate sensitivity to radiative forcing changes. This is because ice-volume variations are a critical factor in the radiative forcing of climate through the ice-albedo feedback process. It is this latter aspect that I will focus on. I will go through the main observational methods that exist for reconstructing past sea-level variations, including their fundamental approaches and assumptions, and hence their limitations and potential. I will conclude with some key examples of how improved understanding of past sea-level variations helps in developing quantitative reconstructions of past equilibrium climate sensitivity.

The first occurrence of ergostane and aromatic ergosteroid in the rock record.

Tharika M. Liyanage[1]*, Eva Sirantoine[1], Janet M. Hope[1], Ilya Bobrovskiy[1], Jochen J. Brocks[1],

[1]The Australian National University, Canberra, ACT 2601, Australia
(corresponding author: u5181755@anu.edu.au)*

The Neoproterozoic Era (1000 – 541 Ma) was a markedly active time in Earth's history, with the occurrence of global glaciations, significant tectonic activity and major leaps in the evolution of complex multicellular life (*1*). Molecular fossils of Neoproterozoic organisms preserve information about biological, ecological and environmental conditions and can be used to clarify the interplay between climatic, tectonic and biological processes through the Era. The proportions of different steranes, the molecular fossils of sterols, provide information about the dominant eukaryotic primary producers and constrain eukaryotic evolution during this period (*2*). Previous work demonstrated that there was an absence of 24-alkylated steranes and an apparent 100% predominance of cholestane in the Tonian (1000-720 Ma) (*3*). Conversely, during the Ediacaran (635-541 Ma), stigmastane was the most prevalent sterane (*4*) with minor contributions from other steranes. These unique signals are considered to be age diagnostic for these periods.

Here we report the discovery of the oldest clearly indigenous steranes alkylated in the side chain in position 24, including saturated ergostane and aromatic ergosteroids. These earliest ergosteroids occur in low relative abundances in immature Tonian deposits that otherwise show a strong cholestane predominance. The recently discovered C_{28} sterane, cryostane (*3*) was also detected. This represents an unprecedented sterane distribution pattern that has never been observed before in the rock record. We also highlight that due to possible preservation biases, it is crucial to account for the aromatic steroids when reconstructing the paleoecology of eukaryotes. The relative proportions of the saturated steranes differ from the analogous aromatic steroids; the origin of this discrepancy is presumably related to the unsaturation pattern of precursor sterols. The unusual distributuion of steranes in sediments of Tonian age challenges current assumptions about the evolutionary state of eukaryotes in the mid-Neoproterozoic and might eventually provide clues about the onset of the Sturtian Snowball Earth (~717 – 660 Ma).

	Steranes				**Triaromatic steroids**		
	cholestane	ergostane	cryostane	stigmastane	TA-cholesteroid	TA-ergosteroid	TA-stigmasteroid
Sample 1	97.94%	1.09%	0.97%	0%	95.69%	4.31%	0%
Sample 2	98.35%	0.74%	0.90%	0%	87.72%	12.28%	0%

Fig. 1. The relative proportions of steranes and triaromatic steroids in two samples from immature Tonian-aged samples.

References

1. A. Knoll, Learning to tell Neoproterozoic time. *Precambrian Res.* **100**, 3–20 (2000).
2. J. J. Brocks, R. E. Summons, in *Treatise on Geochemistry* (2004), vol. 8, pp. 63–115.
3. J. J. Brocks *et al.*, Early sponges and toxic protists: possible sources of cryostane, an age diagnostic biomarker antedating Sturtian Snowball Earth. *Geobiology* (2015), 14, 129-149.
4. P. J. Grantham, G. W. M. Lijmbach, J. Posthuma, Geochemistry of crude oils in Oman. *Geol. Soc. London, Spec. Publ.* **50**, 317–328 (1990).

Geochemical and palynological evidence of the earliest land plants in Middle Ordovician shallow marine environments: Implications for paleoclimate and early plant evolution

Gemma Spaak[1]*, Kliti Grice[1], Clinton Foster[2], Dianne Edwards[3]

[1]Curtin University, WA Organic and Isotope Geochemistry, Department of Chemistry, The Institute for Geoscience Research, GPO Box U1987, Perth, WA 6845, Australia
[2] School of Earth and Environment, The University of Western Australia
[3]Geoscience Australia GPO Box 387, Canberra, ACT 2601, Australia
(corresponding author: gemma.spaak@curtin.edu.au)*

The Early Palaeozoic, specifically the Middle Ordovician, marks a significant period in Earth's history due to the appearance and diversification of life on land. Plant megafossil records indicate vascular plants first appeared in the Early Silurian and by Devonian times had diversified rapidly (e.g. Wellman and Gray, 2000; Steemans et al., 2009; Kenrick et al., 2012; Strother, 2016). However non-vascular plants (bryophytes) predating vascular plants are rarely preserved as body fossils and the bryophyte microfossil record in the lowermost Palaeozoic is scarce. This lack of fossil data severely limits our understanding of life in earliest non-marine environments and the origin of land plants.

In comparison to microfossils, molecular fossils (biomarkers) are far more ubiquitous in the sedimentary record and have a higher preservation potential, thus providing a powerful tool to track terrestrial signals when microfossils are scarce or absent. Molecular proxies such as long chain *n*-alkanes have been used extensively in both modern and ancient environments to identify terrestrial contributions to the organic matter (e.g. Eglinton and Hamilton, 1967; Ficken et al., 2000; Hautevelle et al., 2006). Furthermore, the isotopic composition of these molecules can be used to further distinguish between sources (e.g. Bird et al., 1995; Sikes et al., 2009; Rouillard et al., 2016). That being said, only relatively few studies have combined palynological evidence with geochemical proxies to assess geochemical signatures of early land plants.

This work presents biomarker and palynological data of the Upper Goldwyer Formation (Middle Ordovician) which records the earliest occurrence of land plant microfossils (cryptospores) in Australia. The higher-molecular-weight *n*-alkane distributions and their isotopic compositions recorded in the Upper Goldwyer show high resemblances to modern day bryophytes and aquatic macrophytes. Retene, a biomarker conventionally used as a proxy for gymnosperms, was also identified in some extracts. The presence of retene in Middle Ordovician (this work) and Silurian (Romero-Sarmiento et al., 2010) rocks indicates conifers are not the sole source of this compound.

Linking biomarkers and palynology has shown to be very useful in the study of early land plants where fossil records are sparse. Molecular and isotopic proxies distinctive of these plants can provide a more complete record of the geographical distribution of early land plants, providing useful information to understand their early evolution.

References:

Bird, M.I., Summons, R.E., Gagan, M.K., Roksandic, Z., Dowling, L., Head, J., Fifield, L.K., Cresswell, R.G., Johnson, D.P., 1995. Terrestrial vegetation change inferred from n-alkane δ13C analysis in the marine environment. Geochimica et Cosmochimica Acta 59, 2853–2857.

Eglinton, G., Hamilton, R.J., 1967. Leaf Epicuticular Waxes. Science 156, 1322–1335.

Ficken, K.J., Li, B., Swain, D.L., Eglinton, G., 2000. An n-alkane proxy for the sedimentary input of submerged/floating freshwater aquatic macrophytes. Organic Geochemistry 31, 745–749.

Hautevelle, Y., Michels, R., Malartre, F., Trouiller, A., 2006. Vascular plant biomarkers as proxies for palaeoflora and palaeoclimatic changes at the Dogger/Malm transition of the Paris Basin (France). Organic Geochemistry 37, 610–625.

Kenrick, P., Wellman, C.H., Schneider, H., Edgecombe, G.D., 2012. A timeline for terrestrialization : consequences for the carbon cycle in the Palaeozoic. Philosophical Transactions of the Royal Society B: Biological Sciences 367, 519–536.

Romero-Sarmiento, M.F., Riboulleau, A., Vecoli, M., Versteegh, G.J.M., 2010. Occurrence of retene in upper Silurian-lower Devonian sediments from North Africa: Origin and implications. Organic Geochemistry 41, 302–306.

Rouillard, A., Greenwood, P.F., Grice, K., Skrzypek, G., Dogramaci, S., Turney, C., Grierson, P.F., 2016. Interpreting vegetation change in tropical arid ecosystems from sediment molecular fossils and their stable isotope compositions: A baseline study from the Pilbara region of northwest Australia. Palaeogeography, Palaeoclimatology, Palaeoecology 459, 495–507.

Sikes, E.L., Uhle, M.E., Nodder, S.D., Howard, M.E., 2009. Sources of organic matter in a coastal marine environment : Evidence from *n*-alkanes and their δ13C distributions in the Hauraki Gulf, New Zealand. Marine Chemistry 113, 149–163.

Steemans, P., Hérissé, A. Le, Melvin, J., Miller, M. a, Paris, F., Verniers, J., Wellman, C.H., 2009. Origin and radiation of the earliest vascular land plants. Science (New York, N.Y.) 324, 353.

Strother, P.K., 2016. Systematics and evolutionary significance of some new cryptospores from the Cambrian of eastern Tennessee , USA. Review of Palaeobotany and Palynology 227, 28–41.

Wellman, C.H., Gray, J., 2000. The Microfossil Record of Early Land Plants. Philosophical Transactions of the Royal Society B: Biological Sciences 355, 717–732.

Interpreting shifts in *n*-alkane average chain length in sedimentary records: what are the key drivers?

S. Howard[1], F.A. McInerney[1], E. Reed[1] and M. Farrell[2]

[1]Sprigg Geobiology Centre, University of Adelaide, 5005, Australia
[2]CSIRO Agriculture & Food, Urrbrae, 5064, Australia

Leaf wax n-alkanes (C25-C35) are widely used biomarkers for terrestrial plants, and are pervasive in the sedimentary record compared to macrofossil plants. Where whole leaf fossils are unavailable, n-alkanes can provide a useful means of analysing past ecosystems. In particular, they may be a useful tool for examining the environmental and vegetation changes associated with major biotic events, such as the extinction of Australia's megafauna. Abundant megafauna fossils are found in the Naracoorte Caves, in the SE of South Australia and analysis of the n-alkanes in the sediments associated with these fossils may help to reveal the environmental and vegetation conditions that these animals lived and died with. Understanding these conditions will facilitate a better understanding of what may have lead to the extinction of Australia's megafauna, which may prove useful for species conservation and management into the future. Here, we examine the controls on n-alkane distributions in modern soils in order to interpret changes in leaf wax average chain length in sediments from Naracoorte caves across the megafauna extinction.

In order to understand the signals that leaf wax *n*-alkanes record, it is critical to give consideration to the formation and modification (taphonomy) of *n*-alkane accumulations in soils and sediments. Deposits of *n*-alkanes from plants become integrated into soil as a result of different factors including wind ablation acting on the leaves and leaf fall. Once deposited, leaf wax *n*-alkanes accumulate in the soils and can preserve in sediments for many millions of years. It has been hypothesized that the distribution (average chain length, or ACL) of *n*-alkanes in soils and sediments can provide insight into the types of plants present, as well as the conditions the plants were subjected to, at the time of deposition. Field and experimental studies were conducted to determine whether the *n*-alkane ACL signal recorded in soils is representative of the current plant species present, and to also determine how biodegradation processes occurring within the soils affect that signal.

We expect that the *n*-alkane ACL distribution of the soils will match the distribution of dominant plant species at a site, weighted by their concentration and percent coverage. To explore this, modern plant and soil samples were obtained from a bioclimatic transect made up of a number of TERN biodiversity monitoring plots (AusPlots and TREND) across Australia. Samples of the top three dominant plant species (determined by % cover, n = 59) present at each plot and the surface soil (n = 20) at each plot had *n*-alkanes extracted and analysed for ACL.

Results from the bioclimatic transect field study show that there is a mismatch between the *n*-alkane signals measured in the plants and the soils. This mismatch may be as a result of the timing of sampling which may affect the dominant plant species selected, due to the ephemerality of different plant species. It may also be that percent cover is an inadequate representation of biomass of each species at each site. Also, percent cover of the top three dominant plant species at each site may not account for other *n*-alkane contributors outside of the hectare plots (i.e. wind-blown allochthonous material). As well as this, leaf waxes accumulate over an extended period of time and thus ecological shifts could affect the time-averaged signal recorded in the soils. The mismatch between the plants and the soils is often observed in 'live-dead' studies, where the living assemblage (in this case the plants) represents a snapshot in time, whereas the death assemblage (in this case the soils) represents a temporal and spatial average of contributors.

Further to this, we explored whether post-depositional modification of *n*-alkanes in soils accounts for the soils' mismatch with the dominant plants present. An experimental study analysing the effects of biodegradation of *n*-alkanes in soils over time was conducted utilising incubated soil samples mixed with a variety of different organic amendments, such as green waste, garden clippings, manure and other composts, obtained from CSIRO. Incubation of samples was halted by drying of the soil samples, preventing continued microbial activity. Samples at 0 months and 18 months were analysed for *n*-alkane ACL and concentration.

Results from the experimental study indicate that concentration of *n*-alkanes decreased markedly over the 18 month incubation period. Nonetheless, ACL remained quite steady over the 18 month period. Further to this, the carbon preference index (CPI), which indicates whether there is an odd-over-even predominance of *n*-alkane chain lengths present, showed a decrease over 18 months. This is supports the assertion that CPI decreases as a result of degradation and may be useful as an indicator of *n*-alkane degradation. These results suggest that inputs to soils have a greater influence on *n*-alkane ACL than any post-depositional modification.

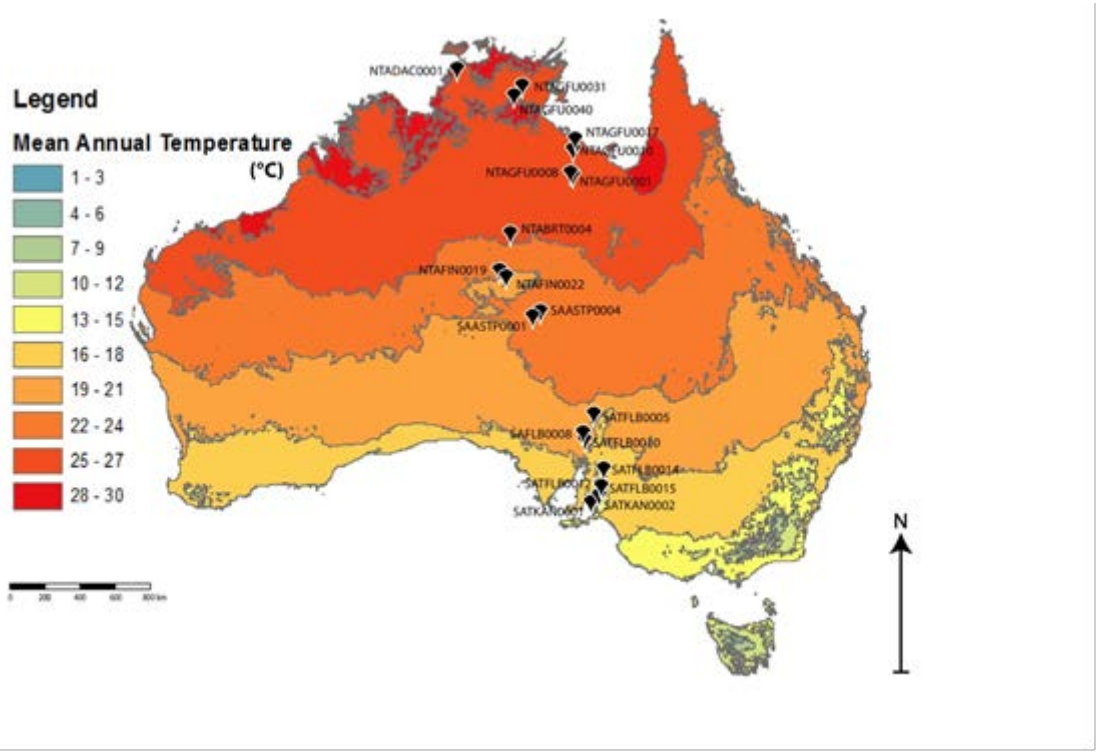

Fig. 1. Location map of selected Ausplots sites (black pins) provided by TERN, across Australia including the TREND sites located in the southern half of South Australia. Location of selected sites with respect to the mean annual temperature is shown. Climate data based on a standard 30-year climatology (1961-1990) and reproduced with permission from Bureau of Meteorology (© Commonwealth of Australia).

Biomarkers from the Ediacaran macrofossil *Beltanelliformis*

Ilya Bobrovskiy*, Janet M. Hope, Tharika M. Liyanage, Jochen J. Brocks

Australian National University, Canberra, ACT 2601, Australia
(corresponding author: ilya.bobrovskiy@anu.edu.au)*

The Ediacara biota (580-540 Ma) marks the first global appearance of complex macroscopic organisms in geological history at a time of transition between microscopic life in the Precambrian world and the animal-dominated world of the Phanerozoic. Although it is clear that the Ediacara biota reflects one of the most important milestones in the evolution of life, their origin remains enigmatic: there is more than one opinion about what the Ediacaran organisms were and what environments they inhabited (e.g. Retallack, 2012; Seilacher, 2007; Tarhan et al., 2015) The controversies about the phylogenetic status of the Ediacaran organisms have raged for several decades, and new advances are needed to provide a breakthrough.

The White Sea region in Russia offers not only one of the most diverse and best preserved impressions of the Ediacara biota in the world, it is also the only place where they occur together with well-preserved biomarkers. Biomarkers may provide new answers about the origin and environments of the Ediacara biota. Here we report the results of the first biomarker analyses of organically preserved Ediacaran macrofossils.

Fig. 1. Organically preserved *Beltanelliformis* from the White Sea region (photo by S.V. Bagirov)

Beltanelliformis is one of the most revisited Ediacaran macrofossils. It has been interpreted as traces of air bubbles, pits, burrows, jellyfish bodies, sedentary polyps, planktonic algae, fungal colonies, colonial cyanobacteria, colonial non-phototrophic bacteria, benthic gametophytes of green algae, and benthic sponge-like animals (for a review see Ivantsov et al., 2014). Organically preserved *Beltanelliformis* impressions in the White Sea region (Fig. 1) show a very different biomarker signal when compared to organic films collected from the same surface surrounding the fossils. The surrounding organic film yields a very dominant signal of steranes over hopanes (S/H = 16.48), and the steranes exhibit a strong C_{29} predominance (87%), implying a prevalent algal source (Fig. 2) (Brocks and Summons, 2004; Volkman, 1986). In contrast, organic matter collected from *Beltanelliformis* yields a distinct biomarker signature: hopane abundances are higher (S/H = 0.67) than in the surrounding film. Steranes are present but show the same distribution as in the surrounding film, pointing to the same algal background signal. The abundant hopanes extracted from the fossil but not from the surrounding organic matter suggest that *Beltanelliformis* were colonial structures of cyanobacteria or aerobic heterotrophic bacteria (Brocks and Summons, 2004).

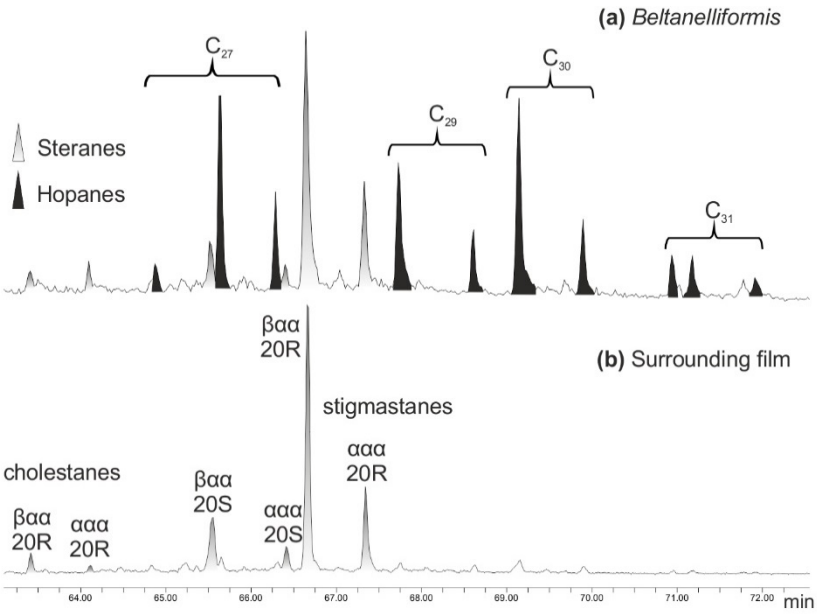

Fig. 2. Sum of MRM traces for C27 to C29 steranes and C27 to C31 hopanes comparing their distribution in (a) organically preserved *Beltanelliformis* and (b) organic film surrounding the fossils

References

Brocks, J.J., Summons, R.E., 2004. Sedimentary Hydrocarbons, Biomarkers for Early Life, in: Schlesinger, W. (Ed.), Treatise on Geochemistry Vol. 8, Biogeochemistry, pp. 63–115.

Ivantsov, A.Y., Gritsenko, V.P., Konstantinenko, L.I., Zakrevskaya, M.A., 2014. Revision of the problematic Vendian macrofossil Beltanelliformis (=Beltanelloides, Nemiana). Paleontological Journal 48, 1415-1440.

Retallack, G.J., 2012. Were Ediacaran siliciclastics of South Australia coastal or deep marine? Sedimentology 59, 1208-1236.

Seilacher, A., 2007. The nature of vendobionts. Geological Society, London, Special Publications 286, 387-397.

Tarhan, L.G., Droser, M.L., Gehling, J.G., 2015. Depositional and preservational environments of the Ediacara Member, Rawnsley Quartzite (South Australia): Assessment of paleoenvironmental proxies and the timing of 'ferruginization'. Palaeogeography, Palaeoclimatology, Palaeoecology 434, 4-13.

Volkman, J.K., 1986. A review of sterol markers for marine and terrigenous organic matter. Organic Geochemistry 9, 83-99.

The Great Oxidation Event and its biological impacts: Insights from geochemistry & molecular clocks

David A Gold[1], Abigail Caron[1], Gregory P Fournier[1] and Roger E Summons[1*],

Department of Earth, Atmospheric and Planetary Science,
Massachusetts Institute of Technology, Cambridge, MA, USA.
(corresponding author: rsummons@mit.edu)*

Molecular oxygen (O_2) has been a primary driver of biological evolution through its roles in respiration and as a key ingredient of biochemistries essential to the radiation of complex multicellular organisms. Although 'whiffs' of oxygen have been claimed for the Archean, O_2 did not accumulate irreversibly until 2.33 billion years ago during what is commonly referred to as the Great Oxidation Event (GOE). The timing and duration of the GOE were recently established through analysis of multiple sulfur isotope data from a continuous and well-dated sedimentary sequence in the Transvaal Supergroup, South Africa (Luo et al., 2016). In the present report we discuss this data and how a molecular clock approach might then determine when O_2-dependent sterol biosynthesis first evolved. We screened databases for the genes that code for squalene monooxygenase (SQMO) and oxidosqualene cyclase (OSC), the first two proteins in the sterol biosynthesis pathway. Additionally, we observe that functionally modern sterol biosynthesis genes shared between bacteria and stem eukaryotes via horizontal gene transfer have a common ancestor around 2.3 Gyr ago, suggesting that sterol biosynthesis most likely originated synchronously with the GOE.

References

Luo G., Ono S., Beukes N.J, Wang D.T., Xie S. and Summons R.E., 2016. Rapid oxidation of Earth's atmosphere 2.33 billion years ago. Science Advances 2: e1600134.

Combined organic and inorganic geochemical characterisation approach of Toarcian carbonate concretions

Chloe Plet[1,*], Kliti Grice[1], Marco J.L. Coolen[1], Anais Pages[2,1], Wolfgang Ruebsam[3], Lorenz Schwark[3,1]

[1]WA-Organic and Isotope Geochemistry, The Institute for Geoscience Research, Department of Chemistry, Curtin University, Perth, 6000, Australia
[2]CSIRO CESRE, Perth, 6000, Australia
[3]Organic Geochemistry workgroup, Christian Albrecht University, Kiel, 24118, Germany
(corresponding author: **chloe.plet@curtin.edu.au**)*

The Posidonia shale was deposited during the Toarcian Anoxic Event (~182.7 Ma) and is host to carbonate concretions containing exceptionally preserved fossils including soft tissue. Calcium carbonate concretions containing well preserved fossils are typically formed under anoxic to euxinic conditions. Organic matter (OM) is decayed by a microbial consortium in sediments and/or at the sediment-water interface and the carbonate preciptates around the OM-rich nucleus giving rise to a carbonate concretion (*e.g.* Coleman and Raiswell, 1995; Melendez et al., 2013a). These conditions allow for exceptional preservation of fossils (Wilson and Brett, 2013) and biolipids (Melendez et al., 2013b). Although carbonate concretions are well-known for containing beautiful morphological fossils, only few studies have investigated biomarker distributions within such concretions (Kiriakoulakis et al., 2000; Plet et al., 2016a) and their encapsulated fossils (Melendez et al., 2013a, 2013b; Plet et al., 2016b).

In this study several concretions from the Posidonia shale and the host shale have been investigated by a multiproxy approach using a combination of organic geochemical methods (*e.g.* Rock Eval and lipid biomarkers, compound specific isotope analyses), classical inorganic geochemical analyses (*e.g.* ICP-MS and $\delta^{13}C_{carb}$) and imaging techniques (*e.g.* optical microscopy, XRF mapping, scanning electron microscopy) (Plet et al., 2016a, 2016b).

The high hydrogen indices in the concretion body (~620 mgH/gTOC) support good preservational conditions for the bulk OM which decreases towards the concretion rim (~535 mgH/gTOC). These results highlight the capacity of preservation of OM within carbonate concretions, suggesting that once triggered around a decaying nucleus, the concretion growth persists with minimal OM degradation.

In one of the concretions an exceptionally well-preserved ichthyosaur vertebra was identified. Lipid biomarker and compound specific isotope analyses revealed the presence of cholesterol largely derived from the ichthyosaur's diet and ethylcholesterol derived from phytoplankton in the ancient water column. In addition a suite of diagenetic and catagenetic steroids were also identified showing the second occurrence of biomolecules and geomolecules ina single sample (cf. Melendez et al., 2013b). Imaging techniques of the vertebra revealed the presence of collagen fibre bundles encrusted with fluorapatite. In comparison with recent work on fibres in dinosaurs (Bertazzo et al., 2015) and with modern day collagen from Australian crocodile bones, our study led to the identification of the oldest reported collagen fibres encapsulated within a thin fluorapatite crust (Plet et al., 2016b). Further analyses of the vertebra revealed the oldest occurrence of red-blood cell like structures (albeit 10 x smaller than modern analogues) identified as stomatocytes (bowl-shaped red blood cells). In conclusion, we report the oldest occurrence of red blood cell-like structures, fossilised collagen and cholesterol (derived from bone marrow and adipose tissue) predating the occurrence of fibres and cell remains preserved in the fossil record by 108 Ma.

References

Bertazzo, S., Maidment, S.C.R., Kallepitis, C., Fearn, S., Stevens, M.M., Xie, H., 2015. Fibres and cellular structures preserved in 75-million–year-old dinosaur specimens. Nat. Commun. 6, 7352. doi:10.1038/ncomms8352

Coleman, M.L., Raiswell, R., 1995. Source of carbonate and origin of zonation in pyritiferous carbonate concretions: evaluation of a dynamic model. Am. J. Sci. 295, 282–308.

Kiriakoulakis, K., Marshall, J.D., Wolff, G.A., 2000. Biomarkers in a Lower Jurassic concretion from Dorset (UK). J. Geol. Soc. London. 157, 207–220. doi:10.1144/jgs.157.1.207

Melendez, I., Grice, K., Trinajstic, K., Ladjavardi, M., Greenwood, P., Thompson, K., 2013a. Biomarkers reveal the role of photic zone euxinia in exceptional fossil preservation: An organic geochemical perspective. Geology 41, 123–126. doi:10.1130/G33492.1

Melendez, I., Grice, K., Schwark, L., 2013b. Exceptional preservation of Palaeozoic steroids in a diagenetic continuum. Sci. Rep. 3, 2768. doi:10.1038/srep02768

Plet, C., Grice, K., Pagès, A., Ruebsam, W., Coolen, M.J.., Schwark, L., 2016a. Microbially-mediated fossil-bearing carbonate concretions and their significance for palaeoenvironmental reconstructions: A multi-proxy organic and inorganic geochemical appraisal. Chem. Geol. 426, 95–108. doi:10.1016/j.chemgeo.2016.01.026

Plet, C., Grice, K., Pages, A., Verrall, M., Coolen, M.J.., Ruebsam, W., Schwark, L., 2016b. Jurassic World: Soft tissue, molecular, and cellular palaeobiology of an ichthyosaur. Nat. Commun. (in Revis.

Wilson, D.D., Brett, C.E., 2013. Concretions as sources of exceptional preservation, and decay as a source of concretions: examples from the middle Devonian of New York. Palaios 28, 305–316. doi:10.2110/palo.2012.p12-086r

Occurrence of microbially mediated black sludge and cobble formations after a cyclonic event in Shark Bay, Western Australia

Matthew Campbell[1a], Prof. Kliti Grice[1b], Assoc. Prof. Marco Coolen[1c], Cornelia Wuchter[1d], Will Di Fulvio[1e], Therese Morris[2], Prof. Pieter Visccher[3], Richard Bush[4a], Girish Choppala[4b]

[1]WA-Organic and Isotope Geochemistry Centre, Curtin University, Kent Street, Bentley WA 6102,
[a]matthew.a.campbell1@postgrad.curtin.edu.au, [b]K.Grice@curtin.edu.au, [c]marco.coolen@curtin.edu.au,
[d]c_wuchter@hotmail.com, [e]william.difulvio@student.curtin.edu.au
[2]Applied Sedimentology & Marine Geoscience, Curtin University, Kent Street, Bentley WA 6102,
therese.morris@postgrad.curtin.edu.au,
[3]Center for Integrative Geosciences, University of Connecticut, Storrs, CT, USA, pieter.visscher@uconn.edu
[4]GeoScience, Southern Cross University, Military Road, East Lismore NSW 2480, [a]richard.bush@scu.edu.au,
[b]girish.choppala@scu.edu.au

On the 13th of March 2015 Shark Bay was hit by a category 3 cyclone, "cyclone Olywn", causing destructive wind gusts of up to 140 kilometres per hour and a record total of 122 mm of rain fell in 24 hours[1]. This event caused significant structural changes to a microbial system found in Hamelin pool. Immediately after the cyclone, Morris observed the formation of a black sludge occurring in the impacted area, this black sludge is currently assumed to be a mixture of reconstituted extracellular polymeric substances (EPS) from impacted microbial mats, anoxic sediments containing iron sulfide minerals, marine debris and terrestrial matter (i.e. plant material). Upon returning to the site on the 7th of July 2016 it was found that the black sludge had turned into mud cobbles (see example in figure below). The cobble formation is likely due to the black sludge rolling back and forth in marine sediments from tidal and wind action; furthermore, active binding of surrounding sediments in the cobbles is likely due to microbial activity (i.e. excretion of EPS)[2]. The central aim will be to investigate how the black sludge differs in organic and inorganic geochemical composition to the mud cobble as well as in microbial taxonomic and functional diversity in order to gain an understanding of how these formations develop. These mud cobbles might represent modern analogues of ancient carbonate concretions which are found throughout the geological record. This project could shed light into the major microbial players involved in concretion formation and provide evidence of how an episodic event such as a cyclone can contribute to the formation of carbonate concretions in microbial systems[3]. The major analytical techniques of this investigation will be X-ray diffraction (XRD)[4], stable carbonate isotope[5], genomic[6], lipid biomarker and compound specific (C, H and S) analyses[7,8]. Additionally, the role of biomolecular sulfurization occurring in the black sludge and mud cobbles will be established using Raney nickel desulfurization procedures to the C-S bound material[9].

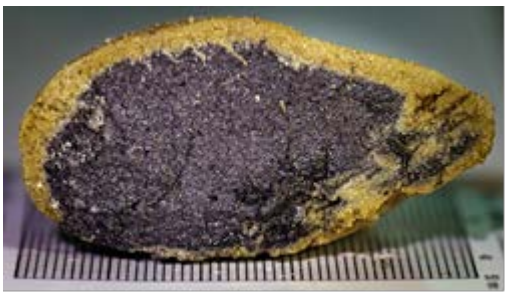

Figure 1. Cross-section of mud cobble (photographer: Aditya Chopra)

References

(1) May, S. M.; Gelhausen, H.; Brill, D.; Callow, N.; Engel, M.; Scheffers, A.; Joannes-Boyau, R.; Leopold, M.; Opitz, S.; Brückner, H. 2016; Vol. 18, p 1475.
(2) Dupraz, C.; Visscher, P. T. *Trends in Microbiology* **2005**, *13* (9), 429–438.
(3) Plet, C.; Grice, K.; Pagès, A.; Ruebsam, W.; Coolen, M. J. L.; Schwark, L. *Chemical Geology* **2016**, *426*, 95–108.
(4) Wang, G.-C.; Lu, T.-M. In *RHEED Transmission Mode and Pole Figures*; Springer New York, 2014; pp 55–71.
(5) Cerling, T. E.; Quade, J. In *Climate Change in Continental Isotopic Records*; Swart, P. K., Lohmann, K. C., Mckenzie, J., Savin, S., Eds.; American Geophysical Union, 1993; pp 217–231.
(6) Coolen, M. J.; Orsi, W. D. *Frontiers in microbiology* **2015**, *6*.
(7) Burlage, R. S. *Techniques in Microbial Ecology*; Oxford University Press, 1998.
(8) Pagès, A.; Grice, K.; Welsh, D. T.; Teasdale, P. T.; Van Kranendonk, M. J.; Greenwood, P. *Microbial ecology* **2015**, *70* (2), 459–472.
(9) Melendez, I.; Grice, K.; Trinajstic, K.; Ladjavardi, M.; Greenwood, P.; Thompson, K. *Geology* **2013**, *41* (2), 123–126.

Molecular, Isotopic and Genetic composition of human gallstones: a Geomedical study

Sureyya H. Kose[1]*, Marco Coolen[1], Kliti Grice[1], Mohammed Ballal[2]

[1]WA-OIGC, Department of Chemistry, Curtin University, WA 6102, Australia
[2]Fiona Stanley Hospital, Perth, Postcode, Australia
(corresponding author: sureyya.kose@postgrad.curtin.edu.au)*

Bacteria in the greater environment are seen to be responsible for a variety of concretions i.e. Stromatolites, oolites and calcium carbonate concretions[1,2]. The structure and shape of their concretionary product is closely linked to the nutrients available in their immediate environment (Ibid). Their environments can be ascertained by studying the molecular and isotopic structure of their fabricated products. It is believed that doing a similar study on human gallstones – as a possible by-product of bacterial metabolism, may yield similar information as to why gallstones form and the reason for their various morphologies/shapes. Long standing debates about the likelihood of biogenic or abiogenic processes developing various concretions in the natural environment are a regular point of contention when dealing with biomineralisation. The most notable of these debates centres on oolites, calcium carbonate nodules and, more recently, calcifications and lipid concretions in the human body. Although the current research has edged towards a more biogenic view with the former two topics, those involving the human body are only at the beginning of such debates. The objective of this study is to identify possible analogues between the human microbiome and the environment that lead to biomineralisation/concretionary structures within these systems. We will aim to investigate whether particular bacterial species are implicated in the crystallisation/accretion of gallstones in the gallbladder. We will compare these results with Oolites; calcium concretions found abundantly in various environmental contexts where bacterial precipitation of the calcium oxalate matrix is well understood. We hope this novel approach will reveal clues to the mechanisms behind lithogenesis of gallstones in the human body.

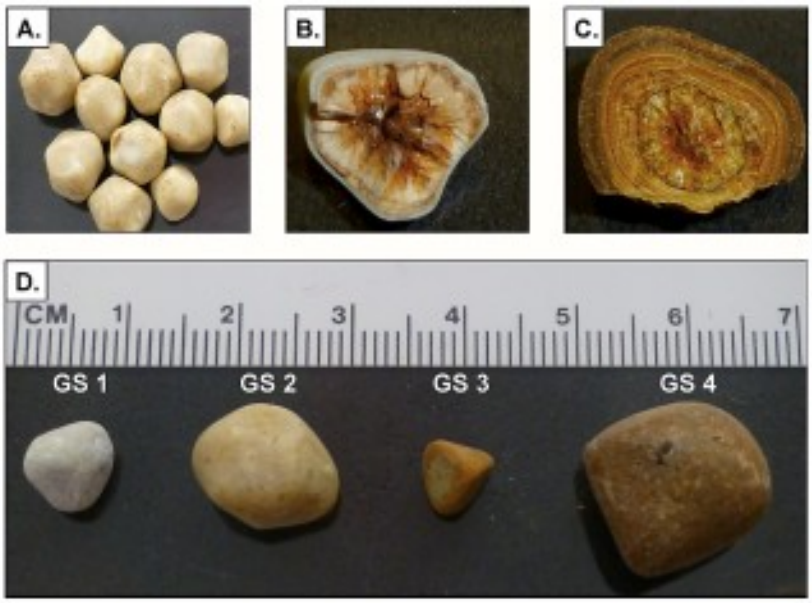

Fig 1[3].

References

1. Grice, K., Melendez, I., Tulipani, S., Jaraula, C. & Lorenz, S. (2014) Similarities between several major extinctions and preservation of life: Biomolecules to Geomolecules: An interdisciplinary approach, AESC abstracts 2014.
2. Summons, R.E., Bird, L.R., Gillespie, A.L., Pruss, S.B., Roberts, M., Sessions, A.L. (2013) Lipid biomarkers in ooids from different locations and ages: evidence for a common bacterial flora, Geobiology 11 (5), 420-436.
3. Marshall, Joanna M.; Flechtner, Alan D.; Perle, Krista M. La; Gunn, John S. (2014): Gross morphological features of patient gallstones employed in this study. Figure_1.tif. PLOS ONE. 10.1371/journal.pone.0089243.g001

A case study of oil-oil correlation in the Tarim Basin, China

Shaojie Li[1], Xuan-Ce Wang[1,*], Keyu Liu[1,2,3], Kliti Grice[4], Alex I. Holman[4], Peter Hopper[4]

[1]Department of Applied Geology, Curtin University, GPO Box U1987, Perth 6845, Australia
[2]Research Institute of Petroleum Exploration and Development, PetroChina, Beijing 100083, China
[3]China University of Petroleum, Qingdao, Shandong 266580, China
[4]Western Australia Organic and Isotope Geochemistry Centre, The Institute for Geoscience Research, Department of Chemistry, Curtin University, GPO Box U1987, Perth, WA 6845, Australia
(corresponding author: X.Wang3@curtin.edu.au)*

Tarim Basin is one of the largest petroliferous basins in China, encompassing over 40 oil and gas fields. However, the origins of the oils discovered are still poorly constrained due mainly to an ambiguous understanding of the major hydrocarbon source rocks and the complex tectonic evolution history of the basin. Biomarker and compound specific isotope analyses were used to investigate the oil-oil correlations in the basin. We presented GC-MS data of saturate and aromatic hydrocarbons on eight oil samples from the Tarim Basin. These data show that the studied samples can be classified into two distinct families. The first oil family is characterised by low pristine to phytane (Pr/Ph=0.84~0.97) and phenanthrene to dibenzothiophene (P/DBT=1.07~1.43) ratios, suggesting that they were derived from the source rock most likely formed in a reducing and sulphate-poor environment. The organic source of the oils is dominated by aquatic plants as indicated by the n-alkane hydrocarbon distribution parameters (e.g. the major n-alkane hydrocarbon of nC_{15} or nC_{14}, terrigenous/aquatic ratio (TAR) =0.18~0.27, $(nC_{21}+nC_{22})/(nC_{28}+nC_{29})$ =2.77~3.03 and $\Sigma nC_{21}-/\Sigma nC_{22}+$=2.25~3.40). Maturity indexes based on aromatic hydrocarbons show that the oils are of medium-high maturity levels. Oils of the first family are biodegraded showing obvious unresolved complex mixtures (UCM) in the total ion chromatograms (TIC) of the saturate hydrocarbons. The source rocks of the second oil family may be formed in a highly reducing and sulphate-poor environment because of their extremely low Pr/Ph (0.41~0.48) but large P/DBT (14.51~28.48) ratios. Aquatic organic matter is the predominant source but terrestrial higher plant may also contribute to the source considering the relative larger carbon number of the major n-alkane hydrocarbon (nC_{22}) and lower $\Sigma nC_{21}-/\Sigma nC_{22}+$ ratios (0.95~1.57). Inconsistencies in the maturity proxies from different aromatic biomarkers are observed in the second oil family. This may be caused by the mixing of oils of various thermal maturity levels. In contrast to the first oil family, there are minor humps on TIC of saturate hydrocarbons of the second oil families. Aromatic hydrocarbons of oils from the first family are characterized by more depleted $\delta^{13}C$ values compared with the second family. The cross-plots of P/DBT-$\delta^{13}C$ of dimethylnaphthalene (DMN) and Pr/Ph-$\delta^{13}C$ of DMN show that the source rocks of the first oil family are deposited in a marine carbonate environment with little or no terrigenous input, whereas oils of the second family might be derived from the source rock(s) with more terrestrial-sourced organic matter. Therefore, combined with traditional biomarkers, carbon isotopic compositions of DMN was suggested to be a potential tool for oil-oil correlations and provide significant insights to the origin of oils in the Tarim Basin.

Helium isotopic distribution of Australian natural gases

Chris J. Boreham[1], D.S. Edwards[1] and R.J. Poreda[2]

1) Resources Division, Geoscience Australia, GPO Box 378, Canberra, ACT 2601, Australia
2) Department of Earth & Environmental Sciences, University of Rochester, Rochester, USA
(corresponding author: chris.boreham @ga.gov.au for oral presentation) eCat 101684*

The isotopic composition of noble gases in natural gas accumulations has been the key to the understanding of their origins and their association with, and alteration of, the natural gas. For helium, the main tool in determining its source is the $^3He/^4He$ ratio (Rc/Ra), with a crustal (radiogenic) origin having a ratio of ~0.01–0.02 Ra (where Ra is the $^3He/^4He$ ratio of air = $1.4x10^{-6}$) and mantle origins ~8 Ra, and higher if mantle-plume associated (Prinzhofer, 2013).

Over 150 natural gases representative of Australia's hydrocarbon-producing sedimentary basins have been analysed for their helium abundance and isotopic composition (supplemented by partial isotopic compositions of the higher noble gases Ne, Ar and Kr). Helium shows abundance up to 1.5 mol% with the highest values in the Amadeus (central Australia) and Gunnedah basins, while $^3He/^4He$ ratios range from around 0.01 to 4.2 Ra (Figure 1). The Gunnedah Basin of south-east Australia and the Bass and Otway basins in southern Australia show the highest $^3He/^4He$ ratios, indicating a significant mantle contribution. Interestingly the adjacent Gippsland Basin has slightly lower $^3He/^4He$ ratios. The associated CO_2 has a relatively low abundance in the Gunnedah Basin (highest $^3He/^4He$ ratio) compared to some extreme concentrations of CO_2 in the Otway Basin, which are associate with recent volcanism. The onshore Bowen and Cooper basins of eastern Australia, where natural gases are predominately sourced from Permian coals, show intermediate $^3He/^4He$ ratios with the former having a higher mantle contribution. At the other end of the spectrum, low $^3He/^4He$ ratios characterise natural gases of the Bonaparte, Browse, Carnarvon and Perth basins in western and northern Australia where radiogenic helium predominates. The minor mantle contribution that is inferred for the He in these samples has a significant contribution from the volcanic and igneous intrusions throughout the region's evolution. The accompanying high CO_2 contents of some of these gases, together with their carbon isotopic composition, infer an inorganic source most likely from thermal decomposition of carbonates.

The geochemical data suggest that the origin of helium in Australian natural gas accumulations is region specific and complex with the component gases originating from multiple sources. The majority of He isotopic data indicate that CO_2 has been lost from most basins. The process by which CO_2 has been lost from the system is likely associated with either the precipitation of carbonates and/or loss through fluid flow (Prinzhofer, 2013).

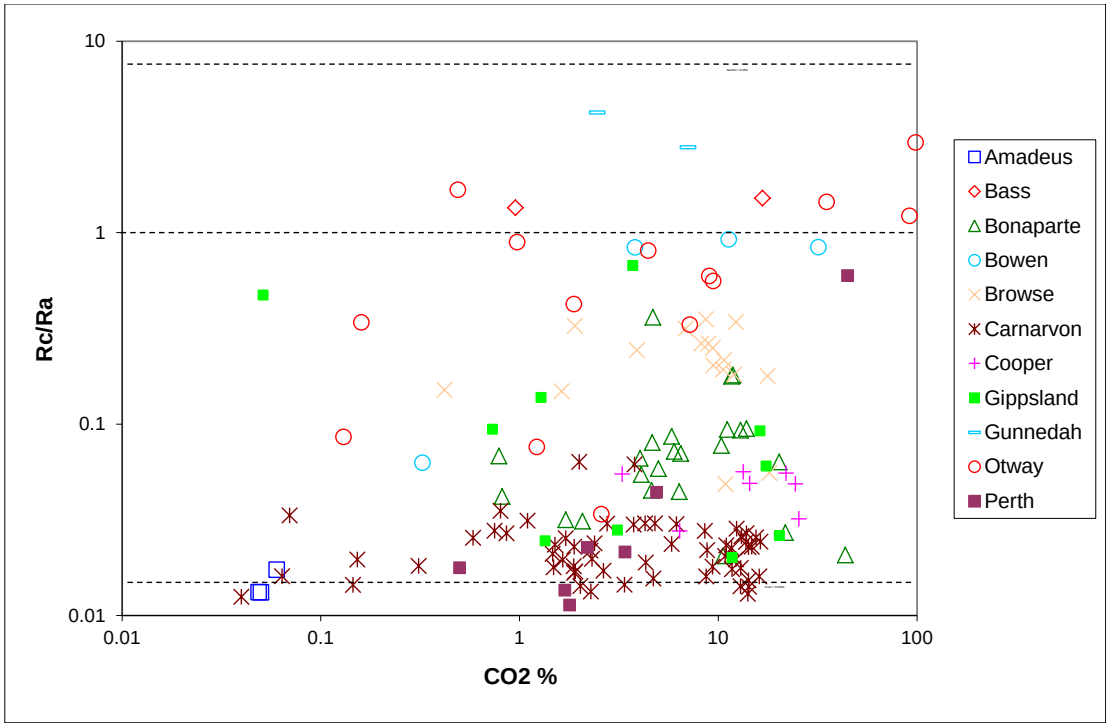

Fig 1. Helium isotopic composition (Rc/Ra) versus mol% CO_2 for Australian natural gases plotted by sedimentary basin. Note: Rc = $^3He/^4He$ ratio of the natural gas and Ra = the $^3He/^4He$ ratio of air.

References

Prinzhofer, A., 2013. Noble Gases in Oil and Gas Accumulations. *The Noble Gases as Geochemical Tracers*. Springer. 225-245.

The stable carbon isotopic compositions of individual n- alkanes and isoprenoids provide evidence of source contributions for petroleum generated from the Xihu Depression, East China Sea

Huiyuan Xu[1,2], Simon C. George[1,*], Dujie Hou[2]

[1] Department of Earth & Planetary Sciences, Macquarie University, North Ryde, Sydney, NSW, Australia
[2] School of Energy Resources, China University of Geosciences (Beijing), Beijing, 100083, China
(corresponding author: huiyuan.xu@students.mq.edu.au)*

n-Alkanes in rocks are derived from algae, photosynthetic bacteria, and leaf waxes of land plants. They are significant for identifying source inputs, and their carbon isotopic ($\delta^{13}C$) compositions provide more accurate biochemical information than molecular information alone. The $\delta^{13}C$ of individual hydrocarbons has been commonly used in making oil-source and oil-oil correlations. It is generally accepted that enrichment in ^{13}C (heavier $\delta^{13}C$ values) of odd carbon number n-alkanes (>n-C_{21}) is a source indicator of the input of higher plants (Collister et al., 1992). However, Zhou et al. (2010) studied the saw-tooth patterns of the $\delta^{13}C$ of these n-alkanes and showed that both odd and even carbon number n-alkanes could have originated from terrestrial higher plants, but via different biochemical pathways. The diverse source inputs shown by this parameter allow us to gain a better understanding of the origin of hydrocarbons from coal-derived petroleum systems.

The Xihu Depression in the East China Sea primarily produces light oil and condensate (low in density and wax content), and has been intensely studied for many years regarding its thermal maturity, redox conditions, and depositional environments. Dominant higher plant inputs to the source rocks are corroborated by abundant β-carotane and diterpenoids, a predominance of C_{29} over C_{27} and C_{28} steranes, and high Pr/Ph ratios (Su et al., 2013; Zhu et al., 2012). These parameters were derived mainly using pyrolysis, molecular biomarkers, or bulk carbon isotope compositions of the fluids. However, what remains unclear is the relative contributions of coal and terrigenous mudstone contributions to the generated oil and gas. Also, little is known regarding the cause of the differences in the compositions of the fluids, e.g. enormous $\delta^{13}C$ excursions (> 4‰) in the long-chain n-alkanes (>n-C_{23}) (Fig. 1), ^{13}C-enrichment or -depletion of n-C_{17} (Fig. 1), saw-tooth pattern in the high molecular weight n-alkanes, and trends of either increasing or decreasing Pr and Ph $\delta^{13}C$ values with depth. These seems to have resulted from (1) complex interbedded coals and mudstones, (2) variations of higher plant biomarker (diterpenoids) contributions between species (Fig. 1), e.g. phyllocladane derived from resins of *Podocarpaceae, Araucariaceae, Taxodiaceae and Cupressaceae* (Noble et al., 1985; Otto et al., 1997; Rieley et al., 1991; Schulze and Michaelis, 1990), and (3) biochemical reworking (Murray et al., 1994). Hence, further research has been undertaken on the precise correlations and specific differences, e.g. variation in n-alkane carbon isotopes for different carbon chain-lengths. A general trend towards isotopically lighter values with increasing carbon numbers is observed, which is consistent with typical fluvial/lacustrine depositional settings (Murray et al., 1994). There are evident differences between the Pinghu and Huangyan oil field samples. The n-alkane $\delta^{13}C$ values of the Pinghu oils are generally heavier (-22‰ to -30‰) relative to the Huangyan oils (-24‰ to -34‰). Surprisingly, $\delta^{13}C$ excursions of short-chain n-alkanes (<n-C_{23}) and long-chain n-alkanes (>n-C_{23}) can be readily identified in the Pinghu and Huangyan oil field samples (Fig. 2). We attributed these phenomena mostly to source input variations between coals and mudstones with respect to algae and terrestrial higher plants (Boreham et al., 1994; Collister et al., 1992; Murray et al., 1994; Sun et al., 2000). In order to discriminate coal or mudstone contributions to the fluids, the $\delta^{13}C$ patterns of coals and mudstones has been established. Oils generated from coals show decreasing $\delta^{13}C$ values with chain-length within a narrow range (approx. 2-3 ‰), whereas oils from the mudstones are more depleted in ^{13}C with increasing carbon number (n-$C_{20\text{-}30}$). Some samples that are exceptions have relatively heavier $\delta^{13}C$ values for low molecular weight n-alkanes, which could be due to their derivation from isotopically heavy algae such as Botryococcus (Boreham et al., 1994). Another noteworthy distinction is that the $\delta^{13}C$ values of Pr are heavier than those of Ph by up to 1.8‰ (on average) for the Huangyan oils, whereas the opposite is true for the Pinghu samples, in which Pr is lighter or similar in $\delta^{13}C$ relative to Ph. This is suggestive of separate origins for the two isoprenoids. These isotope profiles reveal connections between the oils, coals, and mudstones, and allow determination of the patterns and variations for different hydrocarbon contributions. Our results, combined with biomarkers, provide a unique comparison for the genesis and origin of petroleum generated from the Xihu Depression.

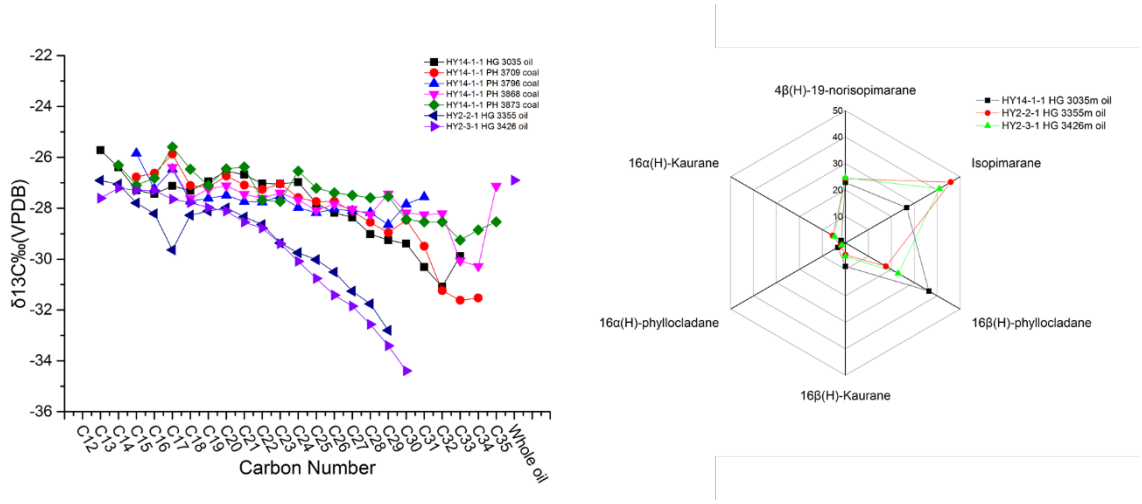

Fig. 1 n-Alkane isotope profiles of oils and coals from the Huangyan oil field and the radar plot graphs of diterpenoids from the Huangyan oils: 4β(H)-19-norisopimarane, isopimarane, 16β(H)-phyllocladane, 16β(H)-Kaurane, 16α(H)-phyllocladane, 16α(H)-Kaurane.

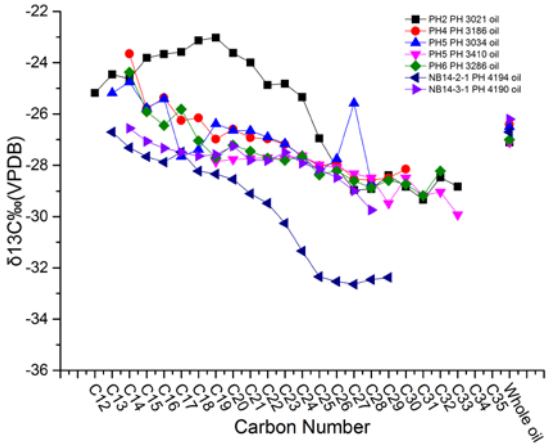

Fig. 2 n-Alkane isotope profiles of oils from the Pinghu oil field.

References

Boreham, C.J., Summons, R.E., Roksandic, Z., Dowling, L.M., Hutton, A.C., 1994. Chemical, Molecular And Isotopic Differentiation Of Organic Facies In the Tertiary Lacustrine Duaringa Oil-Shale Deposit, Queensland, Australia. Organic Geochemistry 21, 685-712.
Collister, J.W., Summons, R.E., Lichtfouse, E., Hayes, J.M., 1992. An isotopic biogeochemical study of the Green River oil shale. Organic Geochemistry 19, 265-276.
Murray, A.P., Summons, R.E., Boreham, C.J., Dowling, L.M., 1994. Biomarker and n-alkane isotope profiles for Tertiary oils: relationship to source rock depositional setting. Organic Geochemistry 22, 521-IN526.
Noble, R.A., Alexander, R., Kagi, R.I., Knox, J., 1985. Tetracyclic Diterpenoid Hydrocarbons in Some Australian Coals, Sediments and Crude Oils. Geochimica Et Cosmochimica Acta 49, 2141-2147.
Otto, A., Walther, H., Puttmann, W., 1997. Sesqui- and diterpenoid biomarkers preserved in Taxodium-rich Oligocene oxbow lake clays, Weisselster basin, Germany. Organic Geochemistry 26, 105-115.
Rieley, G., Collier, R.J., Jones, D.M., Eglinton, G., Eakin, P.A., Fallick, A.E., 1991. Sources Of Sedimentary Lipids Deduced From Stable Carbon Isotope Analyses Of Individual Compounds. Nature 352, 425-427.
Schulze, T., Michaelis, W., 1990. Structure and Origin of Terpenoid Hydrocarbons in Some German Coals. Organic Geochemistry 16, 1051-1058.Su, A., Chen, H., Wang, C., Li, P., Zhang, H., Xiong, W., Lei, M., 2013. Genesis and maturity identification of oil and gas in the Xihu Sag, East China Sea Basin. Petroleum Exploration and Development 40, 558-565.
Sun, Y., Sheng, G., Peng, P.a., Fu, J., 2000. Compound-specific stable carbon isotope analysis as a tool for correlating coal-sourced oils and interbedded shale-sourced oils in coal measures: an example from Turpan basin, north-western China. Organic Geochemistry 31, 1349-1362.
Zhou, Y., Grice, K., Stuart-Williams, H., Farquhar, G. D., Hocart, C. H., Lu, H., & Liu, W. (2010). Biosynthetic origin of the saw-toothed profile in δ 13 C and δ 2 H of n-alkanes and systematic isotopic differences between n-, iso-and anteiso-alkanes in leaf waxes of land plants. Phytochemistry, 71(4), 388-403.
Zhu, Y., Li, Y., Zhou, J., Gu, S., 2012. Geochemical characteristics of Tertiary coal-bearing source rocks in Xihu depression, East China Sea basin. Marine and Petroleum Geology 35, 154-165.

Organic Geochemical Characterisation of Aliphatic Fractions of Pliocene Sapropels From ODP Sites 964 and 967, Eastern Mediterranean Basin

Simon C. George[1,*], Huiyuan Xu[1,2], Stefan C. Löhr[1], Martin J. Kennedy[1]

[1] Department of Earth & Planetary Sciences, Macquarie University, North Ryde, Sydney, NSW, Australia
[2] School of Energy Resources, China University of Geosciences (Beijing), Beijing, 100083, China
(corresponding author: simon.george@mq.edu.au)*

Sapropels are fine-grained, organic carbon-rich sediments that are cyclically interbedded with organic-lean marls. They are a conspicuous feature of the sedimentary record of the Mediterranean Basin (Emeis et al., 2000) and have been extensively studied to assess the relative importance of climatic, oceanographic as well as continental influences on the formation of organic-rich mudstones (Rohling et al., 2015). Their deposition has been linked to orbital forcing of the African monsoon (Rossignol-Strick, 1983), with increased fluvial inputs leading to stratification of the Mediterranean during Northern Hemisphere insolation maxima (Rohling et al., 2015). Deposition of Pliocene sapropels under periodically anoxic to sulphidic conditions is demonstrated by preserved sediment lamination, the absence of benthic fauna and/or the dominance of low-oxygen adapted species (Löhr and Kennedy, 2015; Rohling et al., 1993), elevated concentrations of redox-sensitive trace elements (Nijenhuis et al., 1999), an abundance of framboidal pyrite (Passier et al., 1999), and the presence of isorenieretane or its derivatives (Passier et al., 1999), a biomarker characteristic of anoxygenic photosynthetic green sulphur bacteria. Four microfacies (MF) have been identified on the basis of bulk composition, microfabric, organic matter distribution/morphology, and the degree of biological reworking (Löhr and Kennedy, unpublished data).

Here we examine the organic geochemistry of three sapropels: 284A from 80.2 m in ODP Site 964, and 280C and 284C from 79.5 m and 80.4 m in ODP Site 967. A key motivation for the organic geochemical analyses was to test the relative magnitude of diatom input to the various microfacies. Sapropel 284C has a TOC of 8-10%, and is composed of MF2, which has a high bulk carbonate content (>40%) and a uniform to weakly laminated microfabric. The bulk of the organic carbon is present as organoclay aggregates. Sapropel 284A has a TOC of 11%, and is composed of MF3B which has a low carbonate content uniform and a weakly laminated microfabric. Sapropel 280C has a TOC of 8-15% and is composed of MF3A, which has a low carbonate content and a strongly laminated microfabric, and its reworked equivalent MF4A. On the basis of these properties we predicted that sapropels 284A and 280C would contain more diatom biomarkers relative to the carbonate-rich sapropel 284C.

Highly branched isoprenoids (HBIs) are widely used biomarkers for rhizosolenid diatom input (Sinninghe Damsté et al., 2004). Saturated C_{25} HBI and small amounts of C_{25} HBI dienes and trienes are present in sapropel 284C, but not in the other two sapropels that we interpret to be dominated by mat-forming diatoms (MF3A and 3B) (Fig. 1). Additionally, a series of unknown compounds that may be related to the HBIs were detected only in sapropel 284C. These results show that, in addition to the calcareous plankton input evident from SEM and geochemical analyses, diatoms contributed to MF2. There are several possible explanations for the absence of diatom biomarkers in the other sapropels. Only five out of > 200 diatom genera are known to produce HBIs (*Haslea, Pleurosigma, Rhizosolenia, Navicula, Berkleya*), and not all species within these genera produce these characteristic lipids (Brown et al., 2014). Many hundreds of species of diatoms have not had their lipid geochemistry determined, so possibly a diatom species that does not produce HBIs may have contributed to these sapropels. Another possibility is that the precursor C_{25} HBI alkenes were quantitatively sulphurised during early diagenesis, and are thus present but unanalysed in the polar fraction. This possibility is being tested.

References

Brown, T.A., Belt, S.T. , Cabedo-Sanz, P., 2014. Identification of a novel di-unsaturated C_{25} highly branched isoprenoid in the marine tube-dwelling diatom Berkeleya rutilans. Environmental Chemistry Letters 12, 455–460.
Emeis, K.-C.C., Sakamoto, T., Wehausen, R., Brumsack, H.-J., 2000. The sapropel record of the eastern Mediterranean Sea—results of Ocean Drilling Program Leg 160. Palaeogeogr. Palaeoclimatol. Palaeoecol. 158, 371–395.
Nijenhuis, I.A., de Lange, G.J., 2000. Geochemical constraints on Pliocene sapropel formation in the eastern Mediterranean. Marine Geology 163, 41–63.
Passier, H.F., Middelburg, J.J., de Lange, G.J., Böttcher, M.E., 1999. Modes of sapropel formation in the eastern Mediterranean: some constraints based on pyrite properties. Marine Geology 153, 199–219.
Rossignol-Strick, M., 1983. African monsoons, an immediate climate response to orbital insolation. Nature, 304, 46–49.
Rohling, E.J., de Stigter, H.C., Vergnaud-Grazzini, C., Zaalberg, R., 1993. Temporary repopulation by low-oxygen tolerant benthic foraminifera within an Upper Pliocene sapropel: Evidence for the role of oxygen depletion in the formation of sapropels. Mar Micropaleontol 22, 207–219.
Rohling, E.J., Marino, G., Grant, K.M., 2015. Mediterranean climate and oceanography, and the periodic development of anoxic events (sapropels). Earth-Sci Rev, 143(C), 62–97.
Sinninghe Damsté, J.S., Muyzer, G., Abbas, B., Rampen, S.W., Massé, G., Allard, W.G., Belt, S.T., Robert, J.-M., Rowland, S.J., Moldowan, J.M., Barbanti, S.M., Fago, F.J., Denisevich, P., Dahl, J., Trindade, L.A.F., Schouten, S. 2004. The rise of the rhizosolenid diatoms. Science 304, 584–587.

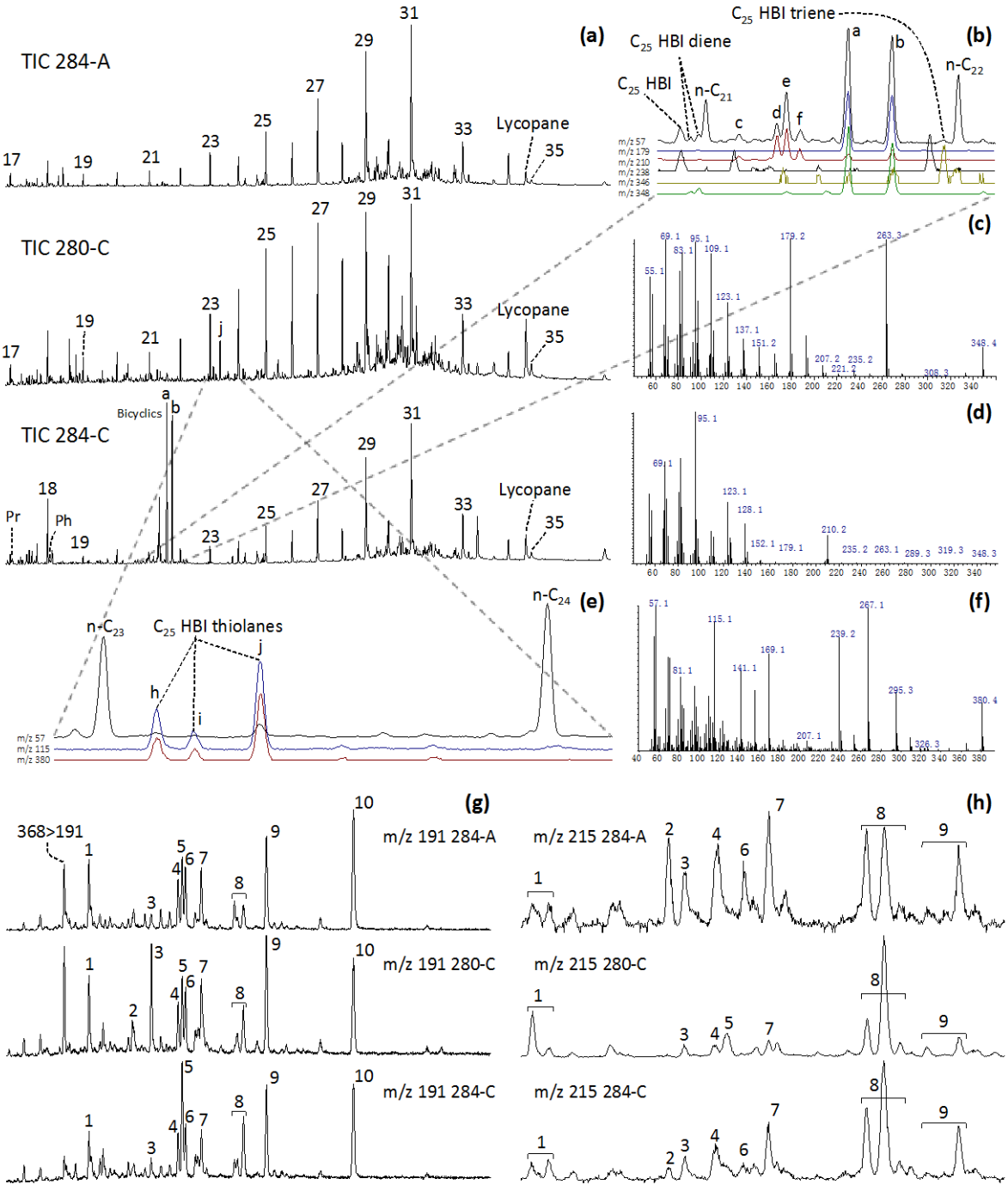

Fig. 1. (a) Total ion chromatograms of the aliphatic fractions of sapropels 284A, 280C, and 284C. (b) Partial mass chromatograms (*m/z* 57, 179, 210, 238, 346, 348) of sapropel 284C, showing the distribution of C_{25} HBI, C_{25} HBI-dienes, C_{25} HBI-triene and C_{25} HBI bicyclic compounds a and b relative to *n*-alkanes. (c) Mass spectra of compound a. (d) Mass spectra of compound d. (e) Partial mass chromatograms (*m/z* 57, 115, 380) of 280-C showing the distribution of C_{25} HBI thiolanes relative to *n*-alkanes. (f) Mass spectra of thiolane peak j. (g) Partial mass chromatograms (*m/z* 191) for sapropels 284A, 280C, and 284C. (h) Partial mass chromatograms (*m/z* 215) for sapropels 284A, 280C, and 284C. Peak identifications for (g): 1 = 17β-22,29,30-trisnorhopane; 2 = C_{29} norneohop-13(18)-ene + C_{29} αβ norhopane; 3 = C_{30} hop-17(21)-ene; 4 = C_{30} αβ hopane; 5 + 6 = C_{30} neohop-13(18)-enes?; 7 = C_{29} ββ norhopane + C_{30} βα moretane; 8 = C_{30} pentacyclic triterpenes; 9 = C_{30} ββ hopane; 10 = C_{31} ββ homohopane. Peak identifications for (h): 1 = C_{27} sterene; 2 = C_{28} steradiene; 3 = C_{27} steradiene + C_{28} steratriene; 4 = C_{28} sterene; 5 = C_{28} sterene; 6 = C_{28} steradiene; 7 = C_{27} sterene + C_{28} steradiene; 8 = C_{29} sterene; 9 = C_{29} steradiene.

Thoughts on the carbon isotopic composition of fluid inclusion gases from Scott Reef area in Browse Basin

Se Gong[1], S. Sestak[1], S[1]. Armand[1], J. van Holst[1], J. Bourdet[2], R. Kempton[2], E, Grosjean[3]

1) CSIRO Energy, North Ryde, NSW, 2113 Australia (Se.Gong@csiro.au)
2) CSIRO Energy, Kensington, WA, 6151 Australia
3) Geoscience Australia, Canberra, ACT, 2601 Australia

Torosa is a gas field located on the northeast oriented Scott Reef Trend in the central part of the Browse Basin. The gas is contained within the Jurassic deltaic sands from the Plover Formation (Fm), containing an intra-formation shale break possibly acting as an internal barrier, sealed by the Lower Vulcan Fm, the Echuca Shoals Fm and the Jamieson Fm. An investigation of the fluid inclusions (FIs) in the gas reservoirs of the Browse Basin has shown the existence of an early oil charge [1] detected just below the seal at North Scott Reef-1. A recently developed technique on carbon isotope analysis of bulk FI gases allowed us to further explore geochemical information on FIs hosted in Torosa-5 and North Scott Reef-1 sandstones with the aim of providing insights on the gas exploration in the Scott Reef area and on the compartmentalization of the gas field.

Four samples have been analysed for carbon isotopes of FI gases. One sample is from an identified palaeo-oil column within the gas zone (4110 m), two samples are from a deeper part of the gas zone below the shale break (4559 m and 4512 m) and one sample is from the water zone (4611 m). Results show carbon isotopes of methane ($\delta^{13}C\ C_1$) and CO_2 ($\delta^{13}C\ CO_2$) trapped in water inclusions in Torosa-5 are ranging from -35.5 ‰ to -39 ‰ and -5.8 ‰ to -3.4 ‰, respectively. The $\delta^{13}C\ C_1$ and $\delta^{13}C\ CO_2$ values of gases associated with oil inclusions in the North Scott Reef-1 are -41.9 ‰ and -11.5 ‰, respectively**.** The $\delta^{13}C\ C_1$ and $\delta^{13}C\ CO_2$ values of current reservoired gases in the Torosa-5 and Torosa-1 are -41.3 ‰ to -39.8 ‰ and -2.7 ‰ to -1.2 ‰, respectively.

Since the technique is based on a crushing method, the carbon isotope signatures of trapped gasses of magmatic origin in quartz grains cannot be deconvolved from diagenetic inclusions. However, insights into the organic origin of gasses could be made from this analysis. The $\delta^{13}C\ CO_2$ value associated with the palaeo-oil column sample in North Scott Reef-1 indicates an organic origin, while the $\delta^{13}C\ CO_2$ value of water inclusions in Torosa-5 does not show the same signature. It can then be speculated that the $\delta^{13}C\ CO_2$ signature from the palaeo-oil zone sample is due to CO_2 with a thermogenic signature associated with the oil. In terms of methane, the $\delta^{13}C\ C_1$ values of the FI gases overall indicate a thermogenic origin. The $\delta^{13}C\ C_1$ values of the current reservoired gases in the Torosa wells is close to that of oil inclusions in North Scott Reef-1, probably indicating a similar source. However more enriched ^{13}C of trapped methane in the gas zone of Torosa-5 below the shale break comparing to the current reservoired gases probably indicates a higher maturity signature, suggesting a possible compartmentalization of the reservoir and the existence of higher maturity gas. Alternatively it might be due to fractionation caused by wettability of the rocks, equilibrium time between water and methane during trapping or diffusion effects during migration [2-3] considering the differences of $\delta^{13}C\ C_1$ and $\delta^{13}C\ CO_2$ values of FI gases between the gas zone and water zone in Torosa-5.

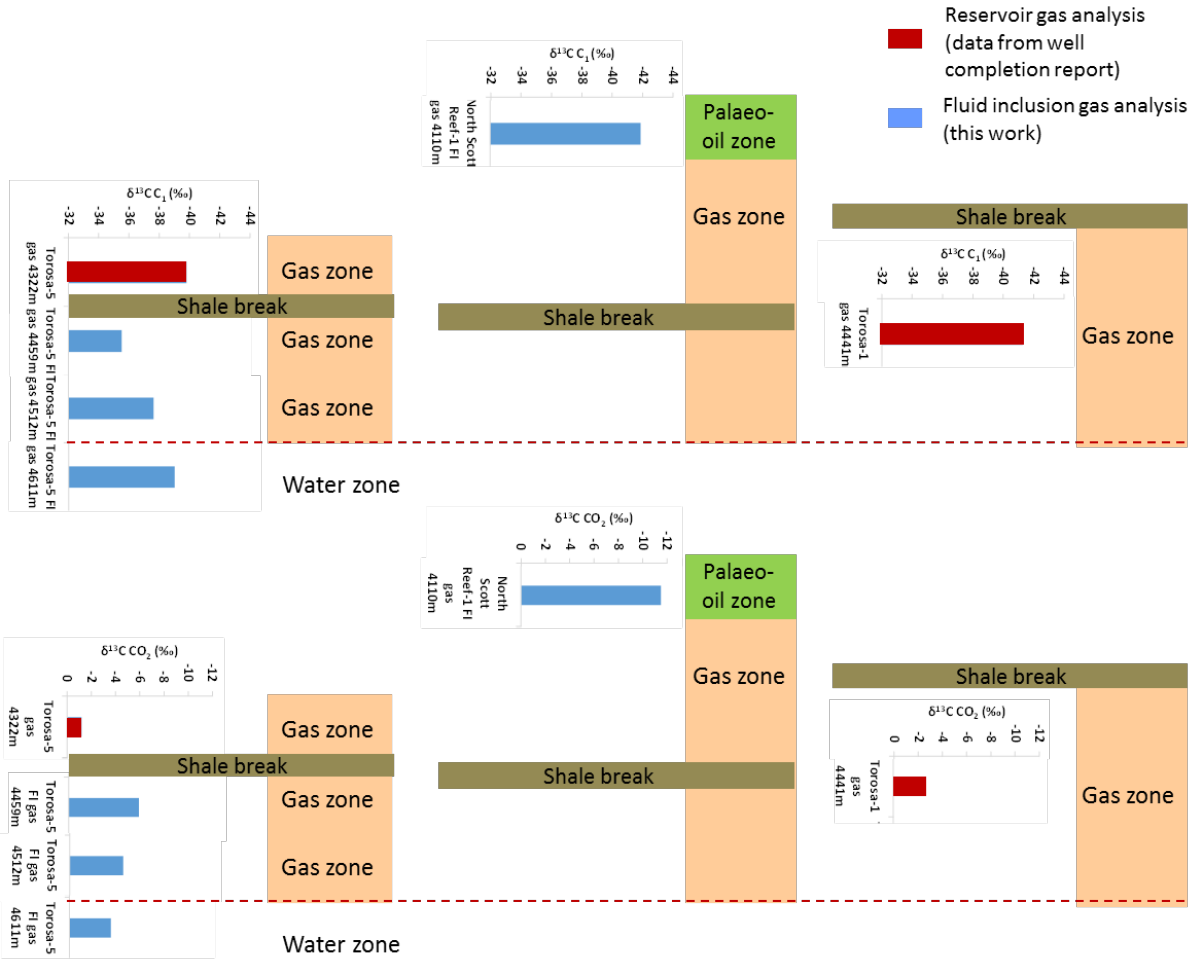

Figure 1: Carbon isotopes of CH_4 (top) and CO_2 (bottom) in the FIs and reservoir gases in the Torosa-5, Torosa-1 and North Scott Reef-1

References:

[1] Brincat, M.P., Lisk, M., Kennard, J.M., Bailey, W.R. & Eadington, P.J., 2004. Evaluating the oil potential of the Caswell Sub-basin: Insights from fluid inclusion studies. In: *Timor Sea Petroleum Geoscience, Proceedings Of The Timor Sea Symposium, Darwin, Northern Territory, 19-20 June 2003* (eds G.K. Ellis, P.W. Baillie and T.J. Munson), Northern Territory Geological Survey, Special Publication 1, pp. 437- 454.

[2] Qin, S., Tang, X., Song, Y. and Wang, H. (2006) Distribution and fractionation mechanism of stable carbon isotope of coalbed methane. *Science in China Series D: Earth Sciences* 49, 1252-1258.

[3] Szaran, J. (1998) Carbon isotope fractionation between dissolved and gaseous carbon dioxide. *Chemical Geology* 150, 331-337.

Shale petroleum resources of Western Australia: an overview

K. Ameed R. Ghori[1]

[1]*Geological Survey of Western Australia, Department of Mines and Petroleum, East Perth, 6004, Australia*

Shale reservoirs are the richest in petroleum (oil and gas) resources because they retain significant amounts of hydrocarbons even after expulsion to conventional reservoirs. Production from these resources in the United States has transformed its energy position from importing to exporting during the last decade. This paper briefly reviews the potential for shale petroleum plays in Western Australia with reference to the development of these resources in the United States. The assessments of basins presented are mainly based on petroleum geochemical studies undertaken by the Geological Survey of Western Australia (GSWA), predominantly for conventional petroleum resources. The stratigraphy and vast geographic extent of onshore Western Australian basins suggest a high potential for shale petroleum resources. Basins rated with high to low potential include the Paleozoic Canning Basin, the Paleozoic–Mesozoic Perth Basin, the Paleozoic Southern Carnarvon Basin, and the Neoproterozoic Officer Basin, respectively (Fig. 1).

The search for shale petroleum resources started with Woodada Deep 1 (2010) and Arrowsmith 2 (2011) in the Perth Basin to evaluate shale-petroleum potential of the Permian Carynginia Formation and the Triassic Kockatea Shale, and Nicolay 1 (2011) in the Canning Basin to evaluate the shale-gas potential of the Ordovician Goldwyer Formation. Estimated total shale-petroleum potential for these formations is about 288 trillion cubic feet (Tcf) gas. Other petroleum source rocks include the Devonian Gogo and Lower Carboniferous Laurel formations of the Canning Basin, the Lower Permian Wooramel and Byro groups of the onshore Carnarvon Basin and the Neoproterozoic shales of the Officer Basin, These source rocks may also host shale-petroleum resources, in addition to the Goldwyer and Carynginia formations and the Kockatea Shale. The Canning and Perth basins are producing petroleum, whereas the onshore Carnarvon and Officer basins are not producing but have indications for petroleum source rocks, generation, and migration from petroleum geochemistry data.

In Western Australia, technically recoverable shale petroleum resources have been estimated for the Permian Carynginia Formation is up to 25 trillion cubic feet (Tcf) gas, and within the Triassic Kockatea shales is up to 8 trillion cubic feet (Tcf) gas with 500 million barrels oil/condensate (Kuuskraa et al., 2013)., and for the Ordovician Goldwyer Formation, Canning Basin at about 229 Tcf gas. These initial estimates were completed as a part of the World Shale Gas Resources study by Advance Resources International Inc. for the United States Energy Information Administration in 2013 (Kuuskraa et al, 2013), and studies are underway to verify these estimates.

All these source rocks are untested for petroleum production potential as compared to the petroleum-rich shales of the United States, which are mostly marine shale source rocks. The Ordovician Goldwyer Formation, Permian Carynginia Formation, and Triassic Kockatea Shale are also marine source rocks, but they may have different petroleum richness, geological and fracturing characteristics required for unlocking the reservoired petroleum (Cooper et.al., 2015). In the United States, shale-plays take up to five years to convert to commercial-plays, where infrastructure is well developed with all necessary facilities and expertise for geological evaluation, drilling, fracturing, and production. These facilities are, currently, lacking in Western Australia and need to be developed. Few vertical shale-gas wells have been completed and successfully fractured, and are the subject of geological studies to understand how shale-petroleum is stored and can be effectively produced. These wells laid the foundation to expand facilities and expertise for shale-petroleum exploration and development in Western Australia. The oil recovery from the Kockatea Shale in Arrowsmith 2 was the first proven shale-oil play in the Western Australia.

Currently, the Ordovician Goldwyer Formation, Permian Carynginia Formation and Triassic Kockatea Shale is a focus for exploration and research to evaluate its tight-petroleum potential. Exploration is at a very early stage and much more work is needed to estimate and verify the shale-petroleum resources of the vastly underexplored onshore Western Australian basins, By comparison, the Western Australian basins have only four vertical shale-plays wells in the last 6 years in comparison with thousands of horizontal wells in the United States.

Keywords: petroleum geochemistry, petroleum systems, source-rock quality, thermal maturity, self-sourcing reservoirs, Western Australia.

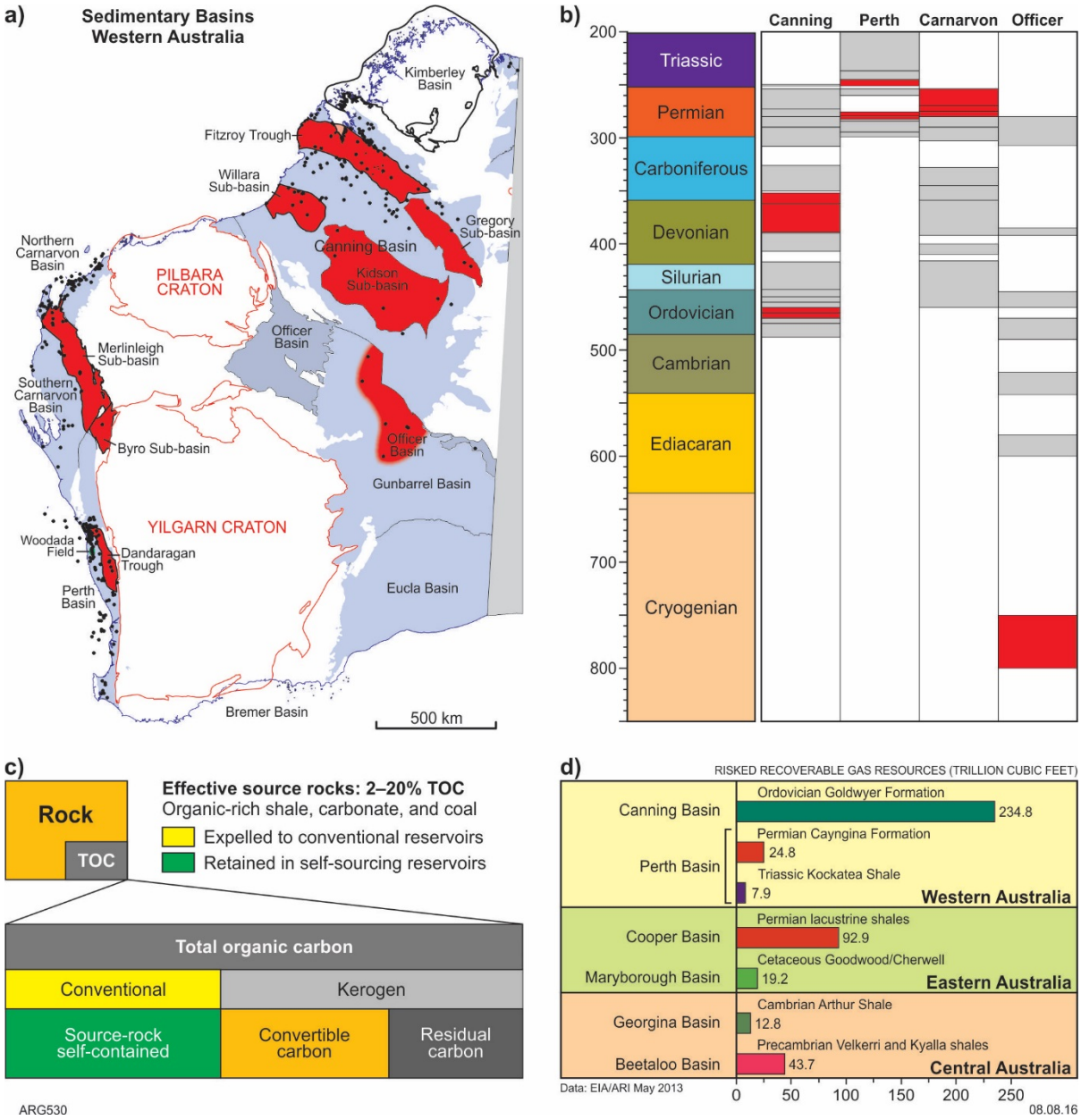

Fig. 1. This figure summarizes: a) map of Western Australia showing depocentre (red) in the Canning, Carnarvon, Officer, and Perth basins, which are target for shale resources; b) generalised stratigraphy of the Canning, Carnarvon, Officer, and Perth basins containing source rocks units (red); c) showing effect source and self-contained reservoirs (green); d) technically recoverable shale resources of Australian basins.

References

Cooper, G., R. Xiang, N. Agnew, P. Ward, M. Fabian and N. Tupper, 2015, A systematic approach to unconventional play analysis: the oil and gas potential of the Kockatea and Carynginia formations, North Perth Basin, Western Australia: APPEA Journal 2015, v. 55, p. 193–214..

Ghori, K. A. R., 2013, Emerging unconventional shale plays in Western Australia: APPEA Journal, v. 53, p.313–336.

Ghori, K. A. R., 2015, Petroleum systems of the Perth Basin, Western Australia: AAPG! SEG International Conference and Exhibition, 13-16 September 2015 Melbourne Australia.

Kuuskraa, V. A., Stevens, S. H., Moodhe, K. D., 2013, Australia, *in* Advanced Resources International Inc. for U.S. Energy Information Administration, technically recoverable shale oil and gas resources: an assessment of 137 shale formations in 41 countries outside the United States, prepared by: US. Department of Energy Washington, DC 20585, p. III-1–III-49.

Geochemistry of dew point petroleum systems, Browse Basin, Australia.

Dianne S. Edwards[1], Emmanuelle Grosjean[1], Tehani Palu[1], Nadege Rollet[1], Lisa Hall[1], Chris J. Boreham[1], Alex Zumberge[2], John Zumberge[2], Andrew P. Murray[3], Prince Palatty[1], Neel Jinadasa[1], Kamal Khider[1] and Tamara Buckler[1]

[1]Resources Division, Geoscience Australia, GPO Box 378, Canberra ACT 2601, Australia
[2]GeoMark Research, Ltd., Houston, Texas, USA
[3]Murray Partners PPSA Pty. Ltd., Perth
(corresponding author: dianne.edwards@ga.gov.au for oral presentation)*

The Browse Basin is located offshore on Australia's North West Shelf and is a proven hydrocarbon province hosting gas with associated condensate; however, oil reserves are small. The assessment of a basin's oil potential traditionally focusses on either the presence or absence of oil-prone source rocks. However, light oil can be found in basins where the primary hydrocarbon type is gas-condensate and oil rims form whenever these fluids migrate into reservoirs at pressures below their dew point (or saturation pressure). The relationship between dew point pressure and condensate-gas ratio (CGR) depends on the liquid composition and is therefore a petroleum system characteristic (Fig. 1). By combining geochemical studies of source rocks and fluids with petroleum systems analysis, the four Mesozoic petroleum systems identified by their geochemical fingerprints (Rollet et al., 2016) can be correlated with several gas-prone (dew point) petroleum systems:

1. Gas-condensates generated and reservoired within the Lower–Middle Jurassic Plover Formation are derived from terrestrial organic matter in fluvio-deltaic to pro-deltaic environments. Such gas is dominated by methane (gas dryness* = 91%), with ideal condensate-gas ratios (CGRs) ranging between 7 and 35 bbl/MMscf. Liquids recovered from wells tested along the Scott Reef Trend (e.g. Calliance, Brecknock and Torosa) comprise pale yellow condensates (49–53° API gravity), as do those from the deepest (Plover) reservoirs within the Ichthys gas accumulation (e.g. Gorgonichthys). These liquids plot on Figure 1 as dew point fluids. The molecular and carbon isotopic signatures of these condensates are similar, classifiying them into a single family (W1_1BRO) in Figure 2. The biomarkers providing the strongest discrimination are the high relative abundances of C_{29} sterane and C_{19} tricyclic triterpane, coupled with an enrichment in $\delta^{13}C$ of their saturated and aromatic hydrocarbon fractions testifies to their terrestrial organic origin.

2. Fluids with similar bulk properties (gas dryness = 91%; ideal CGRs 27–52 bbl/MMscf) to those of the aformentioned Plover-sourced fluids are found in the greater Crux accumulation in the Heywood Graben. The pale yellow condensates (47°API gravity) also exhibit similar biomarker assemblages as the W1_1BRO family. However, due to their greater enrichment in $\delta^{13}C$, the condensates plot as a separate family (W1_2BRO) in Figure 2. A difference in thermal maturity is also noted, with the Crux accumulation having lower maturity (calculated vitrinite reflectance[#] [Rc] = 0.77%) relative to the condensates on the Scott Reef Trend (av Rc = 1.18%). The most likely source rocks for the Crux fluids are the terrestrially-dominated Plover Formation coals and shales, but shaly coals also occur within the thick Upper Jurassic section in the northern part of the basin. These fluids are categorised as a separate dew point system within the Heywood Graben (Fig. 1).

3. Gas-condensates reservoired within the Brewster Member of the upper Vulcan Formation in the Ichthys/Prelude and Burnside accumulations have a greater liquid content than the aformentioned gases, with ideal CGRs of 22–151 bbl/MMscf at Titanichthys 1 and a gas dryness of 84%. The pale yellow condensates have API gravities of 55° and are potentially a separate intraformational dew point petroleum system within the central Caswell Sub-basin. Their biomarker and isotopic signatures indicate derivation from mixed marine and land-plant organic matter and plot as another family (W2W3_1BRO; Fig. 2). The source of these fluids is probably the organic-rich shales of the Upper Jurassic–Lower Cretaceous Vulcan Formation that encase the Brewster Member sandstone reservoir. PVT data for Brewster-reservoired fluids is affected by synthetic mud contamination, which has an impact on the measured dew point pressures. In the absence of measured values, a similar phase behaviour to North Sea (UK) gas-condensates (England, 2002) is assumed.

4. The Cretaceous reservoir in Caswell contains an unbiodegraded brown 'light oil' (47°API gravity) but PVT data are not available. Biomarker and isotope signatures show that the liquids were generated from source rocks containing both marine and terrigenous organic matter lying within the early oil window ($Rc^{\#}$ = 0.75%). They correlate with the Yampi Shelf biodegraded oils (W3_1BRO, Fig. 2), gas at Adele, and with extracts of the Lower Cretaceous Echuca Shoals Formation (Boreham et al., 1997). However, these marine shales have low hydrogen indices (~200 mg hydrocarbons/gTOC) and hence may only be able to expel sufficient hydrocarbons to sustain migration over short distances. Since biodegraded solution gases in the Yampi Shelf accumulations contain *neo*-pentane – a highly resistant compound – with isotopic affinity to Plover Formation generated fluids, it is possible that Cretaceous-sourced liquids were mobilised and carried to the shelf edge by co-migrating Plover-derived gas.

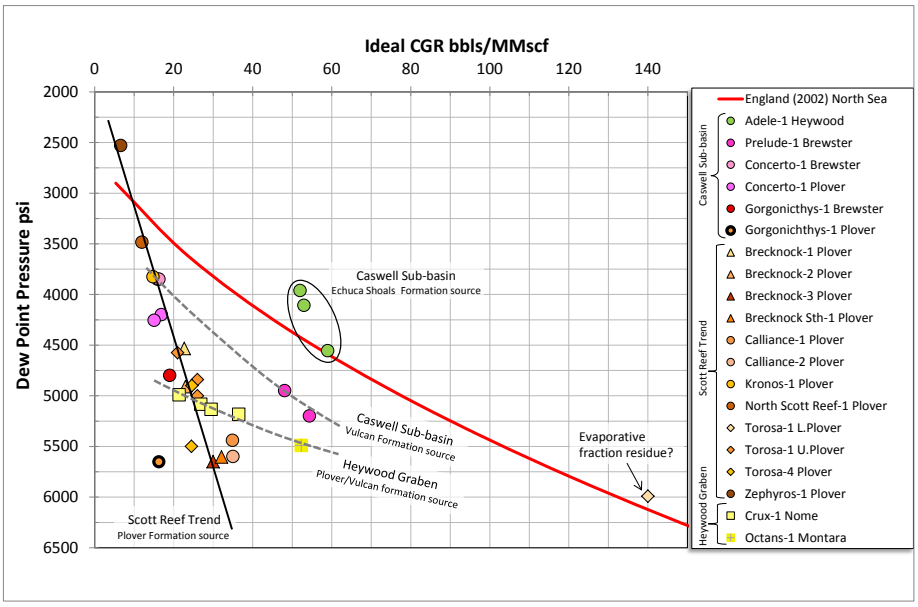

Fig. 1. Pressure, volume and temperature (PVT) test data from wells in the Browse Basin reveal the presence of several dew point petroleum systems. Reservoir formation is indicated in the legend and their source by the colours used in Figure 2.

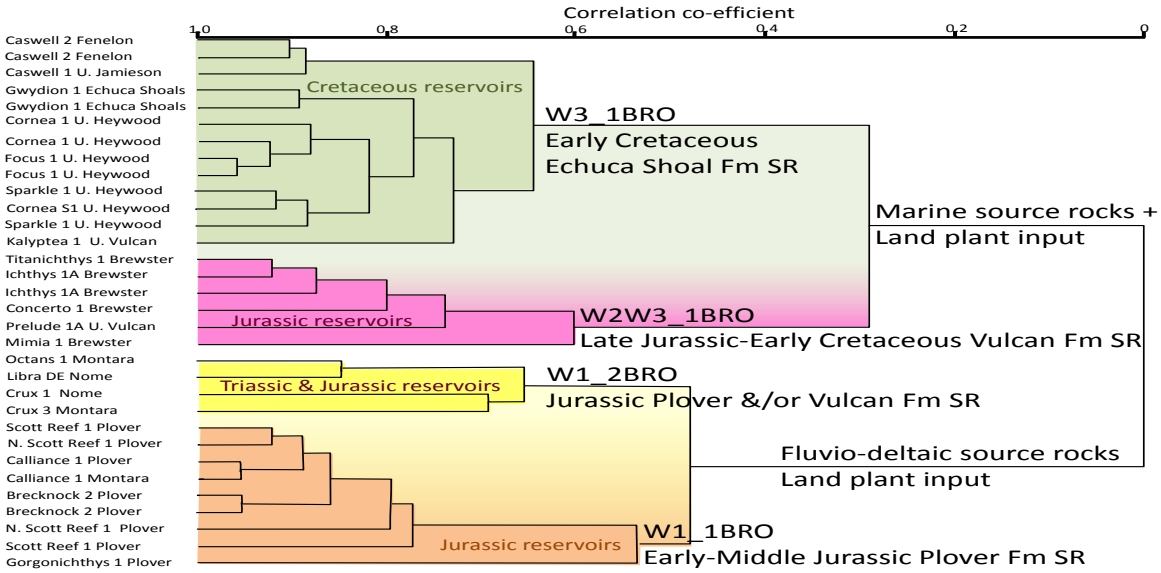

Fig. 2. Hierarchical cluster analysis for oil and condensate families in the Browse Basin (after Edwards and Zumberge, 2005).

References

Boreham, C.J., Roksandic, Z., Hope, J.M., Summons, R.E., Murray, A.P., Blevin, J.E., Struckmeyer, H.I.M., 1997. Browse Basin organic geochemistry study, North West Shelf, Australia. AGSO, Canberra. Record 1997/57.

Edwards, D.S., Zumberge, J.E., 2005. The oils of western Australia II. Geoscience Australia and GeoMark Research Ltd, Canberra and Houston. Record 37512

England 2002, Empirical correlations to predict gas/gas condensate phase behaviour in sedimentary basins. Organic Geochemistry, 33, 665-673.

Le Poidevin, S.R., Kuske, T.J., Edwards, D.S, Temple, P.R., 2015. Australian Petroleum Accumulations Report 7 Browse Basin; 2nd edition. Record 2015/10, Geoscience Australia, Canberra. Record 82545

Rollet, N., Abbott, S.T., Lech, M.E., Romeyn, R., Grosjean, E., Edwards, D.S., Totterdell, J.M., Nicholson, C.J., Khider, K., Nguyen, D., Bernardel, G., Tenthorey, E., Orlov, C., Wang, L., 2016. A regional assessment of CO_2 storage potential in the Browse Basin: results of a study undertaken as part of the National CO_2 Infrastructure Plan. Geoscience Australia, Canberra, Record.2016.017

Multiproxy reconstruction of redox conditions during Permian Kupferschiefer deposition in the Thuringian Basin based on trace elements, molybdenum isotopes and biomarkers

Lorenz Schwark[1,2] Wolfgang Ruebsam[1], Kliti Grice[2], Svenja Tulipani[2], Alex Dickson[3]

[1]Institute of Geoscience, Organic Geochemistry Unit, Christian Albrecht University, Kiel, 24118, Germany
[2]WA-Organic and Isotope Geochemistry, Department of Chemistry, Curtin University, Perth, 6000, Australia
[3]Department of Earth Sciences, University of Oxford, Oxford, UK
(corresponding author: ls@gpi.uni-kiel.de)*

The reconstruction of past environments and the key drivers controlling the redox state of water column and pore waters in low energy environments with restricted water circulation is often based on geochemical proxies, comprising redox-sensitive trace elements (RSTE), molecular biomarkers and with increasing rate of application, trace element isotopes, particularly those of molybdenum. Here we present a study applying a combination of these tools to the Late Permian Kupferschiefer (T1) deposited in the marginal Thuringian Basin, located in the SE of the semi-enclosed intracontinental Zechstein Sea. This setting is similar to that of the Lower Rhine Embayment in the SW Zechstein Sea (Schwark and Pütmann, 1990; Grice et al., 1996) but in addition shows representations of very shallow, above wave base, lagoonal sedimentation regimes.

The detailed study and cross-validation of molecular biomarkers (homohopane index, isorenieratane, DBT/phenanthrenes) with RSTE and molybdenum-isotopes allowed building a palaeodepositional model of the redox and hydrological regime during the deposition of the T1. Enrichment pattern of RSTE and biomarker data attest to the rapid development of euxinic conditions in basin settings during early T1 times, which became progressively less extreme during T1 deposition. Evolution of redox conditions in basinal settings, and the delayed onset of euxinia at shallow marginal sites are attributed to the interaction of sea level change with the basin palaeogeography. Euxinia in the Thuringian Basin of the Kupferschiefer Sea (KSS) did not cause near-quantitative depletion of aqueous molybdenum, due to short deepwater renewal times, a continuous resupply of RSTE upon transgression and declining burial rates of RSTE burial throughout T1. Drawdown of RSTE is indicated for shallow and euxinic lagoon environments in Thuringia. Admixture of riverine freshwater into the lagoon strongly impacted onto the local seawater chemistry and molybdenum isotope composition. A Mo-isotope ratio of ~1.7‰ in basinal sediments indicates a minimum KSS seawater composition of ~2.4‰, similar to the ~2.3‰ estimate for the Permian open ocean, and confirms a hydrographic connection between the intracratonic KSS and the global ocean. The substantial variation in Mo-isotope signatures is paralleled by diagnostic shifts in biomarkers responding to oxygenation in different parts of the water column. Water column chemistry has been affected by variation in sea level, extent of fresh water superposition above saline deep waters, hydrodynamic restriction, riverine fresh water influx and evaporitic conditions in shallow lagoons. Elucidation of the relative role of each driving factor by a single geochemical proxy is not feasible but the complex scenario can be disentangled by a multiproxy approach.

Interpretation of RSTE is commonly based on total rock analysis. Here we present some preliminary results on differentiation of specific RSTE (MO, Ni, P, Zn, Cu) bound to mineral (sulphidic) and organic phases by RSTE analysis of solvent extracted sediments versus solvent retrieved maltene and asphaltene fractions.

References

Grice, K., Schaeffer, P., Schwark, L., Maxwell, J.R., 1996. Molecular indicators of palaeoenvironmental conditions in an immature Permian shale (Kupferschiefer, Lower Rhine Basin, north-west Germany) from free and S-bound lipids. Organic Geochemistry 25, 131 – 147.

Schwark, L., Püttmann,W., 1990. Aromatic composition of the Permian Kupferschiefer in the Lower Rhine Basin, NW Germany. Organic Geochemistry 16, 749 – 761.

Carbon isotope records of thermochemical sulfate reduction corrosion effects on carbonate minerals, Upper Permian and Lower Triassic carbonates, NE Sichuan Basin, China

Kaikai Li[1, 2, *], Simon C. George[2], Chunfang Cai[3]

[1]Energy Resource Department, China University of Geosciences (Beijing), Beijing 100083, PR China
[2]Department of Earth and Planetary Sciences, Macquarie University, NSW, 2109, Australia
[3]Key Lab of Petroleum Resources, Institute of Geology and Geophysics, Chinese Academy of Sciences, Beijing 100029, China
(corresponding author: likaikai@cugb.edu.cn; kaikai.li@mq.edu.au)*

Prolific sour gas has been found worldwide in deep porous dolomite reservoirs adjacent to or interbedded with evaporites. Thermochemical sulfate reduction (TSR) results from the reaction between SO_4^{2-} and hydrocarbons and is responsible for the "souring" by the generated H_2S and CO_2. There is often a positive correlation between H_2S concentrations and porosities in sour gas provinces, and the widespread presence of solution collapse brecciation in MVT-deposits suggest a significant dissolution of carbonates during TSR (Anderson and Garven, 1987). This is supported by experimental simulation and calculation (Vandeginste et al., 2009). However, due to the decrease in the solubility of carbonate as burial depth and temperature increase, TSR is also considered to result in calcite precipitation rather than carbonate dissolution (Hao et al., 2015). Mobile anhydrite is prone to filling older pores and fractures and thus reduces the porosity significantly (Machel and Buschkuehle, 2008). The focus of this study is on assessment of the process of carbonate dissolution and precipitation during TSR in the Upper Permian Changxing (P_3ch) Formation and the Lower Triassic Feixianguan (T_1f) Formation, NE Sichuan Basin, China. Some information about the TSR reaction in the study area, including evidence for TSR, the temperature range, and the reactants and products have already been published (e.g., Cai et al., 2004; Hao et al., 2008).

Theoretically, as the TSR reaction proceeds, the continuous production of TSR-derived CO_2 will result in lighter $\delta^{13}C$ values of CO_2 in a relatively closed system. If substantial dissolution of carbonate occurred, the released inorganic CO_2 would have led to an enrichment in ^{13}C. Therefore, detailed work was conducted by the analysis of the carbon isotopes of the TSR calcites and the CO_2 trapped in fluid inclusions in the calcite; the homogenization temperatures (HTs) of the fluid inclusions were also determined. Investigation of the carbon isotopic behaviour of CO_2 during TSR will lead to great insight into the effect of TSR corrosion on carbonate minerals.

The CO_2 samples were collected from crushed calcite crystals and have $\delta^{13}C$ ratios ranging from -9.3‰ to +8.4‰ PDB (n=12), which are significantly heavier than those from TSR-derived CO_2 based on laboratory experiments (-37.1‰ to -24.9‰). This indicates a substantial contribution of inorganic carbon, either from re-equilibration of CO_2 with the ^{13}C-enriched water-rock system (Hao et al., 2015) or from bulk dolomite dissolution (Cai et al., 2014). It is hard to rule out either of these possibilities. However, the presence of a weak positive correlation between the $\delta^{13}C$ values of CO_2 in the fluid inclusions and the corresponding HTs (Fig. 1a) yields instructive clues regarding constant dissolution as the main process. Compared with CO_2 in the fluid inclusions, most of the TSR-derived calcite crystals have -5‰~-10‰ more negative $\delta^{13}C$ values, ranging from -14.0‰ to +3.6‰. This might be attributed to preferential sequestration of ^{13}C-depleted CO_2 into calcite cements, with a positive shift in $\delta^{13}C$ for the residual CO_2. There is no correlation between the $\delta^{13}C$ values of diagenetic calcite cements and HTs. However, for the TSR-derived calcites (HTs＞119°C) the $\delta^{13}C$ values show a positive correlation (R^2=0.46) with the HTs (Fig. 1b). A similar trend is also present based on the data from others (Jiang et al., 2014, 2015; Jiang, 2009). This is completely opposite to the generalization that carbon isotope ratios of TSR-derived calcites decrease with the extent of TSR (Worden et al., 1996).

The significant discrepancy mentioned above can be attributed to different settings of TSR sites in the gas reservoirs of the Khuff Formation in Abu Dhabi and those in this study, which resulted in distinctive dissolution-precipitation processes. In the Khuff Formation the TSR reaction occurred within anhydrite-bearing strata, and TSR-derived calcites typically occur as replacive masses after anhydrite. This indicates: 1) the presence of a closed hydrodynamical system near the TSR sites, due to the relatively lower porosity and permeability of evaporitic sediments and the occlusion of early pores by anhydrite cements; and 2) a quick saturation of calcium in the pore waters owing to the constant dissolution of anhydrite. Therefore, the growth of calcium carbonate rather than carbonate dissolution seemed likely to be sustained. With the gradual accumulation of organic carbon, ^{13}C of the TSR-derived calcites became more depleted. In contrast, in the P_3ch and T_1f formations of the NE Sichuan Basin, the TSR reaction was confirmed to have occurred in oolitic shoal and reef reservoirs, with barely detectable amounts of solid calcium sulfate associated. The reactive sulfate was demonstrated to have been derived from the early refluxing of evaporative brines from the backreef restricted lagoons. The better petrophysical properties and greater amounts of preserved pore waters offered the possibility of transport of the solutes away from the TSR sites in the overpressured settings. As TSR-derived calcite precipitated elsewhere, Ca^{2+} in the initial water was quickly consumed and Ca^{2+} concentrations decreased rapidly because of no continuous calcium supply from anhydrite dissolution. This might have provided an environment conducive to dissolution of the bulk dolomites. The addition of the released inorganic CO_2 into the system promoted the positive shift in $\delta^{13}C$ of the TSR-derived calcite, as well as those of the CO_2 captured in the fluid inclusions. Clearly,

carbonate dissolution during TSR seems to be influenced by transport of reactants to the surface and transport of products away from the surface, which is supported by simulation experiments on carbonate dissolution with various kinds of acid solutions (e.g., Fredd and Fogler, 1998).

Significant dissolution of dolomite has been proposed to be the result of H^+ release from H_2S precipitation as metal sulfides. However, this mechanism fails to explain: 1) the pyrite that was found to be volumetrically minor in the reservoirs; and 2) the overall positive correlation between H_2S and CO_2 concentrations. As an alternative, CO_2-induced dissolution has also been invoked to explain secondary porosity development during late burial. The addition of CO_2 into a system could lower the pH by 1-2 units and induce organic deposition, causing a change in the core's wettability towards a more water-wet condition (Zekri et al., 2009). The H^+ released from carbonic acid reacting with dolomite would have caused dissolution and HCO_3^- generation. After dissolved HCO_3^- was further consumed by calcite precipitation, the CO_2 concentrations in the system maintained balance and kept the linear correlation with H_2S concentrations. Another available mechanism proposed by Cai et al. (2014) is that dolomite could react directly with anhydrite and hydrocarbons under acidic conditions and produce H_2S and calcite. In any case, the carbonate dissolution-precipitation process did occur in the deep reservoirs and resulted in a redistribution of porosity.

Clark and Vanorio (2016) claimed that the initial porosity and microstructure appeared to be the primary control over mass transport of reactive brines and solutes and the ultimate changes to petrophysical properties. Their reactive fluid experiment showed that the high-porosity cores have the largest quantities of carbonate minerals removed, which was attributed to the positive link between reactive surface area and pore network connectivity (Noiriel et al., 2009), while the pore throats in the tight cores tended to be blocked with dislodged minerals during flow. This generalization and the proposal about the dissolution-precipitation process related to different settings of TSR sites explains well all the phenomena observed in the NE Sichuan Basin, e.g., 1) the vertical and horizontal distribution pattern of the amounts of TSR-derived calcites; 2) different amounts of TSR-derived calcites in various types of dolomites with different porosity and permeability; and 3) the horizontal distribution pattern of the $\delta^{13}C$ values of TSR-derived calcites.

It should be noted that despite the occurrence of TSR-induced dissolution, the dissolved material would have been likely to reprecipitate as calcium carbonates. So limited amounts of new porosity seem to have been created during subsidence, when viewed from the principle of mass-balance. However, as a result of the dissolution-precipitation process during TSR, enhancements and reductions occurred in porous and tight cores, respectively, which had essentially improved the reservoirs to a certain extent.

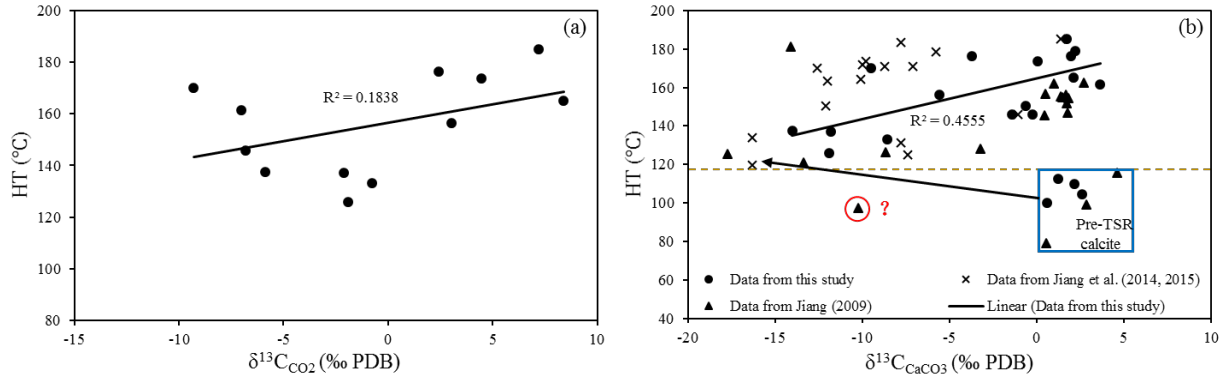

Fig. 1. Cross plots showing relationships of: (a) $\delta^{13}C$ values of CO_2 trapped in fluid inclusions with homogenization temperatures (HTs), and (b) $\delta^{13}C$ values of void-filling calcite cements with HTs. The red circle with the question mark means the data point is considered to be an anomalous value. Since the precipitation temperature is under the thermal limit for TSR, the depletion in ^{13}C is unlikely to originate from oxidation of hydrocarbons by sulfates. The yellow dashed line represents the minimum temperature for TSR (about 119°C) in the study area. The points below this line represent pre-TSR calcite samples with consistent positive $\delta^{13}C$ values, while the other points represent TSR-derived calcite samples with a good correlation between the $\delta^{13}C$ values and HTs.

References

Anderson, G.M., Garven, G., 1987. Sulfate-sulphide-carbonate associations in Mississippi Valley-type lead-zinic deposits. Econ. Geol. 82, 482-488.

Cai, C.F., He, W.X., Jiang, L., Li, K.K., Xiang, L., Jia, L.Q., 2014. Petrological and geochemical constraints on porosity difference between Lower Triassic sour- and sweet-gas carbonate reservoirs in the Sichuan Basin. Mar. Petrol. Geol. 56, 34–50.

Clark, A.C., Vanorio, T., 2016. The rock physics and geochemistry of carbonates exposed to reactive brines. Journal of Geophysical Research: Solid Earth, 121: 1497-1513

Fredd, C.N., Fogler, H.S., 1998. The kinetics of calcite dissolution in acetic acid solutions. Chemical Engineering Science, 53 (22): 3863-3874

Hao, F., Guo, T.L., Zhu, Y.M., Cai, X.Y., Zou, H.Y., Li, P.P., 2008. Evidence for multiple stages of oil cracking and thermochemical sulfate reduction in the Puguang gas field, Sichuan Basin, China. Am. Assoc. Petrol. Geol. Bull 92, 611-637

Hao, F., Zhang, X.F., Wang, C.W., Li, P.P., Guo, T.L., Zou. H.Y., Zhu, Y.M., Liu, J.Z., Cai, Z.X. 2015. The fate of CO_2 derived fromthermochemical sulfate reduction (TSR) and effect of TSR on carbonate porosity and permeability, Sichuan Basin, China. Earth-Science Reviews, 141: 154-177

Jiang, L., Worden, R.H., Cai, C.F., 2014. Thermochemical sulfate reduction and fluid evolution of the Lower Triassic Feixianguan Formation sour gas reservoirs, northeast Sichuan Basin, China. AAPG Bull. 98, 947–973.

Jiang, L., Worden, R.H., Cai, C.F., 2015. Generation of isotopically and compositionally distinct water during thermochemical sulfate reduction (TSR)
in carbonate reservoirs: Triassic Feixianguan Formation, Sichuan Basin, China. Geochimica et Cosmochimica Acta, 165: 249–262

Jiang, T., 2009. The research of reservoir geochemistry characteristics of Upper Permian and Lower Triassic in the NE Sichuan Basin. Chengdu University of Technology, 54p.

Machel, H.G., Buschkuehle, B.E., 2008. Diagenesis of the Devonian Southesk–Cairn Carbonate Complex, Alberta, Canada: marine cementation, burial dolomitization, thermochemical sulfate reduction, anhydritization, and squeegee fluid flow. J. Sediment. Res. 78, 366–389.

Noiriel, C., Luquot, L., Made, B., Raimbault, L., Gouze, P., van der Lee, J., 2009. Changes in reactive surface area during limestone dissolution: An experimental and modelling study, Chem. Geol., 265, 160–170

Vandeginste, V., Swennen, R., Reed, M.H., Ellam, R.M., Osadetz, K., Roure, F. 2009. Host rock dolomitization and secondary porosity development in the Upper Devonian Cairn Formation of the Fairholme carbonate complex (South-west Alberta, Canadian Rockies): diagenesis and geochemical modeling. Sedimentology, 56, 2044-2060

Worden, R.H., Smalley, P.C., 1996. H_2S-producing reactions in deep carbonate gas reservoirs: Khuff Formation Abu Dhabi. Chem. Geol. 133, 157–171.

Zekri, A.Y., Shedid, S.A., Almehaideb, R.A., 2009. Investigation of supercritical carbon dioxide, aspheltenic crude oil, and formation brine interactions in carbonate formations. Journal of Petroleum Science and Engineering, 69: 63-70

Wettability Alteration measurements of Indiana Lime Stone due to Effect of Crude Oil Composition during Immiscible CO2 Flooding

Muhammad Ali[1], Dr. Stefan Iglauer[2], *Naeem Ul. Hussain Dahraj [3], Muhammad Arif [4]*

[1]Curtin University, Australia, muhammad.ali7@postgrad.curtin.edu.au, +61 405 956 284
[2]Curtin University, Australia, stefan.Iglauer@curtin.edu.au, +618 9266 7703
[3](Pakistan Petroleum Ltd), h_naeem@ppl.com.pk, +92 336 568 1188
[4]Curtin University, Australia, muhammad.arif@curtin.edu.au, +61 438 913 050

Carbon dioxide flooding is an EOR technique in which carbon dioxide is injected into the reservoir to improve the oil recovery. The reservoir oil and rock properties are altered when carbon dioxide interacts with the oil and rock present in the reservoir. Carbon dioxide injection alters the oil and rock properties by causing reduction in oil viscosity, oil swelling and wettability alteration of the rock. This paper will present a proposal to study the wettability alteration in carbonate formations during immiscible carbon dioxide flooding. In immiscible carbon dioxide flooding, the injection pressure of carbon dioxide would be kept below the minimum miscibility pressure. Thus carbon dioxide is not miscible with the oil present in the reservoir.

This paper primarily focuses on understanding the effect of crude oil composition on the change in wettability in carbonate rocks during immiscible carbon dioxide flooding. Experiments will be carried out with different crude oils (Heavy, Medium and Light) on the same carbonate rock, at reservoir conditions, in order to observe the change in rock wettability. A time dependent mathematical model, recently built to represent wettability alteration during immiscible carbon dioxide, will also be verified with the results of the experiments.

Carbonate rocks are very special due to the fact that usually carbonate rocks are oil wet and carbon dioxide tends to change the wettability of the carbonate rocks from oil wet to water wet. This change in wettability of the reservoir rock increases the oil recovery. Literature review revealed that considerable amount of research has not been done on the wettability alteration of carbonate rocks during immiscible CO_2 flooding process. Thus this topic needs to be further investigated and studied.

URANIUM RADIOLYTIC IMPACTS ON AROMATIC HYDROCARBON COMPOSITION OF MULGA ROCK SEDIMENTS

Chao Shan[1,2], Paul F. Greenwood[2-4,*], Alex Holman[1], Kliti Grice[1]

[1]Western Australia Organic and Isotope Geochemistry Centre, Curtin University, Bentley, 6102, Australia
[2]Faculty of Earth Resources, China University of Geosciences; Wuhan 430074,China
[3]Centre for Exploration Targeting, UWA, Crawley, 6009, Australia
[4]WA Biogeochemistry Centre and Ecosystems Research Group, The University of Western Australia (UWA), Crawley, 6009, Australia
(* corresponding author: paul.greenwood@uwa.edu.au)

Our groups interest in the effects of ionizing radiation on the molecular and stable isotopic composition of sedimentary organic matter (OM) has extended to the aromatic hydrocarbons of thermally immature sediments from the Mulga Rock Uranium Deposit (Western Australia). Many uranium deposits contain high amounts of sedimentary organic matter (OM) which may have played an important role in metal accumulation or formation of the deposit. Jaraula et al (2015) recently reported several changes in the hydrocarbon distributions of the aliphatic and ketone fractions of sediments spanning a 500 - 5000 ppm radiation gradient across the Eocene uranium deposit at Mulga Rock (W. Australia). This included a reduction in aliphatic chain length (due to radiolytic cracking) and an increasing proportion of alkenones (from the reaction of aliphatics with OH- radicals from radiolysis of water), , particularly alkan-2-ones (due to isomerisation impedance at higher U and concomitant S concentrations). These molecular trends were evident where traditional geological indicators (e.g., pleochroic haloes) were not, indicating a higher sensitivity to relatively low levels or short durations of radiation.

There have been several other studies of the U-impacts on aliphatic hydrocarbons (e.g., Forbes et al., 1988; Dahl et al., 1988,Landais, 1996), but the corresponding impacts on aromatic distributions has been given relatively little attention. With increasing radiation levels the aromatic moiety of a declining bitumen fraction typically increases (and C/H ratio decrease) due the relatively high susceptibility of aliphatic hydrocarbons to free radical polymerisation and functional group's to condensation reactions. These trends were evident in Mulga Rock sediments (Fig. 1A and B) -

This paper will report impacts of U-radiolysis on the aromatic hydrocarbon distributions of the Mulga Rock sediments. Higher plant sourced aromatic (and aliphatic) terpenoids were very abundant in these low thermal maturity sediments (Rr = 0.26%; Tmax < 421oC). Many of the aromatised terpenoids were recognised as intermediate or end products of the diagenetic aromatization of diterpane (e.g..,cadilane) and triterpane (e.g., amyrin) precursors. □13C data of individual aromatic compounds were measured to help identify the reaction pathways. The sediment with the highest U content of > 5000 ppm showed only diterpenoids and low MW PAHs, reflecting complete radiolytic removal of higher MW terpenoids. At low U levels the radiolysis was shown to variedly impact the rates of different aromitisation schemes. For instance, higher abundances of triaromatic C ring-cleaved and aromatic des-A hydrocarbons were measured in higher U content sediments across the range of 640 ppm to 1700 ppm (e.g., Fig 1C and D) possibly assisted by radiolytic oxidation, e.g., uranium oxide catalysis of dehydrogenation reactions. A slight □13C depletion increasingly aromatised triterpenoids may reflect preferential H-abstraction from 12C.

Radiolytic affects can significantly alter organic matter composition and a greater understanding of the reaction pathways and controls on this type of alteration may help to more fully appreciate the robustness (or secondary influences) of other traditional organic geochemical parameters (e.g., thermal maturity indicators based on the relative abundances of aromatic compounds, such as triaromatic steroids) and may even contribute organic based parameters useful for locating U-rich sediments.

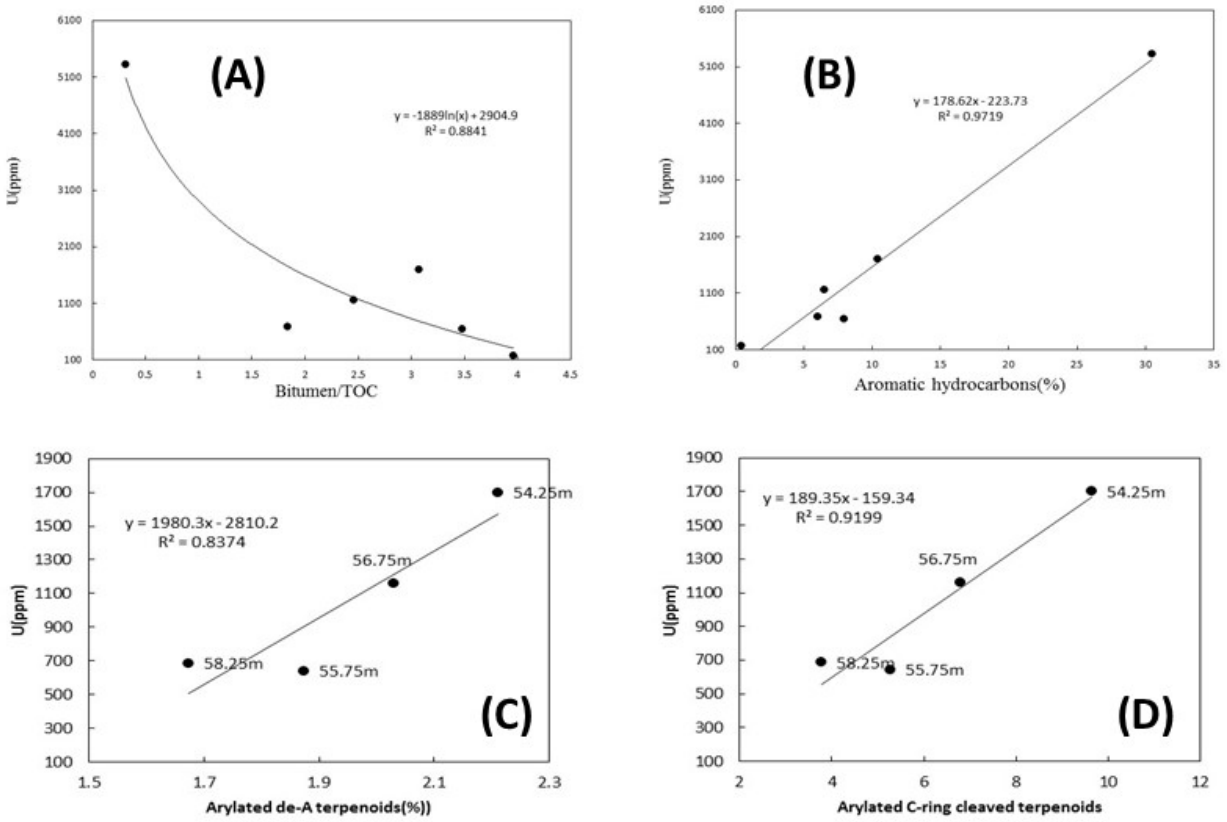

Fig. 1. Profiles of (A) Bitumen content; (B) Aromatiuc fraction (%); and (C-D) arylated terpenoid concentrationss versus U concentration.

References

Dahl, J., Hallberg, R., Kaplan, I. R., 1988. Effects of irradiation from uranium decay on extractable organic matter in the Alum Shales of Sweden. Organic Geochemistry. 12(6), 559–571.

Forbes, P., Landais, P., Bertrand, P., Brosse, E., Espitalie, J., Yahaya, M., 1988. Chemical transformations of type-III organic matter associated with the Akouta uranium deposit (Niger); geological implications. Chem. Geol. 71(4), 267–282.

Jaraula, C.M.B., Schwark, L., Moreau, X., Pickel, W., Bagas, L., Grice, K., 2015. Radiolytic alteration of biopolymers in the Mulga Rock (Australia) uranium deposit. Applied Geochemistry. 52, 97–108

Landais, P., 1996. Organic geochemistry of sedimentary uranium ore deposits. Ore Geology Reviews, 11(1-3), 33-51

Unusual association of organic matter and metals in the Cambrian black shales of South China

Anais Pagès, [1,2*] Steve Barnes, [1] Susanne Schmid,[1] Margaux Le Vaillant[1], Chris Ryan[3], David Paterson[4], Haifeng Fan[5], Hanjie Wen[5]

[1] CSIRO, Mineral Resources National Flagship, 26 Dick Perry Avenue, Kensington WA
[2] WA Organic and Isotope Geochemistry Centre, Department of Chemistry, The Institute for Geoscience Research, Curtin University, GPO Box U1987, Perth, WA 6845, Australia
[3] CSIRO Mineral Resources, Normanby Road, Clayton VIC 3168, Australia
[4] Australian Synchrotron, Blackburn Road, Clayton VIC 3168, Australia
[5] State Key Lab of Ore Deposit Geochemistry, Institute of Geochemistry, Chinese Academy of Sciences, 46 Guanshui Road, Guiyang, 550002, Guizhou Province, P. R. China
(corresponding author: **Anais.pages@csiro.au**)*

A transition from oxygen-deficient to oxygenated oceans triggered the evolution of complex multicellular life at the Precambrian-Cambrian boundary, 542 million years ago. At this time, both the evolution of metazoan radiation and the genesis of sub-economic Ni, Mo, Rare Earth Elements (REE) and Platinum Group Element (PGE) deposits were triggered in shallow water environments, on the Yangtze platform in China. Euxinic bottom waters have been associated with the Cambrian explosion, based on negative Mo isotopic excursion and enrichment of redox-sensitive TE in the black shales of the Niutitang Formation. However, the identification of numerous benthic animals (e.g. sponges and arthropods) suggest oxic to dysoxic environmental conditions underneath the bottom waters (Zhou and Jiang, 2009), in contradiction with geochemical results.

To date, the formation of the Ni-Mo-PGE-Au ore deposit concomitant with the Cambrian explosion in South China also remains highly debated (Embso et al., 2005; Pasava et al., 2008; Xu et al., 2013). The thin accumulation of Ni, Mo, Au, Ag, Se, Cr, V, Zn, U and PGEs and other metals including REE is developed within the Lower Cambrian Niutitang formation, and can be traced along the same stratigraphic horizon over distances of several hundreds of kilometres (Xu et al., 2013). This is one of the most enigmatic examples of a sediment-hosted base and precious metal deposit showing an association of ore-grade metals with organic matter. The genesis of this and other such strata-bound deposits is poorly understood.

The present study aims to investigate in details the spatial distribution of metals in this rare ore layer, providing further insights into the genesis of this ore layer and paleoenvironmental conditions associated with the Cambrian explosion in South China. Complimentary techniques such as microbeam XRF mapping and XRF microscopy combined with the Maia detector (384 detector array (Paterson et al., 2011; Ryan et al., 2016); Australian Synchrotron) were used to investigate specific microscale distributions of phosphorite nodules, metals and organic-rich matrix. The strong variations in metal distributions highlight rapid shifts in redox conditions. This fine-scale study of metals, organic-rich matrix and phosphorite nodules allows a greater understanding of metal associations in this unique, highly anoxic and sulfidic sedimentary system, in the context of the Cambrian bioradiation of metazoans.

References

Emsbo, E., Hofstra, H., Johnson, C.A., Koenig, A., Grauch, R., Zhang, X., Hu, R., Su, W., Pi, D., 2005. Lower Cambrian metallogenesis of south China: interplay between diverse basinal hydrothermal fluids and marine chemistry. J. Mao, F.P. Bierlein (Eds.), Mineral Deposit Research: Meeting the Global Challenge. Proceedings of the Eighth Biennial SGA Meeting Bejing, Springer, Berlin (2005), pp. 115–118

Pašava, J., Kr˘íbek, B., Vymazalová, A., Sýkorová, I., Žák, K., and Orberger, B., 2008, Multiple sources of metals of mineralization in Lower Cambrian black shales of South China: Evidence from geochemical and petrographic study. Resource Geology, 58, 25–42.

Paterson, D., de Jonge, M.D., Howard, D.L., Lewis, W., McKinlay, J., Starritt, A., Kusel, M., Ryan, C.G., Kirkham, R., Moorhead, G., Siddons, D.P., 2011. The X-ray fluorescence microscopy beamline at the Australian Synchrotron. AIP Conf. Proc. 1365, 219-222.

Ryan, C.G., Fisher, L.A., Le Vaillant, M., Pagès, A., Siddons, D.P., Kirkham, R., Paterson, D.J., de Jonge, M.D., Howard, D.L., Barnes, S.J., Moorhead, G.F., Laird, J.S., 2016. High throughput quantitative per pixel XFM element imaging using Maia for complex natural samples. XRM Conference, Oxford.

Xu, L.G., Lehmann, B., and Mao, J.W., 2013, Seawater contribution to polymetallic Ni-Mo-PGE-Au mineralization in Early Cambrian black shales of South China: Evidence from Mo isotope, PGE, trace element, and REE geochemistry. Ore Geology Reviews, 52, 66–84

Zhou, C., Jiang, S.-Y., 2009. Palaeoceanographic redox environments for the lower Cambrian Hetang Formation in South China: Evidence from pyrite framboids, redox sensitive trace elements, and sponge biota occurrence. Palaeogeography, Palaeoclimatology, Palaeoecology 271, 279-286.

Sulfur isotope variability of DMS(P) in specific aquatic environments and phytoplankton species

Alon Amrani and Ward Said-Ahmad

The Institute of Earth Sciences, The Hebrew University, Givat Ram, 91904, Jerusalem, Israel
(corresponding author: alon.amrani@mail.huji.ac.il)*

Dimethylsulfoniopropionate (DMSP) is a widespread and important metabolite in marine ecosystems, mainly produced by marine microalgae. It is involved in multiple cross-scale processes, from cell physiology to ecosystem functioning. Enzymatic processes break it to a volatile organosulfur compound, dimethylsulfide (DMS) in the surface ocean. Oceanic emissions of volatile DMS represent the largest natural source of biogenic sulfur to the global atmosphere. However, there are other sources of DMS (e.g. coral reefs, lakes, wetlands, anoxic sediments) that may controlled by other biogeochemical mechanisms, and may contribute to the DMS flux to the atmosphere. Oxidation processes in the atmosphere transform DMS into sulfuric and methanesulfonic acids, that were postulated to be important participants of cloud formation and may regulate local climate. This hypothesis (CLAW) of a feedback loop between phytoplankton DMS production, cloud formation and climate regulation remains controversial for the last three decades. To better understand this complex system, it is essential to study the processes controlling DMSP production by microalgae, and to assess how much of its degradation product, DMS, is effectively transferred to the atmosphere and contribute to aerosols

Sulfur isotope ratios ($^{34}S/^{32}S$ ratio, $\delta^{34}S$) of DMS and DMSP may provide a useful tool to follow processes and constrain the contribution of the end members based on specific S isotope signatures. Because of the low oceanic concentrations of DMS/P (few nanomolars), we applied a new and sensitive method for the analysis of $\delta^{34}S$ in individual compounds (Amrani et al., 2009). This method was modified for DMS analysis based on purge and trap of seawater and a subsequent injection to a gas chromatograph coupled with inductively coupled plasma mass spectrometer (GC/MC-ICPMS) (Said-Ahmad and Amrani 2013). We then applied this method in a range of marine environments, from oceanic water to sea ice and lake water and sediments. In addition, we measure species-specific $\delta^{34}S$ values in DMSP of several phytoplanktom species. Here we will review the main results of these measurements and their potential implications.

Surface water DMSP collected from six different ocean provinces around the world revealed a remarkable consistency in $\delta^{34}S$ values ranging between +18.9 and +20.3‰ (Amrani et al., 2013). Sulfur isotope composition of DMS analyzed in freshly collected seawater was similar to $\delta^{34}S$ of DMSP, showing that the in situ fractionation between these species is small (< +1‰). Based on volatilization experiments, emission of DMS to the atmosphere results in a relatively small fractionation (-0.5±0.2‰) compared to the seawater DMS pool. Since $\delta^{34}S$ values of oceanic DMS closely reflect that of DMSP, we conclude that the homogenous $\delta^{34}S$ of DMSP at the ocean surface represent the $\delta^{34}S$ of DMS emitted to the atmosphere, within +1‰.

This apparent homogeneity for surface seawater DMS(P) may hide larger variability in specific microalgae and their symbionts. We isolated specific microalgae species that were collected from whole seawater of the Red Sea (Eilat, Israel) (Gutierrez-Rodriguez et al., In Press). The mean $\delta^{34}S$-DMSP in isolated holobiont specimens of Acantharia-Phaeocystis sp. were very similar to each other, and also to the natural microbial assemblage coexisting in the same surface water (19.7 ± 0.4‰). In contrast, the Collodaria-Brandtodinium holobiont showed a very distinct DMSP isotopic composition (23.5±0.8‰), significantly ^{34}S enriched not only compared to other symbiotic groups (Acantharia and Foraminifera) and microbial assemblage, but also compared to seawater sulfate (21.1‰). Culture experiments of sulfate (with distinct $\delta^{34}S$ values) assimilation by different species of microalgae, showed that Collodaria holobionts did not assimilate sulfate during the experiment while all the other species did. This may suggest a different metabolic pathway for the formation of DMSP of this species that eventually affect its $\delta^{34}S$ values.

Specific marine environments can also have $\delta^{34}S$ variability. Antarctic sea ice microalgal communities are known to produce very large amounts of DMSP. Despite several field measurements of bulk ice DMS(P) concentrations, punctual measurements of sea ice-atmosphere DMS fluxes, and experiments with isotopically-labelled DMS(P) in brine, our knowledge of the sea ice DMS cycle remains very limited. We report the first profiles of the $\delta^{34}S$ of DMS(P) in natural sea ice cores from the Ross Sea and Weddell sea, by combining dry crushing extraction of DMS(P), and $\delta^{34}S$ analysis with GC-MC-ICPMS (Carnet et al., in preparation). Depth-profiles of $\delta^{34}S$ of DMSP revealed considerable variability between regions, across seasons, and between sea ice horizons, with values ranging between 9.2 and 21.9‰. This variability is remarkable considering the relative sulfur isotopic homogeneity of DMSP in oceanic waters and much higher than those observed for specific microalgae species (Gutierrez-Rodriguez et al., In Press). Moreover, this S isotope fractionation in the formation of DMSP is much larger than the published assimilatory sulfate reduction fractionation during biosynthesis of organosulfur compounds (in the range of 1-3‰, Kaplan and Rittenberg, 1964). The most ^{34}S depleted values, and highest spatial variability, were mainly observed in surface and interior ice in the winter and early spring, where adapted microalgae thrive in the extreme conditions (e.g. temperature and salinity) of brine microenvironments as shown by ancillary physical and biological data . This, combined with the remarkable consistency (~21‰) of the $\delta^{34}S$ of sulfate in the same ice samples, suggests that the observed variability in DMSP probably originated from distinct metabolic pathways of DMSP synthesis.

Another example for large variability of DMS(P) was observed in Lake Kineret , a monomictic freshwater lake (Israel). Profiles of DMS in the epilimnion during March and June 2014 showed sulfur isotope ($\delta^{34}S$) values that were enriched by up to 4.8‰ compared with DMSP and sulfate $\delta^{34}S$ values in the epilimnion at that time (~13‰) (Sela-Adler et al., 2016). During the stratified period, the $\delta^{34}S$ values of DMS in the hypolimnion decreased to -7.0‰, close to the $\delta^{34}S$ values of coexisting H_2S derived from dissimilatory sulfate reduction in the reduced bottom water and sediments. This indicates that H_2S was methylated by unknown microbial processes to form DMS. In the hypolimnion during stratified period DMSP was significantly ^{34}S enriched relative to DMS reflecting its different S source, which was mostly from sulfate assimilation with small isotopic fractionation. This in turn demonstrates the multiple sources of DMS in stratified water bodies and complex DMSP/DMS dynamics that are linked to the various biogeochemical processes within the sulfur cycle.

References

Amrani, A., Sessions A.L., Adkins J. 2009. Compound-specific $\delta^{34}S$ analysis of volatile organics by coupled - GC/ Multicollector - ICPMS. Analytical Chemistry 81, 9027-9034.

Said-Ahmad W, Amrani, A. 2013 A sensitive method for the sulfur isotope analysis of DMS and DMSP in seawater. Rapid Communication in Mass Spectrometry (RCM) 27, 2789-2796.

Amrani A., Said-Ahmad W., Shaked Y. Kiene R.P. (2013) Sulfur isotope homogeneity of oceanic DMSP and DMS. Proceedings of the National Academy of Sciences (PNAS) vol 110, (46), 18413-18418.

Carnat, G. Said-Ahmad, W., Fripiat, F., Tison J.-L. Amrani A. (2016) Sulfur isotope variability of DMS(P) production by antarctic sea ice microalgal communities. Goldschmidt meeting 2016, Yokohama , Japan.

Gutierrez-Rodriguez A., Pillet L., Biard T., Said-Ahmad W., Amrani A., Simo R., Not F. (2016) Dimethyl sulfur compounds in symbiotic protists: A potentially important source for marine DMS(P). Limnology and Oceanography. Accepted.

Kaplan, I. R. Rittenberg, S.C.. (1964) Microbiological Fractionation of Sulphur Isotopes. J. Gen. Microbiol., 34,195.

Sela-Adler, M., Said-Ahmad, W., Sivan, O., Eckert, W., Kiene, R. P. , Amrani, A. (2016) Isotopic evidence for the origin of DMS and DMSP-like compounds in a warm-monomictic freshwater lake. Environmental Chemistry. 13, 340–351.

$\delta^{34}S$ of Organic Sulfur Compounds and the Sulfur Cycle of Petroleum Systems

Nannan He[1,*], Kliti Grice[1] and Paul Greenwood[1,2]

[1]The Western Australian Organic & Isotope Geochemistry, Department of Chemistry, Curtin University, Australia
[2] School of Earth and Environment, The University of Western Australia, Australia
(corresponding author: nannan.he@postgrad.curtin.edu.au)*

This study makes use of recently invented Compound Specific Sulfur Isotope analysis (CS-S-IA) to investigate the incorporation and fate of sulfur in petroleum systems. Sulfur is usually incorporated into fossil fuels via secondary processes (Peters et al., 2005), most significantly by thermochemical sulfate reduction (TSR). The $\delta^{34}S$ of organo sulphur compounds (OSCs) in oils can be significantly influenced by TSR, as well as by other factors such as depositional environment and thermal maturity. Bulk $\delta^{34}S$ values of petroleum can vary over a wide range (8 to 32%; Faure and Mensing, 2005) and have traditionally proved quite useful for oil–oil correlations (see e.g., Gaffney et al.1980). CS-S-IA has already been applied to several S-rich oils from different parts of the world (Amrani et al., 2009; 2012; Greenwood et al., 2014; Li et al., 2015; Cai et al., 2015; Gvirtzman et al., 2015) with the $\delta^{34}S$ values measured ranging from -15 to +40 ‰, and with co-occurring OSCs in a single oil varying by as much as 30 ‰ – reflecting the impact of different controls that would not be resolved by bulk $\delta^{34}S$ analysis. A more sophisticated understanding of the $\delta^{34}S$ relationships of specific S-sources and alteration events, however, requires further CS-S-IA research and application to a variety of petroleum samples

We are conducting a CS-S-IA study of oils from the Tarim Basin (W. China) to help resolve the controversy about the source of deep oil in the Tarim Basin. CS-S-IA has already been used in correlation studies of oils from the Tarim Basin (Li et al., 2015; Cai et al., 2015), but a clear distinction of a Cambrian or Ordovician source of these oils was often not established. We aim to use $\delta^{34}S$ signatures to help resolve the respective contribution of these sources, as well as provide a more comprehensive evaluation of the $\delta^{34}S$ values and relationships with TSR which have significantly impacted a number of deep (>6000m) Tarim Basin oils.

We are also interested in the potential $\delta^{34}S$ dynamics associated with the biodegradation of oils by microbial communities. Biodegradation is a common and detrimental alteration process in petroleum systems when the temperature in reservoirs is cooler than approximately 80 °C. A number of molecular based biodegradation scales based on the different vulnerability of aliphatic and aromatic hydrocarbons to biodegradation have been defined from many organic geochemical studies (e.g. Volkman et al., 1984; Grice et al., 2000; Larter et al., 2012), and are now commonly used to assess the extent to which crude oils have been biodegraded. Biodegradation can also lead to varied ^{13}C and D fractionation of different hydrocarbons, and $\delta^{13}C$/ [illegible] have also been defined (Asif et al., 2009). The vulnerability of OSCs to biodgradation, however, has attracted very little previous attention. We plan to evaluate the abundance and $\delta^{34}S$ relationships of the OSCs to biodegradation through the analysis of S-rich reservoir oils exposed to different levels of biodegradation and also by simulating the biodegradative processes on selected oils under laboratory controlled conditions. The outcome of this CS-S-IA based research will shed further light on biogeochemical S cycles, help contribute to the discovery and more efficient utilisation of new natural energy resources, and provide a better appreciation of S species and hydrocarbon reaction mechanisms during eogenesis.

References

Amrani, A, Sessions, A.L., and Adkins, J.F., 2009. Compound-Specific delta(34)S Analysis of Volatile Organics by Coupled GC/Multicollector-ICPMS. Analytical Chemistry 81, 9027-9034.

Amrani, A, Sessions, A.L., Tang, Y., Adkins, J.F., Hills, R.J., Moldowan, M.J., Wei, Z., 2012. The sulfur-isotopic compositions of benzothiophenes and dibenzothiophenes as a proxy for thermochemical sulfate reduction. Geochimica et Cosmochimica Acta 84, 152-164Cai CF et al. (2015b) Application of sulfur and carbon isotopes to oil–source rock correlation: A case study from the Tazhong area, Tarim Basin, China. Organic Geochemistry, 83-84, 140-152.

Asif, M., Grice, K., Fazeelat, T., 2009. Assessment of petroleum biodegradation using stable hydrogen isotopes of individual saturated hydrocarbon and polycyclic aromatic hydrocarbon distributions in oils from the Upper Indus Basin, Pakistan. Organic Geochemistry 40 (3), 301-311.

Faure, G., Mensing, T.M. , 2005. Isotopes, Principles and Applications, Third Edition. John Wiley & Sons, Inc., Hoboken, New Jersey.

Gaffney J.S., Premuzic E.T., Manowitz B., 1980. On the usefulness of sulfur isotope ratios in crude oil correlations. Geochimica Cosmochimica Acta 44, 135-139.

Greenwood, P. F., Amrani, A., Sessions, A., Raven, M. R., Holman, A., Dror, G., Grice, K., McCulloch, M. T., and Adkins, J. F. (2014) In: Principles and Practice of Analytical Techniques in Geosciences, K Grice ed. Royal Soc. Chem., Oxford.

Grice, K., Alexander, R., Kagi, R. 2000. Diamondoid hydrocarbon ratios as indicators of biodegradation in Australian crude oils. Organic Geochemistry 31, 67-73.

Larter, S., Huang, H., Adams, J., Bennett, B., Snowdon, L. R. (2012) A practical biodegradation scale for use in reservoir geochemical studies of biodegraded oils. Organic Geochemistry, 45, 66-76.

Li SM et al. (2015) Origin and quantitative source assessment of deep oils in the Tazhong Uplift, Tarim Basin. Organic Geochemistry, 78, 1-22.

Peters, K.E., Walters, C.C., Moldowan, J.M. The Biomarker Guide, Cambridge University Press, Cambridge, 2nd edn, 2005. Acta, 1980, 44, 135–139.

Volkman, J.K., Alexander, R., Kagi, R.I., Roeland, S. J., Sheppard, P. N. (1984) Biodegradation of aromatic hydrocarbons in crude oils from the Barrow Subbasin of Western Australia. Organic Geochemistry, 6, 619–632.

Developments in new conversion processes of biomass to liquid fuels versus the formation of high-end energy saving chemicals

Elad Meller, Yoel Sasson and Zeev Aizenshtat

Currently, most of the commercially available **biofuels** are produced from edible resources. Biofuels, derived from renewable biomass platform molecules such as starch, triglycerides and lignocellulose, are considered to be the ideal substitutes of petroleum resources. Unlike petroleum resources, which consist mainly of alkanes, biomass molecules are functionalized compounds. Out of the three types mentioned above, triglycerides are the least oxygenated type of biomass and therefore are much easier to convert to liquid fuels. Three of the projects are aimed at both developments of new and innovative catalysts to enable both green chemistry in the processes and use of inedible source of rough matter. Also if possible it is suggested not to replace fossil fuels as such but to lower the use of these by providing additives to enhance more energy and better performance. The "second generation" modification to enable better energy input and rheology achieved *via* innovative catalytic treatments will be discussed[1,2].

A more challenging undertaking of our groups is the production of high-end energy saving chemicals derived from cellulose or lignocellulose. Lignocellulose is a non-edible feedstock of natural organic carbon. It is the most abundant raw material in nature and therefore it attracted much attention in the last decade. Cellulose has a very high degree of crystallinity and as a result it is a difficult material to process. In our research we have developed a process for the production of 5-methylfurfural that can serve as fuel candidate or preferably as fuel additive. In future work we suggest one pot synthesis of 5-methyl furfural from lignocellulosic waste, as initial results imply the great potential of this kind of process especially *via* CMF. One pot synthesis can save time consuming steps and increase potential applicability of the process. In addition, as was mentioned above, exploring for robust and cheaper catalysts can contribute to the economic feasibility of the process. Here too a promising catalyst can be found in the polyoxometalates family[3].

References

E. Meller, U. Green, Z. Aizenshtat, Y. Sasson. Catalytic deoxygenation of castor oil over Pd/C for the production of cost effective biofuel Fuel **133** (2014) 89–95.
Meller E, Aviv A, Aizenshtat Z, Sasson Y, Catalytic hydrocracking –hydrogenation of castor oil fatty acid methyl esters over nickel substituted polyoxometalate catalyst RSC Advances 6, 2016, 36069-36076
Meller E, Sasson Y, Aizenshtat Z. Palladium catalyzed hydrogenation of biomass
derived halogenated furfurals. Submitted to RSC Advances 2016.

Challenges in Rhenium-Osmium (Re-Os) Isotope Dating of Hydrocarbons in Petroleum Systems

Zhen Li[1, 2, *], Xuan-Ce Wang[1, 2], Keyu Liu[3], Xue-Mei Yang[1]

[1]The Institute for Geoscience Research (TIGeR), Department of Applied Geology, Curtin University, Perth, WA 6845, Australia
[2]The School of Earth Science and Resources, Chang'an University, Xi'an 710054, P.R. China
[3]School of Geosciences, China University of Petroleum, Qingdao 266555, P.R. China
*(*corresponding author: zhen.li@curtin.edu.au)*

Direct dating of hydrocarbons is crucial for petroleum exploration. The Re-Os isotopic method was proposed to be one of most promising techniques to constrain the timing of oil formation, migration or charge in petroleum systems. Our pilot studies imply that, in some cases, the Re-Os radiometric system could be a highly potential geochronometer for petroleum dating, but ongoing uncertainties are hindering the use of the Re-Os isotopes in providing reliable dating for petroleum system analysis.

The mechanism capable of fractionating Re/Os in a petroleum system is still unclear. Early studies (e.g., Selby and Creaser, 2005) speculated that precipitation of asphaltenes during oil migration, mixing, and charging into reservoirs may fractionate Re/Os ratios that can satisfy the requirement of the Re-Os isochron dating technique. However, experiment simulating the sequential asphaltene precipitation in a petroleum system suggests that the asphaltene precipitation has little effect on the Re/Os ratio, and is unlikely to perturb the Re–Os geochronometer (Mahdaoui et al., 2013). Furthermore, hydrous pyrolysis experiments indicated that the bitumen generation is capable of both homogenizing the Os isotopes and fractionating the Re/Os ratios at a local scale (Rooney et al., 2012; Cumming et al., 2014), whereas only low concentrations of Re and Os were found in the oils expelled in these experiments, implying negligible transfer of Re and Os from kerogen into oil. More importantly, the results of recent hydrothermal experiments (Mahdaoui et al., 2015) challenged the traditional viewpoint. Although the results have been questioned due to poor consistency of their data and overestimation of the partition rate of Re and Os in natural water-bearing petroleum systems (Wu et al., 2016), the work of Mahdaoui et al. (2015) provides a fresh perspective on Re/Os fractionation in complex petroleum systems. If the deduction in Mahdaoui et al. (2015) is true, the Re-Os isochrones obtained from hydrocarbons may represent the timing of the latest hydrodynamic closure of the traps.

Thermal cracking of low-maturity bitumen and crude oil (Huc et al., 2000) is an important way to produce dry gas and pyrobitumen. This process may play a key role in redistributing Re-Os in petroleum systems. Therefore, the behaviour of the Re-Os isotope system in this process is fundamental to interpret the obtained Re-Os isochron age on bitumen. Previous researchers proposed that thermal cracking may have minimal or no effect on the Re–Os systematics in hydrocarbons (Lillis and Selby, 2013). However, case studies on bitumen of different maturity from the Xuefeng uplift in China argued that thermal cracking could reset the Re-Os systematics, thus considered the Re-Os isochron age of high-maturity bitumen as the timing of thermal cracking in petroleum systems (Ge et al., 2016). More recently, our pilot studies on Neoproterozoic bituminous sandstone intruded by two gabbro-diabase sills (ca. 66-80 m thick) suggest that the Re–Os radiometric system in high-maturity bitumen (pyrobitumen) were totally perturbed and unable to yield any meaningful isochrones. This further makes the issue on the effect of thermal cracking on the Re–Os isochrones more complex.

In summary, the detailed behaviour and fractionation mechanism of Re and Os in petroleum systems remain controversial. These uncertainties have led to the current lack of well-accepted sampling strategies, analysing protocols, and guidelines of data interpretations for Re-Os isotope dating of hydrocarbons in petroleum exploration. Filling such a knowledge gap requires the integration of both organic and inorganic geochemistry approaches. It requires research to take a critical step to accomplish a valuable application guide for petroleum industry end-users on direct Re-Os dating of petroleum systems.

References

Cumming, V.M., Selby, D., Lillis, P.G., Lewan, M.D., 2014. Re–Os geochronology and Os isotope fingerprinting of petroleum sourced from a Type I lacustrine kerogen: Insights from the natural Green River petroleum system in the Uinta Basin and hydrous pyrolysis experiments. Geochimica et Cosmochimica Acta 138, 32-56.
Ge, X., Shen, C., Selby, D., Deng, D., Mei, L., 2016. Apatite fission-track and Re-Os geochronology of the Xuefeng uplift, China: Temporal implications for dry gas associated hydrocarbon systems. Geology 44, 491-494.
Huc, A.Y., Nederlof, P., Debarre, R., Carpentier, B., Boussafir, M., Laggoun-Défarge, F., Lenail-Chouteau, A., Bordas-Le Floch, N., 2000. Pyrobitumen occurrence and formation in a Cambro–Ordovician sandstone reservoir, Fahud Salt Basin, north Oman. Chemical Geology 168, 99-112.
Lillis, P.G., Selby, D., 2013. Evaluation of the rhenium–osmium geochronometer in the Phosphoria petroleum system, Bighorn Basin of Wyoming and Montana, USA. Geochimica et Cosmochimica Acta 118, 312-330.
Mahdaoui, F., Michels, R., Reisberg, L., Pujol, M., Poirier, Y., 2015. Behavior of Re and Os during contact between an aqueous solution and oil: Consequences for the application of the Re–Os geochronometer to petroleum. Geochimica et Cosmochimica Acta 158, 1-21.

Mahdaoui, F., Reisberg, L., Michels, R., Hautevelle, Y., Poirier, Y., Girard, J.-P., 2013. Effect of the progressive precipitation of petroleum asphaltenes on the Re–Os radioisotope system. Chemical Geology 358, 90-100.
Rooney, A.D., Selby, D., Lewan, M.D., Lillis, P.G., Houzay, J.-P., 2012. Evaluating Re–Os systematics in organic-rich sedimentary rocks in response to petroleum generation using hydrous pyrolysis experiments. Geochimica et Cosmochimica Acta 77, 275-291.
Selby, D., Creaser, R.A., 2005. Direct radiometric dating of hydrocarbon deposits using rhenium-osmium isotopes. Science 308, 1293-1295.
Wu, J., Li, Z., Wang, X.-c., 2016. Comment on “Behavior of Re and Os during contact between an aqueous solution and oil: Consequences for the application of the Re–Os geochronometer to petroleum” by Mahdaoui et al. (2015). Geochimica et Cosmochimica Acta.

NanoMin; a quantum step in understanding the diagenetic and depositional history of organic carbon rich shale

Martin Kennedy[1,*], Stefan Loehr[1], Habibur Rahman[1], Soumaya Abassi[1]

[1] Department of Earth and Planetary Sciences, Macquarie University, Sydney 2109, Australia
(corresponding author: ben.bloggs@company.com)*

Spatially resolved chemistry, phase (mineralogical) identification, and quantification are essential to many fields of scientific enquiry, particularly at the critical nanoscale at which many natural environmental processes occur. Sub micron scale mineral growths within shale can determine the viability of a hydrocarbon reservoir by occluding porosity and influencing the composition of hydrocarbons generated from primary organic particles by catalytic reactions. Studies of coarse-grained materials routinely depend on the determination of minerals and their distribution using simple optical petrography or spatially resolved electron probe data such as QEMSCAN (Quantitative Evaluation of Minerals by SCANning electron microscopy) or MLA (Mineral Liberation Analyser) systems. However, spatially resolved mineral identification has long proven a challenge in fine-grained materials, whether engineered, geological or biological in origin, where individual mineral grains are commonly smaller than the resolving power or analytical volumes of the techniques used. This broad class of material is most commonly studied using bulk characterisation approaches such as X-ray diffractometry and FTIR spectroscopy of powders. The loss of spatial and contextual information leads to inferences of importance based simply on abundance, which is of particular concern with these techniques because of their poor detection limits.

Here we apply a new system called NanoMin capable of sub µm quantitative mineral mapping based on FEG-SEM-EDS (Field Emission Gun Scanning Electron Microscope - Energy Dispersive X-ray spectrometry). At present, the most advanced commercial SEM-based mineral mapping systems (QEMSCAN and MLA) are fundamentally limited in their characterisation of mixed phase X-ray spectra. Mixed spectra are obtained when multiple phases (minerals) are presented in the electron-beam excitation volume. QEMSCAN and MLA can only assign a single mineral to each 5 µm pixel area (Fig 1). NanoMin quantitatively resolves multiple minerals within the excitation volume of every single pixel allowing for multiple phase determinations. The spectral deconvolution engine and standard mineral spectra database that form part of NanoMin allow each analysed micro-spot to be decomposed into up to three component minerals, an approach which explicitly acknowledges the common presence of mixed mineralogies in each analysed volume/spot. This capability opens up analysis of complex fine-grained materials in which quantitative mineral mapping has not previously been possible, resulting in greater accuracy in mineral identification, spatial understanding of trace minerals, quantification and analysis of spatial relationships between phases.

NanoMin data are compared between two late Permian aged shale reservoirs in South Australia; the lacustrine REM interval of the Cooper Basin and adjacent marine Stuart Range Formation in the Arckaringa Basin (Figure 1). Both show systematic distributions of early carbonate cements. The REM lacustrine depositional environment resulted in early diagenetic low S, high Fe cements (siderite) that were preferentially formed in coarser grained portions of laminae. These cements parse the reservoir by restricting migrating hydrocarbons to finer grain size intervals. By contrast, S availability in the marine Stuart Range Fm. led to sequestration of Fe in pyrite prohibiting the formation of siderite. Excess S resulted in sulfurization reactions that preserved lipid-rich type II organic matter. Pyritic intervals dominated by type II kerogen alternated with Mn-carbonate cemented intervals dominated by type III (refractory terrestrial) OM in varved intervals with the distribution controlled by oscillations in basinal redox conditions. The dominance of one cycle over the other influences hydrocarbon potential as well as brittleness and reservoir compartmentalization where Mn-carbonate intervals increase. While Mn-carbonate and siderite were present in trace amounts in many of the samples analysed by powder X-ray diffraction, the spatial data from the *insitu* technique provided the environmental significance and the ability to better understand basinal trends in source, reservoir, and rock properties.

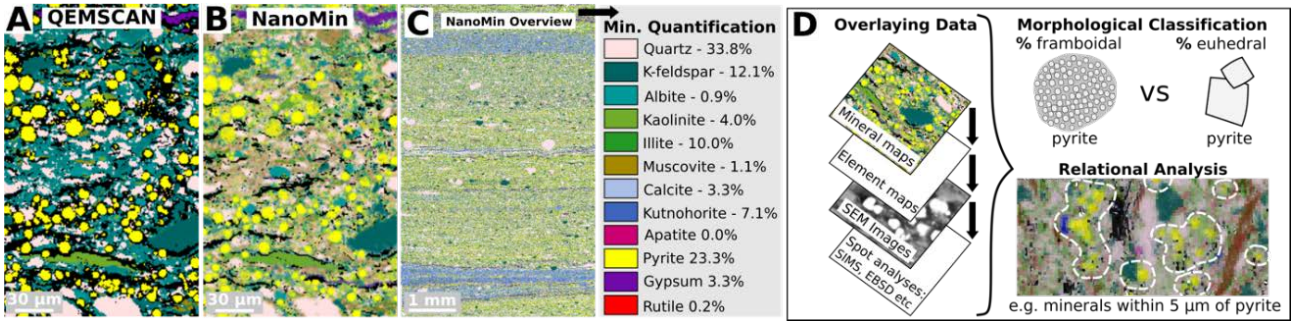

Fig 1: The NanoMin system is the first SEM-based mineral mapping system specifically designed for grain determination in mudstones. Comparison of mineral maps of a Permian-aged Australian mudstone collected with QEMSCAN vs. NanoMin show that QEMSCAN erroneously maps the heterogeneous fine-grained matrix comprising clays and mica **(B)** as homogeneous feldspar **(A)**. **(C)** Mn-carbonate (kutnohorite) is present in trace amounts in many of the samples analysed by powder X-ray diffraction The spatial data from the NanoMin maps identify that it is concentrated in cyclical laminae recording basinal changes in redox conditions of the water column. **(D)** The NanoMin system simultaneously collects elemental maps, mineral distribution maps, organic matter distribution maps, and seamlessly stitched, nm-resolution electron microscope images of samples up to several cm in size. The maps can be used to define regions of interest, ranging in size from only a few μm^2 to several cm^2, from which to extract quantitative mineralogy. This data can be overlaid so that each mineral can be quantified, grain and organic matter morphotypes can be distinguished, and spatial associations between particular mineral phases can be statistically assessed. The overlays provide base maps to identify and locate representative grains for detailed crystallographic, compositional or isotopic analysis using other *in situ* tools.

Constraining the impact of benthic meiofaunal activity on organic carbon burial in ancient oxygen-depleted sedimentary environments

Stefan C. Löhr[1,]*, Martin J. Kennedy[1] & Simon C. George[1]

[1]Department of Earth & Planetary Sciences, Macquarie University, North Ryde 2109, Australia
(corresponding author: stefan.loehr@mq.edu.au)*

The dynamic interaction between marine sediments and burrowing fauna represents one of the key biogeochemical processes on Earth. Benthic animals facilitate sediment irrigation and oxygen ingress through burrowing, and accelerate organic matter (OM) degradation through ingestion, physical comminution and enzymatic breakdown. Since their proliferation in the Cambrian, animal burrowers have left an indelible signature on the sedimentary record in almost all marine environments, with the seeming exception of low oxygen environments (Bromley, 1996). However, sub-mm benthic animals (termed meiofauna) adapted to low oxygen conditions are ubiquitous in modern sediments (Levin, 2003). Since they leave few recognisable traces their influence on ancient sediments is generally overlooked, and almost nothing is known about their impact on biogeochemical cycling in the past.

We have recently developed a novel imaging approach comprising back scatter electron (BSE) microscopy of Ar-ion polished samples to identify meiofaunal trace fossils. Using this approach we have shown, in Pliocene-aged sapropels from the Eastern Mediterranean, the first reported trace fossil evidence of meiofaunal activity and its relation to changing oxygenation (Löhr and Kennedy, 2015). Pliocene sapropels are a classic anoxic facies, but we show meiofauna to have reworked the uppermost 3-4 cm of several sapropels under conditions sufficiently oxygen-depleted to exclude benthic macrofauna. The meiofauna fragmented and ingested organic material formerly concentrated in discrete laminae, emplacing 15-70 µm diameter faecal pellets without visibly influencing the macroscopic sediment fabric (Fig. 1).

Sapropels are commonly used as a model system for anoxic preservation of OM, and they may also be representative of meiofaunal modification that has as yet gone unnoticed in other fine- grained sediments from low-oxygen settings. An important question that remains unresolved is to what extent meiofaunal reworking impacts both the quantity and the quality of the organic matter preserved in low-oxygen settings. Comparison to similar modern environments suggests a strong meiofaunal influence on sediment biogeochemistry and organic matter preservation (e.g. Aller and Aller, 1992), but this question remains untested in ancient examples.

Here we study sapropel cycles from two locations in the Mediterranean to determine the magnitude of OM mineralization attributable to meiofaunal burrowing, it's influence on the molecular composition of the organic matter, as well as the redox conditions under which meiofaunal burrowing commenced and intensified. We use high resolution backscatter electron mapping of organic matter distribution and morphology to: 1) identify the onset of meiofaunal and macrofaunal burrowing, and 2) quantify the proportion of OM at each depth present in intact OM laminae, fragmented OM laminae or faecal material. Our results confirm that there is a clear threshold at which both meiofaunal and macrofaunal burrowing become pervasive, with close to 100% of organic material present within fecal pellets or <100 µm laminae fragments. An unexpected result is the observation of vertically and horizontally discontinous pockets (<500 µm) of meiofaunally bioturbated material embedded in otherwise laminated sediment, implying that short-lived episodes of benthic amelioration and recolonisation occurred prior to fully-fledged benthic reworking.

We combine this information with bulk geochemical characterization of samples collected at a mm scale (TOC, biogenic Ba, redox sensitive trace metals, GC-MS). Bulk geochemical characterisation is ongoing. Once completed the changes in the TOC/Ba_{bio} ratio, molecular composition of OM and trace element concentrations of the sediment will be related to the magnitude of meiofaunal burrowing at each depth interval. Biogenic barium is a proxy for OC flux and is widely applied to reconstruct pre-diagenetic OC concentrations in sapropels (de Lange et al., 2008), allowing us to determine the proportion of OM delivered to the sea floor that was ultimately preserved at each depth. Concentrations of redox sensitive trace metals will be combined with organic redox proxies to determine the conditions under which meiofaunal reworking commenced and/or intensified, while molecular characterisation of OM will identify qualitative changes to organic matter composition attributable to meiofaunal activity.

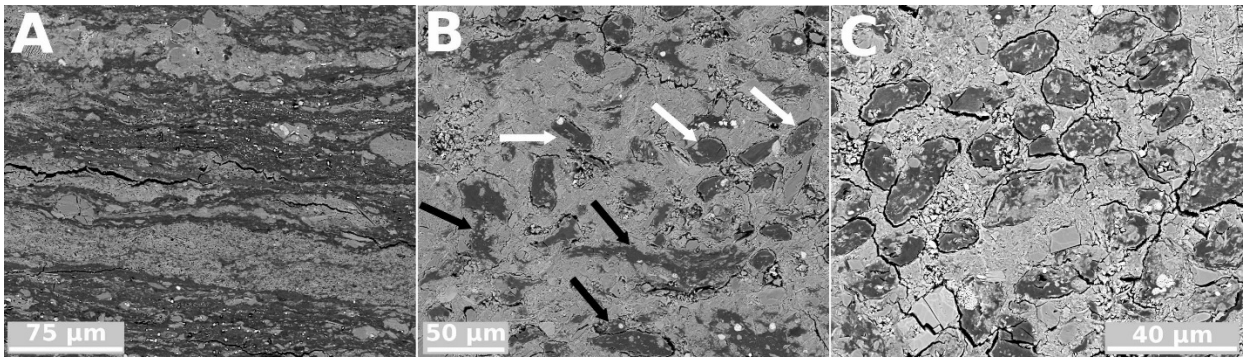

Fig. 1. (A) BSE image showing OM concentrated in discrete laminae in a Pliocene sapropel from ODP Site 969. Where meiofaunal bioturbation has occurred (B+C), OM laminae are fragmented (black arrows) or reworked into faecal pellets (white arrows). The sudden onset of meiofaunal reworking identifies an environmental threshold, after which the extent of reworking increases steadily upsection.

References

Aller, R.C., Aller, J.Y., 1992. Meiofauna and Solute Transport in Marine Muds. Limnology and Oceanography 37, 1018–1033.

Bromley, R.G., 1996. Trace Fossils, 2nd ed. Chapman & Hall.

de Lange, G.J., Thomson, J., Reitz, A., Slomp, C.P., Speranza Principato, M., Erba, E., Corselli, C., 2008. Synchronous basin-wide formation and redox-controlled preservation of a Mediterranean sapropel. Nat Geosci 1, 606–610. doi:10.1038/ngeo283

Levin, L.A., 2003. Oxygen minimum zone benthos: Adaptation and community response to hypoxia. Oceanography and Marine Biology: an Annual Review 41, 1–45.

Löhr, S.C., Kennedy, M.J., 2015. Micro-trace fossils reveal pervasive reworking of Pliocene sapropels by low-oxygen-adapted benthic meiofauna. Nature Communications 6, 1–8. doi:10.1038/ncomms7589

Iron cemented sandstone in coastal regions of Western Australia: Mechanisms of Formation and Impacts on Groundwater

Mehwish Ali[1], Anna Heitz*[2]

[1]Department of Civil Engineering, Curtin University
[2]Department of Civil Engineering, Curtin University
(corresponding author: A.Heitz@curtin.edu.au)*

Degradation of groundwater quality is an ongoing problem around the coastal aquifers of the world. The coastal aquifers of Western Australia are affected due to various factors including salt water intrusion, groundwater acidity and climate change. An important determinant of the susceptibility to degradation is the hydrogeological setting of an aquifer. Many settings contain sandy formations which have been indurated over time and formed units of cemented sediments, colloquially known as “Coffee Rock”. This material is found to be the part of coastal aquifers in many parts of south-western Australia but its role and formation process is still unclear. This research is investigating the nature, distribution and mechanism of formation of “Coffee Rock” and its role in the degradation of groundwater. The study is determining the hydrogeological, geochemical and geotechnical characteristics of “coffee rock” and its influence, on water quality and water movement along coastal aquifers in Southern Western Australia. Numerical models will be developed on the basis of results obtained to determine the potential for further formation of these cemented iron materials and their future potential to affect aquifer characteristics and groundwater quality. The outcome of this work has the potential to contribute to ground water management plans of coastal aquifers.

Colloquially known “Coffee Rock” is observed on beachlines near Esperance in South Western Australia. It is hypothesized that this rock-like material is presently being formed and is at different stages of diagenesis. The formation process involves transport of iron and/or organic matter through groundwater movement, leading to cementation of silica grains by formation of an iron-hydroxide mineral material, suggested to be hematite by preliminary testing. To investigate the process of formation of these rocks, different samples were collected and analysed by examining the mineralogy, elemental composition and physical properties. A TESCAN Integrated Mineral Analyser (TIMA) technique has been used to study the minerals and elemental distribution of the sample. Thermogravimetric analysis has been used to determine the organic and inorganic carbon content of the cementing material. Index engineering properties of the material will be determined by performing geotechnical tests which will help in engineering classification of the material. Further examination will determine its role as aquifer forming units.

References

Cox M., Harbison J., Ezzy T., Preda M., Brooke B., Lee R., Lester J., Oberhardt M. and Laycock J. (2000), “Coffee Rock”: an Overview of its Character and Occurrence in the Pumicestone Rgion”, Pumicestone Passage & Deception Bay Catchment Conference, PASSCON 2000.

Cox M., Brooke B., Preda M., Lee R., Olley J., Pietsch T. and Price D. (2008), “Development, composition and age of indurated sand layers in the Late Quaternary coastal deposits of northern Moreton Bay, Queensland, Australian”, Journal of Earth Sciences, 55:2,141-157, DOI: 10.1080/08120090701689316

Chandrasekar N, Selvakumar S., Srinivas Y., Wilson J.S.J., Peter T.S., Magesh N.S. (2013), “Hydrogeochemical assessment of groundwater quality along the coastal aquifers of southern Tamil Nadu, India”, Springer-Verlag Berlin Heidelberg 71:4739–4750, DOI: 10.1007/s12665-013-2864-3

Davidson, WA (1995), “Hydrogeology and Groundwater Resources of the Perth Region, Western Australia”: Geological Survey of Western Australia, Bulletin 142.

Department of Environment and Conservation, Gov. of WA. 2009. “Understanding soil processes controlling landscape acidity and heavy metal mobilisation in Aquic Podosols on the Swan Coastal Plain”, https://www.water.wa.gov.au/__data/assets/pdf_file/0011/5123/86706.pdf

Farmer V.C. (1983), “Genesis of humus B horizons in hydromorphic humus podzols”, Nature 304. 0028-0836/83/300342

Lee S.Y. and Gilkes R.J. (2004), “Groundwater geochemistry and composition of hardpans in Southwestern Australian regolith.” Geoderma 126:59-84. DOI:10.1016/j.geoderma.2004.11.007

Löhr S., Grigorescu M., Fraser S.J. and Cox M (2010), “Iron occurrence in soils and sediments of a coastal catchment a multivariate approach using self-organizing maps”, Geoderma 156(3-4):253-266. DOI: 10.1016/j.geoderma.2010.02.025

Morse J.W., Cornwell J.C, Arakak T., Lin S., and Huerta-Diaz M. Diaz (1992), “Iron Sulfide and Carbonate Mineral Diagenesis in Baffin Bay, Texas”, Journal of Sedimentary Petrology, 62(4):671-680, 0022-4472/92/0062-0671

Prakongkep N., Gilkes R.J., Singh B. and Wong S (2010), “The Morphology and Composition of Pyrite in Sandy Podosols in The Swan Coastal Plain”, 19th World Congress of Soil Science, Soil Solutions for a Changing World, 1-6 August 2010, Brisbane, Australia. Published on DVD

Ramana J.V., Rao M.J., Venngopal R., Rao M.C., Avataram N. (2007), “Characterization of Beach Rock- underlying placer mineral sand deposits, Vishakapatanam Coast, Andhraha Pardesh”, Journal of Geological Society of India 70(6): 975-980, 0016-7622/2007-70-6-975

Tarawneh K., Alnawafleh H., Harahsheh M., Radaideh N., Shreideh S., Moumani k., Tarawneh B. and Abdelghafoor M (2011), “”Minerology, Geochemistry and Genesis of the ferruginous sndstone in Batn al Ghul Area, Southern Jordan, Annual of the University of Mining and Geology, ST. IVAN RILSKI, 54(1):89-94, www.researchgate.net/publication/281509895

Poster Presentation Abstracts

Sub-marine mass slide as a potential biomarker reservoir: Preliminary results from IODP Expedition 355, Arabian Sea

Sophia Aharonovich[1*], Denise K. Kulhanek[2], Peter D. Clift[3], and Simon C. George[1]

[1]Macquarie University, North Ryde, Sydney, NSW, 2109, Australia
[2]Texas A&M University, College Station, Texas, 9547, USA
[3]Louisiana State University, Baton Rouge, LA, 70803, USA
(corresponding author: sophia.aharonovich@mq.edu.au)*

The study of mass transport deposits (MTDs) is an important field of research due to the potential insights into catastrophic events in the past and modern geohazard threats (e.g. tsunamis). Submarine mass movements are very significant processes in sculpturing the structure of continental margins, particularly in their extent and magnitude that have consequences both in the modern day as well as in the geological past. In addition, the high volume of many mass movements and the rapid burial of the sediments means that post-depositional alteration of the organic matter will be minimised, so preservation potential of any biomarkers is high. An understanding of the complex stratigraphy of a submarine mass transport deposit might help in reconstructing the provenance and transport pathways of the material and thus give important insights into sedimentary dynamics and processes triggering specific events.

Drilling operations during the International Ocean Discovery Program (IODP) Expedition 355 - Arabian Sea Monsoon took place during April and May 2015, with two cored sites in the Laxmi Basin (Pandey et al., 2015). Site U1456 was cored to 1109.4 m below seafloor (mbsf), with the oldest recovered rock dated to 13.5-17.7 Ma. Site U1457 was cored to 1108.6 mbsf, with the oldest rock dated to 62 Ma. The sites contain 330 m and 190 m of MTD material, respectively. The MTD layers mainly consist of interbedded lithologies of dark grey claystone, light greenish calcarenite and calcilutite, and conglomerate/breccia (Fig.1), with ages based on calcareous nannofossil and foraminifer biostratigraphy ranging from the Eocene to the early Miocene (Pandey et al., 2015). This MTD, known as the Nataraja Slide, is the third largest MTD known from the geological record, and the second largest on a passive margin. Calvés et al. (2015) identified a potential source area offshore of Sourashstra on the Indian continental margin, and invoked a single step mass movement model to explain the mechanism of emplacement.

The purpose of this study is to understand the depositional and post-depositional processes of the sedimentary layers in the MTD. Initial shipboard work demonstrated a high variability in total organic carbon (TOC) and total nitrogen (TN) levels in different depth within the MTD, might suggest multiple step mass movement model with some variations in deposited organic matter.

Here we present the biomarker signature of the material based on gas chromatography-mass spectrometry (GC-MS) and high performance liquid chromatography-mass spectrometry (HPLC-MS) analyses (Fig. 1 and 2). High carbon preference index values ($CPI_{22\text{-}32}$ >1.5) and highly branched glycerol dialkyl glycerol tetraethers (GDGTs) index values (BIT >0.85) suggest high terrestrial lipid input with some variation in the oxicity of depositional environment through the MTD. A contribution of shallow marine biomarker input is suggested based on the sterane data. Sea surface temperature (SST) reconstruction based on the unsaturated alkenone index ($U^{K'}_{37}$) suggest very little variation through the MTD, with an average around 27.6°C. In contrast, the isoprenoid GDGT based index (TEX^{H}_{86}) shows a much more diverse temperature range (22-30°C).

The unique opportunity of collaborative, multi-disciplinary data collection produced on-board the JOIDES Resolution, together with post-cruise research, allows us to create a better understanding of the processes involved in creation of one of the largest MTDs on Earth and its geological potential.

References

Calvès, G., Huuse, M., Clift, P.D. and Brusset, S., 2015. Giant fossil mass wasting off the coast of West India: The Nataraja submarine slide. *Earth and Planetary Science Letters*, **432**, pp. 265-272.
Pandey, D.K., Clift, P.D., Kulhanek, D.K., et al., 2015. Expedition 355 Preliminary Report: Arabian Sea Monsoon. International Ocean Discovery Program. http://dx.doi.org/10.14379/iodp.pr.355.2015

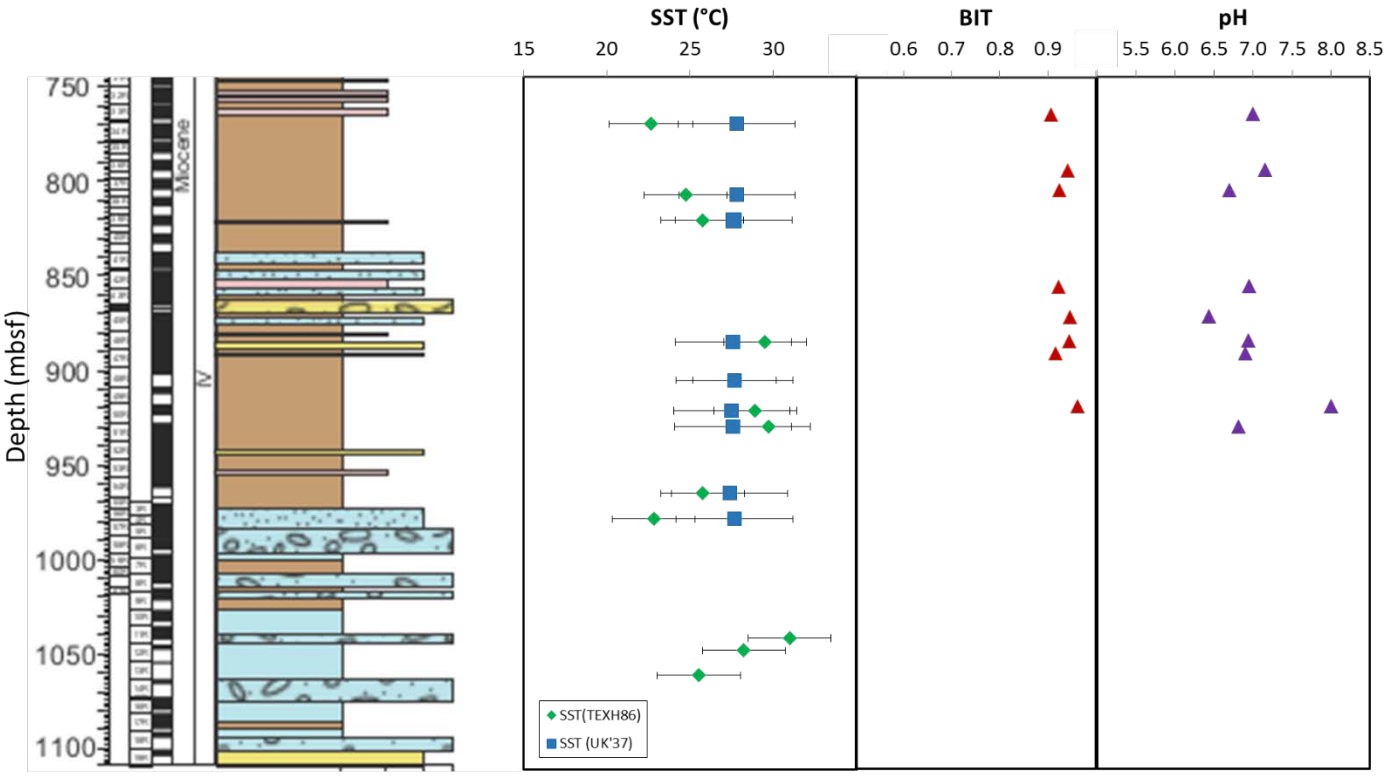

Fig. 1: IODP Expedition 355 Site U1456 unsaturated alkenones, isoprenoid GDGTs, and branched GDGTs data relative to the lithology of the mass transport deposit.

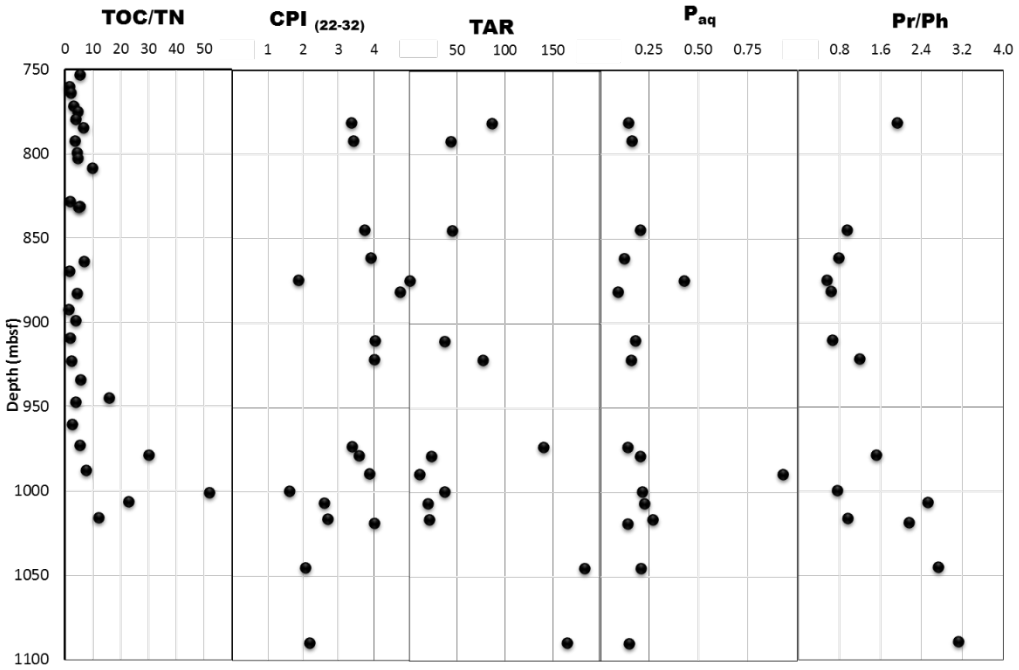

Fig. 2: IODP Expedition 355 organic composition of mass transit deposit from detected at the Site U1456 relative to the depth, where TAR – terrigenous/aquatic ratio, P_{aq} – submerged/floating aquatic macrophyte input vs. emergent and terrestrial input, Pr- pristane, and Ph – phytane.

Chemistry Honours Project: Using GC x GC-TOF-MS to identify individual naphthenic acids within a degraded crude oil sample

Callum Bonnar[1*], Alan Scarlett[1], Kliti Grice[1]

1. Western Australia Organic and Isotope Geochemistry Centre (WA-OIGC), Department of Chemistry, Curtin University, Bentley, WA 6102, Australia
(Corresponding author: callum.bonnar@student.curtin.edu.au)

Historically the characterisation of individual molecular components in complex petrochemical mixtures has been difficult and poorly realized, especially for the heavier fractions. This is in spite of great effort and skill devoted to the study of petroleum composition (1). Analytical methods for volatile compounds such as fractionation or gas chromatography would seem relevant, but the vast number of components with similar column partition behaviour has previously restricted progress (2). However advances in multidimensional instrumental methods have greatly improved the ability to characterise the individual structure of similar compounds (3, 4).

A class of compounds within petroleum that is of particular interest are the naphthenic acids, which cause corrosion in refineries and toxic pollution in process waters (5). Naphthenic acids are formally defined as carboxylic acids with the formula $\mathbf{C_nH_{2n-z}O_2}$, where **z** is equal to the hydrogen deficiency caused by the presence of saturated rings. Typically 5- and 6- member rings are present in varying numbers and arrangements, although other structures including n-alkane and benzyl compounds also appear.

This project applies the method of two-dimensional gas chromatography/ time of flight mass spectrometry (GC x GC – TOF MS) to the analysis of an extract of highly degraded crude oil. Success in identifying individual naphthenic acid molecules has been previously achieved using a non-polar primary column and a polar secondary column in such instruments (6). Following on from these successes, it is hoped that a method can be optimised to identify the naphthenic acid compounds within crude oil samples. There are two areas to consider for the method development of this project. The first is the extraction or clean-up of the raw oil sample prior to chromatography. The second aspect is optimisation of GC x GC parameters for the best separation of components within the sample.

Extraction Techniques: A variety of different techniques can be used for isolation of naphthenic acids in crude oil, to reduce the number of possible interferences during gas chromatography. These include silica gel columns to separate the polar fraction, base extraction, and non-aqueous ion exchange solid phase extraction among others (7, 8). The isolated polar fraction is then often modified to turn carboxylic acids into the respective –methyl or –silyl esters to somewhat reduce reactions with polar columns. The particular combination of these techniques may affect naphthenic acids differently depending on their unique structure, so comparison is needed (9).

Optimisation of GC x GC Method: Once the acidic fraction has been pre-separated and derivatised, there are a number of factors that can be optimised in the GC x GC-TOF-MS method. These include the choice of column stationary phase, whether to use polar->non-polar or non-polar->polar configurations, column length, heating regimes, modulation time between columns etc. A given set of parameters can cause better resolution between some peaks but co-elution between others, so may have to be adjusted empirically to achieve the best results (10).

Once a method is developed, it can be applied to one or several samples of degraded crude oil to study the presence and structure of naphthenic acids. The information can then be used to explore patterns between different samples and the geochemical history of each oils' formation.

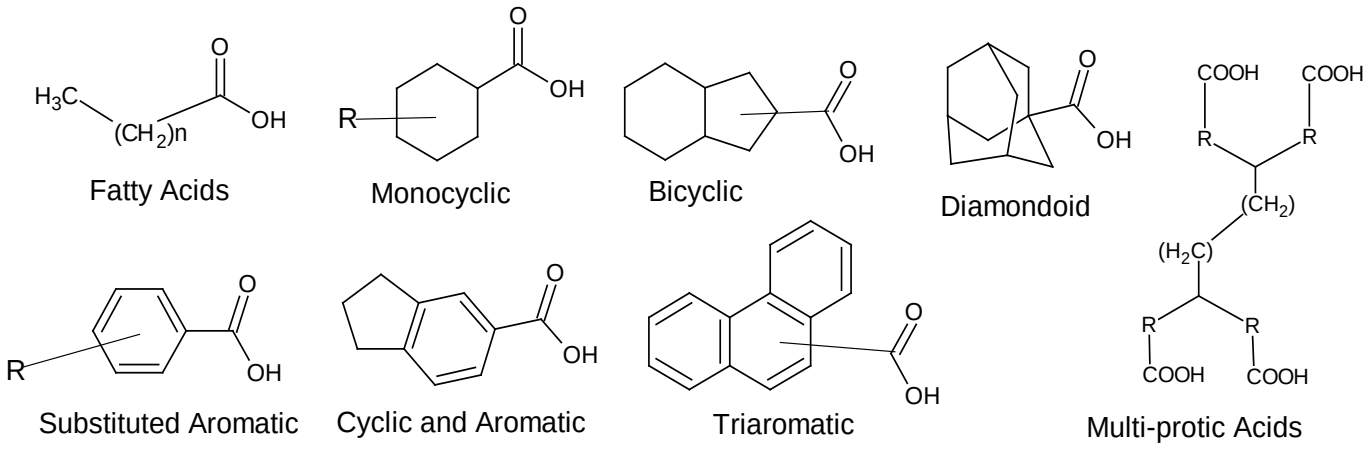

Fig. 1. Some potential naphthenic acid structures

References

1. Rossini FD. Hydrocarbons from petroleum: the fractionation, analysis, isolation, purification, and properties of petroleum hydrocarbons: an account of the work of the American Petroleum Institute Research Project 6. In: American Petroleum I, editor.: New York: Reinhold; 1953.
2. Beens J, Brinkman UAT. The role of gas chromatography in compositional analyses in the petroleum industry. Trends in Analytical Chemistry. 2000;19(4):260-75.
3. Liu Z, Phillips JB. Comprehensive two-dimensional gas chromatography using an on-column thermal modulator interface. Journal of Chromatographic Science. 1991;29(5):227-31.
4. Giddings JC. Two-dimensional separations: concept and promise. Analytical chemistry. 1984;56(12):1258A.
5. Clemente JS, Fedorak PM. A review of the occurrence, analyses, toxicity, and biodegradation of naphthenic acids. Chemosphere. 2005;60(5):585-600.
6. Rowland S, Scarlett A, Jones D, West C, Frank R. Diamonds in the rough: Identification of individual naphthenic acids in oil sands process water. 2011.
7. Bastow TP, van Aarssen BGK, Lang D. Rapid small-scale separation of saturate, aromatic and polar components in petroleum. Organic Geochemistry. 2007;38(8):1235-50.
8. Jones D, West CE, Scarlett AG, Frank RA, Rowland SJ. Isolation and estimation of the 'aromatic' naphthenic acid content of an oil sands process-affected water extract. Journal of Chromatography A. 2012;1247:171-5.
9. Ahmed M, George SC. Changes in the molecular composition of crude oils during their preparation for GC and GC–MS analyses. Organic Geochemistry. 2004;35(2):137-55.
10. Eiserbeck C, Nelson RK, Grice K, Curiale J, Reddy CM. Comparison of GC–MS, GC–MRM-MS, and GC×GC to characterise higher plant biomarkers in Tertiary oils and rock extracts. Geochimica et Cosmochimica Acta. 2012;87:299-322.

Geochemical and sedimentological characterisation of the shallow marine-fluvial Permian succession, Cadda Terrace, northern Perth Basin.

Caroline Butland* and Annette D. George

School of Earth & Environment, University of Western Australia, Perth, 6009, Australia.
(corresponding author: caroline.butland@research.uwa.edu.au)*

The Perth Basin is a proven petroleum basin with producing wells both onshore and offshore in the northern part of the basin. There are a number of source rock intervals (Irwin River Coal Measures, Carynginia Formation, Kockatea Shale) supplying oil and gas to conventional reservoirs, with the Lower Triassic Kockatea Shale identified as a source for oil, and all formations recognised as sources for gas in the region. Recent national exploration activity has focussed on source rocks from productive petroleum basins including the Perth Basin. Renewed interest in unconventional and conventional resources in this area has provided an opportunity to undertake geological and geochemical characterisation of the Permian succession on the Cadda Terrace.

Organic geochemical data (Rock Eval, TOC and VR) have been analysed from several wells located on the Cadda Terrace to distinguish patterns in kerogen type and maturity across this part of the basin (Fig. 1). Three maturation subgroups (low, medium and high) have been identified, based on their thermal maturity (Hydrogen Indices and Tmax). Type II/III kerogens in the Carynginia Formation are associated with moderate to low hydrogen content, restricted oxygenation during deposition and typically represent transgressive depositional phases. On the Cadda Terrace, the Carynginia Formation is dominated by organic-rich black shale. A shallow marine (shoreface) to proximal inner shelf depositional setting has been interpreted from sedimentary facies analysis and contains characteristic trace fossils of the *Cruziana* Ichnofacies.

Mean vitrinite reflectance, Ro, in the Carynginia Formation ranges from 0.53 % to 2.78 %, increasing towards the east, with the same easterly trend measured in the Irwin River Coal Measures. Ro ranges from 0.82% to 3.82%, with the majority of samples in the early peak gas – peak gas hydrocarbon window for gas-prone kerogens. The same easterly trend in reflectance is evident in mean inertinite reflectance across the Cadda Terrace for the Carynginia Formation and Irwin River Coal Measures. This contrasts with the overlying Kockatea Shale that shows a southerly trend in both mean vitrinite and inertinite reflectance, ranging from 0.44% to 1.82% and 1.13% to 1.92%, respectively.

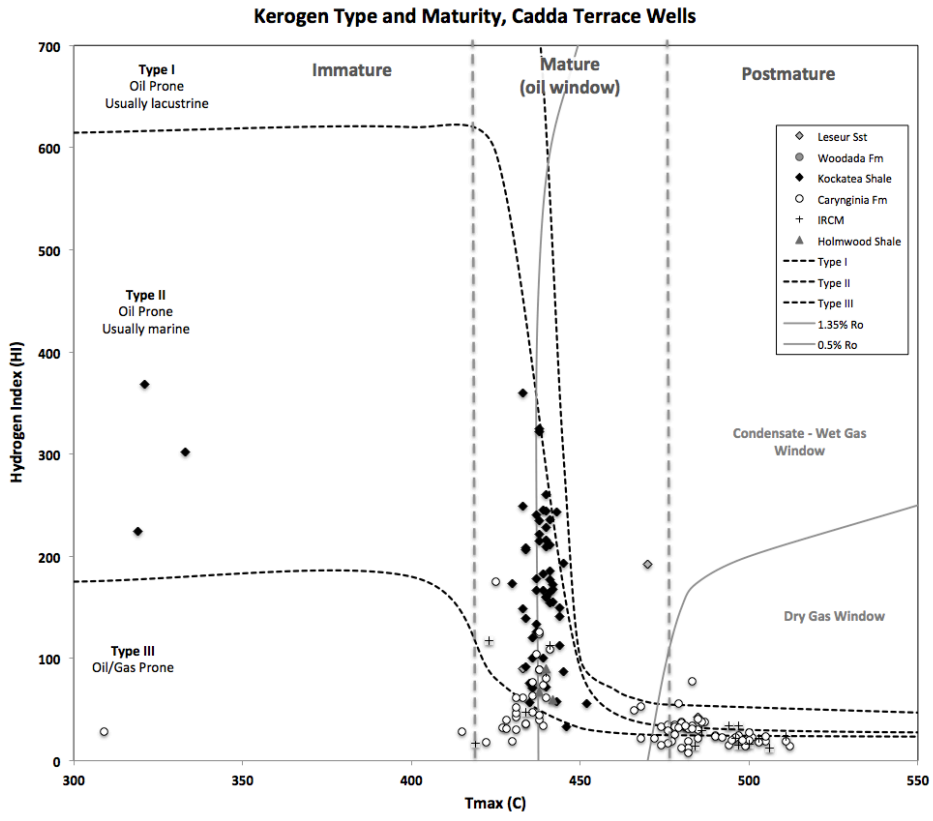

Fig. 1. Kerogen type and thermal maturity for the major source rock intervals (Kockatea Shale, Carynginia Formation, Irwin River Coal Measures) obtained from selected wells in the Cadda Terrace, northern Perth Basin.

Diamond Like Carbon (DLC) Coating in Combat for Flow Assurance.

Jamie M. Burgess[1], Amy E. Kelly[2,*], Nancy Utech[2]

[1]Shell Australia Limited, Perth 6000, Australia
[2]Shell International E&P, Houston, 77082, USA
(corresponding author: amy.a.kelly@shell.com)*

In the drive for economic development of the world's remaining hydrocarbon resources Diamond Like Carbon (DLC) coatings offer the potential to downsize both investment capital and ongoing operating expenditure. This is particularly the case for subsea completed long-offset gas condensate production in which scale and wax management can present a challenge. DLC coatings are applicable to a variety of Flow Assurance phenomena and may be applied in different operational scenarios.

Reservoired hydrocarbons of the Asia-Pacific region commonly originate from dominantly terrestrial source facies. As a result the wax property variability and related data contrast in particular with petroleum systems featuring non-terrigenous petroleum source. In Asia-Pacific fluids normal paraffins in the nC20+ range do not necessarily exhibit an exponential distribution of relative abundance like they commonly do elsewhere. Both cloud point and pour point data for Asia-Pacific oils and condensates exhibit a wide range and in places are further varied by differing degrees of secondary alteration. The Jurassic sourced gas condensates of Australia's greater northwest margin form an interesting dataset in which to compare wax properties with respective source facies.

Efficient characterisation of the challenges posed by subsea production of gas condensate fluids is provided by Shell's robust FEAST (Fluid Evaluation and Sampling Technologies)-Flow Assurance workflow. Application of DLC coating to downhole and subsea tubulars can result in minimisation of chemical service and the infrastructure required to deliver it.

Biodegradation of tricyclic terpanes in crude oils from the Bohai Bay Basin

Xiong Cheng [a,b,*] Dujie Hou [a,b,*], Changgui Xu [c], Feilong Wang [c]

[a] *School of Energy Resources, China University of Geosciences, Beijing 100083, China*
[b] *Key Laboratory of Marine Reservoir Evolution and Hydrocarbon Accumulation Mechanism, Ministry of Education, China University of Geosciences, Beijing 100083, China*
[c] *Exploration and Development Research Institute, Tianjin Branch of China National Offshore Oil Corporation, Tianjin 300452, China*
(Corresponding authors: xcheng2015@cugb.edu.cn (X. Cheng), hdj@cugb.edu.cn (D. Hou))*

A suite of 33 biodegraded crude oils from the Miaoxi Depression and Liaodong Bay, Bohai Bay Basin, China have been analyzed to investigate the effect of biodegradation on biomarkers. Amongst these samples, a sequential biodegradation of tricyclic terpanes was observed in the most degraded crude oils, in which C_{27}–C_{29} regular steranes and hopanes were almost completely removed (Fig. 1). This suggests that alteration of tricyclic terpane occurs when almost all hopanes and steranes have been removed. The C_{21}–C_{22} steranes and diasteranes were unaffected in the crude oil samples, and so they can be used as conserved ''internal standards'' to evaluate the biodegradation of tricyclic terpanes (Volkman et al., 1983). The tricyclic terpanes distributions, absolute concentrations and their relative abundance to the biodegradation resistant components show systematic changes with increasing biodegradation. The results illustrate that the tricyclic terpanes with different carbon numbers are degraded concurrently, but the relative susceptibility of the tricyclic terpane family to biodegradation decreases with increasing carbon number, with an exception of the C_{20} tricyclic terpane. No demethylated tricyclic terpanes were detected, indicating that tricyclic terpanes were biodegraded without microbial demethylation to generate demethylated counterparts (17-nor-tricyclic terpanes). Refer to the biodegradation pathways of hopanes (e.g., Watson et al., 2002; Bennett et al., 2007; Lamorde et al., 2015). Tentatively, we predict that the biodegradation pathways of tricyclic terpanes are: (a) microbial oxidation of the methyl group of the side chain to a carboxyl group with formation of tricyclic terpanoic acids, and followed by (b) demethylation of the tricyclic terpanoic acids at C-10 and generation of demethylated tricyclic terpanoic acids. Verification of this predicted biodegradation pathway will require analytical data of the related biodegradation products.

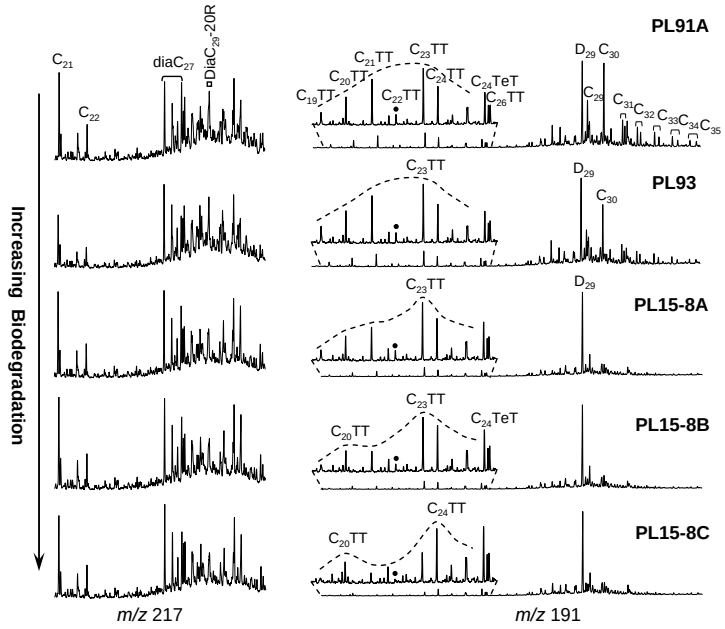

Fig. 1. Representative mass chromatograms (*m/z* 217 and *m/z* 191) showing the distributions of steranes (left), tricyclic terpanes (middle) and pentacyclic triterpanes (right) in crude oils with different biodegradation extents from the Miaoxi Depression. C_{21}–C_{22}: C_{21}–C_{22} steranes; diaC_{27}: C_{27} diasteranes; diaC_{29}-20R: C_{29} 13β(H),17α(H)-diasteranes(20R); C_{19}–C_{26}TT: C_{19}–C_{26} tricyclic terpanes; C_{24}TeT: C_{24} trecyclic terpane; C_{29}–C_{35}: C_{29}–C_{35} hopanes; D_{29}: C_{29} 25-norhopane.

References

Bennett, B., Aitken, C.M., Jones, D.M., Farrimond, P., Larter, S.R., 2007. The occurrence and significance of 25-norhopanoic acids in petroleum reservoirs. Organic Geochemistry 38, 1977–1985.

Lamorde, U.A., Parnell, J., Bowden, S.A., 2015. Constraining the genetic relationships of 25-norhopanes, hopanoic and 25-norhopanoic acids in onshore Niger Delta oils using a temperature-dependent material balance. Organic Geochemistry 79, 31–43.

Volkman, J.K., Alexander, R., Kagi, R.I., Woodhouse, G.W., 1983. Demethylated hopanes in crude oils and their applications in petroleum geochemistry. Geochimica et Cosmochimica Acta 47, 785–794.

Watson, J.S., Jones, D.M., Swannell, R.P.J., van Duin, A.C.T., 2002. Formation of carboxylic acids during aerobic biodegradation of crude oil and evidence of microbial oxidation of hopanes. Organic Geochemistry 33, 1153–1169.

Using *neo*-pentane to probe the source of gases in accumulations of the Browse and northern Perth basins

Emmanuelle Grosjean*, Dianne Edwards, Chris Boreham, Ziqing Hong, Junhong Chen, Jacob Sohn

Geoscience Australia, Canberra ACT 2601, Australia

(corresponding author: emmanuelle.grosjean@ga.gov.au)*

Mapping the geographic and stratigraphic extents of a given petroleum system requires robust oil and gas to source correlations. Correlating gases to source rocks is notoriously difficult, as it relies only on a handful of parameters (namely, the molecular and isotopic compositions of individual C_1–C_5 hydrocarbons). Adding to the difficulty is the sensitivity of these parameters to processes such as thermal maturity, biodegradation, water-washing and migration and a sound understanding of the degree to which these parameters have been affected by such processes is crucial for valid interpretation. In recent years, the carbon isotopic composition of *neo*-pentane has been shown to provide a powerful correlation tool as *neo*-pentane is strongly resistant to biodegradation and least influenced by thermal maturation (Boreham and Edwards, 2008). Examples of how this tool has been applied to decipher the origin of gases in Australia's Browse and northern Perth basins are presented here.

The Browse Basin on Australia's North West Shelf hosts considerable undeveloped gas accumulations in the central Caswell Sub-basin (Ichthys, Prelude and Concerto), along the Brecknock-Scott Reef Trend (Calliance, Brecknock, Torosa and Poseidon) and in the Heywood Graben (Crux). Oil discoveries are limited and restricted to the central Caswell Sub-basin and to the Yampi Shelf. The compound-specific carbon isotopic analysis of alkanes in gases and oils is effective at discriminating fluids in the Browse Basin and enables the identification of four petroleum systems: a basin-wide gas system sourced by the Lower–Middle Jurassic Plover Formation and three systems sourced by more liquid-prone Jurassic and Lower Cretaceous source rocks (Rollet et al., 2016). The origin of fluids found on the Yampi Shelf is more challenging to establish due to the impact of biodegradation on geochemical parameters. Microbial degradation is pervasive in these shallow Cretaceous reservoirs due to reservoir temperatures low enough (< 80°C) to allow bacteria to thrive. While biodegraded oils on the Yampi Shelf can still be reliably correlated to the sediments of the Lower Cretaceous Echuca Shoals Formation (Blevin et al., 1998), gases have been altered to the extent that their molecular and isotopic compositions are too compromised for reliable interpretation. Indeed, gases on the Yampi Shelf are dry as a result of the preferential removal of wet gases by microbes and significant enrichment in ^{13}C of the residual C_2-C_5 hydrocarbons are observed due to the bacterial selectivity towards ^{12}C during biodegradation. However, the carbon isotopic compositions of *neo*-pentane for Yampi Shelf gases in Caspar 1A, Cornea South 2 and Macula 1 all fall within the range expected for Plover-sourced gases (Fig. 1), supporting the fact that these gases have been charged by the Lower–Middle Jurassic Plover Formation. As the co-reservoired oils are derived from marine organic matter within the Echuca Shoals Formation, this highlights the existence of multiple hydrocarbon charges towards the basin margins.

Compared to the gases from the Browse Basin, the majority of gases from the northern Perth Basin show depleted values in ^{13}C (Fig. 2), consistent with sourcing from the marine Lower Triassic Kockatea Shale (Boreham et al., 2011). Only three gases are isotopically enriched in ^{13}C, pointing to ^{13}C-enriched Permian (Elegans 1) and Jurassic (Gingin West 1 and Warro 3) sources. The Kockatea Shale-sourced gases have been generated from a wide range of thermal maturities. As thermal maturity drives carbon isotopic compositions towards more ^{13}C-enriched values, the ability of discriminating between an overmature Kockatea Shale-sourced gas and the Permian and Jurassic-sourced gases comes into question. However, thermal maturity exerts only a weak control on the carbon isotopic composition of *neo*-pentane (Boreham and Edwards, 2008). Redback South 1 and Redback 2 represent dry mature gases, yet the strong depletion in ^{13}C value of *neo*-pentane unambiguously attests to a Kockatea Shale source (Fig. 2), proving the effectiveness of *neo*-pentane as a strong source indicator.

References

Blevin, J.E., Boreham, C.J., Summons, R.E., Struckmeyer, H.I.M., Loutit, T.S., 1998. An effective Lower Cretaceous petroleum system on the North West Shelf: evidence from the Browse Basin, in: Purcell, P.G., Purcell, R.R. (Eds.), The Sedimentary Basins of Western Australia 2: Proceedings of the Petroleum Exploration Society of Australia Symposium, Perth, 1998, pp. 397-420.

Boreham, C.J., Chen, J., Grosjean, E., Poreda, R., 2011. Hedberg Conference Natural Gas Geochemistry, Beijing, China, 9-12 May 2011.

Boreham, C.J., Edwards, D.S., 2008. Abundance and carbon isotopic composition of neo-pentane in Australian natural gases. Organic Geochemistry 39, 550-566.

Rollet, N., Abbott, S.T., Lech, M.E., Romeyn, R., Grosjean, E., Edwards, D.S., Totterdell, J.M., Nicholson, C.J., Khider, K., Nguyen, D., Bernardel, G., Tenthorey, E., Orlov, C., Wang, L., 2016. A regional assessment of CO2 storage potential in the Browse Basin: results of a study undertaken as part of the National CO2 Infrastructure Plan. Geoscience Australia, Canberra, Record.2016.017.

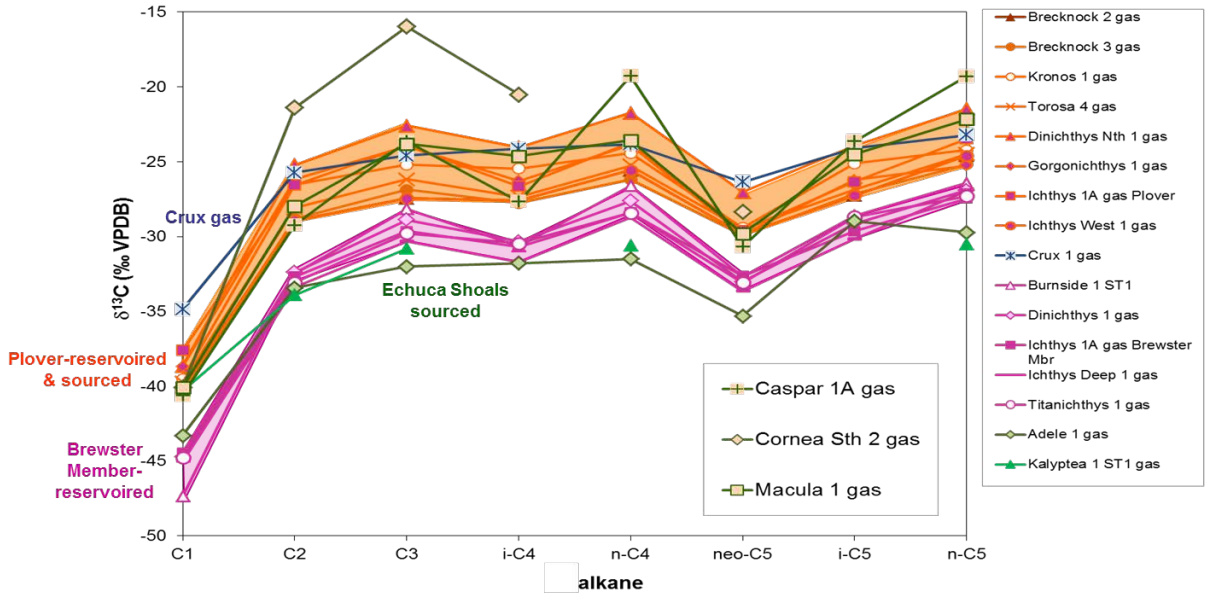

Fig. 1. Carbon isotopic composition of C_1-C_5 alkanes highlighting the occurrence of four Mesozoic gas families in the Browse Basin. Dry gases found in the Plover reservoirs of the Brecknock-Scott Reef Trend and Ichthys fields (orange) are primarily sourced by the fluvio-deltaic sediments of the Lower to Middle Jurassic Plover Formation. Wet gas accumulations reservoired within the Upper Jurassic Brewster Member of the Ichthys and Prelude/Concerto fields (pink) are likely derived from the Upper Jurassic to Lower Cretaceous Vulcan Formation. The ^{13}C-enriched gases from the Crux field in the Heywood Graben (blue) are thought to derive from coal-rich facies within thick Jurassic syn-rift sediments. Gases at Adele and Kalyptea (green) are isotopically more depleted in ^{13}C than any other gases generated from the Browse Basin and are sourced by marine source rocks within the Lower Cretaceous Echuca Shoals Formation.

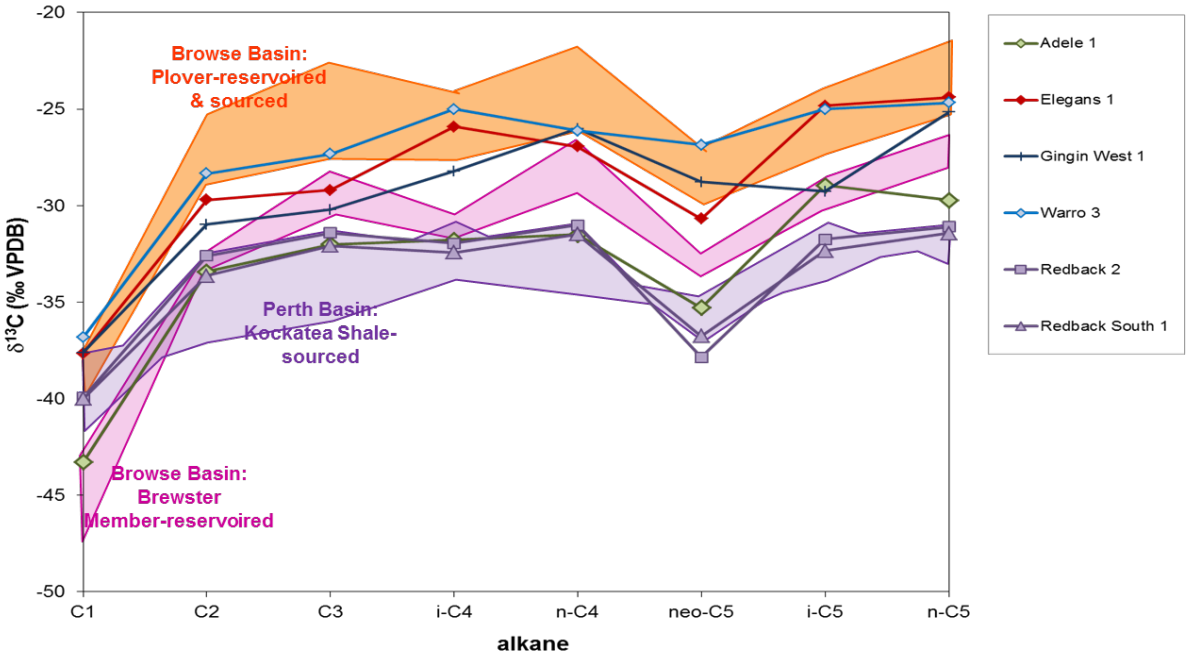

Fig. 2. Carbon isotopic composition of C_1-C_5 alkanes from gases of the Browse and northern Perth basins. Gases of the northern Perth Basin (purple) sourced by the Lower Triassic Kockatea Shale show a strong depletion in ^{13}C. The ^{13}C-enriched gas in Elegans 1 (red) reservoired in the Permian Irwin River Coal measures is attributed to a Permian source, whereas Jurassic source rocks have charged the ^{13}C-enriched gases at Gingin West 1 and Warro 3.

Sulphur isotopic composition of individual organic sulphur compounds and pyrite during the Permian/Triassic extinction

Hendrik Grotheer[1*#], Paul F. Greenwood[1,2], Michael Böttcher[3], Roger Summons[4], Kliti Grice[1]

[1] WA-OIGC, Dept. of Chemistry, Curtin University, Perth, Australia
[2] Centre for Exploration Targeting, UWA, Crawley, Australia
[3] IOW, Geochemistry and Stable Isotope Biogeochemistry, Warnemünde, Germany
[4] MIT, Dept. of Earth, Atmospheric and Planetary Sciences, Cambridge, MA, USA
(corresponding author: h.grotheer@curtin.edu.au)*
([#]current address: Alfred-Wegener-Institute, Marine Geochemistry, Bremerhaven, Germany)

The ~251 Ma ago Permian/Triassic (P/T) extinction was the most severe of the Phanerozoic, with a disappearance of 95 % of marine and 70 % of terrestrial species (e.g., Erwin et al., 2002) over a very short interval (~ 60 ±48 kyr; Burgess et al., 2014). Like other major extinction events, the P/T extinction was associated with a period of increased volcanic activity related to the tectonic evolution of the planet. The volcanic activity, namely the formation of the Siberian Trap basalts, was believed to have significantly impacted the Earth's climate causing global warming, sea level rise, global anoxia and eutrophic oceans (e.g., Hallam and Wignall, 1997; Grice et al., 2005) and large amounts of H_2S were expelled during the eruptions.

P/T extinction intervals have shown a shift in the ^{34}S isotopic composition of pyrite which has been attributed to a change in the redox conditions due to the formation of a stratified water column as a result of global warming and sea level rise (Grice et al., 2005). Generally, the ^{34}S of pyrite, has shown a positive shift when toxic H_2S from anoxic bottom waters reached the photic zone creating widespread euxcinic conditions (rapid burial of pyrite) such as near the boundary interval and a negative shift when hydrogen sulphide was rapidly oxidised such as during the end of the Permian (Fenton et al., 2007; Nabbefeld et al., 2010). The $\delta^{34}S$ values of sedimentary OSCs, now possible to analyse with the development of advanced GC-ICPMS technology, could further illuminate the sulphur cycles associated with these key evolutionary periods. For instance, measurement of the $\delta^{34}S$ values of carotenoid biomarkers (e.g. isorenieratane) specific to *Chlorobi* (biological proxies of photic zone euxinic conditions) or other OSCs in sediments spanning these boundaries should help reveal the extent and consequences of euxinic conditions during the mass extinction periods and subsequent recovery phases.

Here we report $\delta^{34}S$ data of aromatic thiophenes (likely representative of the organic S pool) and pyrite (representative of the inorganic S pool) measured in sediments covering the P/T boundary sections from i) Western Australia (Hovea-3) and ii) South China (Meishan). The $\delta^{34}S$ profiles of pyrite and DBT for these two sections are shown in Figure 1. DBT was quite enriched relative to pyrite in Hovea-3 ($\Delta^{34}S_{Pyrite\text{-}DBT}$ = -40 to -10 ‰), but less so in Meishan ($\Delta^{34}S_{Pyrite\text{-}DBT}$ = -15 to +10 ‰). These differences may be due to the different proportion of inorganic and organic S-pools at these two sites or other differences in local basin biogeochemistry. $\delta^{34}S_{DBT}$ may be influenced by the pyrite burial rate and related preferential removal of depleted HS^-. Variations of $\delta^{34}S_{pyrite}$ by as much as 30 ‰ and $\delta^{34}S_{DBT}$ up to 12 ‰ were observed through the sections. The Hovea-3 data reflects a general increase in the $\delta^{34}S$ of both inorganic and organic S though the Permian (in particular) and Triassic, although these trends are less obvious in the Meishan core.

A large and abrupt perturbation in the $\delta^{34}S_{pyrite}$ and $\delta^{34}S_{DBT}$ profiles was evident near the boundary of both cores, although intriguingly the direction of the isotopic excursion was not the same. In Hovea-3, inorganic S becomes more depleted and organic S more enriched near the boundary (($\Delta^{34}S_{Pyrite\text{-}DBT}$ approaches -20 ‰) whereas the Meishan sediments showed the exact opposite excursion (($\Delta^{34}S_{Pyrite\text{-}DBT}$ approaches +10 ‰). Whilst the reason for the opposite nature of these trends is not clear (but likely also influenced by local biogeochemical or depositional differences), clearly the $\delta^{34}S$ measurements of the OS pool – via molecular proxies such as individual aromatic thiophenes – can complement $\delta^{34}S$ sulphide data in studies of the S-cycle through Earth's history. The pronounced $\delta^{34}S$ decoupling of organic and inorganic S near the P/T boundary reflects the high sensitivity of these parameters to extreme S-dynamics such as associated with the P-T extinction.

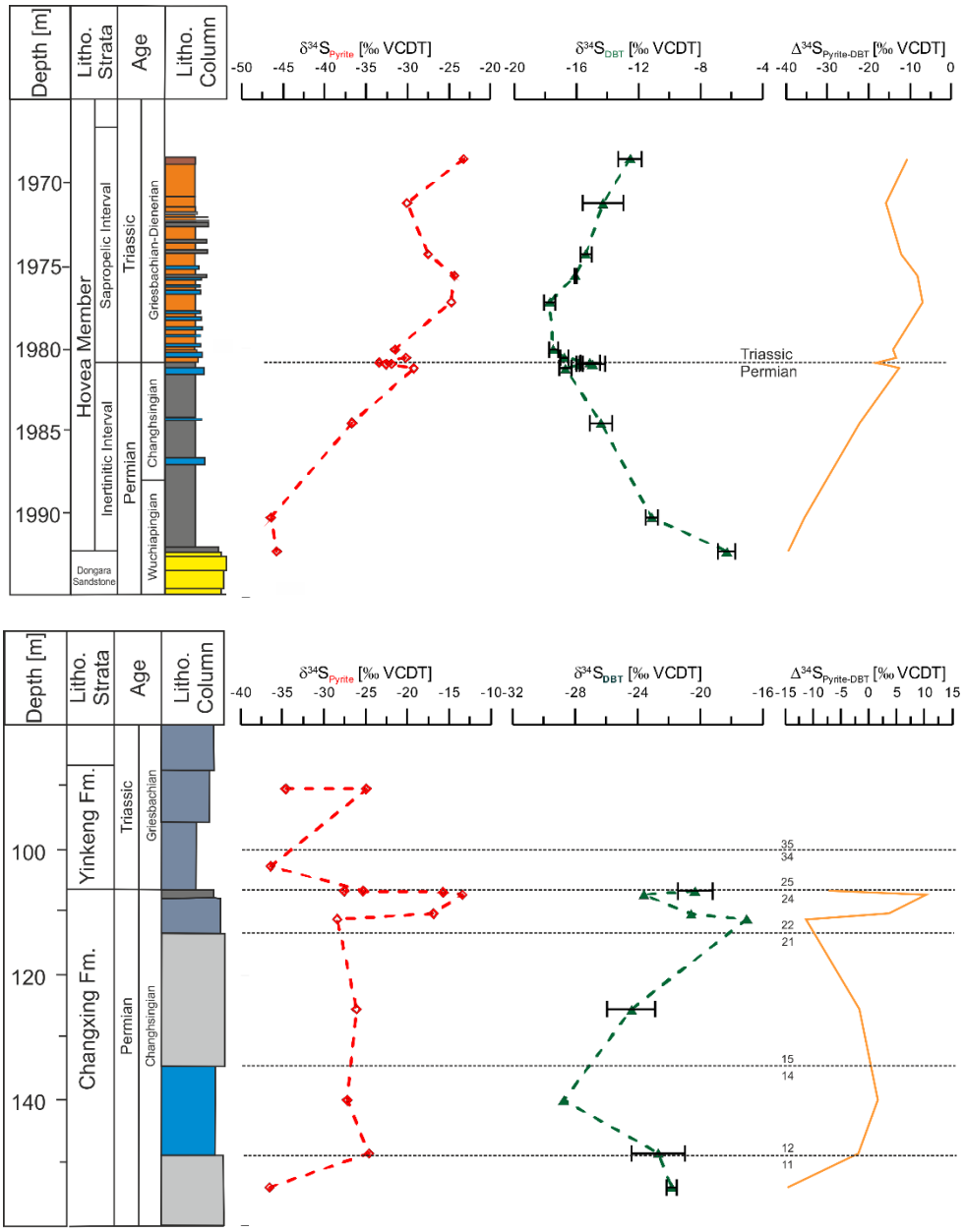

Fig. 1. Stratigraphic details & $\delta^{34}S_{Pyrite}$, $\delta^{34}S_{DBT}$ and $\Delta^{34}S_{Pyrite\text{-}DBT}$ values from the globally distant Hovea-3 (top) and Meishan (bottom) sections.

References

Burgess, S.D., Bowring, S.A., Shen, S.Z., 2014. High-precision timeline for Earth's most severe extinction. Proceedings of the National Academy of Sciences 111, 3316–3321.

Erwin, D.H., Bowring, S.A., Yugan, J., 2002. End-Permian mass extinctions: A review. Geological Society of America Special Paper 365, 363–383.

Fenton, S., Grice, K., Twitchett, R., Bottcher, M., Looy, C., Nabbefeld, B., 2007. Changes in biomarker abundances and sulfur isotopes of pyrite across the Permian--Triassic (P/Tr) Schuchert Dal section (East Greenland). Earth and Planetary Science Letters 262, 230–239.

Grice, K., Cao, C., Love, G.D., Böttcher, M.E., Twitchett, R.J., Grosjean, E., Summons, R.E., Turgeon, S.C., Dunning, W., Jin, Y., 2005. Photic zone euxinia during the Permian-triassic superanoxic event. Science 307, 706–709.

Hallam, A., Wignall, P.B., 1997. Mass Extinctions and their Aftermath. Oxford University Press.

Nabbefeld, B., Grice, K., Twitchett, R.J., Summons, R.E., Hays, L., Böttcher, M.E., Asif, M., 2010. An integrated biomarker, isotopic and palaeoenvironmental study through the Late Permian event at Lusitaniadalen, Spitsbergen. Earth and Planetary Science Letters 291, 84–96.

Microbial diversity and palaeoenvironmental reconstruction of the 1.4 Ga Roper Seaway, McArthur Basin, northern Australia.

Amber J M Jarrett[1,*], Grant M Cox[2], Jochen J Brocks[3], Chris J Boreham[1], Dianne S Edwards[1]

[1]Geoscience Australia, Canberra, 2015, Australia
[2]Curtin University, Perth, 6102, Australia
[3]The Australian National University, Canberra, 2105, Australia
(corresponding author: Amber.Jarrett@ga.gov.au)*

The 1.4 Ga Roper Group of the McArthur Basin, northern Australia is one of the most extensive Proterozoic hydrocarbon-bearing basins preserved in the geological record (Jackson et al. 1984). It is interpreted to have been deposited in a large redox stratified epeiric sea known as the Roper Seaway (Abbott & Sweet, 2000; Cox et. al. 2016). Black shales from the Velkerri Formation, a deep water lowstand systems tract, thermally well preserved in drillcore Altree 2, were analysed to assess microbial diversity and palaeoenvironment, and compared with previously published inorganic geochemistry and microfossils (Cox et al., 2016; Javaux et al., 2001; Fig. 1).

Indigenous biomarkers describe a microbial environment dominated by bacteria. All extracts are characterised by a large unresolved complex mixture (UCM) and high ratios of monomethyl alkanes relative to *n*-alkanes—characteristic features of indigenous Proterozoic bitumen (Pawlowska et al., 2013). Regular hopanes in the C_{27} to C_{35} range and their diagenetically rearranged isomers were detected in all samples from 410.55 to 793.37 m. C_{29} to C_{36} 3β- and 2α-hopanes were detected in low concentrations. The combination of these biomarkers describes a water column dominated by bacteria with heterotrophic reworking of the organic matter.

Steranes, biomarkers for single-cell and multicellular eukaryotes, were below detection limits in all extracts analysed, although eukaryotic microfossils have been identified in the same drillcore (Javaux et al., 2001). These results suggest that eukaryotes, while present in the Roper Seaway, were ecologically restricted and contributed little to the net biomass.

The dibenzothiophene/phenanthrene (DBT/P) ratio increases from the upper Velkerri Formation to the middle and lower Velkerri Formation, broadly correlating with increasing sulphide concentrations in the deep water column (Fig. 1). The elevated sulphide concentration would have been subsequently incorporated into the organic matter (Hughes et al. 1995), broadly consistent with the onset of euxinia (based on elevated Mo, V and U enrichments) at similar depths in the drillcore (Cox et al., 2016; Figure 1). The 2,3,4- and 2,3,6-trimethyl arylisoprenoids are in low concentrations or absent through the Velkerri Formation. The absence is not due to thermal destruction since the maturity level at the base of the analysed interval is pre-oil window. Hence the water column at the time of high total organic carbon (TOC) deposition was not euxinic in the photic zone, but likely only euxinic at depth.

The biomarker composition and water column chemistry in the Roper Group described in this study is in contrast to the 1.64 Ga Barney Creek Formation of the McArthur Basin where pervasive euxinia extended into the photic zone (Lee and Brocks, 2011). This contrast demonstrates that microbial environments and water column geochemistry was heterogeneous during the Mesoproterozoic.

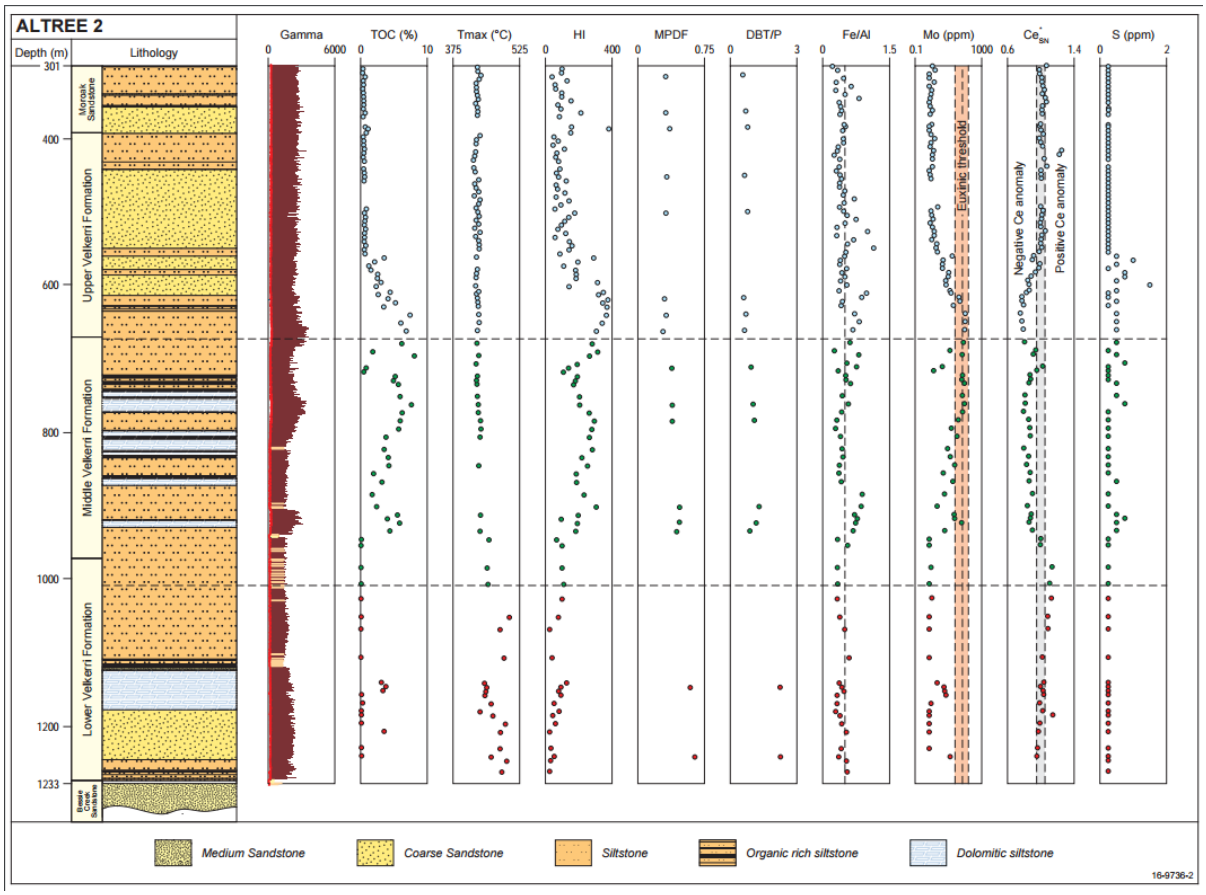

Fig 1. Stratigraphic log of drillcore Altree 2 demonstrating variation in organic and inorganic composition through the Velkerri Formation showing Gamma log; Total Organic Carbon (TOC %); Tmax (°C); Hydrogen Index (HI = (S2/TOC) x 100, mg HC/g rock); Methylphenanthrene distribution factor (MPDF = (3+2)/(3+2+9+1)-methylphenanthrene); Dibenzothiophene/Phenanthrene (DBT/P); Fe(wt %)/Al(wt %). Dashed line at 0.5 differentiates between oxic and anoxic conditions (Lyons and Severmann, 2006); Molybdenum (Mo ppm), shaded area indicates the approximate threshold value for indicating intermittent to persistent euxinia (Lyons et al., 2009); Ce anomaly calculated as $Ce^*_{SN} = Ce_{SN} / [0.5(La_{SN} + Pr_{SN})]$ where SN refers to shale normalisation using PAAS (Nance and Taylor, 1976); Sulphur (S, ppm). Trace element data (Al, Ce*, Fe, Mo, S) is replotted from Cox et al. (2016).

References

Abbott, S.T., Sweet, I.P., 2000. Tectonic control on third-order sequences in a siliciclastic ramp-style basin: An example from the Roper Superbasin (Mesoproterozoic), northern Australia. Australian Journal of Earth Sciences 47, 637-657.

Cox, G.M., Jarrett, A.J.M., Edwards, D.S., Crockford, P., Halverson, G.P., Li, Z.X., Colins, A.S., 2016. Basin redox and primary productivity within the Mesoproterozoic Roper Seaway. Chemical Geology 440, 101-116

Hughes, W.B., Holba, A.G., Dzou, L.I.P., 1995. The ratios of dibenzothiophene to phenanthrene and pristane to phytane as indicators of depositional environment and lithology of petroleum source rocks. Geochimica et Cosmochimica Acta 59, 3581-3598.

Jackson, M.J., Powell, T.G., Summons, R.E., Sweet, I.P., 1986. Hydrocarbon shows and petroleum source rocks in sediments as old at 1.7 Ga. Nature 322, 727-729.

Javaux, E.J., Knoll, A.H., Walter, M.R., 2001. Morphological and ecological complexity in early eukaryotic ecosystems. Nature 412, 66-69.

Lee, C., Brocks, J.J., 2011. Identification of carotane breakdown products in the 1.64 billion year old Barney Creek Formation, McArthur Basin, northern Australia. Organic Geochemistry 42, 425-430

Lyons, T.W., Severmann, S., 2006. A critical look at iron paleoredox proxies: New insights from modern euxinic marine basins. Geochimica et Cosmochimica Acta 70, 5698-5722.

Lyons, T.W., Anbar, A.D., Severmann, S., Scott, C., Gill, B.C., 2009. Tracking Euxinia in the Ancient Ocean: A Multiproxy Perspective and Proterozoic Case Study. Annual Review of Earth and Planetary Sciences 37, 507-534

Nance, W.B., Taylor, S.R., 1976. Rare earth element patterns and crustal evolution- I. Australian post-Archean sedimentary rocks. Geochimica et Cosmochimica Acta 40, 1539-1551.

Pawlowska, M.M., Butterfield, N.J., Brocks, J.J., 2013. Lipid taphonomy in the Proterozoic and the effect of microbial mats on biomarker preservation. Geology 41, 103-106.

Petroleum Analysis and Fingerprinting Using Comprehensive Two-dimensional Gas Chromatography (GC×GC)

Robert K. Nelson and Christopher M. Reddy

Dept. Marine Chemistry & Geochemistry
Woods Hole Oceanographic Institution
Woods Hole, MA, USA 02543

Comprehensive two-dimensional gas chromatography (GC×GC) is highly effective for the separation, identification, and quantification of complex organic mixtures, including crude oil and petroleum products. This technique is applied widely in petroleum characterization, since it can provide valuable information on the age, thermal maturity, and source material of crude oil. GC×GC employs two serially joined capillary GC columns of differing stationary phases to separate compounds based on two independent physical–chemical properties. This substantially increases the overall peak capacity of the chromatogram, compared to conventional GC. In the case of oil analysis, GC×GC typically involves a nonpolar first-dimension column to separate compounds based on their vapor pressure and a shorter polar second-dimension column housed in a separate GC oven to separate compounds based on their polarity. These columns are joined in series such that compounds eluting from the first column are refocused (continually trapped and intermittently released) at the head of the shorter second column by one of several thermal or differential-flow techniques. The length of the modulation period is chosen to ensure that all released compounds elute from the second column prior to the introduction of the compounds trapped during the following modulation. This instrument configuration produces highly structured GC×GC chromatograms where compounds with similar properties elute in predictable regions or fairways.

Understanding natural analogues of mineral carbonation to inform the development of industrial CO_2 storage

Hans C. Oskierski*; Bogdan Z. Dlugogorski

School of Engineering and IT, Murdoch University, Murdoch, 6150 WA, Australia
(corresponding author: hans.oskierski@murdoch.edu.au)*

Natural examples of mineral carbonation, the conversion of Mg-silicate to Mg-carbonate and silica, are common in ultramafic rocks throughout the world and reflect the thermodynamic instability of Mg-silicate minerals in the presence of CO_2. However, the industrial implementation of mineral carbonation as a means of safely storing CO_2 in the form of carbonate minerals is hampered by slow kinetics and the cost associated with heat-activation and carbonation reactors at high pressures and temperatures[1,2].

In the Great Serpentinite Belt, New South Wales, Australia, natural carbonation occurs in the form of weathering-derived magnesite deposits, carbonate crust on ultramafic mine tailings and hydrothermal silica-carbonate alteration. At Attunga, low temperature (10 to 50 °C) meteoric waters have altered serpentinite to typical cauliflower-like magnesite nodules and veins, usually accompanied by late stage amorphous silica. Consistently low $\delta^{13}C$ and small radiocarbon contents point to overlying soil as the source of carbon in the magnesite[3]. Textural observations suggest carbonation progressed via fractures and porosity created by weathering of the host-rock, producing intermediate phases with decreased Mg/Si ratios in the process. For the mine tailings of the Woodsreef Asbestos Mine a relationship between textures, mineral content and isotopic fingerprint indicates that carbonate crusts covering the tailings formed from evaporating meteoric fluids, which absorbed CO_2 directly from the atmosphere[4]. Rate estimates based on the carbonate content and time since closure of the mine indicate that carbonation of the mine tailings proceeds at much higher rates than background uptake of CO_2 by chemical weathering. Lensoid masses of silica-carbonate rock and magnesite veins at the Piedmont magnesite deposit formed by hypogene replacement of serpentinite at temperatures between 165 and 225 °C[5]. The magnesite is usually Fe-rich, indicating reducing conditions during formation, and often accompanied by dolomite and quartz with alteration fluids ascribed to hydrothermal and magmatic sources[5].

Each of the above processes created a distinct set of textures, minerals and isotope-geochemical signatures which reflect conditions and mechanisms favourable for carbonation, but also the associated limitations that need to be overcome for industrial implementation. A better understanding of natural analogues to mineral carbonation informs the development of accelerated carbonation processes for large scale industrial storage of CO_2 in carbonate minerals.

References

Dlugogorski, B.Z., Balucan R., 2014. Dehydroxilation of serpentine minerals: Implications for mineral carbonation. Renewable and Sustainable Energy Reviews 31, 353-367.

Power I.M., Harrison A.L., Dipple G.M., Wilson S.A., Kelemen P.B., Hitch M., Southam G., 2013. Carbon mineralization: from natural analogues to engineered systems. Reviews in Mineralogy & Geochemistry 77, 305-360.

Oskierski, H.C., Dlugogorski, B.Z., Jacobsen, G., 2013. Sequestration of atmospheric CO_2 in a weathering-derived, serpentinite-hosted magnesite deposit: 14C tracing of carbon sources and age constraints for a genetic model. Geochimica et Cosmochimica Acta 122, 226-246.

Oskierski, H.C., Dlugogorski, B.Z., Jacobsen, G., 2013. Sequestration of atmospheric CO_2 in chrysotile mine tailings of the Woodsreef Asbestos Mine, Australia: Quantitative mineralogy, isotopic fingerprinting and carbonation rates.Chemical Geology 358, 156-169.

Ashley, P.M., 1997. Silica-carbonate alteration zones and gold mineralisation in the Great Serpentinite Belt, New England Orogen, New South Wales. In: Ashley, P.M., Flood, P.G. (Eds.), Tectonics and metallogenesis of the New England Orogen Geological Society Australia Special Publication 19, 212-225.

Investigations of metal-rich black shales of South China and the Nick prospect

Anais Pagès[1,2], Steve Barnes[1], Ray Coveney[3], Susanne Schmid[1], Margaux Le Vaillant[1], Chris Ryan[4], David Paterson[5], Haifeng Fan[6], Hanjie Wen[6]

[1] CSIRO, Mineral Resources National Flagship, 26 Dick Perry Avenue, Kensington WA 6151, Australia
[2] *WA Organic and Isotope Geochemistry Centre, Department of Chemistry, The Institute for Geoscience Research, Curtin University, GPO Box U1987, Perth, WA 6845, Australia*
[3] Department of Geosciences, University of Missouri-Kansas City, Missouri 64110-2499, US
[4] *CSIRO Mineral Resources, Normanby Road, Clayton VIC 3168, Australia*
[5] *Australian Synchrotron, Blackburn Road, Clayton VIC 3168, Australia*
[6] State Key Lab of Ore Deposit Geochemistry, Institute of Geochemistry, Chinese Academy of Sciences, 46 Guanshui Road, Guiyang, 550002, Guizhou Province, P. R. China
(* corresponding author: **Anais.pages@csiro.au**)

Shale-hosted Ni-Cu-PGE sulfide occurrences can be associated with large amounts of Mo, Zn, Mn, V and U and represent economic resources. In recent years, metalliferous black shales have proven to represent a valuable resource for Ni (Talvivaara mine in Finland) and other base metals (Red Dog and Howards Pass Pb-Zn deposits, USA and Canada).

In South China, during the Early Cambrian, a thin accumulation of phosphorite, Ni, Mo, Au, Ag, Se, Cr, V, Zn, U and PGEs occurred in shallow water environments, on the Yangtze platform. This narrow mineralised layer, within 10 m of the Proterozoic-Cambrian boundary, crops out for up to 2000 kilometers. This thin ore horizon is particularly enriched in organic matter (OM) (> 10 % TOC), in Mo-Ni-Re-Os-Se-As-Hg-Sb (> 1000*continental crust) and Ag-Au-Pt-Pd (> 100*continental crust) (Xu et al., 2013). This is one of the most enigmatic examples of a sediment-hosted base and precious metal deposit showing an association of ore-grade metals with OM.

Of all known deposits, the Ni-Mo sulfide beds of the Devonian Nick prospect in the Selwyn Basin, Canadian Yukan, present the strongest similarities with the South China black shales (Coveney and Nansheng, 1991). The bed thickness varies between 5 and 15 cm, it is associated with a significant unconformity at the edge of the basin and contains abundant Ni (7.8 % Ni), Mo (0.4 %) and PGE (up to 1050 ppb). The Nick prospect shows a less complex mineralogy than the Niutitang shales, but they both display clastic textures and abundant vaesite. The Nick prospect also preserves plant material, suggesting an input of terrestrial material. Although a SEDEX mineralisation has been suggested for the Nick deposit (Hulbert et al., 1992), very few studies have focused on the detailed associations and origin of the metals.

XFM combined with the Maia detector (384 detector array) was performed on the Australian Synchrotron XFM beamline (Paterson et al., 2011) to investigate the fine-scale distribution of metals in these rare mineralised horizons. The high-definition images obtained with the Maia detector allow the detection of metal segregation on a wide range of spatial scales (Ryan et al., 2016). For the first time, detailed mineral structures and spatial associations with OM were investigated in the South China shales and the Nick prospect to gain further understanding of metal deposition in these complex organic-rich sedimentary systems, based on a comparison of two distinct localities.

References

Coveney, R.M., Nansheng, C., 1991. Ni-Mo-PGE-Au-rich ores in Chinese black shales and speculations on possible analogues in the United States. Mineralium Deposita 26, 83-88.
Hulbert, L.J., Carne, R.C., Gregoire, D.C., Paktunc, D., 1992. Sedimentary nickel, zinc, and platinum-group-element mineralization in Devonian black shales at the Nick Property, Yukon, Canada; a new deposit type. Exploration and Mining Geology 1, 39-62.
Paterson, D., de Jonge, M.D., Howard, D.L., Lewis, W., McKinlay, J., Starritt, A., Kusel, M., Ryan, C.G., Kirkham, R., Moorhead, G., Siddons, D.P., 2011. The X-ray fluorescence microscopy beamline at the Australian Synchrotron. AIP Conf. Proc. 1365, 219-222.
Ryan, C.G., Fisher, L.A., Le Vaillant, M., Pagès, A., Siddons, D.P., Kirkham, R., Paterson, D.J., de Jonge, M.D., Howard, D.L., Barnes, S.J., Moorhead, G.F., Laird, J.S., 2016. High throughput quantitative per pixel XFM element imaging using Maia for complex natural samples. XRM Conference, Oxford.
Xu, L.G., Lehmann, B., and Mao, J.W., 2013, Seawater contribution to polymetallic Ni-Mo-PGE-Au mineralization in Early Cambrian black shales of South China: Evidence from Mo isotope, PGE, trace element, and REE geochemistry. Ore Geology Reviews, 52, 66–84

Vibrational Spectroscopy Characterisation of Shales from the Canning and Perth Basins

Bobby Pejcic*, Claudio Delle Piane, Charles Heath

CSIRO, Energy, Kensington, 6151, WA, Australia
(corresponding author: bobby.pejcic@csiro.au)*

There is an increasing focus on the development of unconventional shale gas and liquid plays to meet future energy needs. The Canning and Perth Basins in Western Australia have been identified as locations that are likely to hold commercial shale gas accumulations. The Ordovician Goldwyer Formation is the main source rock in the Canning Basin and it varies from mudstone dominated in basinal areas to limestone-dominated in some platform and terrace areas. As for the Perth Basin, the Triassic Kockatea shale Formation is one of the source rocks and it consists of dark shale, micaceous siltstone along with minor sandstone and limestone.

Gas chromatography/mass spectrometry based techniques are frequently used to characterise and provide geochemical information on the organic matter and hydrocarbons that are present in geological systems [1-3]. Although these methods provide highly valuable data, they do require a chemical treatment and extraction step prior to the analysis of the isolated organic material. Infrared (IR) and Raman spectroscopy are relatively non-destructive techniques that can directly and rapidly investigate the chemical properties of sediments and rocks. Furthermore, they are able to provide information on the organic structure at the micrometer scale and can generate a chemical map of the different types of organic macerals. The potential of micro-Fourier transform infrared spectroscopy (micro-FTIR) as a tool to assess the organic matter dispersed in sedimentary rocks and understand its thermal maturity has been established [4]. However, very few studies have been undertaken using IR spectroscopy to characterise the organic matter in shales. In this study, shale samples from the Canning and Perth Basins, with vitrinite reflectance values ranging from 0.78% to 1.88%, were analysed by micro-FTIR.

The objective of this paper was to evaluate the potential of micro-FTIR to determine the type of organic matter and its thermal maturity in shales from the Perth and Canning Basins. Micro-FTIR spectra were acquired on various shale samples taken from different wells and Figure 1 shows some typical spectra. All measurements were made in reflectance mode using an aperture size of 30x30 µm. IR bands were detected in the region between 3000-2800 cm^{-1} and this is consistent with the presence of aliphatic C-H bond vibrations. It was revealed that the IR spectra were not completely identical when investigating different regions of organic matter on the same sample. Although the C-H vibrations were detected on most samples that were analysed, the shape and intensity of the peak depended significantly on the type of organic matter and its thermal maturity. In this paper, we discuss the micro-FTIR spectroscopy results and compare it to the information obtained by conventional petrographic methods (i.e. vitrinite reflectance).

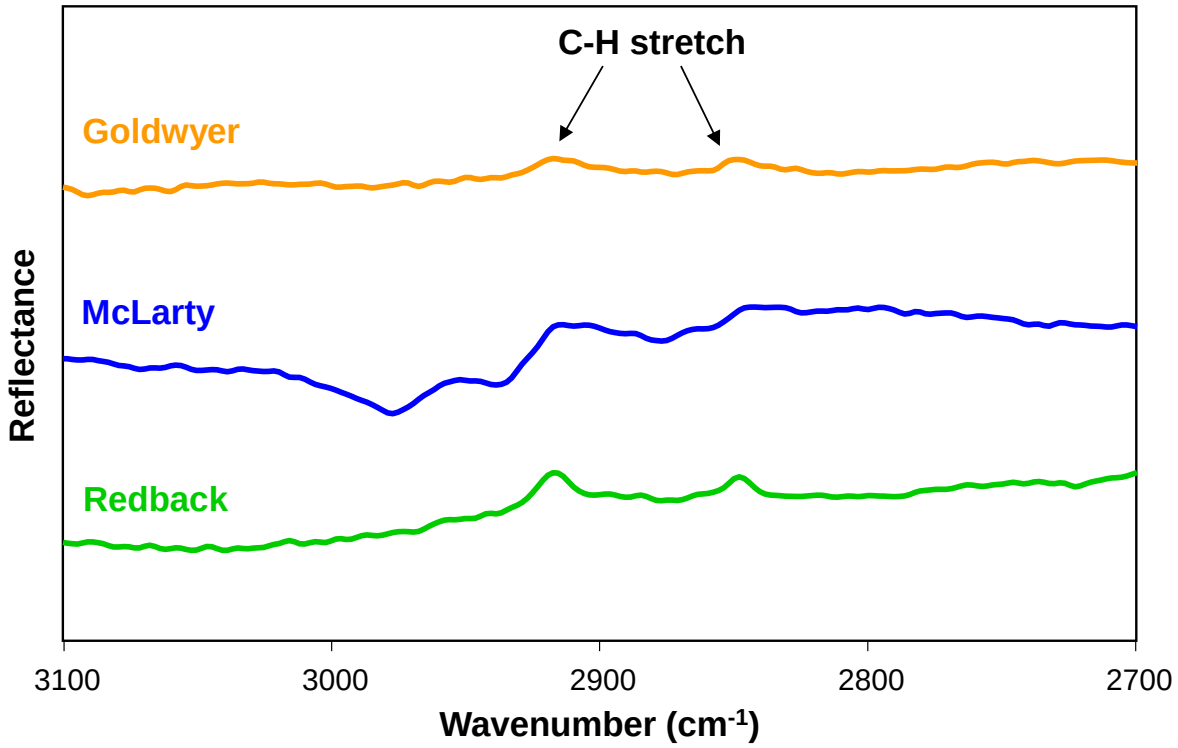

Fig. 1. Micro-FTIR spectra obtained on selected organic macerals in various shale samples.

References

1. Hoffmann, C.F., Foster, C.B., Powell, T.G., and Summons, R.E., *Hydrocarbon biomarkers from Ordovician sediments and the fossil alga Gloeocapsomorpha prisca Zalessky 1917*, Geochimica et Cosmochimica Acta, 1987, **51**(10), 2681-2697.
2. Barber, C.J., Grice, K., Bastow, T.P., Alexander, R., and Kagi, R.I., *The identification of crocetane in australian crude oils*, Organic Geochemistry, 2001, **32**(7), 943-947.
3. Boreham, C.J., Powell, T.G., and Hutton, A.C., *Chemical and petrographic characterization of the Australian Tertiary Duaringa oil shale deposit*, Fuel, 1988, **67**(10), 1369-1377.
4. Chen, Y., Zou, C., Mastalerz, M., Hu, S., Gasaway, C., and Tao, X., *Applications of micro-fourier transform infrared spectroscopy (FTIR) in the geological sciences—A Review*, International Journal of Molecular Sciences, 2015, **16**(12), 30223-30250.

Combining GCxGC and CSIA of diamondoids to unravel the sources of (biodegraded) hydrocarbons in the Browse Basin

Gemma Spaak[1]*, Kliti Grice[1], Dianne Edwards[2], Alan Scarlett[1], Emmanuelle Grosjean[2]

[1]Curtin University, WA Organic and Isotope Geochemistry Centre, Department of Chemistry, The Institute for Geoscience Research, GPO Box U1987, Perth, WA 6845, Australia
[2]Geoscience Australia GPO Box 387, Canberra, ACT 2601, Australia
(corresponding author: gemma.spaak@curtin.edu.au)*

The Browse Basin, situated in the offshore Northwest region of Australia, is part of a world class hydrocarbon province hosting vast reserves of gas and condensate (Le Poidevin et al., 2015). In addition, both non-biodegraded (Caswell) and biodegraded (Cornea and Gwydion) oil fields are present. The primary source of gas is thought to be a Lower-Middle Jurassic fluviodeltaic sequence whereas Upper Jurassic to Lower Cretaceous marine sequences are the most likely source of liquid hydrocarbons (Rollet et al., 2016). Complex fill histories, mixed marine and terrestrial biomarker signatures and, on the Yampi Shelf, the addition of biogenic methane, have made it difficult to understand the charge history of accumulations in the basin.

This study combines comprehensive two dimensional gas chromatography coupled to time-of-flight mass spectrometry (GC×GC-TOFMS) and compound specific isotope analyses (CSIA) of *n*-alkanes, aromatic hydrocarbons and diamondoids to identify numerous hydrocarbon contributions to the accumulations in the Browse Basin. The absolute concentrations, ratios and isotopic composition of diamondoids have been shown to be source-specific and highly resistant to both thermal maturity and biodegradation (e.g Dahl et al., 1999; Grice et al., 2000; Moldowan et al., 2015). Diamondoid analysis and quantitation was performed on GC×GC-TOFMS as it minimises interference of co-eluting compounds and allows whole oil injection, eliminating potential losses from sample preparation (Silva et al., 2013; Wang et al., 2013).

The non-biodegraded Caswell oils contained high diamondoid concentrations, well above diamondoid yields recovered from laboratory oil cracking experiments (Dahl et al., 1999; Fang et al., 2012), indicating the contribution of a high maturity fluid (wet gas – early dry gas). Contrastingly, typical biomarker parameters indicate that these fluids have been generated from a marine source rock within the oil window (methylphenanthrene index[1] = 0.4). Thefore, by combining the information from routine biomarker analyses with quantitative diamondoid analysis, the Caswell accumulation can be demonstrated to consist of a mixture of hydrocarbons. Furthermore no gas was recovered from this field, which is in disagreement with the high diamondoid concentrations found in the fluids. This indicates that gas has escaped from the structure, leaving behind a hydrocarbon field that initially seems to consist of marine oil but actually contains a mixture of hydrocarbons.

Although the biodegraded oils displayed even higher diamondoid concentrations than the Caswell oils, a similar mixed hydrocarbon signature cannot be confirmed from quantitative diamondoid analysis as biodegradation increases the concentration of these compounds. However due to their high abundance, carbon isotopic composition of individial diamondoids could be measured in the biodegraded oils. The $\delta^{13}C$ values of methyladamantanes in biodegraded oils become progressively more depleted with increasing biodegradation and the depletion is more pronounced for dimethyladamantane. As biogenic methane is isotopically depleted compared to thermogenic methane, these results suggest that alteration of adamantanes could have occurred during the biodegradation process.

Diamondoid concentrations and their stable isotopic signatures provide further insight into the multiple sources of hydrocarbons that are contained within the Browse Basin acumulations and furthermore provide insight into the formation and occurrence of diamondoids in biodegraded oil fields.

References

Dahl, J.E., Moldowan, J.M., Peters, K.E., Claypool, G.E., Rooney, M.A., Michael, G.E., Mello, M.R., Kohnen, M.L., 1999. Diamondoid hydrocarbons as indicators of natural oil cracking. Nature 399.

Fang, C., Xiong, Y., Liang, Q., Li, Y., 2012. Variation in abundance and distribution of diamondoids during oil cracking. Organic Geochemistry 47, 1–8.

Grice, K., Alexander, R., Kagi, R.I., 2000. Diamondoid hydrocarbon ratios as indicators of biodegradation in Australian crude oils. Organic Geochemistry 31, 67–73.

Le Poidevin, S.R., Kuske, T.J., Edwards, D.S., Temple, P.R., 2015. Australian Petroleum Accumulations Report 7 Browse Basin: Western Australia and Territory of Ashmore and Cartier Islands adjacent area, 2nd edition. Record 2015/10. Geoscience Australia, Canberra.

Moldowan, J.M.M., Dahl, J., Zinniker, D., Barbanti, S.M., 2015. Underutilized advanced geochemical technologies for oil and gas exploration and production-1 . The diamondoids. Journal of Petroleum Science and Engineering 126, 87–96.

Rollet, N., Grosjean, E., Edwards, D., Palu, T., Abbott, S., Totterdell, J., Lech, M.E., Khider, K., Hall, L., Oolov, C., Nguyen, D., Nicholson, C., Higgins, K. and Mclennen, S., 2016. New insights into the petroleum prospectivity of the Browse Basin: results of a multi-disciplinary study. The APPEA Journal, 483–494.

[1] Methylphenanthrene index = Σ(3-,2-methylphenenathrene)/Σ(3-,2-,9-,1-methylphenanthrene)

Silva, R.C., Silva, R.S.F., Castro, E.V.R. De, Peters, K.E., Azevedo, D.A., 2013. Extended diamondoid assessment in crude oil using comprehensive two-dimensional gas chromatography coupled to time-of-flight mass spectrometry. Fuel 112, 125–133.
Wang, G., Shi, S., Wang, P., Wang, T., 2013. Analysis of diamondoids in crude oils using comprehensive two-dimensional gas chromatography / time-of-flight mass spectrometry. Fuel 107, 706–714.

AN ORGANIC GEOCHEMICAL INVESTIGATION OF THE LATE HOLOCENE VEGETATION AND HYDROLOGICAL DYNAMICS OF THE TROPICAL ARID PILBARA (NW AUSTRALIA)

Alexandra Rouillard[1], Paul F. Greenwood[1-3,*], Kliti Grice[3], Grzegorz Skrzypek[1], Shawan Dogramaci[4], Chris Turney[5], Pauline F. Grierson[1]

[1]WA Biogeochemistry Centre and Ecosystems Research Group, The University of Western Australia (UWA), Crawley, 6009, Australia
[2]Centre for Exploration Targeting, UWA, Crawley, 6009, Australia
[3]Western Australia Organic and Isotope Geochemistry Centre, Curtin University, Bentley, 6102, Australia
[4]Rio Tinto Iron Ore, Perth, 6001, Australia
[5]*Climate Change Research Centre, University of New South Wales (UNSW), Kensington, 2052, Australia*
(corresponding author: paul.greenwood@uwa.edu.au)*

We have conducted an organic geochemical study of a multi-dated (^{210}Pb, ^{137}Cs and ^{14}C) late Holocene sedimentary core from the Fortescue Marsh (Pilbara, NW Australia) to investigate the hydroclimate history of this presently arid region of Australian. Morphological (particle size, molecular fossils) and bulk geochemical (C and N %, δ^{13}C, δ^{15}N) analyses on the same core (collected from Fortescue Marsh in 2012) identified the occurrence of centennial and millennial flooding (Rouillard et al., 2015, 2016), which was also supported by an appraisal of paleohydrological records (Rouillard et al., 2015). We now evaluate the potential of using the hydrocarbon products and δ^{13}C values of plant waxes detected in these sediments for reconstructing catchment vegetation and hydroclimatic histories of this arid environment.

Saturate and aromatic fractions from four separate sections (P1-P4) of the sedimentary core, corresponding to distinct stratigraphic periods of the past 2000 years (Rouillard et al., 2016), were separately analysed by GCMS (P1-P3 data shown in Figure 1).

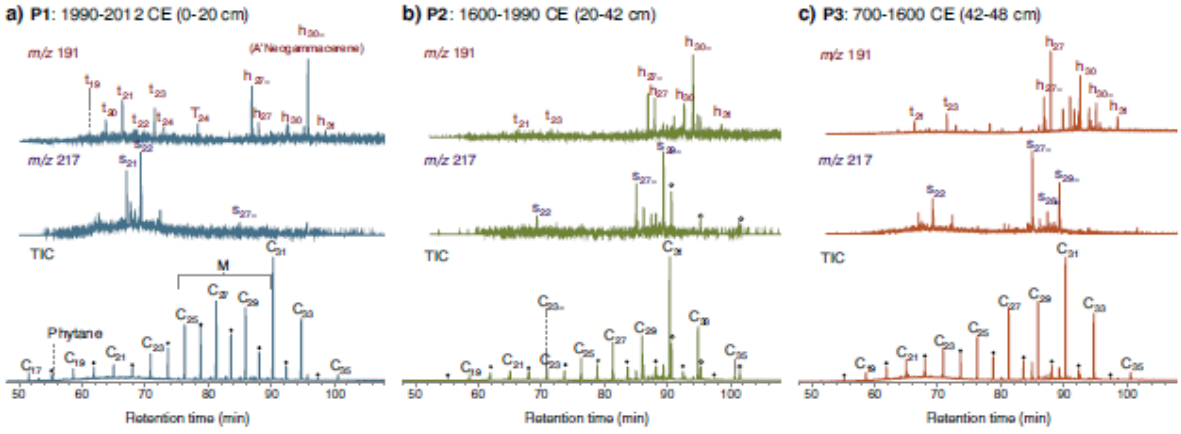

Fig. 1. GC–MS data of (a) P1, (b) P2 and (c) P3. Products include *n*-alkanes, tricyclic terpanes (t), tetracyclic terpanes (T), steroids (s), hopanoids (h) methylated alkane series range (M). Cn corresponds to n-alkane carbon number; open circles = even numbered n-alkanes; and = to unsaturated products.

The low total carbon (TC) content (<1.4%) of the core – consistent with the low OM contents of modern Pilbara soils and typical of both oligotrophic aquatic systems and dry stream-bed sediments - challenged the sensitivity of these analyses. Indeed no products were detected from the deepest section of the core (P4, corresponding to *Common Era (CE) years <100 - 700*). The aromatic fractions of P3 (*CE 700- 1600*), P2 (*CE 1600 – 1990*) and P1 (*CE 1990 – 2012*) also yielded very few products; however, their saturated fractions revealed a wide distribution of aliphatic hydrocarbons. The main aliphatic products included: *n*-alkanes, regular isoprenoids (e.g., phytane), branched alkanes and alkenes and saturated and unsaturated hopanoids and steroids. The δ^{13}C values for the most abundant hydrocarbon products were able to be measured by GCirMS. Several relative abundance and δ^{13}C features of the aliphatic products were reflective of the major organic input. For example, these included a prominence of high MW n-alkanes displaying a distinctive odd over even carbon number preference ($CPI_{nC23\text{-}nC33}$ = 3 to 6) typical of terrestrial plant sources; δ^{13}C values of most *n*-alkanes were −29 ± 2‰ indicated a mixed input of C3 and C4 plant sources; and low P_{aq} values (< 0.3) and a discernible ^{13}C depletion of low MW n-alkanes (Cf. higher C numbers) were indicative of aquatic macrophytes.

The aliphatic product distribution of P1- P3 were generally similar, but subtle product variations across the core (e.g. isoprenoids and short chain sterenes only in more recent P1) reflected the temporal flux of some sources. Some of the differences detected might be due to changes in hydroclimatic over the last ~2000 years (i.e., the late Holocene). For instance, the absence of any products from P4 is consistent with notably drier conditions than pesent in the inland Pilbara region identified from our earlier study (Rouillard et al., 2016). The relatively lower $\delta^{13}C$ values of long chain n-alkanes in modern sediments reflected the emergence of wetter conditions through the late Holocene, and particularly over recent decades.

The relative contribution of C3 and C4 plant sources in P1-P3 were estimated by a mixing model developed using the mean $\delta^{13}C$ values of n-alkanes from C3 or C4 sources from a literature survey of arid zone studies. Our model suggests C4 plants make 41–50% median contribution towards the n-alkanes detected. Interestingly, this was notably lower than the current 64% (aboveground biomass) landscape dominance of grasses. The large riparian fringe of the Fortescue Marsh may contribute to this discrepancy. Riparian vegetation can produce slightly ^{13}C depleted n-alkanes compared to most other C3 plant sources. However, the $\delta^{13}C$ signatures of lacustrine sediments can also be influenced by several other environmental (e.g. water stress, intermittent water flow) and biological (microbial dynamics) variables .

These results show that it is possible to extract organic molecular fossil distributions and $\delta^{13}C$ of n-alkanes from lake sediments of low OM content in tropical arid ecosystems. The stable isotopic signatures measured for several of the more abundant n-alkanes provided additional C source information that can be useful for paleoclimate reconstructions.

References

Rouillard, A., Skrzypek, G., Dogramaci, S., Turney, C., Grierson, P.F., 2015. Impacts of high inter-annual variability of rainfall on a century of extreme hydrologic regime of northwest Australia. Hydrol. Earth Syst. Sci. 19, 2057–2078.
Rouillard, A., Skrzypek, G., Turney, C., Dogramaci, S., Hua, Q., Zawadzki, A., Reeves, J., Greenwood, P., O'Donnell, A., Grierson, P., 2016. Evidence for 'megafloods' in arid subtropical Western Australia during the Little Ice Age Chronozone. Quat. Sci. Rev. 144, 107–122.

Unravelling the food-web structure of the subterranean invertebrate communities of arid zone Western Australia

Mattia Saccò[1,2] *, Alison Blyth[1,2], Bill Humphrey[3], Bill Bateman[4], Kliti Grice[2]

[1]Department of Applied Geology, Curtin University, Perth, 6102, WA (Australia)
[2]WA-Organic Isotope Geochemistry, Department of Chemistry, The Institute for Geoscience Research, Curtin University, Perth, 6102, WA (Australia)
[3]Western Australian Museum, Perth, 6000, WA (Australia)
[4]Department of Environment and Agriculture, Curtin University, Perth, 6102, WA (Australia)
(corresponding author: mattia.sacco@postgrad.curtin.edu.au)*

Groundwater constitutes the largest reservoir of freshwater in the world. 97% of all unfrozen freshwater is subsurface, with lakes and rivers representing less than 2% (Gibert et al., 1994). Subsurface water represents a life-sustaining source that supplies water to billions of people and plays a central part in irrigated agriculture (Gleeson et al., 2012). With an aridifying climate, ground water is especially important to Australian society, industry and the environment (O'Grady et al., 2010). Subterranean environments are closely connected to surface water bodies, along a hydrological continuum. Understanding these connections is fundamental to understanding the overall dynamics of groundwater and surface hydrological systems (Brunke & Gosner, 1997). Aquifers are not inert environments, but complex ecosystems that harbour a huge range of biodiversity patterns. Australia hosts a great variety of subterranean habitats and associated faunas in karst and non-karst environments (Guzik et al., 2008). The Yilgarn and Pilbara regions (WA), specifically, harbour a myriad of short-range endemic invertebrate species (Bradford et al., 2010; Humphreys & Adams 2001; Harvey et al., 2008) (Figure 1). However, these ecosystems are poorly understood: ~90% of the 4,000+ species are undescribed and we know little about ecosystem function in terms of food webs and energy sources (Humphrey, 2009). In addition, the overall collapse of biodiversity, particularly at the basal level of the trophic chain, is currently accelerating due to water pollution, deforestation, and industrial forest plantation, among others. Our research on subterranean habitats will contribute to a wide exploration of habitat patterns that will aid future management of our rapidly deteriorating ecosystems.

Few papers in the field of groundwater research have considered in detail the study of the trophic relationships in these systems (Marmonier et al., 1993; Danielopol et al., 2000). This means that our current understanding of key biogeochemical processes, diversity of the microbes and, of the trophic stages responsible for ecosystem functioning is still insufficient for most groundwater ecosystems (Humphrey, 2009).

This investigation focuses on the diversity, assessment and food-web structure of the subterranean invertebrate communities of arid zone Western Australia. Specifically, the study will involve compound specific isotopic analysis of the trophic relationships and energy fluxes in groundwater environments of Pilbara and Yilgarn regions. The project has three objectives: 1) recover quantified information about trophic position of various subterranean fauna, 2) identify the energy sources within the ecosystem and 3) investigate the ecological status of the ecosystems by using macroinvertebrates as biological indicators.

Fig 1. Examples of subterranean invertebrates from Western Australia. (*a*) Troglobitic spider (*b*) stygobitic parabathynellid,; (*c*) stygobitic amphipod,; (*d*) troglobitic dipluran,; (*e*) troglobitic beetle, (*f*) troglobitic millipede, (*g*) stygobitic ostracod,; (*h*) stygobitic beetle. (Photos by Giulia Perina (*a*–*g*) and Kate Muirhead (*b*–*f*), Subterranean Ecology Pty Ltd (www.subterraneanecology.com.au) (Copyright); photo *h* by Chris Watts.)

The main methodological approach will focus on compound specific nitrogen and carbon stable isotope analysis of amino acids. The analysis of $\delta^{15}N$ and $\delta^{13}C$ has been widely used in ecology to recover data about food web composition (Yoshii et al., 1999; Hondula et al., 2014; Du et al., 2015). However, the most common approach of bulk tissue analysis gives only a limited depth of information, as source, trophic and other biochemical fractionation signals can become homogenised (Boecklen et al., 2011). By analysing specific amino acids it is possible to separate the source and trophic isotopic signals, and so study the changes in the trophic levels in quantitative detail (Chikaraishi et al., 2007; Steffan et al., 2013; Ishikawa et al., 2014). Analysis of source and trophic amino acids can also be paired with the analysis of other molecules to better understand energy transfer within the system (Grice et al., 1998). To date, the CSIA of amino acid $\delta^{15}N$ has been used to estimate the trophic position of consumer species in marine, freshwater, and terrestrial ecosystems (Steffan et al., 2013). However, the study of the trophic interactions and associated geochemical patterns is still in its infancy in groundwater environments (Bradford et al., 2014) and the application of compound specific amino acid analysis is highly novel in this context.

The capacity of CSIA to accurately characterize the trophic flows within the WA groundwater systems will provide important insights into the fundamental processes that control biodiversity in some of Australia's unique and most fragile ecosystems.

References

Boecklen, W. J., Yarnes, C. T., Cook, B. A., & James, A. C. 2011. On the use of stable isotopes in trophic ecology. Annual Review of Ecology, Evolution, and Systematics, 42, 411-440.

Bradford, T., Adams, M., Humphreys, W. F., Austin, A. D., & Cooper, S. J. B. 2010. DNA barcoding of stygofauna uncovers cryptic amphipod diversity in a calcrete aquifer in Western Australia's arid zone. Molecular Ecology Resources, 10(1), 41-50.

Bradford, T. M., Humphreys, W. F., Austin, A. D., & Cooper, S. J. 2014. Identification of trophic niches of subterranean diving beetles in a calcrete aquifer by DNA and stable isotope analyses. *Marine and Freshwater Research*,*65* (2), 95-104.

Brunke, M., & Gonser, T. O. M. 1997. The ecological significance of exchange processes between rivers and groundwater. Freshwater biology, 37(1), 1-33.

Chikaraishi, Y., Kashiyama, Y., Ogawa, N. O., Kitazato, H., & Ohkouchi, N. 2007. Metabolic control of nitrogen isotope composition of amino acids in macroalgae and gastropods: implications for aquatic food web studies. Marine Ecology Progress Series, 342, 85-90.

Danielopol, D.L., Baltamls, A & Humphreys, W.F. Groundwater calcrete aquifers. 2000. Danielopolina kornickeri sp. n. (Ostracoda: Thaumatocypridoidea) from a western Australian anchialine cave - morphology and evolution. Zoologica Scripta 29: 1-16.

Du, J., Cheung, W. W., Zheng, X., Chen, B., Liao, J., & Hu, W. 2015. Comparing trophic structure of a subtropical bay as estimated from mass-balance food web model and stable isotope analysis. Ecological Modelling, 312, 175-181.

Gibert, J., Vervier, P., Malard, F., Laurent, R., & Reygrobellet, J. L. 1994. Dynamics of communities and ecology of karst ecosystems: example of three karsts in eastern and southern France. Groundwater Ecology. Academic Press, Inc., San Diego, 425-450.

Gleeson, T., Wada, Y., Bierkens, M. F., & van Beek, L. P. 2012. Water balance of global aquifers revealed by groundwater footprint. Nature, 488(7410), 197-200.

Grice, K., Klein Breteler, W.C., Schouten, S., Grossi, V., De Leeuw, J.W., & Sinninghe-Damsté J.S. 1998. The effects of zooplankton herbivory on biomarker proxy records. Paleoceanography 13, 686-693.

Guzik, M. T., Abrams, K. M., Cooper, S. J. B., Humphreys, W. F., & Cho, J.-L. 2008. Phylogeography of the ancient Parabathynellidae (Crustacea: Bathynellacea) from the Yilgarn region of Western Australia. *Invertebrate Systematics* **22**, 205–216. doi: 10.1071/IS07040

Harvey, M. S., Berry, O., Edward, K. L., & Humphreys, G. 2008. Molecular and morphological systematics of hypogean schizomids (Schizomida:Hubbardiidae) in semiarid Australia. *Invertebrate Systematics* **22**, 167–194. doi:10.1071/IS07026

Hondula, K. L., Pace, M. L., Cole, J. J., & Batt, R. D. 2014. Hydrogen isotope discrimination in aquatic primary producers: implications for aquatic food web studies. Aquatic sciences, 76(2), 217-229.

Humphreys, W. F. 2009. Hydrogeology and groundwater ecology: Does each inform the other?. *Hydrogeology Journal*, *17*(1), 5-21.

Humphreys, W. F., & Adams, M. 2001. Allozyme variation in the troglobitic millipede *Stygiochiropus communis* (Diplopoda: Paradoxosomatidae) from arid tropical Cape Range, northwestern Australia: population structure and implications for the management of the region. *Records of the Western Australian Museum* Supplement 64, 15–36.

Ishikawa, N. F., Kato, Y., Togashi, H., Yoshimura, M., Yoshimizu, C., Okuda, N., & Tayasu, I. 2014. Stable nitrogen isotopic composition of amino acids reveals food web structure in stream ecosystems. *Oecologia*, *175*(3), 911-922.

Marmonier, P., Vervier, P., Gibert, J. & Dole-Olivier, M.-J. 1993. Biodiversity in ground waters. Trends in Ecology and Evolution 8: 392-395

O'Grady, A., Carter, J., & Holland, K. 2010. Review of Australian groundwater discharge studies of terrestrial systems. CSIRO Water for a Healthy Country.

Steffan, S. A., Chikaraishi, Y., Horton, D. R., Ohkouchi, N., Singleton, M. E., Miliczky, E., Hogg, D. B. & Jones, V. P. 2013. Trophic hierarchies illuminated via amino acid isotopic analysis. PloS one, 8(9), e76152.

Yoshii, K., Melnik, N. G., Timoshkin, O. A., Bondarenko, N. A., Anoshko, P. N., Yoshioka, T., & Wada, E. 1999. Stable isotope analyses of the pelagic food web in Lake Baikal. Limnology and Oceanography, 44(3), 502-511.

Analyses of biomarkers using reverse-phase comprehensive two-dimensional gas chromatography time-of-flight mass spectrometry (GC×GC-TOFMS) employing an extremely polar ionic liquid capillary GC columns

Alan G Scarlett[1]*, Peter Hopper[1], Kliti Grice[1]

[1]Western Australian Organic and Isotope Geochemistry Centre, Department of Chemistry, The Institute for Geoscience Research, Curtin University, GPO BOX U1987 Perth, WA 6845, Australia
(corresponding author: Alan.Scarlett@curtin.edu.au)*

Since its development in the 1950s, gas chromatography coupled with mass spectrometry (GC-MS) has developed into an essential instrument for the analysis of organic compounds. In parallel with the evolution of the instrument, capillary GC columns have undergone huge improvements in performance and now a vast diversity of columns are available with different stationary phases providing a range of polarities and separation capabilities. Probably the most commonly used capillary GC columns have a polysiloxane-based phase e.g. non-polar dimethylpolysiloxane and the slightly polar 5%-Phenyl-methylpolysiloxane columns. Such columns are ideal for routine analyses of diverse organic compounds with separation mainly based on volatility. For the analysis of highly complex mixtures of organic compounds, such as crude oil, comprehensive two-dimensional gas chromatography time-of-flight mass spectrometry (GC×GC-TOFMS) has literally added another dimension (reviewed by e.g. Adahchour et al., 2006; Dallüge et al., 2003; Meinert and Meierhenrich, 2012) and has proven to be very useful for identification of biomarkers ('molecular fossils') in the field of biogeochemistry e.g. (Eiserbeck et al., 2012; Eiserbeck et al., 2011; Spaak et al., 2016). The coupling of two columns with different phases theoretically provides a resolving power that is the product of the individual columns. As with GC-MS, 100% polysiloxane-based columns (and 5% Phenyl) are typically used as the primary column i.e. the first separation, with a medium polar (50% phenyl/50% dimethylpolysiloxane) column used for the second dimension separation. These column combinations are an excellent choice for many applications but sometimes so much more can be achieved by making use of the full range of capillary GC columns that are now commercially available.

A relatively recent addition to the suite of commercially available capillary GC columns are those based on an ionic liquid stationary phase. Such columns have extreme polarity. In fact the SLB-IL111 (Supelco®) is considerably more polar than wax-based capillary GC columns which, until recently, were considered to be the most polar. This column has previously been employed in both 1D (GC) and 2D (GC×GC) systems where its main advantage has been that alkanes elute much earlier than standard columns allowing better resolution of low-molecular-weight aromatic hydrocarbons and fatty acid methyl esters (FAMES) (Hantao et al., 2016; Kilulya et al., 2014; Krupcik et al., 2013). It has also been used as a secondary column in GC×GC for the separation of polychlorinated biphenyls (PCBs), achieving better resolution for some PCBs that normally co-elute (Zapadlo et al., 2010). Reinardy et al (2013) used a SLB-IL111 as a primary column in conjunction with a mid-polar BPX50 secondary column (SGE) in order to fully resolve an aromatic acid fraction (as methyl esters) extracted from oil sands process-affected water. This demonstrates that ionic liquid capillary GC columns have the potential to improve resolution or even to achieve separations not possible with more commonly used systems.

Numerous molecular fossils have been established as biomarkers to provide information on past climatic and ecological environments (reviewed by Brocks and Grice, 2011; Grice and Brocks, 2011). Co-elution can occur which may interfere with either quantification or isotopic signal but there can be chromatographic solutions to this e.g. recently Spaak et al (2016) were able to separate crocetane from phytane, which co-elute on non-polar columns, using a mid-polarity capillary column without losing resolution of sterane and hopane biomarkers. Here we have explored the use of SLB-IL111 in GC-MS, and in GC×GC-TOFMS as a primary column in conjunction with a mid-polar secondary column (termed reverse phase) to help with the separation and identification of a range of biomarkers found in crude oils and source rocks.

References

Adahchour, M., Beens, J., Vreuls, R.J.J., Brinkman, U.A.T., 2006. Recent developments in comprehensive two-dimensional gas chromatography (GC X GC) I. Introduction and instrumental set-up. Trac-Trends Anal. Chem. 25, 438-454.

Brocks, J.J., Grice, K., 2011. Biomarkers (ancient biomolecules, evolution) Encyclopaedia of Geobiology. (Editors Thiel & Reitner), pp.167-182; Springer. Encyclopedia of Earth Science Series.

Dallüge, J., Beens, J., Brinkman, U.A.T., 2003. Comprehensive two-dimensional gas chromatography: a powerful and versatile analytical tool. J. Chromatogr. A 1000, 69-108.

Eiserbeck, C., Nelson, R.K., Grice, K., Curiale, J., Reddy, C.M., 2012. Comparison of GC-MS, GC-MRM-MS, and GC x GC to characterise higher plant biomarkers in Tertiary oils and rock extracts. Geochim. Cosmochim. Acta 87, 299-322.

Eiserbeck, C., Nelson, R.K., Grice, K., Curiale, J., Reddy, C.M., Raiteri, P., 2011. Separation of 18 alpha(H)-, 18 beta(H)-oleanane and lupane by comprehensive two-dimensional gas chromatography. J. Chromatogr. A 1218, 5549-5553.

Grice, K., Brocks, J.J., 2011. Biomarkers (organic, compound specific isotopes) Encyclopaedia of Geobiology. (Editors Thiel & Reitner), pp.147-167; Springer. Encyclopedia of Earth Science Series.

Hantao, L.W., Toledo, B.R., Augusto, F., 2016. Ionic liquid stationary phases in gas chromatography: Fundamentals, recent advances, and perspectives. Quim. Nova 39, 81-93.

Kilulya, K.F., Msagati, T.A.M., Mamba, B.B., 2014. Ionic Liquid-Based Extraction of Fatty Acids from Blue-Green Algal Cells Enhanced by Direct Transesterification and Determination Using GC x GC-TOFMS. Chromatographia 77, 479-486.

Krupcik, J., Gorovenko, R., Spanik, I., Bockova, I., Sandra, P., Armstrong, D.W., 2013. On the use of ionic liquid capillary columns for analysis of aromatic hydrocarbons in low-boiling petrochemical products by one-dimensional and comprehensive two-dimensional gas chromatography. J. Chromatogr. A 1301, 225-236.

Meinert, C., Meierhenrich, U.J., 2012. A New Dimension in Separation Science: Comprehensive Two-Dimensional Gas Chromatography. Angew. Chem.-Int. Edit. 51, 10460-10470.

Reinardy, H.C., Scarlett, A.G., Henry, T.B., West, C.E., Hewitt, L.M., Frank, R.A., Rowland, S.J., 2013. Aromatic Naphthenic Acids in Oil Sands Process-Affected Water, Resolved by GCxGC-MS, Only Weakly Induce the Gene for Vitellogenin Production in Zebrafish (Danio rerio) Larvae. Environmental Science & Technology 47, 6614-6620.

Spaak, G., Nelson, R.K., Reddy, C.M., Scarlett, A.G., Chidlow, G.E., Grice, K., 2016. Advances on the separation of crocetane and phytane using GC-MS and GC x GC-TOFMS. Organic Geochemistry 98, 176-182.

Zapadlo, M., Krupcik, J., Majek, P., Armstrong, D.W., Sandra, P., 2010. Use of a polar ionic liquid as second column for the comprehensive two-dimensional GC separation of PCBs. J. Chromatogr. A 1217, 5859-5867.

Hydrocarbon-source correlation of the post-mature Neoproterozoic Dengying giant gas system from the Sichuan Basin, southwestern China: insights from carbon isotopes of individual *n*-alkanes

Chunhua Shi[1,2], Jian Cao[1,*], Kliti Grice[2], Alex Holman[2], Xiucheng Tan[3], Bing Luo[4], Wei Zeng[3], Wenxuan Hu[1]

[1] State Key Laboratory for Mineral Deposits Research, School of Earth Sciences and Engineering, Nanjing University, Nanjing, Jiangsu, 210023, China

[2] Western Australian Organic and Isotope Geochemistry Centre, Department of Chemistry, The Institute for Geoscience Research, Curtin University, GPO Box U1987, Perth, WA 6845, Australia

[3] State Key Laboratory of Oil and Gas Geology and Exploitation, School of Geoscience and Technology, Southwest Petroleum University, Chengdu, Sichuan, 610500, China

[4] Research Institute of Exploration and Development, PetroChina Southwest Oil and Gas Field Company, Chengdu, Sichuan 610051, China

(corresponding author: jcao@nju.edu.cn)*

It is a great research challenge for hydrocarbon-source correlation under post-mature conditions during past decades. Here, we explore the application of carbon isotopes of individual *n*-alkanes based on a case study in the Neoproterozoic (Sinian) Dengying Formation in the Sichuan Basin of southwestern China, which has obtained great natural gas exploration breakthroughs recently. Six source rock samples were collected from candidate source rock sequences, including lower Cambrian Qiongzhusi shales, lower Cambrian Maidiping argillaceous dolomites, mudstones of the third member of the Sinian Dengying Formation, Sinian Dengying algal dolomites, and Sinian Doushantuo shales (Fig. 1). Three reservoir bitumen samples were collected from the Dengying Formation (Fig. 1). Both the source rock and the reservoir samples were extracted by solvent (DCM:MeOH=9:1), and the extracted products were further separated into saturated, aromatic and polar fractions. The saturated fractions were analysed by GCirMS for carbon isotopic compositions of individual *n*-alkanes. Results show that carbon isotope of *n*-alkanes (nC_{16}-nC_{22}) of the six source rock samples is as follows, -29.4~-28.9‰ with average of -29.2‰ (Ap1q), -29.8~-28.5‰ with average of -29.3‰ (Zi4q), -30.1~-29.3‰ with average of -29.6‰ (Zi4m), -30.7~-28.5‰ with average of -29.8‰ (Gk1dy3), -31.0~-29.4‰, with average of -30.3‰ (Ap1dy), and -30.0~-25.8‰ with average of -28.7‰ (XFDst). And carbon isotope of *n*-alkanes (nC_{16}-nC_{22}) of the three reservoir samples is as follows, -30.6~-28.9‰ with average of -29.8‰ (Ap1-5049), -29.5~-28.2‰ with average of -29.1‰ (Wei113-3186), -30.1~-28.7‰ with average of -29.6‰ (Zi4-3073). Samples Gk1dy3 (the third member of the Sinian Dengying Formation), Ap1dy (the Sinian Dengying Formation) and XFDst (the Sinian Doushantuo Formation) are a little different from other source rock and reservoir bitumen samples. First, carbon isotope of nC_{18} of Gk1dy3 is -30.5‰, lower than both the average of source rocks (-29.4‰) and the average of reservoir bitumen (-29.1‰). Second, carbon isotope of nC_{17}, nC_{19}, nC_{20} and nC_{21} of Ap1dy is lower than that of any other samples. Third, carbon isotope of nC_{16} of XFDst is -25.8‰, higher than both the average of source rocks (-28.7‰) and the average of reservoir bitumen (-28.6‰). Based on these results, we tentatively conclude that the three sets of source rocks (i.e., the third member of the Sinian Dengying Formation, the Sinian Dengying Formation, and the Sinian Doushantuo Formation) may contribute little to reservoir bitumens. By comparing the rest three source rock samples, Ap1q (the Qiongzhusi Formation), Zi4q (the Qiongzhusi Formation) and Zi4m (the Maidiping Formation), with the three reservoir bitumen samples, Ap1-5049, Wei113-3186 and Zi4-3703 (the Dengying Formation), we found that their distribution patterns are similar. Therefore, we infer that the bitumen and associated oil-cracking gas in the Dengying reservoir is dominantly sourced from the Qiongzhusi shales and Maidiping argillaceous dolomites.

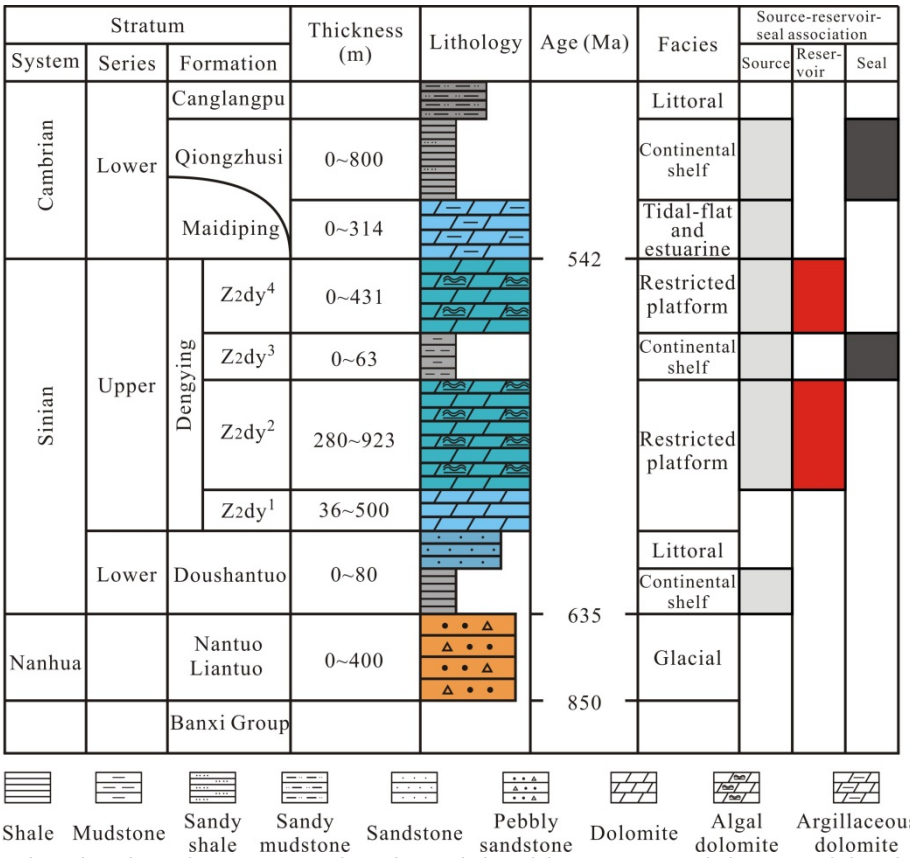

Fig. 1. Generalized stratigraphy and source-reservoir-seal association of the Neoproterozoic-lower Cambrian giant gas system in the Sichuan Basin, southwestern China

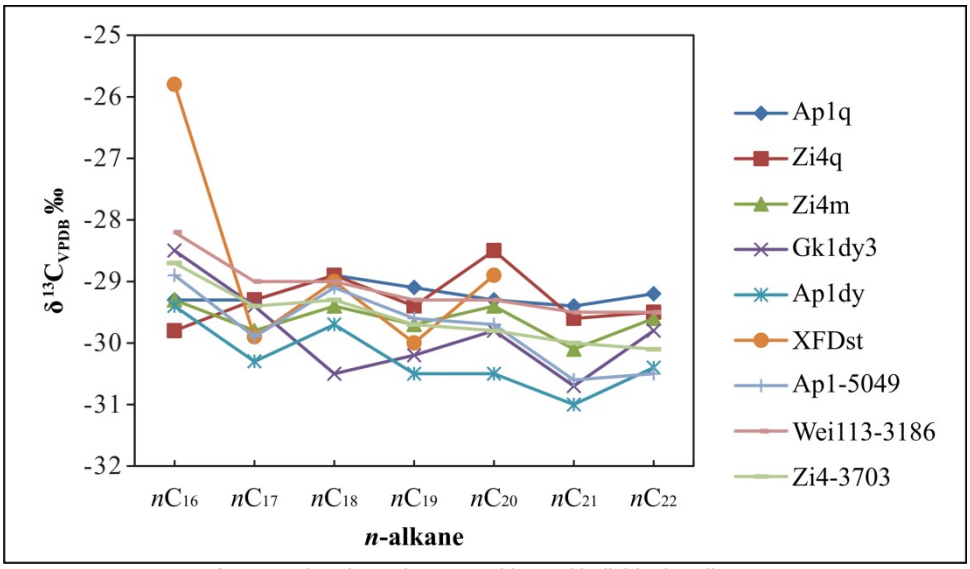

Fig. 2. Carbon isotopic compositions of individual *n*-alkanes

Source rock samples: Ap1q and Zi4q (shales, the Qiongzhusi Formation); Zi4m (argillaceous dolomites, the Maidiping Formation); Gk1dy3 (mudstones, the third member of Dengying Formation); Ap1dy (algal dolomites, the Dengying Formation); and XFDst (shales, the Doushantuo Formation).

Reservoir bitumen samples: Ap1-5049, Wei113-3186, and Zi4-3703 (dolomites, the Dengying Formation).

Classification of Australian crude oils by artificial neural network and geochemical hydrocarbon characteristics

Jacob Sohn*, Dianne Edwards, Junhong Chen, Chris Boreham

Geoscience Australia, Canberra ACT 2601, Australia
(corresponding author: Jacob.sohn@ga.gov.au)*

In this study, an artificial neural network (ANN) and a data set of geochemical hydrocarbon characteristics consists of carbon isotopic signatures, biomarker and molecular data of oil samples, were used to develop a classification model. The ANN classification model was further generalised to accurately classify oils geographically that were not used to design the ANN model.

The 239 oil samples were collected from four different Australian basins [Edwards and Zumberge, 2005; Geoscience Australia and GeoMark, 2002). The number of oil samples from the Bowen/Surat (BS), Carnarvon (Barrow Sub-basin) (CB), Cooper/Eromanga (CE) and Gippsland (G) basins are 42, 45, 91 and 61 samples, respectively. Each oil sample contains $\delta^{13}C$ values of its saturated and aromatic hydrocarbon fractions ($\delta^{13}C_{sats}$, $\delta^{13}C_{arom}$), biomarker (C19/C23, C22/C21, C24/C23, Tet/C23, C27T/C27, C28/H, C29/H, C30X/H, C31R/H, S/H, %C27, %C28, %C29, S1/S6, DM/H) and molecular (Pr/Ph) compositional data and its basin code (BS=1. CB=2; CE=3, G=4).
The data set matrices consist of 22 rows including 4 rows of basin codes and 239 columns. In order to make the data set for neural network training, these data files were restructured into two matrices, the input matrix and the target matrix. Each i_{th} column of the input matrix has 21 elements representing the characteristics of oil whose basin is already known, while each corresponding column of the target matrix will have four elements, consisting of three '0' and a '1' in the location of the associated basin.

The data set with 239 samples was randomly divided up into three subsets, *i.e.*, Training (70%, n = 167), Validation (15%, n = 36) and Testing (15%, n = 36). The Training and Validation subsets were used to develop the ANN model. The Testing subset has no effect on the training process of ANN model and is used as a tool to provide an independent measure of network performance.

The architecture of the ANN chosen for this study was a two-layer feed-forward neural network, which has a sigmoid transfer function in the hidden layer and softmax output neurons in the output layer. The training algorithm used to set the ANN weight matrix was the scaled conjugate gradient backpropagation available in MATLAB's Neural Network Toolbox 7.0. This training algorithm is regarded as one of the fastest methods for training moderate-sized (up to several hundred weights) backpropagation neural networks. It has also shown high performance in pattern recognition, particularly in a supervised learning problem (Sohn et al., 2008).

It is important to determine the number of neurons in the hidden layer in order to build an ANN. The ANN with too few hidden neurons has a tendency to produce a high training error and a high generalisation error due to under-fitting and high statistical bias. The ANN with too many hidden neurons can show low training error, but high generalisation error due to overfitting. Generally, the number somewhere between the input layer size and the output layer size is recommended by 'the rule of thumb' (Sohn et al., 2003). The network with 5, 10, 20 and 30 hidden neurons were simulated to find the optimal number of hidden neurons. Although there seems to be no upper limit in the neural network, it is not necessary to use too many hidden neurons because it needs more computation time and memory requirements. With the increase in the number of neurons in the hidden layer, a decrease in the Cross-Entropy and Percent Error (%E) was observed. The neural network showed best performance at 20 hidden neurons. The values of the Cross-Entropy and %E in 5, 10, 20 and 30 hidden neurons are presented in Table 1.

The confusion matrix shows the percentages of correct and incorrect classification. The green squares on the matrices diagonal constitute the correct classifications, and incorrect classifications form the red squares in the matrix. The simulation results, as demonstrated in the confusion matrices, have shown that the two-layer feed-forward neural network, can be trained to classify oil samples from four different Australian basins correctly with a low percentage error; 5.55% from the testing data set and 4.20% from the all data sets as shown in Figure 1. There was no misclassification from the oil samples collected from Bowen/Surat basins whilst the oil samples from Carnarvon (Barrow) basin shows the highest misclassification rate of 15.6% (7 out of 45 samples). The 85.6% (6 of 7) of misclassified samples in the Carnarvon (Barrow) basin is misclassified to Bowen/Surat basins due to their similarities in isotopic signatures and biomarker characteristics inherited from these Permian and Jurassic source rocks. The trained ANN model was able to classify oil samples into four basins from each oil's geochemical hydrocarbon characteristics with the overall percentages of correct and incorrect classification, 95.8 and 4.2%, respectively. Further study is required to refine this ANN modelling technique to provide a statistical measure of the closeness of fit, especially for oils on the outer edge of the cluster of oils from the same basin and for oils with unknown origin.

Table 1
The artificial neural network simulation results for 5, 10, 20 and 30 hidden neurons

	The ANN simulation				
Hidden Neurons	3	5	10	20	30
Epoch	21	37	22	19	20
Cross-Entropy (CE)	1.75×10^{-3}	2.27×10^{-4}	4.09×10^{-3}	2.16×10^{-4}	7.95×10^{-4}
Gradient	4.35×10^{-3}	8.65×10^{-4}	7.20×10^{-3}	6.10×10^{-3}	1.96×10^{-3}

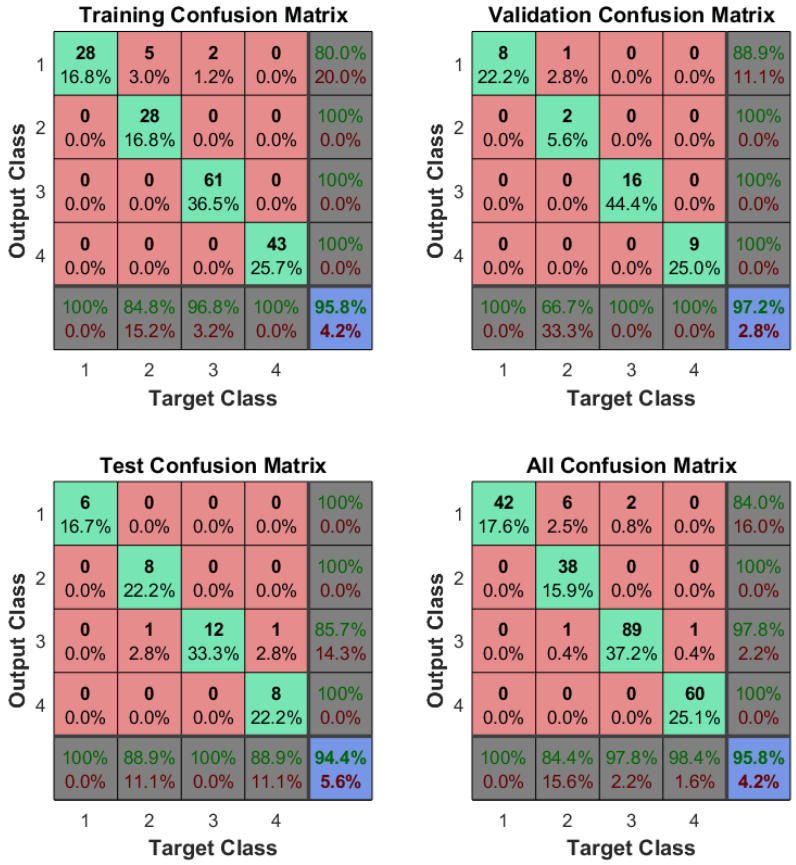

Fig.1. Confusion matrix results from the two-layer feed-forward neural network trained with a data set of 239 Australian oils collected from four different basins. The overall classification performance of the designed artificial neural network is 95.8%, *i.e.*, 229 out of 239 oil samples are correctly classified. Note: 1 = Bowen/Surrat, 2 = Carnarvon/Barrow, 3- Cooper/Eromanga, 4 = Gippsland.

References

Edwards, D.S., Zumberge, J.E., 2005. The oils of western Australia II. Regional petroleum geochemistry and correlation of crude oils and condensates from western Australia and Papua New Guinea. Geoscience Australia and GeoMark Research Ltd, Canberra and Houston. Record 37512

Geoscience Australia and GeoMark, 2002. The Oils of Eastern Australia. Petroleum Geochemistry and Correlation Volume 2. Geoscience Australia and GeoMark Research, Inc., Proprietary report, Canberra and Houston, unpublished.

Sohn J. H., Smith, R., Yoong, E., Leis, J., Galvin, G., 2003. Quantification Of Odours From Piggery Effluent Ponds Using An Electronic Nose And An Artificial Neural Network. Biosystems Engineering 86(4), 399-410

Sohn, J. H., Atzeni, M., Zeller, L., Pioggia, G., 2008. Characterisation Of Humidity Dependence Of A Metal Oxide Semiconductor Sensor Array Using Partial Least Squares, Sensor & Actuators B 131(1), 230-235

Coagulation optimisation using aluminium sulphate for the removal of natural organic matter from a surface water source in the southwest of Western Australia

Madina N. Tsuntsaeva*, Anna Heitz

Curtin University, Perth, 6102, Australia
*(*madina.tsuntsaeva@postgrad.curtin.edu.au)*

The high level of natural organic matter (NOM) in water from a surface water in the southwest of Western Australia has been found as a cause of excessive colour and precursors of disinfection by-products (DBPs) in drinking water supplied from this reservoir (Kristiana, Joll, Heitz 2011; Miller 2005)**.** NOM comprises a complicated matrix of different organic matter materials containing particulate and dissolved organic carbon (DOC) compounds. NOM matter in surface water can be derived from biodegradation products of aquatic plants and micro-organisms and is characterised as humic and non-humic fractions, as well as fractions of different molecular weights (Chow et al. 2009). DOC has to be removed from the raw water because it can react with chlorine to form DBPs such as trihalomethanes, haloacetic acids and chlorophenols (Kristiana, Joll, Heitz 2011; Hussain et al. 2013).

The aim of this study was to optimize the treatment process for this water, based on alum coagulation in combination with powdered activated carbon (PAC) to minimize the chemical dosages for reduction of DOC and ultraviolet absorbance at 254nm (UV_{254}). Ultraviolet absorbance at 254nm (UV_{254}) is associated with the presence of aquatic humic matter contaminants and high DBP formation potential. Specific ultraviolet absorbance ($SUVA_{254}$) calculation (UVA/DOC*100) was applied to characterise NOM fractions in untreated and treated water samples at the optimal conditions of the coagulation-flocculation process. One of the objectives of the study was to determine the impact of changing the order of addition of alum coagulant and PAC for optimal removal of residual low molecular weight (MW) pollutants which cannot be removed by coagulation only because of their low aromaticity and high hydrophilicity properties.

Coagulation water treatment process optimization was carried out using a jar test apparatus, pH meter, and aluminium sulphate as the coagulant. In the raw and treated water samples UV_{254} absorbance and DOC were measured using a UV/Vis spectrophotometer at a wavelength of 254 nm and TOC analyser, respectively. The samples were filtered before measuring UV_{254} and DOC using a membrane filter with 0.45 micron pore size. The values of $SUVA_{254}$ were calculated as the ratio of measured UV_{254} values to DOC values (Edzwald et al. 2008).

Surface raw water quality parameters were determined as UV_{254} = 0.432 (1/cm), DOC = 11.89 (mgC/L) and $SUVA_{254}$ - 3.63 ($mg^{-1}\ m^{-1}\ L$), respectively. Further alum coagulation optimization by pH change was carried out to reduce absolute values of UV_{254}, DOC and $SUVA_{254}$ in the water samples using a jar test apparatus. Figure 1 shows the maximum reduction of UV_{254}, DOC and $SUVA_{254}$ values as following 82%, 50%, and 64% at the optimum alum dose of 25ppm of aluminium at pH 6. While UV_{254} absorbance reduction was significant, DOC reduction was minor in comparison. High percent removal of UV_{254} absorbance in comparison to DOC suggested that surface raw water contains a high concentration of aquatic humic matter compounds. It is well known that aquatic humic matter contaminants have a higher UV_{254} absorbance than other types of NOM constituents (Edzwald et al. 2008). An alum coagulation removes organic matter such as humic and fulvic acids by destabilisation of negatively charged high molecular weight pollutants with positively charged aluminium species and adsorption within aluminium hydroxide precipitates (Shen and Chaung 1998). The significantly reduced $SUVA_{254}$ value of the treated water revealed that the remaining 50% DOC low molecular weight (MW) non-humic organic matter pollutants which are hydrophilic in nature, less aromatic and recalcitrant to removal by alum treatment (Shen and Chaung 1998; Chow et al. 2009). The coagulation results showed that the optimised alum coagulation process effectively removed high MW organic components of NOM that have negatively charged functional groups (and/or negatively charged surface charges in the case of larger colloidal material) but that the process is less effective in removing low MW, uncharged and non-humic organic compounds (Shen and Chaung 1998; Uyak and Toroz 2007). Further investigation is required to determine the impact of the order of addition of alum coagulant and PAC. The integrated water treatment system will allow maximum removal of recalcitrant uncharged and non-humic matter pollutants which are recalcitrant to removal by single alum coagulation.

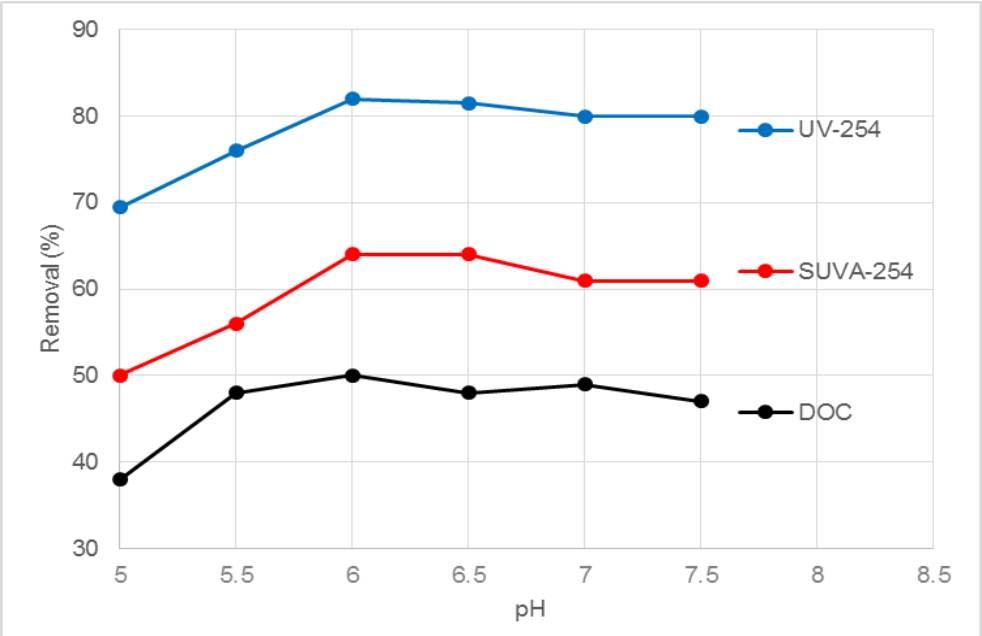

Fig. 1. Reduction of UV_{254}, DOC, $SUVA_{254}$ at different pH level using aluminium sulphate coagulation at optimal alum dose of 25ppm of aluminium.

References

Chow, C.W.K., Leeuwen, J.A., Fabris, R., Drikas, M., 2009. Optimised coagulation using aluminium sulfate for the removal of dissolved organic carbon. Desalination 245, 120-134.

Edzwald, J.K., Dee, P.E., Kaminski, G.S., 2008. A practical method for water plants to select coagulant dosing. New England Water Work Association, 11-27.

Hussain, S., Leeuwen, J., Chow, C., Beecham, S., Drikas, M., Aryal, R., 2013. Removal of organic contaminants from river and reserverentoir waters by three different aluminum-based salts: Coagulation adsorption and kinetics studies. Chemical Engineering 225, 394-405.

Kristiana, I., Joll, C., Heitz, A., 2011. Powdered activated carbon coupled with enhanced coagulation for natural organic matter removal and disinfection by-produt control: Application in a Western Australian water treatment plant. Chemosphere 5, 661-667.

Miller, R., 2005. Honours thesis, Natural organic matter in Quickup reservoir: Sources and Fluctuations. University of Western Australia.

Shen, Y.H, Chaung, T.H., 1998. Removal of dissolved organic carbon by coagulation and adsorption from polluted source water in Southern Taiwan. Environment international 24, 497-503.

Uyak, V., Toroz, I., 2007. Disinfection by-product precursors reduction by various coagulation techniques in Istanbul water supplies. Journal of Hazardous materials 141, 320-328.